PLACE IN RETURN BOX to remove this checkout from your record.

TO AVOID FINES return on or before date due.

DATE DUE	DATE DUE	DATE DUE

1/98 c:/CIRC/DateDue.p65-p.14

EFFECTS OF METHYLMERCURY ON CENTRAL SYNAPTIC TRANSMISSION IN RAT BRAIN SLICES

By

Yukun Yuan

A DISSERTATION

Submitted to
Michigan State University
in partial fulfillment of the requirements
for the degree of

DOCTOR OF PHILOSOPHY

Department of Pharmacology and Toxicology

1997

ABSTRACT

EFFECTS OF METHYLMERCURY ON CENTRAL SYNAPTIC TRANSMISSION IN RAT BRAIN SLICES

By

Yukun Yuan

Effects of MeHg on central synaptic transmission were examined in rat hippocampal and cerebellar slices using electrophysiological methods. Bath application of MeHg initially stimulated and then suppressed synaptic transmission in the CA1 region of hippocampal slices. 4 - 100 µM MeHg blocked action potentials and hyperpolarized and then depolarized CA1 neuronal membranes. The primary sites of action of MeHg appeared to be the postsynaptic CA1 pyramidal cells, although multiple effects were involved. Inhibitory synaptic transmission appeared to be more sensitive to MeHg than was excitatory synaptic transmission. After pretreatment of hippocampal slices with bicuculline, a GABA receptor antagonist, MeHg only suppressed population spikes and excitatory postsynaptic potentials (EPSPs); no early stimulation of these responses occurred. MeHg also blocked responses evoked by GABA, receptor agonist muscimol. Thus, a preferential block by MeHg of GABA, receptor-mediated responses appeared to be primarily responsible for the initial enhancement of hippocampal synaptic transmission.

Similarly, MeHg caused a biphasic effect on field potentials recorded from the molecular layer of the cerebellar slices. To identify sites of action, effects of MeHg on EPSPs evoked by stimulating the parallel or climbing fibers and repetitive firing of Purkinje cells evoked by injecting depolarizing current at the soma were compared. MeHg blocked all voltage-dependent responses, including Na⁺-dependent, fast somatic spikes and Ca²⁺-dependent, slow dendritic spike bursts. MeHg appeared to affect voltage-dependent responses and glutamate receptor-mediated responses differently. Similarly, MeHg hyperpolarized and then depolarized Purkinje cell membranes. Moreover, MeHg changed the patterns of repetitive firing of Purkinje cells from predominantly Na⁺-dependent, fast somatic spikes to predominantly Ca²⁺-dependent, low amplitude, slow dendritic spike bursts, suggesting that MeHg may affect Purkinje cell membrane ionic conductances. Apparently, MeHg acts primarily at the postsynaptic Purkinje cells to block cerebellar synaptic transmission, multiple effects are involved. Thus, effects of MeHg on hippocampal and cerebellar synaptic transmission are generally similar.

ACKNOWLEDGMENTS

I would like to thank my mentor, Dr. William D. Atchison, for providing me with the opportunity to work and study in his lab for the past several years, which will be a very important period of time in my career. Under his guidance, I understood a simple but very important philosophy: Learn to walk before run. I am very grateful for his great efforts and patient in helping me to improve my oral and writing skills. I would also like to thank the rest members of my dissertation committee: Drs. Peter JR. Cobbett, Gerard L. Gebber, Kenneth E. Moore and Monte M. Piercey, for their great efforts and helpful advice. Special thanks are extended to Dr. James J. Galligan for his help and suggestions in the setting up of the electrophysiological experiments.

I would also like to take this opportunity to thank everyone in Dr Atchison's lab, John, Tim, Cindy, Michael, Mike, Lynne, Jay, Ravindra, Sue, Yao, Laura and Youfen, for their assistance and friendship during my stay. Especially, I'd like to thank Michael, Mike and Jay for teaching me the "kid language". I also want to thank all the graduate students in this department, especially my classmates Amy, Courtney, Frederick, Ken and Rosie, for their support and friendship. Special thanks are extended to the department office staffs, Diane, Nelda and Mickey for their great help in all the paper work.

I'd also like to thank my family, especially my parents, for their

understanding and constant support. I also want to thank my daughter and son, Lucy and Daniel, for giving me lots of extra fun.

Finally, I want to express my gratitude to my wife and colleague, Hong, for her constant support, understanding, suggestion and love. Without her encouragement and help, I can't image how difficult it would be for me to accomplish my work.

TABLE OF CONTENTS

LIST OF TABLES	vii
LIST OF FIGURES	viii
LIST OF ABBREVIATIONS	xiii
CHAPTER ONE: INTRODUCTION	1
A. Methylmercury neurotoxicity	2
B. Effects of MeHg on peripheral synaptic transmission	4
C. Effects of MeHg on central synaptic transmission	8
D. Specific aims	16
CHAPTER TWO: THE PREPARATION AND USE OF BRAIN SLICES FOR ELECTROPHYSIOLOGICAL STUDIES OF CENTRAL SYNAPTIC TRANSMISSION	18
A. The advantages of in vitro brain slice techniques	19
B. The organization of neurons and synaptic circuits the hippocampal slice	21
C. The organization of neurons and synaptic circuits of cerebellar slices	27
D. Preparation of brain slices	34
1) Preparation of hippocampal slices	34
2) Preparation of cerebellar slices	35
E. Methods for electrophysiological studies of synaptic transmission in brain slices	39
1) Extracellular recording	39
2) Intracellular recording	44

3) Sharp single-electrode voltage clamp recording	45
4) Whole-cell patch recording	51
CHAPTER THREE: METHYLMERCURY ACTS AT MULTIPLE SITES TO BLOCK HIPPOCAMPAL SYNAPTIC TRANSMISSION	55
A. Abstract	56
B. Introduction	58
C. Materials and Methods	60
D. Results	65
E. Discussion	94
CHAPTER FOUR: ACTION OF METHYLMERCURY ON GABAARECEPTOR-MEDIATED INHIBITORY SYNAPTIC TRANSMISSION IS PRIMARILY RESPONSIBLE FOR ITS EARLY STIMULATORY EFFECTS ON HIPPOCAMPAL	
CA1 EXCITATORY SYNAPTIC TRANSMISSION	104
A. Abstract	105
B. Introduction	107
C. Materials and Methods	110
D. Results	113
E. Discussion	142
CHAPTER FIVE: COMPARATIVE EFFECTS OF METHYLMERCURY ON PARALLEL-FIBER AND CLIMBING-FIBER RESPONSES	
IN RAT CEREBELLAR SLICES	150
A. Abstract	151
B. Introduction	154
C. Materials and Methods	157
D. Results	168

E. Discussion	209
CHAPTER SIX: SUMMARY AND CONCLUSIONS	
A. Summary	221
B. Conclusion	237
C. Future direction	238
BIBLIOGRAPHY	240

LIST OF TABLES

Table 2.1.	Putative neurotransmitter in the major intrinsic pathways of hippocampus.	26
Table 3.1.	Time to MeHg-induced block of action potentials evoked at the threshold and maximum stimulation of Schaffer collaterals.	68
Table 3.2.	Amplitudes of action potentials and the resting membrane potentials just before or at the time that action potentials were blocked by MeHg.	70
Table 6.1.	Comparison of time to MeHg-induced block of population spikes and field excitatory postsynaptic potentials in the CA1 region of hippocampal slices.	235
Table 6.2.	Comparison of times to MeHg-induced block of parallel-fiber volley, parallel-fiber postsynaptic response and climbing-fiber response in cerebellar slices.	235
Table 6.3.	Comparison of times to MeHg-induced block of action potentials evoked by stimulating Schaffer collaterals and by current-injection in CA1 pyramidal cells of hippocampal slices.	236
Table 6.4.	Comparison of times to MeHg-induced block of parallel- fiber excitatory postsynaptic potentials, climbing- fiber excitatory postsynaptic potentials and repetitive firing of Purkinje cells evoked by current injection in cerebellar slices.	236

LIST OF FIGURES

Figure 1.1.	Time course of effects of 4-500 μM MeHg on amplitude of population spikes, field excitatory postsynaptic potentials and antidromically-activated population spikes.	11
Figure 1.2.	Time course of reversal of effects of MeHg (100 μ M) on population spikes, field excitatory postsynaptic potentials, or antidromically-activated population spikes by washing with MeHg-free ACSF or D-penicillamine.	13
Figure 1.3.	Effects of increasing stimulating intensity on population spike responses in hippocampal slices blocked irreversibly by 100 μM MeHg.	15
Figure 2.1.	Schematic diagram of structure and intrinsic synaptic circuits of a transverse hippocampal slice.	23
Figure 2.2.	Schematic diagram of organization of neurons and synaptic circuits of the transverse and sagittal cerebellar slices.	29
Figure 2.3.	Diagrammatic depiction of arrangement of the agar and cerebellar tissue blocks on the tissue pedestal of an oscillatory slicer.	38
Figure 2.4.	Representative demonstration of the field potentials recorded from the CA1 region of a hippocampal slice and the molecular layer of a cerebellar slice using extracellular recording techniques.	43
Figure 2.5.	Representative example of responses recorded from individual CA1 pyramidal cells of a hippocampal slice and Purkinje cells of a cerebellar slice using intracellular recording techniques.	47
Figure 2.6.	Schematic diagram of the principle of sharp single-electrode voltage clamp technique.	49
Figure 3.1	Diagrammatic depiction of the synaptic circuits of a traverse hippocampal slice and methods for recording action potentials in the CA1 pyramidal cells.	64

Figure 3.2.	Time courses of effects of 4, 20 and 100 μM MeHg on action potentials of hippocampal CA1 pyramidal cells.	67
Figure 3.3.	Time courses of 4 - 100 μM MeHg on resting membrane potentials of hippocampal CA1 pyramidal cells.	73
Figure 3.4.	The maximum hyperpolarization of CA1 neuronal membrane caused by 4 - 100 μM MeHg.	s 76
Figure 3.5.	Effects of increased [Ca ²⁺] _e on time to MeHg-induced block of action potentials evoked at threshold and maximum stimulation of Schaffer collaterals.	80
Figure 3.6.	Comparison of times to MeHg-induced block of action potentials evoked by different stimulation methods.	83
Figure 3.7	Time course of effect of 20 μ M MeHg on action potentials evoked by depolarizing current injection through a recording electrode at the CA1 pyramidal cell soma.	85
Figure 3.8.	Comparison of times to block by 100 μ M MeHg of responses of CA1 neurons to electrical stimulation of presynaptic terminals and to iontophoretic application of glutamate on the apical dendrites of CA1 pyramidal cells.	88
Figure 3.9.	Comparison of time course of effects of 100 μM MeHg on EPSPs and IPSPs.	91
Figure 3.10.	MeHg-induced changes in IPSP amplitudes at 0, 10 and 35 min and changes in EPSP amplitudes of hippocampal CA1 pyramidal cells at 0, 40 and 60 min.	93
Figure 4.1.	Comparison of times to block of recurrent IPSPs and EPSPs or IPSCs and EPSCs by 100 µM MeHg or Hg ²⁺ .	115
Figure 4.2.	Time course of effect of 100 µM MeHg on EPSCs recorded from CA1 pyramidal cells of hippocampal slices using sharp single-microelectrode voltage-clamp techniques.	118
Figure 4.3.	Effects of 100 μM MeHg on IPSCs recorded at different holding potentials.	121
Figure 4.4.	Effects of 100 µM Hg ²⁺ on IPSCs recorded at different holding potentials	123

Figure 4.5.	Comparison of effects of 100 µM MeHg and Hg ²⁺ on the current-voltage relationship (I/V curve) of IPSCs recorded in the CA1 pyramidal cells.	125
Figure 4.6.	Comparison of effects of MeHg and bicuculline on population spikes of hippocampal CA1 pyramidal cells.	128
Figure 4.7.	Time courses of effects of MeHg on population spikes of hippocampal CA1 pyramidal cells with or without pretreatment of slices with bicuculline or strychnine.	131
Figure 4.8.	Time course of effects of 100 µM MeHg on EPSPs of hippocampal CA1 pyramidal cells evoked by stimulating Schaffer collaterals in the presence of bicuculline.	135
Figure 4.9.	Effects of 20 μM bicuculline and 100 μM MeHg on muscimolevoked responses in hippocampal CA1 pyramidal cells.	137
Figure 4.10.	Comparison of the maximum enhancement of population spikes of CA1 hippocampal pyramidal cells by strychnine, bicuculline and MeHg alone, with the combinations of MeHg with bicuculline or strychnine.	, 141
Figure 5.1.	Diagrammatic depiction of the structure of the cerebellar cortex in sagittal and transverse slices and methods for recording field potentials of Purkinje cells following activation of parallel-fibers or climbing-fibers.	160
Figure 5.2.	Effects of DNQX and AP-5 on field potentials evoked by stimulating the parallel or climbing fibers in cerebellar slices.	163
Figure 5.3.	Effects of stimulus intensity on the parallel and climbing fiber responses.	166
Figure 5.4.	Time course of effects of 100 and 20 μ M MeHg on field potentials recorded from the molecular layer following stimulation of the parallel fibers in transverse cerebellar slices.	170
Figure 5.5.	Time course of effects of 100 and 20 µM MeHg on field potentials recorded from the molecular layer following stimulation of the climbing fibers in sagittal cerebellar slices.	173

Figure 5.6.	Comparison of times to block by 100 and 20 µM MeHg of field potentials representing the parallel fiber volleys, postsynaptic responses and climbing fiber responses.	175
Figure 5.7.	Time course of effects of 100 and 20 µM MeHg on field responses representing the parallel fiber volleys, postsynaptic responses and climbing fiber responses.	177
Figure 5.8.	Time courses of effects of 100 and 20 µM MeHg on PF- EPSPs recorded from Purkinje cell soma by stimulation of the parallel fibers in the transverse cerebellar slices	181
Figure 5.9.	Time courses of effects of 100 and 20 µM MeHg on CF- EPSPs recorded from Purkinje cell soma by stimulation of the climbing fibers in the sagittal cerebellar slices.	183
Figure 5.10.	Time courses of effects of 100 and 20 μM MeHg on resting membrane potentials of Purkinje cells.	186
Figure 5.11.	Time course of effects of 100 μM MeHg on responses evoked by injection of depolarizing current through the recording electrode at Purkinje cell soma.	189
Figure 5.12.	Comparison of time courses of effects of 100 μ M MeHg on PF-EPSPs evoked by stimulation of the parallel fibers and repetitive responses evoked by injection of depolarizing current at Purkinje cell soma.	192
Figure 5.13.	Comparison of time courses of effects of 20 μ M MeHg on PF-EPSPs evoked by stimulation of the parallel fibers and repetitive responses evoked by injection of depolarizing current at Purkinje cell soma.	195
Figure 5.14.	Comparison of time courses of effects of 100 μM MeHg on CF-EPSPs evoked by stimulation of the climbing fibers and repetitive responses evoked by injection of short duration depolarizing currents at Purkinje cell soma.	197
Figure 5.15.	Comparison of times to block of PF-EPSPs, CF-EPSPs and repetitive firing responses (Soma) of Purkinje cell by 100 and 20 μ M MeHg.	200
Figure 5.16	Spontaneous repetitive firing of a Purkinje cell just after	

	penetration with a glass recording microelectrode.	203
_	Effects of 100 μM MeHg on spontaneous repetitive firing of Purkinje cells.	205
_	Effects of 100 μ M MeHg on spontaneous firing of Purkinje cells recorded from the Purkinje cell layer of a transverse cerebellar slice using extracellular recording techniques.	207

LIST OF ABBREVIATIONS

ACh acetylcholine

ACSF artificial cerebrospinal fluid

AP-5 amino-5-phosphonopentanoic acid

EF-EPSPs climbing fiber excitatory postsynaptic potentials

CFRs climbing-fiber responses

CNS central nervous system

CNQX 6-cyano-7-nitroquinoxaline-2,3-dione

[Ca²⁺]_e extracellular Ca²⁺ concentration

[Ca²⁺]_i intracellular Ca²⁺ concentration

DMSO dimethyl sulfoxide

DNQX 6,7-dinitroquinoxaline-2,3-dione

EPPs end-plate potentials

EPSPs excitatory postsynaptic potentials

EPSCs excitatory postsynaptic currents

fEPSPs field excitatory postsynaptic potentials

GABA γ-aminobutyric acid

GABA A type of GABA receptor

GABA_B B type of GABA receptor

Hg²⁺ inorganic mercury

IP₃ inositol-1,4,5-tris-phosphate

IPSPs inhibitory postsynaptic potentials

IPSCs inhibitory postsynaptic currents

I/V curve voltage-current relationship

MeHg methylmercury

MEPP miniature end-plate potential

min minute

mM millimole

ms millisecond

mV millivolt

 $M\Omega$ megohm

NMDA N-methyl-D-aspartate

PF-EPSPs parallel fiber excitatory postsynaptic potentials

PFVs parallel-fiber volleys

PSRs postsynaptic responses

SE standard error of mean

sSEVC sharp single-electrode voltage-clamp recording

TTX tetrodotoxin

μM micromole

v/v volume per volume dilution

CHAPTER ONE

INTRODUCTION

A. Methylmercury neurotoxicity

Methylmercury (MeHg) is a well-known environmental contaminant. Even today, mercury pollution remains an important global environmental problem (Evans, 1986; Wendro, 1990; Nriagu et al., 1992; Nater and Grigal, 1992; Nriagu, 1993). Sources of mercury contamination are generally from industrial, agricultural and other anthropogenic activities and natural events from geological formations. MeHg can be converted from inorganic mercury, via methylation by microorganisms in the sediments of river and lake bottoms. and then concentrated in fish tissues within the food chain. This is thought to be primarily responsible for the chronic events of MeHg poisoning events in Minamata Bay and the Niigata district of Japan in the 1950s. The mean biological half-life of MeHg is about 70 days in the human body (Nelson et al., 1971; Birke et al., 1972) and much longer in brain (Komulainen, 1988). MeHg is soluble in both water and lipid with a high lipid/water partition coefficient, which confers on it the ability to cross the blood-brain barrier more readily than other mercurial compounds. Therefore it accumulates in the brain following chronic exposure. The distribution of MeHg in the brain is generally uniform, however, the areas which attain the maximum concentrations of MeHg following subacute or chronic exposure were the cerebral cortex, hippocampus and the cerebellar cortex (Olserwski et al., 1974; Chang, 1980; Møller-Madsen, 1990, 1991). Regional variations in distribution of MeHg have also been demonstrated between experimental animal species, sex and patterns

of administration of MeHg (Yoshino et al., 1966a; Yasutake and Hiyama, 1986; Omata et al., 1986; Thomas et al., 1986; Møller-Madsen, 1990, 1991). The critical target organ of MeHg is the nervous system, particularly the central nervous system (CNS). Acute and chronic exposure to MeHg disrupts sensory and motor functions and causes a series of peripheral and central nervous system disorders of human and experimental animals (Takeuchi et al., 1959; Kurland et al., 1960; Tokuomi et al., 1961; Takeuchi et al., 1962; Miyakawa et al., 1970; Bakir et al., 1973; Rustam and Hamdi, 1974; Chang, 1977, 1980). The typical symptoms and signs of MeHg poisoning include extremity weakness, cerebellar ataxia, visual damage (tunnel-vision), loss of hearing, disturbances of sensory functions and so on (Kurland et al., 1960; Tokuomi et al., 1961; Bakir et al., 1973; Rustam and Hamdi, 1974; Chang, 1977, 1980). The underlying mechanisms responsible for these effects remain poorly understood. Multiple mechanisms may be involved, as MeHg has been reported to interfere with intracellular homeostasis of Ca2+ (Komulainen and Bondy, 1987; Kauppinen et al., 1989; Levesque and Atchison, 1991; Hare and Atchison, 1992b, Hare et al., 1993; Denny et al., 1993; Sarafian, 1993; Hare and Atchison, 1995a,b; Marty and Atchison, 1997), to affect Ca²⁺ channels (Atchison et al., 1986; Shafer and Atchison, 1989; Shafer et al., 1990; Shafer and Atchison, 1991, 1992; Hewett and Atchison, 1992; Leonhardt et al., 1996; Sirois and Atchison, 1996), K⁺ and Na⁺ channels (Shrivastav *et al.*, 1976; Quandt et al., 1982; Shafer and Atchison, 1992; Sirois and Atchison, 1995;

Leonhardt et al., 1996), to inhibit protein phosphorylation and synthesis (Yoshino et al., 1966b; Syversen, 1981; Sarafian and Verity, 1990a,b Sarafian, 1993), to inhibit activity of some enzymes (Taylor, 1963; Tunnicliff and Wood, 1973; Verity et al., 1975; Omata et al., 1982; Dyck and O'Kusky, 1988; Kishimoto et al., 1995), to affect neurotransmitter release and disrupt peripheral synaptic transmission (Juang and Yonemura, 1975; Juang, 1976a,b; Bondy et al., 1979; Minnema et al., 1989; Atchison and Narahashi, 1982; Atchison, 1986; Traxinger and Atchison, 1987a,b; Levesque et al., 1992), to induce cell death (Sarafian et al., 1989; Sarafian and Verity, 1990a; Sarafian et al., 1994; Nagashima et al., 1996; Kunimoto and Suzuki, 1997), to depolarize neuronal membranes (Juang, 1976; Shrivastav et al., 1976; Quandt et al., 1982; Kauppinen et al., 1989; Hare and Atchison, 1992a) and to have other neurotoxic effects (Chang, 1980; Atchison, 1987b). It is generally believed that effects of MeHg on both peripheral and central synaptic transmission may play an important role in its neurotoxicity.

B. Effects of MeHg on peripheral synaptic transmission.

In experimental animals with subacute MeHg poisoning, pathological examination indicated that MeHg first or selectively affected the peripheral nerves, especially the sensory nerve fibers, (Miyakawa et al., 1970; Chang and Hartmann, 1972). In the Iraq MeHg poisoning episode, individuals also exhibited neuromuscular weakness which was similar to myasthenia gravis,

suggesting that MeHg may disrupt peripheral motor synaptic transmission (Rustam et al., 1975). Thus, early mechanistic studies have extensively examined the effects of MeHg on synaptic transmission at vertebrate peripheral synapses such as the neuromuscular junction and autonomic ganglia. Acute bath application of MeHg irreversibly blocks synaptic transmission at these synapses (Juang and Yonemura, 1975; Juang, 1976a,b; Atchison and Narahashi, 1982; Atchison, 1986; Traxinger and Atchison, 1987a,b). In neuromuscular preparations, MeHg caused a biphasic effect on spontaneous release of acetylcholine (ACh). Release, measured as a change of miniature end-plate potential (MEPP) frequency, is stimulated and then depressed to block by MeHg in the concentration range of 4 - 100 µM (Atchison and Naraharshi, 1982; Atchison, 1986, 1987a; Traxinger and Atchison, 1987 a,b; Levesque and Atchison, 1987, 1988). Effects of MeHg on synaptic function are not limited to spontaneous release of ACh. MeHg also affects nerve-evoked release of ACh, measured as changes in amplitude of end-plate potentials (EPPs) (Atchison and Narahashi, 1982; Atchison et al., 1986; Traxinger and Atchison, 1987b). In some cases MeHg also transiently increased the amplitude of EPPs prior to block (Manalis and Cooper, 1975; Juang, 1976b; Traxinger and Atchison, 1987b). Using mouse triangularis sterni motor nerves, Shafer and Atchison (1992) directly examined effects of MeHg on functions of presynaptic nerve terminal Ca2+ and Na+ channels at intact neuromuscular junctions. At micromolar levels (20, 100 µM), MeHg rapidly and irreversibly blocked both Ca²⁺- and Na⁺-mediated potential components evoked by stimulating presynaptic nerve fibers, suggesting that MeHg may decrease motor nerve excitability and block neurotransmitter release by disrupting function of Na⁺ and Ca²⁺ channels on nerve terminals. None of these effects described above were reversed completely by washing neuromuscular preparations with MeHg-free solution. However, partial reversal of effects of MeHg on synaptic functions occurred under certain conditions such as by washing neuromuscular preparations with MeHg-free solution in conjunction with increasing stimulus intensity or duration or by increasing extracellular Ca2+ concentrations (Von Burg and Landry, 1976; Alkhadhi and Taha, 1982; Atchison, 1986; Traxinger and Atchison, 1987b). The mechanisms responsible for these effects caused by MeHg on peripheral synaptic transmission are generally considered to be predominantly presynaptic (Atchison and Narahashi, 1982; Atchison, 1986, 1987; Levesque and Atchison, 1987, 1988; Shafer and Atchison, 1991, 1992), because at relatively high concentrations (40 or 100 µM), MeHg has no effects on either action potentials (twitches) evoked by direct stimulation of muscle fibers or resting membrane potentials of postsynaptic muscle fibers despite block of neuromuscular transmission (Juang, 1976a). Moreover, MEPPs of normal amplitude and duration still occur and responses of end-plates to iontophoretic application of ACh were unaffected by 100 µM MeHg at times that EPPs were blocked (Atchison and Narahashi, 1982).

These model peripheral synapses, which are well characterized physiologically and anatomically, have been useful systems in which to detail some of the early effects of MeHg on synaptic function such as neuromuscular weakness in those Iraqi poisoning patients. However, the clinical symptoms and signs and pathologic lesions in human and experimental animals with MeHg poisoning, especially following chronic exposure, suggest that the major neurotoxic target is the central nervous system, particularly the cerebellum and the visual cortex of the occipital lobe (Hunter and Russell, 1954; Kurland et al., 1960; Tokuomi et al., 1961; Takeuchi et al., 1962; Bakir et al., 1973; Rustam and Hamdi, 1974; Chang, 1977, 1980), although differences in the sites, degree and sequence of MeHg-induced neuropathologic lesions in the CNS exist among experimental animal species (Yoshino et al., 1965; Shaw et al., 1975). Moreover, central synapses have a number of unique characteristics such as the presence of significant Ca²⁺-mediated action potentials in dendrites of some neurons (Llinás and Hess, 1976; Schwartzkroin and Slawsky, 1977; Wong and Prince, 1978; Wong et al., 1979; Llinás and Sugimori, 1980b; Kimura et al., 1985; Llinás and Walton, 1990; Johnston et al., 1996), which are not present at the neuromuscular junction. Thus, MeHg may affect central synaptic function in a manner different from that on peripheral somatic nerve transmission.

C. Effects of MeHg on central synaptic transmission.

The effects of MeHg on central synaptic transmission have not been as well studied as its effects on peripheral synaptic transmission. Thus, little is known of the mechanisms by which MeHg acutely and chronically alters central synaptic functions. In vitro, however, exposure to MeHg alters neurotransmitter release from brain homogenates or synaptosomes (Bondy et al., 1979; Minnema et al., 1989; Levesque et al., 1992), depolarizes synaptosomal and intraterminal mitochondrial membranes (Kauppinen et al., 1989; Hare and Atchison, 1992a), affects Ca²⁺ channels in synaptosomes and primary cultures of cerebellar granule cells (Shafer and Atchison, 1989; Shafer et al., 1990; Hewett and Atchison, 1992; Sirois and Atchison, 1996), and disturbs intracellular homeostasis of Ca2+ of synaptosomes and intact neurons (Komulainen and Bondy, 1987; Kaupppinen et al., 1989; Levesque and Atchison, 1991; Hare and Atchison, 1992b; Denny et al., Marty and Atchison, 1996; 1997). Thus, it is likely that MeHg also blocks synaptic transmission at intact central synapses.

Using extracellular microelectrode recording techniques I initially examined the effects of MeHg on the field potentials [including population spikes, field excitatory postsynaptic potentials (fEPSPs) and antidromically-activated population spikes] recorded from the CA1 pyramidal cells of hippocampal slices (Yuan and Atchison, 1993, 1994). Acute bath application of 4 - 500 µM MeHg caused a concentration- and time-dependent biphasic

effect on these field potentials (Figure 1.1). Specifically, MeHg initially increased and then decreased to complete block population spikes, fEPSPs and antidromically-activated population spikes. However, the characteristics of block of these field potentials by MeHg differed somewhat in terms of the time courses and degree of reversibility. Block of orthodromically- and antidromically-activated population spikes was at best only partially reversible by washing slices with MeHg-free artificial cerebrospinal fluid (ACSF) or 1 mM D-penicillamine, a MeHg chelator, whereas block of fEPSPs was partially reversible by washing slices with MeHg-free ACSF and quickly and completely reversible by D-penicillamine (Figure 1.2). In those slices refractory to reversal by washing with either MeHg-free ACSF or D-penicillamine, increasing the stimulus intensity slightly could induce temporary recovery of the population spikes (Figure 1.3). These results suggest that acute bath application of MeHg may alter hippocampal CA1 neuronal membrane excitability and act at multiple sites to disrupt synaptic transmission.

Figure 1.1. Time course of effects of MeHg on amplitude of population spike (PS), field excitatory postsynaptic potential (fEPSP) and antidromically-activated population spike (Anti-PS). Slices were perfused continuously with MeHg--containing ACSF at 4, 20 100 and 500 µM. PSs and fEPSPs were recorded at the CA1 pyramidal cell soma and apical dendritic region, respectively, by stimulation of Schaffer collaterals at 0.25 Hz. Anti-PSs were recorded at the CA1 pyramidal soma region by stimulating the alveus. Values obtained before perfusion with MeHg were considered as pretreatment control. All values are the mean ± SE of 6-11 individual experiments. Only one slice per rat was used.

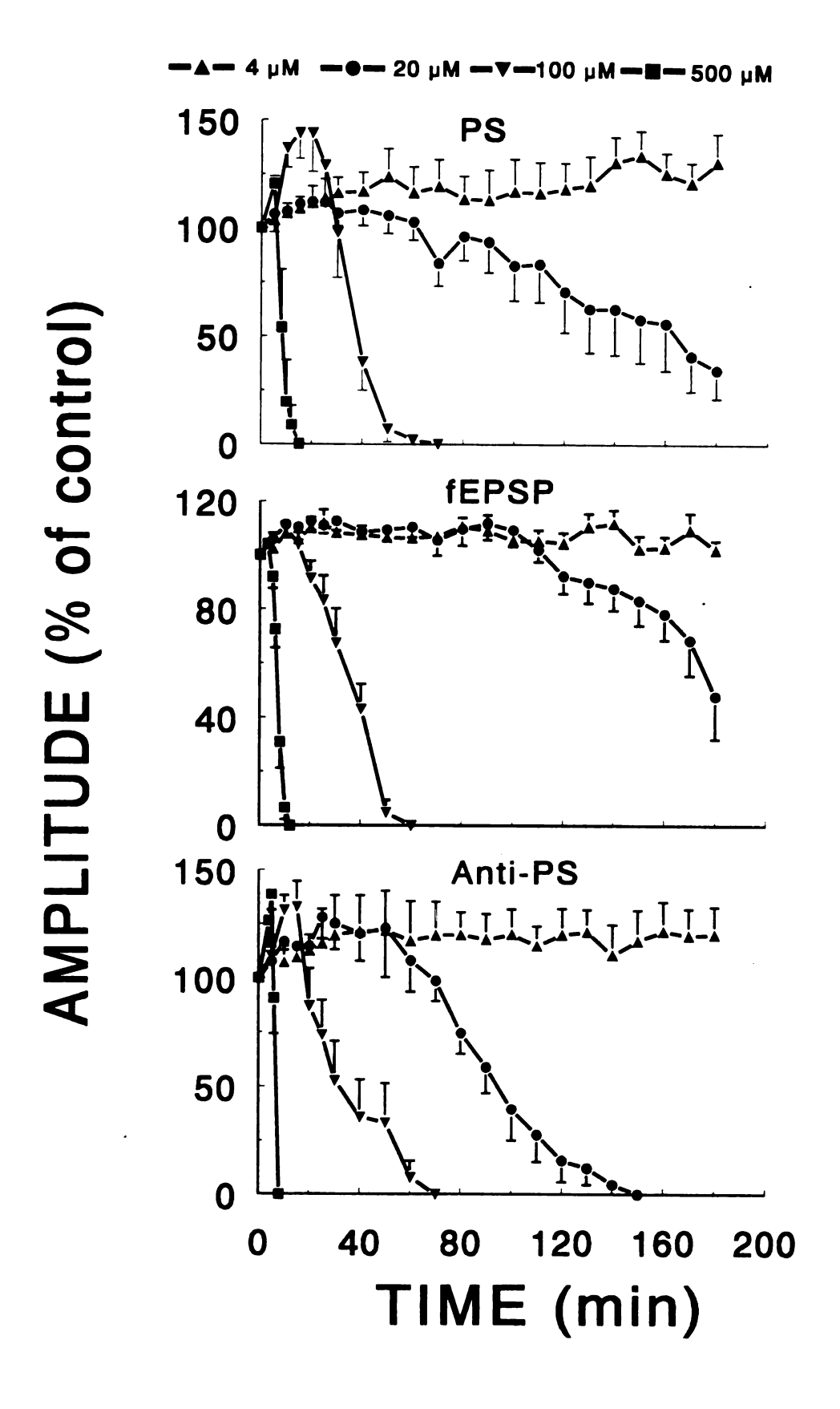


Figure 1.2. Time course of reversal effects of MeHg (100 μ M) on population spikes (PSs), field excitatory postsynaptic potentials (fEPSPs), or antidromically-activated population spikes (Anti-PSs) by washing with MeHg-free ACSF or D-penicillamine. Slices were washed with MeHg-free ACSF or 1 mM D-penicillamine after the amplitudes of PSs, fEPSPs or Anti-PSs were reduced by MeHg to 50% of their pretreatment control level. Values are the mean \pm SE of 5-10 individual experiments.

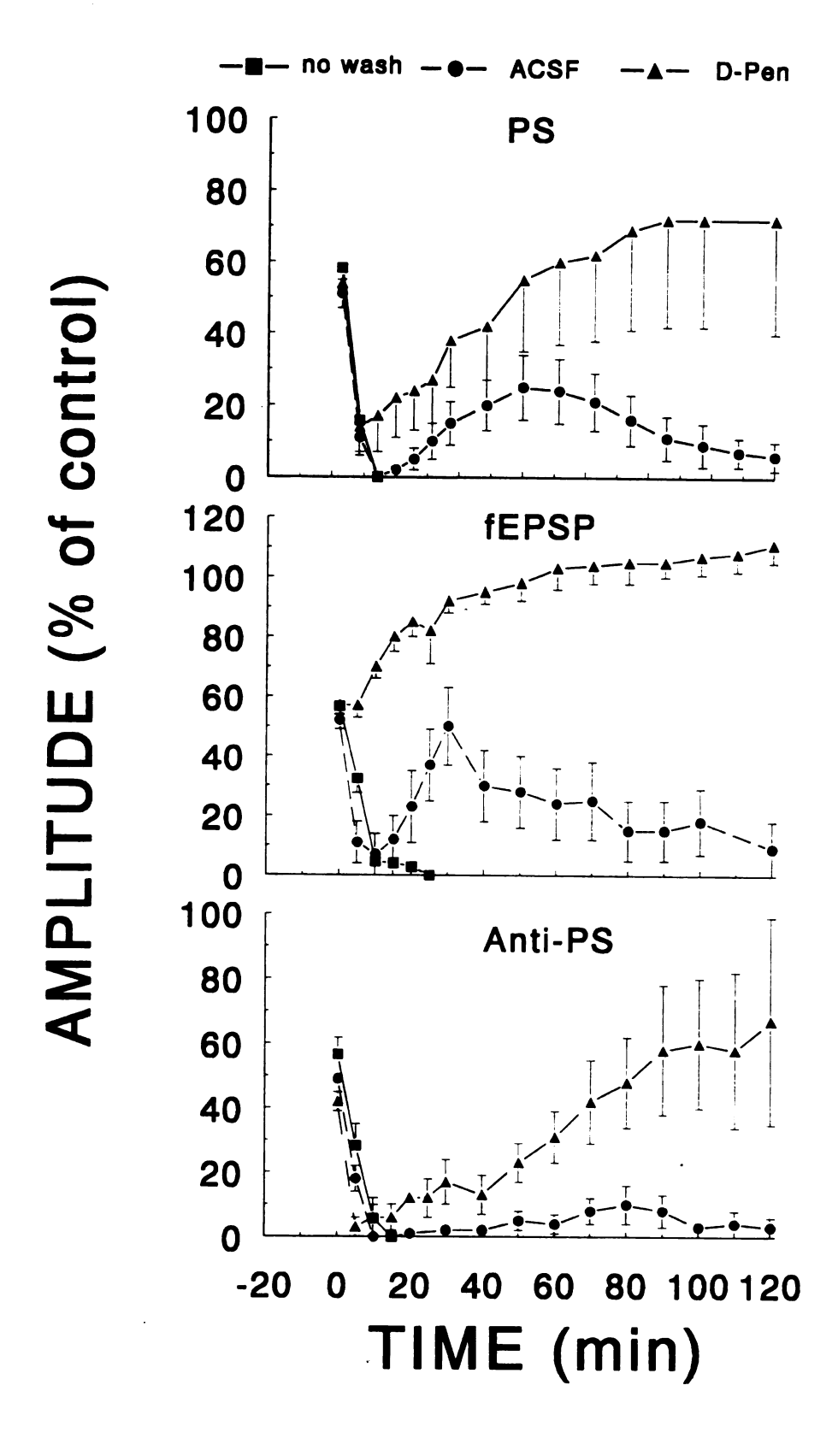
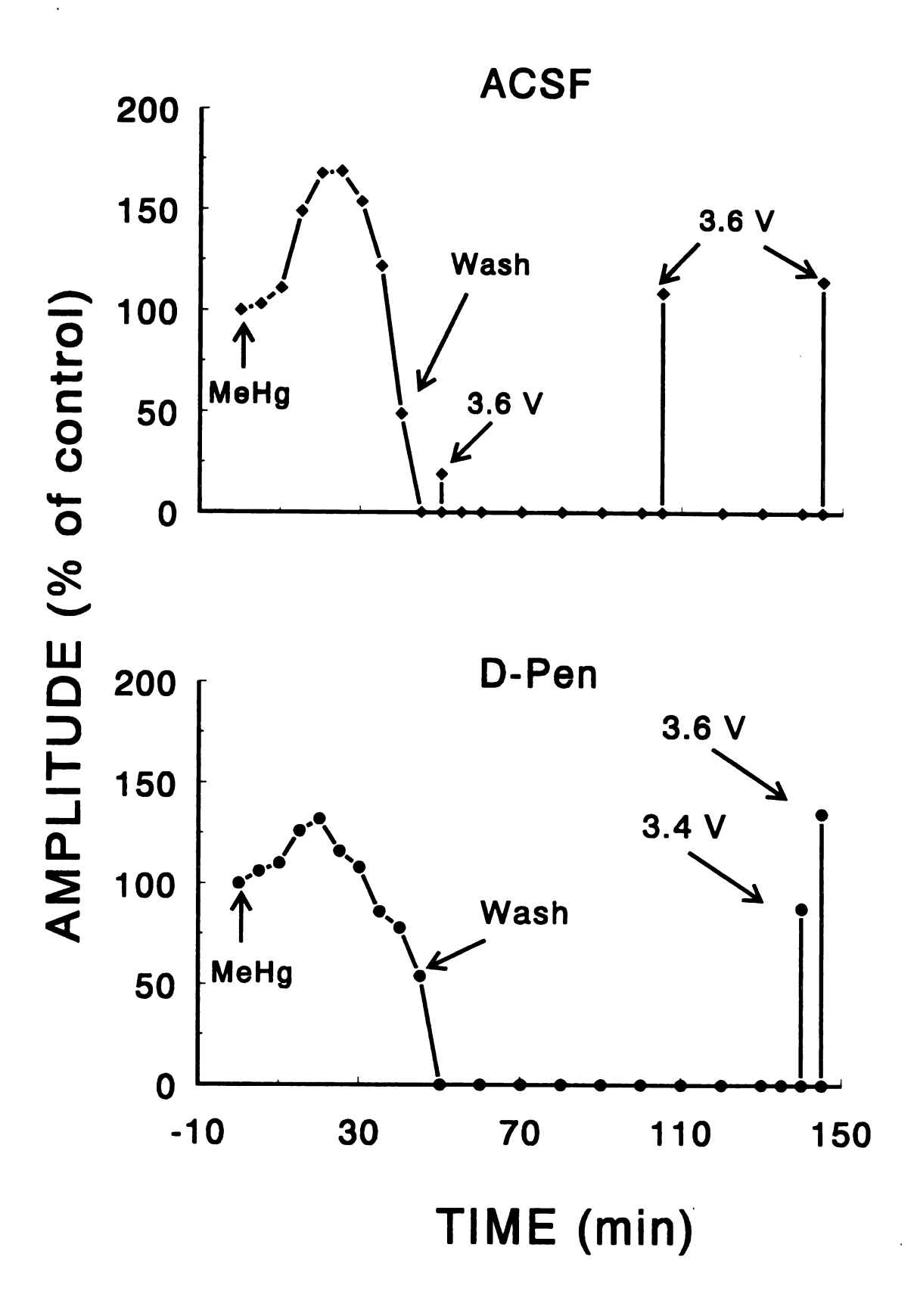


Figure 1.3. Effects of increasing stimulating intensity on population spike (PS) responses in slices blocked irreversibly by 100 μM MeHg. After PS amplitude was increased and then decreased to 50% of control, the slice was washed with MeHg-free ACSF (Top) or 1 mM D-penicillamine (Bottom). PSs were induced and maintained by repeated single shock stimulation of 3.2 V (A) or 3.0 (B) at 0.25 Hz. After PSs were blocked completely, increasing stimulation intensity from 3.2 V to 3.6 V at 5, 60 and 90 min (Top) or from 3.0 V to 3.4 or 3.6 (Bottom) could still induce PS responses. Upon returning stimulation intensity to 3.2 V or 3.0 V, PS responses again disappeared.



Due to the limitations of extracellular recording techniques, it is difficult to specify where and how MeHg acts to block hippocampal synaptic transmission. In addition, it is unknown if these effects occur similarly in other brain regions such as the cerebellar cortex. Thus, in order to characterize further the effects of MeHg on central synaptic transmission, extracellular and intracellular microelectrode recordings, sharp single-electrode voltage-clamp recordings and iontophoresis techniques were applied in this dissertation to examine effects of MeHg on synaptic transmission in both hippocampal and cerebellar slices of rat brain.

D. Specific aims.

The general objective of this dissertation is to characterize *in vitro* acute effects of MeHg on central synaptic transmission in brain slices, to explore the potential mechanisms underlying these effects and, to collect basic information for future design of studies of the subchronic and chronic effects of MeHg on the CNS. Specifically, the questions to be asked in this dissertation are:

- (1). Does MeHg affect neuronal membrane excitability or alter the threshold for neuronal excitation?
- (2). Are the mechanisms responsible for effects of MeHg on synaptic transmission in a given region of brain slices pre- or postsynaptic?
- (3). Does MeHg also affect inhibitory synaptic transmission in addition to its effect on excitatory synaptic transmission?

- (4). Are effects of MeHg on synaptic transmission in hippocampal and cerebellar slices similar?
- (5). Are effects of MeHg on central synaptic transmission similar to those of MeHg on peripheral somatic synaptic transmission?

To answer these questions, hippocampal and cerebellar slices prepared freshly from rat brain were used as the central synaptic circuit model in this dissertation.

CHAPTER TWO

THE PREPARATION AND USE OF BRAIN SLICES FOR ELECTROPHYSIOLOGICAL STUDIES OF CENTRAL SYNAPTIC TRANSMISSION

Central synaptic transmission can be studied in freshly isolated brain slice preparations (Lynch, 1980; Schwartzkroin, 1981; Langmoen and Anderson, 1981; Alger et al., 1984; Johnston and Brown, 1984; Teyler, 1986). Since its introduction in the 1920s, especially after the 1970s, the in vitro brain slice technique has been widely used in electrophysiological, morphological, biochemical, and pharmacological studies. This is because it offers several major technical advantages over in vitro invertebrate model, cell culture, whole brain in situ, and in vivo methods for the investigation of mammalian CNS neurobiology and neurophysiology.

A. The advantages of in vitro brain slice techniques.

First, the brain slice provides simple and precise control over experimental conditions such as pH, temperature and concentrations of tested chemicals, compared to the variables that must be controlled in in vivo studies. There is no blood pressure to monitor, no expired CO₂ concentration to maintain, no heart rate to stabilize and no anesthetics, paralytics or foreign agents need be used in slice preparations from small animals and during experiments.

Second, the brain slice preparation provides direct visual control over the placement of both recording and stimulating electrodes in the desired sites, avoiding the hazards and ambiguities of stereotaxic techniques. The neurons being targeted can be located, identified, and accessed easily. Third, in contrast to most cell culture systems, the normal anatomical relationships and synaptic circuits remain intact and healthy in a properly-oriented brain slice. This is of particular advantage in a laminated structure such as the hippocampus and cerebellar cortex.

Fourth, the brain slice greatly improves the stability of electrophysiological recording. There are no mechanical disturbances caused by heart beat and respiration. Therefore, it is possible to make high-quality, long-lasting intracellular recordings from neurons in isolated brain slices with relative ease.

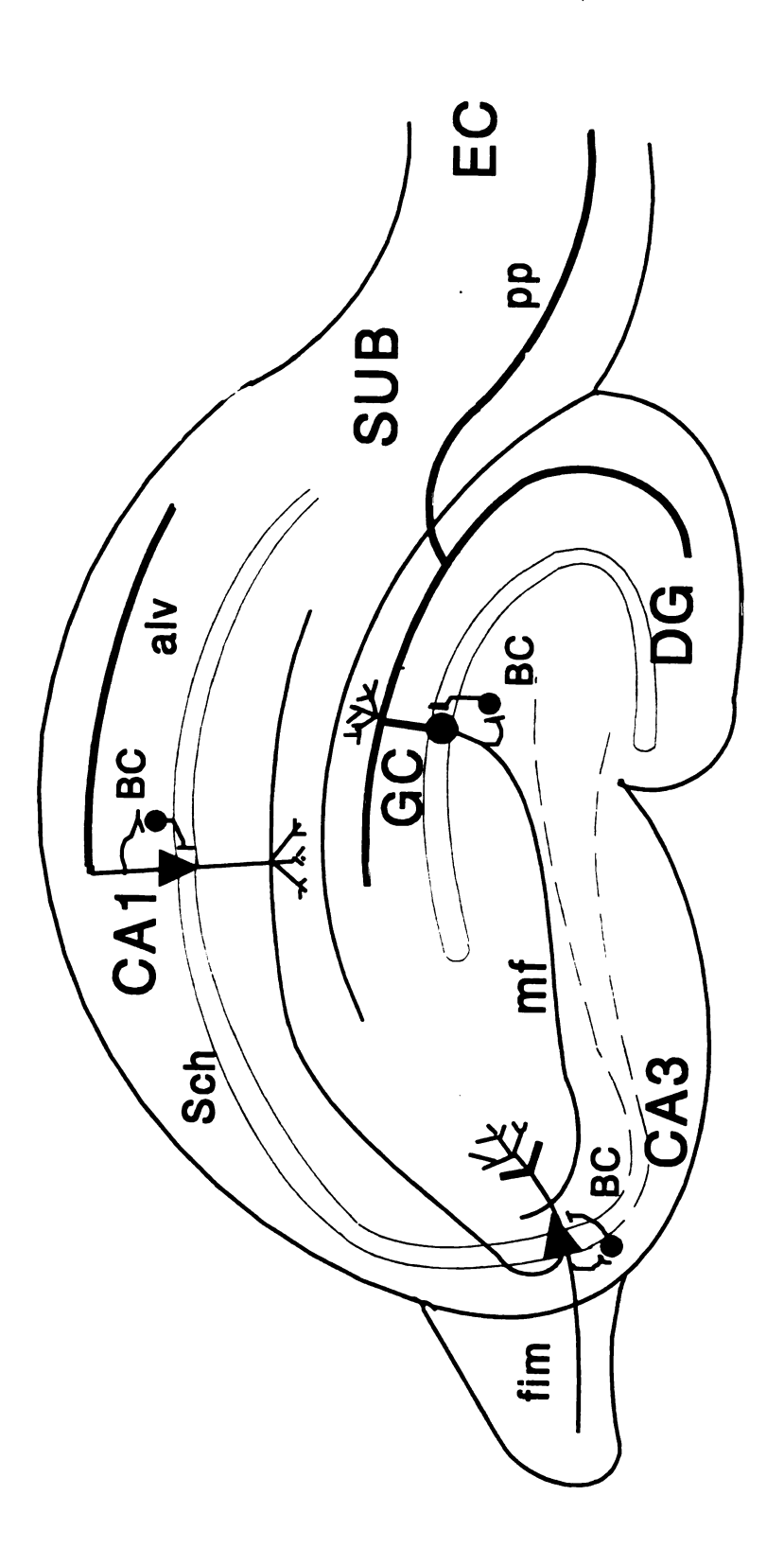
Fifth, both side hippocampi from one animal can be sectioned into 5 to 10 slices. Thus, one animal is possibly used to do several experiments with different objectives such as concentration-dependent effects.

In short, the *in vitro* brain slice technique combines many of the technical advantages of whole brain *in situ* and cell culture simplicity with normal complex organization of mammalian CNS tissue, and has greatly facilitate our investigation of the electrical properties and function of neurons in the CNS. Use of the brain slice has also greatly increased our knowledge of the effects of many neurotoxic chemicals on the mammalian CNS in the last decade. The brain slices can be made from almost any region of the brain. In this dissertation, both rat hippocampal and cerebellar slices were used as model central synapses to examine *in vitro* acute effects of MeHg on central synaptic transmission.

B. The organization of neurons and synaptic circuits of the hippocampal slice.

The hippocampal slice preparation has been the most commonly-used model for studying central synaptic function, due to (1) its relatively simple organization of a few major types of cells (pyramidal, granule and basket cells) with well-characterized synaptic pathways; (2) the entire hippocampus can be easily removed from the brain with a minimum of manipulation, while its size is optimal for slice preparation with very simple equipment, and hippocampal slice is easy to prepare and maintain; (3) the layers of pyramidal and granule cell bodies and several important fiber tracts (perforant path, mossy fibers, the commissural-Schaffer collaterals and alveus) can be easily discerned with a dissecting microscope; (4) most of the major intrinsic and extrinsic hippocampal fiber systems are organized according to a "lamellar" plane in which they travel at right angles to the longitudinal axis of the structure (Figure 2.1). Thus, a transverse hippocampal slice (see "Preparation of hippocampal slices") will contain a variety of projections whose axons extend for some distance along that cross section that are amenable to the study of several different synaptic circuits in a single slice. In addition, interest in hippocampal slice is also due to the fact that the hippocampus plays an important role in certain aspects of learning and memory and is a target of some degenerative disorders such as Alzheimer's disease and many neurotoxic agents (Walsh and Emerich, 1988).

Figure 2.1. Schematic diagram of structure and intrinsic synaptic circuits of a transverse hippocampal slice. Abbreviations: EC, entorhinal cortex; SUB, subiculum; pp, perforant path; DG, dentate gyrus; GC, granule cell; BC, basket cell; mf, mossy fiber; CA3, pyramidal cell in CA3 region; fim, fimbria; Sch, Schaffer collaterals; CA1, pyramidal cell in CA1 region; alv, alveus.



The organization of neurons and synaptic connections in the transverse hippocampal slice are relatively simple (Dingledine, 1984; Franck et al., 1989; Brown and Zador, 1990; Kennedy and Marder, 1992). It is composed of two sheets of two principal neurons that are highly interconnected with each other. The first sheet consists of three contiguous areas of cortex-CA fields (Cornu Ammonis), the subicular complex, and the entorhinal cortex (Figure 2.1). The CA fields are composed of a large flap of tightly packed CA1-C4 pyramidal cells (CA2 and CA4 have rarely been used as designating terms; they are not substantially different from those pyramidal cells of CA1 and CA3 regions). The sizes of pyramidal cells become larger as they extend from the CA1 region to the CA3 region; in the CA3 region the pyramidal cell bodies condense into monolayer. The second sheet of neurons is the dentate gyrus, in which are small, round and highly packed granule cells.

The major input to hippocampus is the axons from neurons of the entorhinal cortex via the perforant pathway to make the first set of synapses on the dendritic trees of the granule cells in dentate gyrus (perfront pathway also projects to pyramidal cells in the CA field, not shown in Figure 2.1). The granule cells send axons, known as mossy fibers, to make the second set of synapses on the dendrites of CA3 pyramidal cells. One mossy fiber synaptically contacts a long row of CA3 pyramidal cells; the mossy fiber contacts are always near the base of the apical dendrites of the CA3 pyramidal cells. The CA3 pyramidal cells in turn send one axon branch to project out of

the hippocampus (principally to the septum), the other axon branches, known as Schaffer collaterals, extends to make the third set of synapses on the apical dendrites of CA1 pyramidal cells. These cells send axons, within the alveus, which is the major output from the hippocampal formation, to the subiculum and entorhinal cortex to complete the so-called **trisynaptic loop**. The principal putative excitatory transmitters in these intrinsic excitatory pathways are glutamate and/or aspartate (Table 2.1). In addition to these intrinsic excitatory synaptic pathways, intrinsic inhibitory pathways also exist between basket cells and granule cells or pyramidal cells. Anytime when granule cells or pyramidal cells are activated, their axons will in turn activate basket cells to release γ -aminobutyric acid (GABA) to act on GABA_A or GABA_B receptors on granule cells or pyramidal cells to cause so-called recurrent inhibition of granule cells or pyramidal cells via both pre- and postsynaptic mechanisms.

Table 2.1. Putative neurotransmitters in the major intrinsic pathways of hippocampus¹

Synapse	Transmitter	Receptor	Ionic effect
pp-GC ²	glutamate	Kainate/AMPA(?)	1 1G _{Na+,K+}
		NMDA (?)	$\uparrow G_{Ca2+}, \uparrow G_{Na+,K+}$
	Met, Leu-enkephalin(?)	(?)	(?)
mf-CA3	glutamate/aspartate	Kainate/AMPA	↑G _{Na+,K+}
		NMDA	$\uparrow G_{Ca2+}, \uparrow G_{Na+.K+}$
	Dynorphin (?)	(?)	(?)
Sch-CA1	glutamate/aspartate	Kainate/AMPA	↑ G _{Na+,K+}
		NMDA	$\uparrow G_{Ca2+}, \uparrow G_{Na+.K+}$
		mGluR	$\uparrow [Ca^{2+}]_i, \downarrow G_{K+}$
BC-GC	GABA	GABA _A	1G _{Cl} ⁺
		GABA _B	11G _{K+}
BC-CA3	GABA	GABA _A	↑G _{C1} +
		GABA _B	↑G _{K+}
BC-CA1	GABA	GABA _A	↑G _{CI} +
		GABA _B	11G _{K+}

¹. Based on references (Dingledine, 1984; Franck et al., 1988; Collingridge and Singer, 1990; Baskys, 1992; Sommer and Seeburg, 1992; Shirasaki et al., 1994; Nadler et al., 1994; Spuston and Sakmann, 1995).

² Abbreviations: pp-GC, perforant path-granule cell synapse; mf-CA3, mossy fiber-CA3 pyramidal cell synapse; Sch-CA1, Schaffer collaterals-CA1 pyramidal cell synapse; BC-GC, basket cell-granule cell synapse; BC-CA3, basket cell-CA3 pyramidal cell synapse; BC-CA1, basket cell-CA1 synapse; AMPA, α-amino-3-hydroxy-5-methyl-4-isoxzoleproprionic acid; NMDA, N-methyle-D-aspartate; mGluR, metabotropic glutamate receptor; G_X , ionic conductance; $[Ca^{2+}]_i$, intracellular Ca^{2+} concentration.

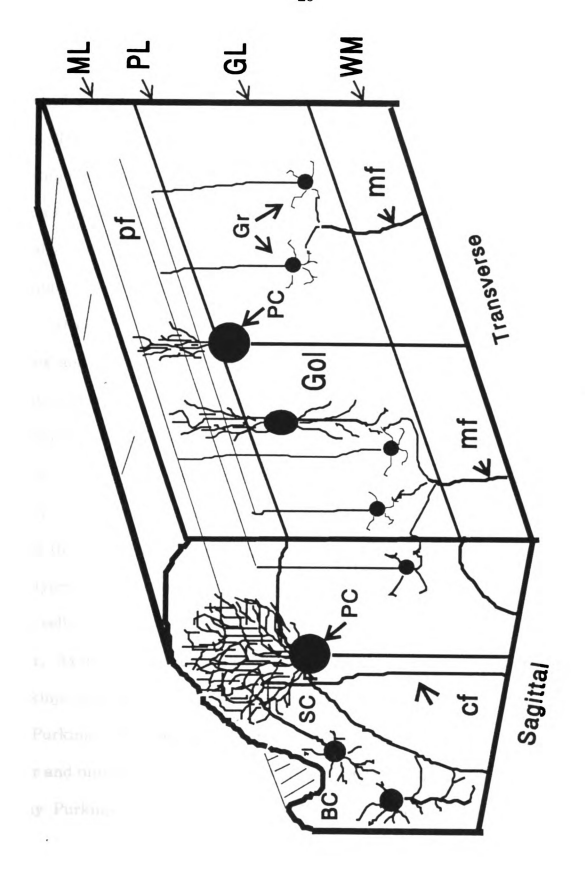
C. The organization of neurons and synaptic circuits of cerebellar slices.

The cerebellum is an outgrowth of the pons and consists of a three-layered cortex overlying deep nuclear groups of cells. Structurally, the cerebellum consists of (1) a superficial gray mantle, the cerebellar cortex; (2) an internal white mass, the medullary substance; and (3) four pairs of intrinsic nuclei (dentate nucleus, globose nucleus, emboliform nucleus and fastigial nucleus) embedded in the white matter. The cerebellum is divided into a median portion-the cerebellar vermis, and two lateral lobes-the cerebellar hemispheres (Anderson, 1989; Shepherd, 1990; Carpenter, 1991; Nicholls et al., 1992). The cerebellar cortex receives two major sets of afferent, the climbing and the mossy fibers, and generates a single output system, the axons of Purkinje cells. The cerebellar nuclei receive collaterals from the climbing and mossy fibers and are the main targets for the Purkinje cell axons.

The cerebellar cortex is uniformly structured in all parts and is composed of three layers containing five major different types of neurons. These layers from the deepest to the surface are (1) the granular layer, (2) the Purkinje cell layer, and (3) the molecular layer (Figure 2.2).

The granular layer is the thickest and deepest, lying adjacent to the white matter. This layer is tightly packed with **granule** cells (estimated number between 10¹⁰ and 10¹¹ cells in human brain), which are round or oval and 5 - 8 µm in diameter. Each granule cell has four or five short dendrites.

Figure 2.2. Schematic diagram of organization of neurons and synaptic circuits of the transverse and sagittal cerebellar slices. Abbreviations: BC, basket cell, cf, climbing fiber; Gol, Golgi cell; GL, granular layer; Gr, granule cell; mf, mossy fiber; ML, molecular layer; PC, Purkinje cell; pf, parallel fiber; PL, Purkinje cell layer; SC, stellate cell; WM, white matter.



Granule cells send their unmyelinated axons outward to the molecular layer to form Parallel Fibers, which run throughout the molecular layer and are oriented perpendicular to the sagittal fan-shaped dendrites of the Purkinje cells. The synaptic contacts between the parallel fibers and the dendrites of Purkinje cells are called the "cross-over" synapses. The dendrites of a typical human Purkinje cell may make as many as 200,000 synaptic contacts with parallel fiber afferents. Also in this layer, mainly in the upper parts of the granular layer, are larger (9-16 µm in diameter) and less numerous Golgi cells. Dendrites of these cells extend throughout all layers of the cerebellar cortex and are contacted by parallel fibers in the molecular layer and by climbing and mossy fiber collaterals in the granular layer. Axons of Golgi cells terminate on granule cell dendrites within the cerebellar glomeruli and release GABA as their major neurotransmitter. The outermost layer, the molecular layer, is made up primarily of the parallel fibers (bifurcating axons of granule cells), the dendrites of cells (Purkinje cells and Golgi cells) in deeper layer and two types of interneuron (outer stellate cells and basket cells). Dendrites of both cells and axons of the outer stellate cells are confined to the molecular layer. Axons of outer stellate cells make synaptic contacts with dendrites of Purkinje cells. Basket cells, located in deep parts of the molecular layer near the Purkinje cell bodies, give rise to dendrites that ascend into the molecular layer and unmyelinated axons that form synaptic contacts with the somata of many Purkinje cells. Both outer stellate cells and basket cells provide

inhibitory inputs to Purkinje cells. Separating the granular and the molecular layers is the **Purkinje** cell layer. The dendrites of Purkinje cells extend toward the cortical surface and divide into an elaborate dendritic tree within the molecular layer. The dendritic tree of Purkinje cells branches profusely, but it does so primarily in a single plane perpendicular to the long axis of the folium and thus to the course of the parallel fibers passing though it. The axons of Purkinje cells are the only output that leaves the cerebellar cortex. Purkinje cell axons are myelinated, pass though the granular layer and white matter, and make synaptic contacts with the deep cerebellar nuclei. Most Purkinje cells contain GABA as their principal neurotransmitter to modulate activity of the deep cerebellar nuclei.

The major inputs to the cerebellar cortex are the Mossy Fibers and Climbing Fibers. The mossy fibers originate from many sources, including the cerebral cortex via the cortico-ponto-cerebellar pathway, the vestibular sense organs via the vestibular nuclei and vestibulocerebellar tracts, spinal cord and the reticular formation. Mossy fibers branch when they enter the cerebellum and send axon collaterals both to the deep cerebellar nuclei and to the cerebellar cortex. In the cerebellar cortex, mossy fibers lose their myelin sheath and form excitatory synaptic connections with granule and Golgi cells. The dendrites of granule cells constitute the postsynaptic element. Golgi cells function as a negative feedback to the mossy fiber-granule cell relay. The mossy fibers constitute the principal mode of termination of most cerebellar

afferent systems. No candidates have been clearly identified as the neurotransmitter released from the mossy fibers (Shepherd, 1990). However, recent evidence indicates that glutamate may be at least one of the neurotransmitters released from the mossy fibers (Garthwaite and Brodbelt, 1989; Traynelis et al., 1993; D'Angelo et al., 1995; Silver et al., 1996). The second major input to the cerebellum is the climbing fibers that arise in the contralateral inferior olive nucleus of the medulla. The main inputs to the inferior olive are from the spinal cord, the brainstem, the cerebellar nuclei and the motor cortex. The climbing fibers pass through the granular and Purkinje cell layers and make excitatory synaptic contacts directly with Purkinje cell dendrites as they ascend in the molecular layer. A single Purkinje cell receives terminals from only one climbing fiber axon. However, a given inferior olivary cell axon may branch to form several climbing fibers and each climbing fiber can make as many as 200 synapses with each Purkinje cell. Stimulation of a group of climbing fibers produces a powerful excitation of Purkinje cells. When a climbing fiber discharges, the Purkinje cell also discharges. stimulation of climbing fibers not only excites Purkinje cells, but also excites a number of Golgi cells, which then inhibit granule cells and the inputs from the mossy fibers to granule cells. By this feedforward inhibition, when climbing fibers fire, their targeted Purkinje cells are dominated by these climbing fiber inputs. In short, in cerebellar cortex, a single Purkinje neuron receives two major excitatory inputs: mossy fiber-parallel fiber-Purkinje cell pathway and climbing-Purkinje cell pathway. The mossy fibers presumably release glutamate and/or other transmitter to excite granule cells, and in turn the axons (parallel fibers) of granule cells release glutamate as their principal transmitter to excite Purkinje cells. Simultaneously, parallel fibers also activate the outer stellate and basket cells, which in turn modulate Purkinje cell excitability, and Golgi cells to produce feedback inhibition of granule cells. The climbing fibers presumably release glutamate/aspartate as their transmitter to excite Purkinje cells. Unlike the majority of neurons, the Purkinje cells generate two types of responses to these two excitatory synaptic inputs (Anderson, 1989; Shepherd, 1990). One is a simple, single-peaked action potential, the simple spike or somatic spike, and the other is a multipeaked action potential, the complex spike or dendritic spike. It has been shown that the simple spikes are produced by activation of the mossy fiber-granule cell-parallel fiber pathway, whereas complex spikes are produced by activation of climbing fibers. The complex and simple spikes result from voltage-gated Ca2+ and Na+ channels that are distributed along different parts of the cell membrane. In cerebellar slice, it has been shown that action potentials generated in the soma-initial segment region are Na⁺-dependent (Llinás and Sugimori, 1980a; Anderson, 1989, Shepherd, 1990; Stuart and Häusser, 1994) and are blocked by tetrodotoxin (TTX), whereas those generated in the dendrites are Ca2+-dependent and resistant to TTX (Llinás and Hess, 1976; Llinás and Sugimori, 1980a,b; Kimura et al., 1985; Ross and Werman, 1987; Llinás and Walton, 1990). Climbing fibers produce a large, synchronous depolarization of the dendrites, thus they activate the dendritic Ca2+ channels and initiate action potentials there to generate the complex spikes. Parallel fibers, however, each produce a small synaptic current that must sum at the initial segment to produce an action potential. consequence, parallel fiber input leads to Na⁺-dependent simple spikes whose frequency is graded as a function of the summed synaptic current from many parallel fiber synapses. However, a recent study showed that TTX-sensitive Na⁺ channels are also present in Purkinje cell dendrites at a density high enough to produce Na⁺ action potentials and synaptic inputs to the dendrites via either parallel fibers or climbing fibers can elicit Na⁺ action potentials in these dendrites (Regehr et al., 1992). On the other hand, studies also showed that in Purkinje cells, even single synaptic climbing fiber-mediated responses produce spike-like increases in [Ca2+], not only in dendrites but also in a narrow somatic submembrane shell (Ellers et al., 1995). The sole output of cerebellar cortex is the axon of Purkinje cell, which projects on the deep nuclei to modulate ongoing activity of these nuclei.

D. Preparation of brain slices.

1) Preparation of hippocampal slices.

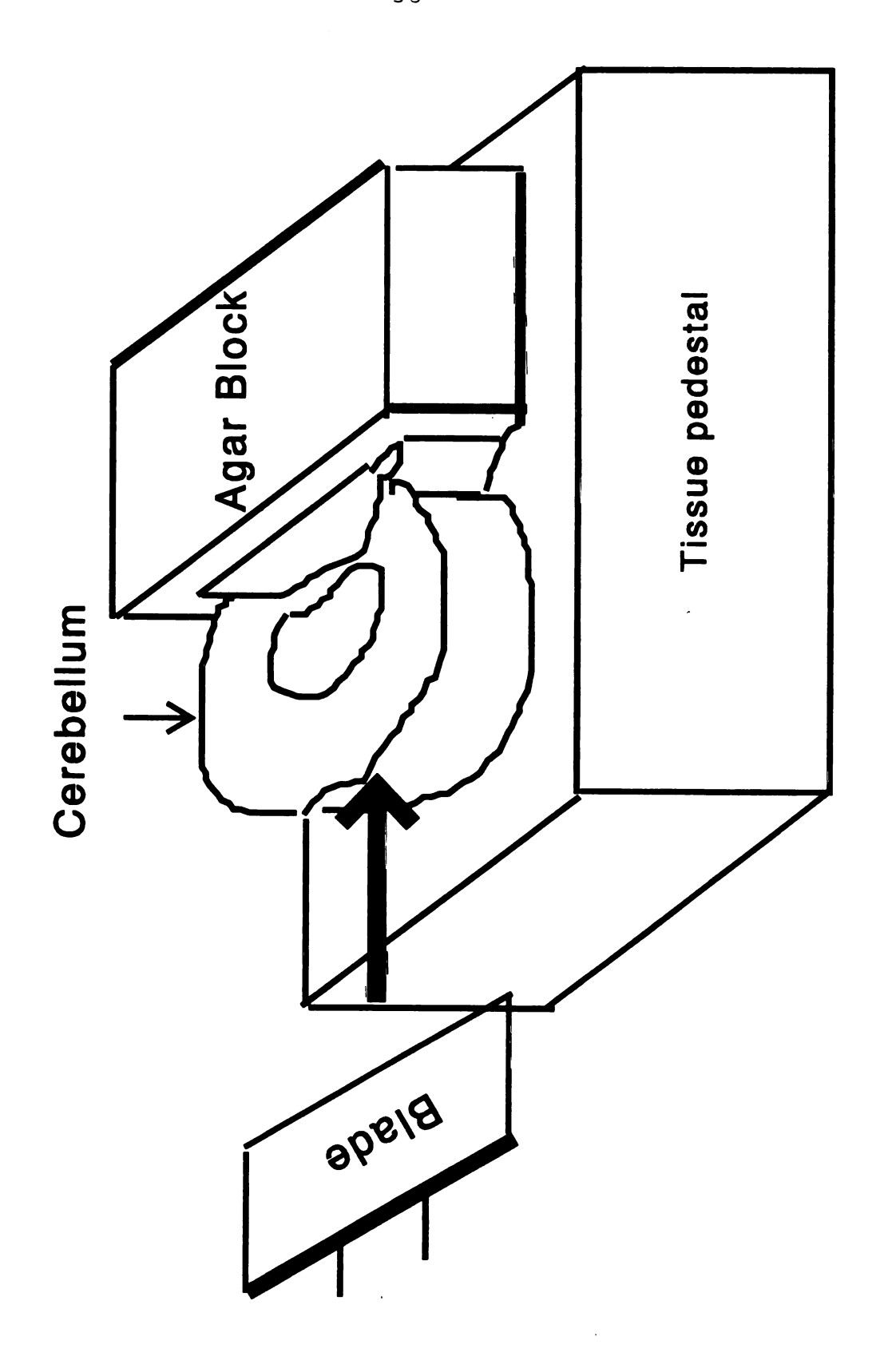
Hippocampi of both sides are isolated quickly from brains of male Sprague-Dawley rats (180-220 g) after decapitation. One hippocampus is then placed on the platform of the tissue chopper and sectioned transversely to the longitudinal axis of hippocampus to slices of approximately 400 μm thickness using methods described by Teyler (1980). Slices were transferred immediately to a recording chamber, where they were superfused continuously with oxygenated ACSF. The composition of ACSF (in mM): NaCl, 124; KCl, 5; MgSO₄, 2; KH₂PO₄, 1.25; NaHCO₃, 26; CaCl₂, 2 and D-glucose, 20. The pH of ACSF was adjusted to 7.4 using HCl after solution was bubbled with 95% O₂-5% CO₂ for 15-30 min. A humidified gas mixture of 95% O₂/5% CO₂ was circulated over the slices by bubbling in water. Slices were incubated in the recording chamber for at least 60 min before electrophysiological recording began.

2) Preparation of cerebellar slices.

Cerebellar slices were prepared using methods modified slightly from those of Llinás and Sugimori (1980a); Crepel et al. (1981); Kimura et al. (1985); Edwards, et al., 1989; Konnerth et al. (1990); Llano et al. (1991); Momiyama and Takahashi (1994) and Mintz et al. (1995). In general, the process of preparation of cerebellar slices is similar to that of preparation of hippocampal slices. In brief, the cerebellum was removed quickly from the brain of Sprague-Dawley rat (15 - 20 days postnatal) and immersed immediately in cold oxygenated modified ACSF, containing 125 mM NaCl; 2.5 mM KCl; 1 mM MgCl₂; 1.25 mM KH₂PO₄; 26 mM NaHCO₃; 2 mM CaCl₂ and 20 mM D-glucose

(pH 7.4) for 1 - 3 min. A portion of vermis (for sagittal slices), isolated by two sagittal cuts, or the whole cerebellum (for transverse slices) was glued on the tissue pedestal of an OTS-3000-05 Automatic Oscillating Slicer (FHC, Brunswick, ME 04011) with cyanoacrylate glue. The tissue block was then transected either sagittally or transversely depending on the purpose of an individual experiments (Figure 2.3). The thickness of cerebellar slices was about 300-350 µm for conventional extracellular and intracellular recording. Sometimes, 200 µm sagittal slices were used for the purpose of identifying whether or not the parallel fiber-Purkinje cell pathway contaminated recordings of effects of MeHg on responses of climbing fiber-Purkinje cell synaptic transmission. One cerebellar slice was transferred to the recording chamber and the remaining slices were incubated in a holding chamber for later use. The entire process from decapitating the rat to transferring the slices into the recording or holding chamber was usually finished in less than 10 min and under 4 °C. The slice in the recording chamber was incubated and superfused (1 - 1.2 ml/min) continuously with modified ACSF saturated with $95\%~O_2~/5\%~CO_2$ for at least 60~min before electrophysiological recordings begin.

Figure 2.3. Diagrammatic depiction of arrangement of the agar and cerebellar tissue blocks on the tissue pedestal of an oscillatory slicer. A cerebellar tissue block is glued on the pedestal with cyanoacrylate glue (Supper glue). The blade is positioned at a 10° angle. The tissue is cut with a very slow advancement speed and a very high vibration rate without distorting the tissue during slicing.



E. Methods for electrophysiological studies of synaptic transmission in brain slices.

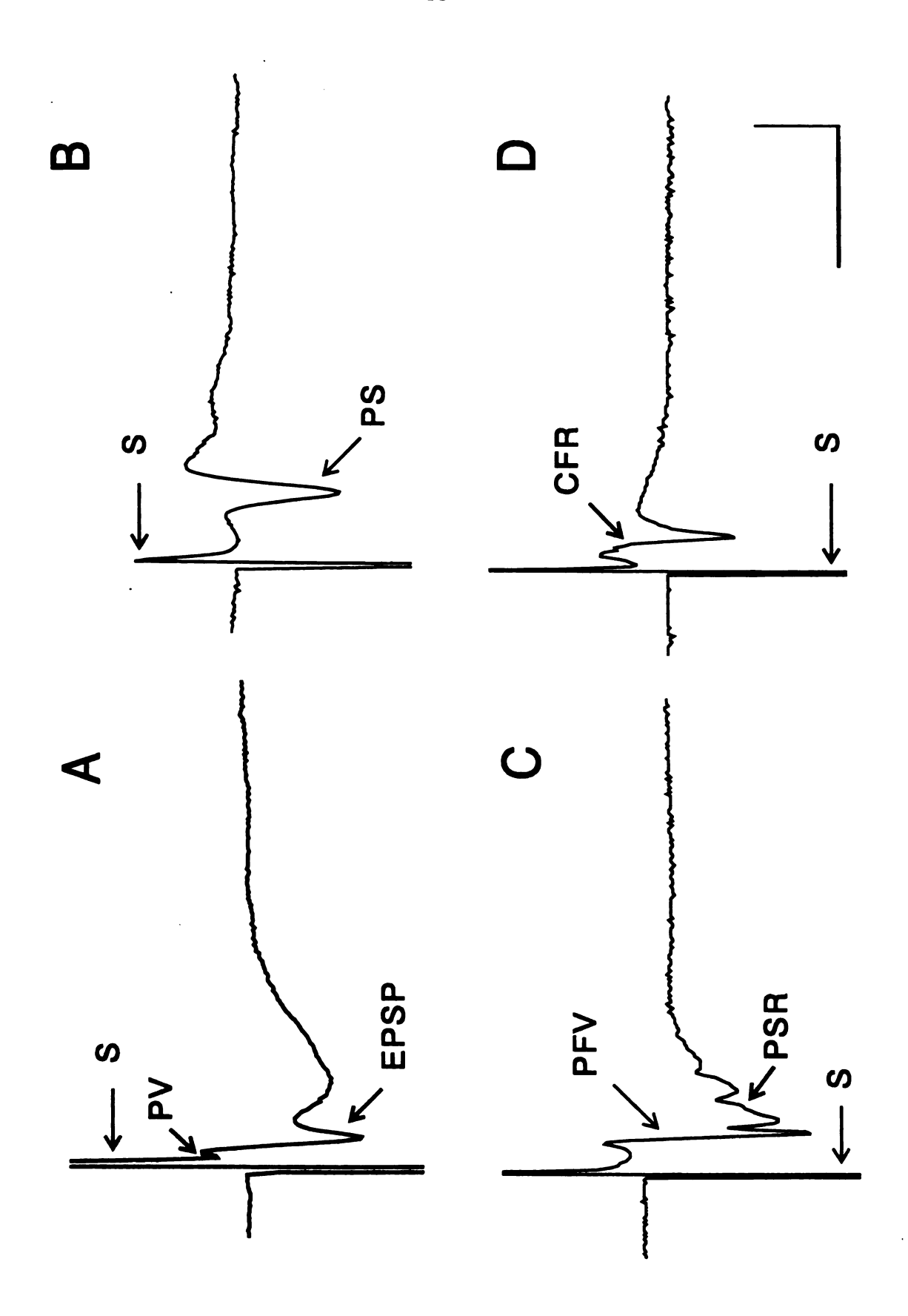
Electrical stimulation of neurons usually generates two main types of signals that are either gradual changes in the membrane potentials (EPSPs) or all-or-none spikes (action potentials). These electrical signals can be recorded by placing a recording electrode close to a cell or a cell population (extracellular recording) or by penetrating the cell membrane with a sharp fluid-filled glass electrode (intracellular recording) or by forming gigaohm seal of a fire-polished fluid-filled glass electrode onto the plasma membrane of an intact cell and subsequently rupturing the membrane to gain access to the cell interior (whole-cell patch-clamp recording). Each of these recording techniques has been successfully applied to the brain slice preparations (Műller, 1992; Henderson, 1993).

1) Extracellular recording.

Extracellular recording refers to recording potential change across cell membrane without penetrating the cell with a microelectrode. The extracellular signal is generated due to (1) the conductance or resistance of the extracellular fluid is not zero; (2) a cell whose membrane potential is changed non-uniformly so that one part of the membrane is depolarized more than another will have current flow within it. Corresponding to the intracellular current, there is certainly a flow of current in the extracellular media to

complete the current path. The extracellular current is then can be picked up with an extracellular recording electrode. In general, extracellular signals are very small and therefore require extensive amplification. Since the signals recorded by extracellular recording electrodes are responses of a single neuron or population of neurons, larger responses can be generated only when the firing of many neighboring neurons is highly synchronized and the dipole orientation of these cells is uniform. The responses of extracellular recording are referred to as field potentials or population spikes. The amplitude of population spikes is proportional to the number of neurons firing. Usually, extracellular recording electrodes can pick up several signal components, these indicate the presynaptic volley corresponding to afferent spike activity. summed fEPSPs, and population spikes. The shape and polarity of field potentials in a given slice structure may vary depending on the location of the recording electrodes. Extracellular recording may sometimes be sufficient to answer general questions about effects of chemicals on synaptic transmission in brain slices, depending on the aims of the experiments. For these experiments, borosilicated glass microelectrodes having impedances of 5 - 10 MΩ when filled with either ACSF or 3 - 4 M NaCl (K⁺ is avoid to prevent nerve depolarization) are generally used as extracellular recording electrodes. A bipolar or monopolar tungsten electrode is used as the stimulating electrode. The activity of pyramidal cells in the cortical structure is well suited for extracellular recording. In hippocampal slices, extracellular recordings can be made in any regions of CA field or dentate gyrus. Figure 2.4A,B representatively demonstrates the fEPSPs and population spikes recorded from the apical dendritic and cell soma layers, respectively, of the CA1 pyramidal cells of hippocampal slice by stimulation of Schaffer collaterals. Extracellular recordings can be also made in the molecular layer of the cerebellar cortex to record activities of parallel fiber-Purkinje cell synapses or climbing fiber-Purkinje cell synapses (Figure 2.4C,D). The major advantage of extracellular recording is that it is relatively easy to make stable recordings of long duration. The main disadvantages of extracellular recording are (a) since the very weak extracellular signals require higher amplification, the noise levels will be also likely amplified. Therefore it is important to use low-impedance electrodes, a low-noise amplifier, and good shielding of the recording system; (b) the technique cannot provide information of changes in some specific responses such as resting membrane potentials and input resistance; and (c) it is nearly impossible to compare amplitudes of field potentials from different experiments, because the overall amplitudes of responses are influenced by the location of recording electrode. Amplitudes of population spikes may vary greatly in different slices of the same animals, in different locations of recording electrodes in the same slice or even in the same region of the same slice but with different depths of the electrode tips in tissue.

Figure 2.4. Representative demonstration of the field potentials recorded from the CA1 region of a (A) prevolley (PV) and field excitatory postsynaptic potential (fEPSP) are recorded from the dendritic region of CA1 pyramidal cells of the hippocampal slice by stimulating the Schaffer collaterals. (B) The population spike (PS) is recorded from the CA1 pyramidal soma area of hippocampal slice by stimulating the Schaffer collaterals. (C) The parallel fiber volley (PFV) and postsynaptic response (PSR) are recorded from the molecular layer by stimulation of parallel fibers. (D) The climbing fiber response (CFR) is Artefacthippocampal slice and the molecular layer of a cerebellar slice using extracellular recording techniques. stimulus artefact. Calibration bars: vertical, 5 mV for A,B and 2.5 mV for C,D; horizontal, 10 ms. recorded from the molecular layer by stimulation of the6 climbing fibers in white matter.



2) Intracellular recording.

Unlike extracellular recording, an intracellular recording electrode penetrates the cell membrane to measure transmembrane potential response of a single neuron. Therefore it is possible to measure changes in the electrical behavior including resting membrane potentials, input resistance, whole cell capacitance and action potentials of individual neurons. It is also possible to do quantal analysis of synaptic transmission, estimate the reversal potentials of a synaptic response and identify if a given chemical affects functions of the presynaptic nerve terminals. Moreover, equipped with a bridge circuit in the intracellular recording amplifier, one can inject DC current into cell through the same recording electrode to change the resting membrane potentials or directly excite the targeted cell. This allows me to analyze the site and mechanism of action of a given chemical on individual neurons. The electrodes used for intracellular recording usually are sharp with impedance of 60 - 120 $M\Omega$ when filled with 3 M potassium acetate (Cl is avoid to prevent diffusion of large amount of Cl into cell). In my experiments, the impedances of recording electrodes were 80 - 120 and 60 - 80 M Ω , respectively, for the pyramidal cells in the CA1 region of hippocampal slices and for Purkinje cells in cerebellar slices. The disadvantages of intracellular recording are (a) it is difficult to obtain a proper cell penetration and maintain it for a long duration in the small neurons; (b) before penetration of a cell, even during recording, the bridge balance and electrode capacitance must be properly adjusted and compensated, otherwise all measurements will be inaccurate; (c) resting membrane potentials are influenced by the electrode tip potentials, and the tip potentials are influenced by the ionic microenvironment, which can be changed after penetration of a cell or by test chemicals. Thus, an exact measurement of the true membrane potential may not be possible, and (d) penetration of cell may cause some damage to the cell membrane and hence lead to an unstable recording. Figure 2.5 representatively shows EPSPs and action potentials recorded from a CA1 pyramidal cell of a hippocampal slice (A, B and C) and from two Purkinje cells of a transverse (D) and a sagittal cerebellar slices (E and F).

3) Sharp single-electrode voltage-clamp (sSEVC) recording.

Similar to the conventional intracellular recording or current-clamp recording, the sSEVC recording also uses a sharp microelectrode to penetrate the cell membrane. However, the response recorded from individual neurons by sSEVC recording is current instead of voltage. In sSEVC the single intracellular microelectrode functions as both the voltage-recording and current-passing electrode, usually with a duty cycle of 70% voltage recording and 30% current passing, *i.e.* the two functions are time-shared and do not interact (Figure 2.6). The success of a sSEVC recording depends on several factors. First, the electrode resistance for sSEVC recording should be as low as possible, but it should not sacrifice the consistency of successful intracellular penetrations. Second, the capacitance neutralization should be

Representative example of responses recorded from individual CA1 pyramidal cells of a The excitatory postsynaptic potential (EPSP) is recorded from a CA1 pyramidal cell soma by stimulation (C) this AP is recorded from a CA1 pyramidal cell soma by injection of depolarizing current through the activated action potential occurs prior to the CF-EPSP or "complex spikes". (F) repetitive firing of Purkinje cell is evoked by injection of depolarizing current at the Purkinje cell soma. S in each trace is recorded from a CA1 pyramidal cell soma by a suprathreshold stimulation of the Schaffer collaterals. (E) The climbing fiber EPSP (CF-EPSP) is recorded from a Purkinje cell soma by stimulation of the indicates the stimulus artefact. Calibration bars: vertical, 5mV for A and 20 Mv for B-F, horizontal, 20 of Schaffer collaterals at a level that does not generate action potentials. (B) The action potential (AP) recording electrode. (D) The parallel fiber EPSP (PF-EPSP) is recorded from a Purkinje cell soma by stimulation of the parallel fibers at the surface of the molecular layer in a transverse cerebellar slice. Note that a single antidromicallyhippocampal slice and Purkinje cells of a cerebellar slice using intracellular recording techniques. climbing fibers in the white matter in a sagittal cerebellar slice. ms for A-E and 100 ms for F. Figure 2.5.

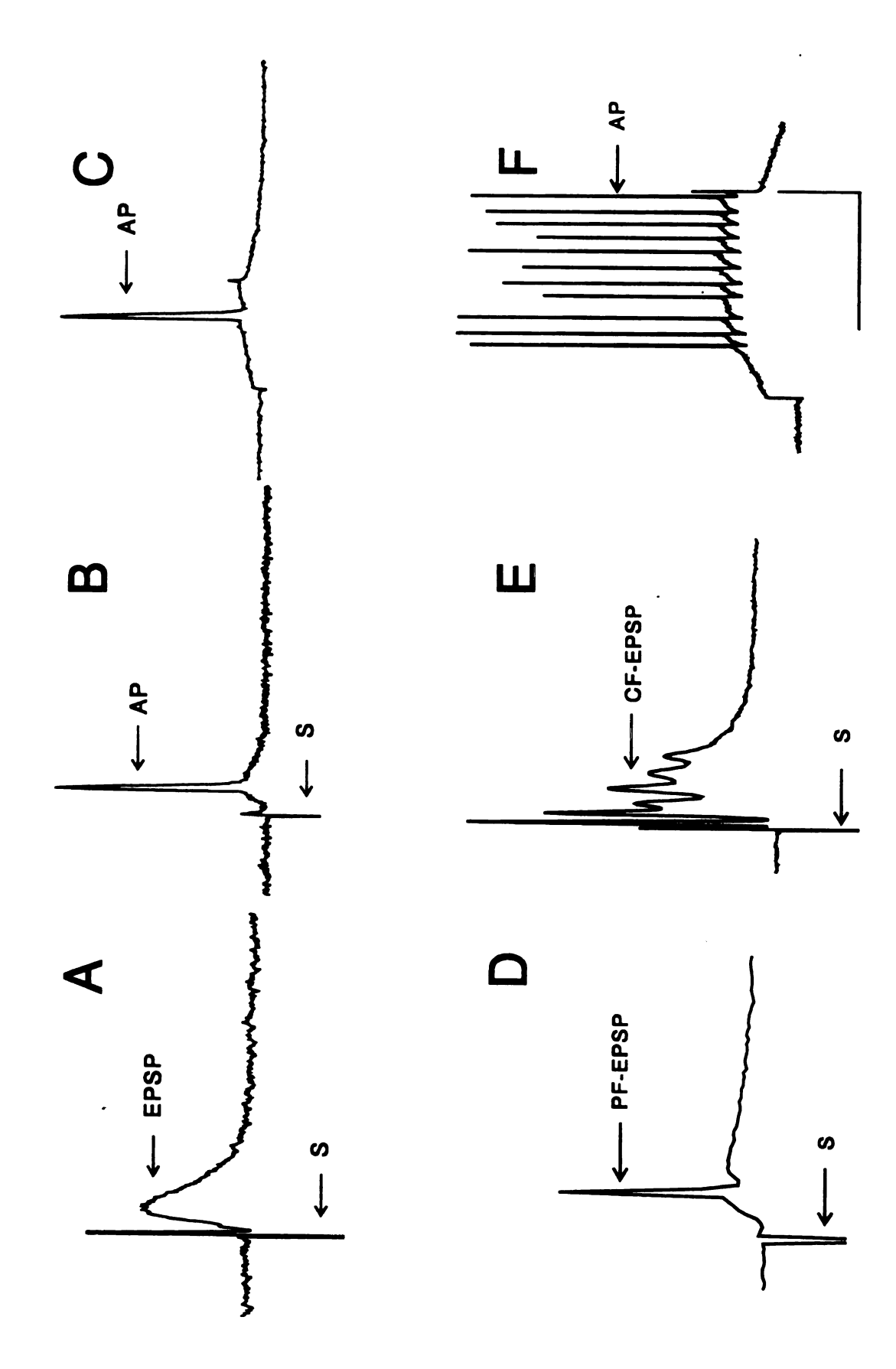
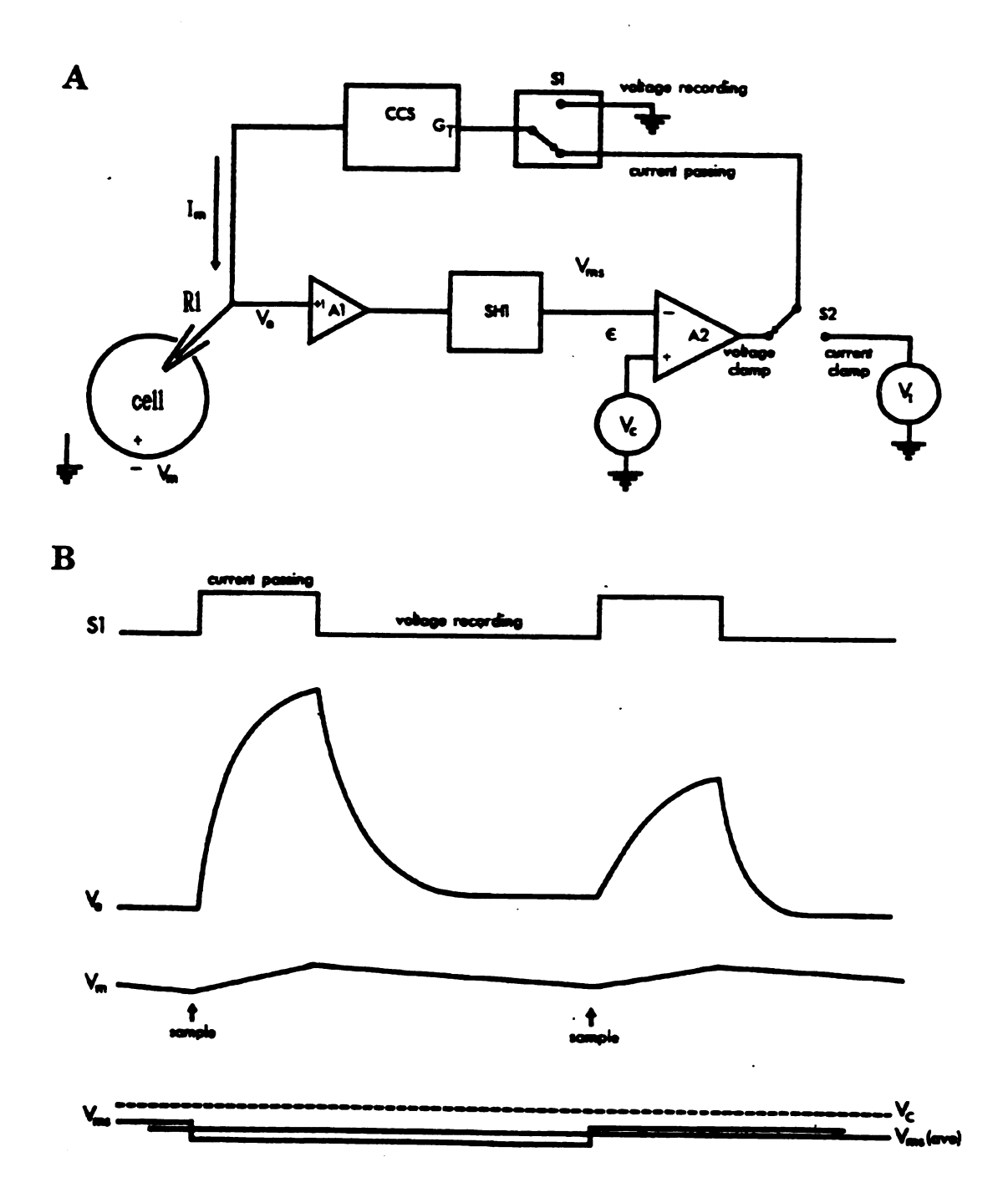


Figure 2.6. Schematic diagram of the principle of sharp single-electrode voltage clamp technique. Top circuit: A recording microelectrode (R1) penetrates the cell (Cell). Voltage (Va) recorded by R1 is buffered by a unitary gain headstage (A1). Ve is the sum of the membrane potential (V_m) and the voltage drop developed on the R1 resistance and capacitance by the applied current. A sample-and-hold circuit (SH1) sample V_e at the times indicated by the arrows and hold the values (V_{ms}) for the rest of the cycle. The sampled potential is compared with the command potential (V_c) in a differential amplifier (A2). The putput of this amplifer becomes the input of a controlled current source (CCS) if the switch (S1) is in the current pasing position. This circuit has a transconductance G_T and it injects a current I_m into the R1 which is directly proportional to the voltage at the input of the CCS irrespective of the R1 resistance. Bottom: diagrammatc illustration of the period of applied current injection. S1 is shown in the current-passing position during which a square pulse of current is injected into R1. The rate of rise of the electrode voltage is determined by the R1 resistance, the R1 capacitance, and the A1 input capacitance. S1 then switchs to the voltage recording position (input to CCS is 0 V). I_m become zero and V_e decays passively. The V_e decays towards zero with a time constant determined by R1 resistance and total parasitic capacitance, while V_m decays towards ist resting level with a time constant determined by the neuronal membrane. Sufficient time must be allowed for V_e to reach within a millivolt or less of V_{ms} . This requires the R1 time constant to be at least an order of magnitude smaller than the cell time constant. At the end of the voltage recording period a new sample of V_m is taken and a new cycle begins. (Modified from Redman, 1992).



properly adjusted to ensure that the microelectrode voltage decays to membrane potentials within the time allotted in each cycle for passive recording. Third, the sampling frequencies should be as high as possible in order to maintain stable sSEVC recording. If the sampling frequency is too low, the sSEVC recording will be unstable due to that long periods of current passing between sample allows the membrane potential to overshoot the command potential to result in larger error signals and larger currents with each cycle. In addition, the gain and the anti-aliasing filter of voltage-clamp circuit should be also adjusted properly. Compared with the conventional intracellular recording or current-clamp, the sSEVC does not have the problem of non-linear summation of the postsynaptic responses to neurotransmitter. Normally, as the stimulus intensity applied to the presynaptic fibers is increased, the amounts of transmitter release are increased. In current-clamp, however, the amount of potential changes evoked in the postsynaptic neurons do not increase linearly with the amounts of transmitter changes; as the potential changes in response to the transmitter release, it moves towards the equilibrium potentials for the response and thus reduces the driving force for subsequent potential change as transmitter release increases. In voltageclamp mode, the current flow through the membrane is measured in response to neurotransmitter under conditions in which the membrane potential and thus the driving force are held constant completely. Compared with the twoelectrode voltage-clamp technique, which is somewhat impractical for using in brain slices due to the small size of most CNS neurons and the difficulty in visualizing individual cell bodies in brain slices, sSEVC recordings can be applied to any neurons that are suitable for conventional intracellular recordings. Compared with the whole-cell patch recording, sSEVC has the major advantage of not suffering an error due to voltage drop across the electrode resistance. On the other hand, however, the sSEVC is much harder to set up than whole-cell patch recording and requires frequent fine-adjustment of the controls as the microelectrode resistance drifts. Also, you generally cannot clamp very fast responses or very large responses. In addition, the amount of noise in sSEVC is about two to three times greater than that in whole-cell patch-clamp recording.

4) Whole-cell patch recording.

The patch-clamp technique is one of the electrophysiological methods that allows to record macroscopic whole-cell or microscopic single-channel currents flowing cell membranes through ion channels, including voltage-gated, receptor-gated and second-messenger-activated channels. Generally, the patch-clamp technique refers to both voltage-clamp and current-clamp measurements using microelectrode with lower impedance (usually a few $M\Omega$) when filled with appropriate internal solutions. Voltage-clamp measurement refers to the technique that allows the investigators to study the voltage-dependence of ion channels by experimentally manipulating the voltage across the patch or whole cell membranes, while current-clamp measurement refers to the technique that

allows one to monitor membrane potential changes by experimentally controlling currents flowing across ion channels.

The patch-clamp recording technique has been widely used to study synaptic transmission in brain slices (Blanton et al., 1989; Edwards et al., 1989; Honnerth, 1990; Stuart, 1993; Blitzer and Landau, 1994; Sakmann and Stuart, 1995; Plant et al., 1995), because it offers many advantages by combing the brain-slice technique with the power of the patch-clamp techniques. Synaptic currents can be recorded in both relatively thick (individual cells not necessarily visualized) or thin (neuron cell soma or dendrites can be visualized with an upright microscope equipped with Nomaski optics) brain slices. To date, three main techniques have been developed for making whole-cell patchclamp recording in brain slices. The "cleaning" method was first introduced by Edwards et al., (1989). In this method, the surface tissue and cell debris over the targeted cells in the thin (150 - 200 µM) brain slices are first teased apart by gentle application of positive pressure to a broken tip pipette to eject a stream of bath solution and then removed by careful suction to exposure the targeted cell membrane. The second method is the so-called "blind" technique introduced by Blanton et al., (1989). This procedure is similar to that used for conventional intracellular recording in thick brain slices (400 - 500 µM) and no specific optics, physical cleaning or enzymatic treatment of tissue are required. When the recording patch electrode tip contacts the cell membrane, as indicated by an increase in apparent resistance, as the pipette advances through the slice, a slight negative pressure is applied to the recording electrode to form a gigaseal and whole-cell recording. The third technique is called the "blow and seal" technique (Stuart et al., 1993), and is a hybrid of the first two methods. In this procedure, the surface neuropile over the neurons to be recorded from is cleaned by gentle application of positive pressure to the recording electrode, similar to the "blind" technique, however, the advancement and placement of recording electrode in brain slices is performed under visual control as in the "clean" procedure. Whole-cell patch recording, using the continuous single-electrode voltage-clamp technique, has several advantages over the sSEVC. First, whole-cell patch-clamp recording significantly improves the signal-to-noise ratio. Thus, it is better suited for recording relatively small amplitude events such as spontaneous miniature EPSCs than are conventional intracellular recording and sSEVC recording (Henderson, 1993; Blitzer and Landau, 1994). Second, in whole-cell patch recording, access to the cell interior is much greater. Thus, relatively large molecules can enter the cytosol by diffusion from the electrode, permitting the design of experiments involving the intracellular injection of proteins and peptides. Third, the low-resistance recording electrodes used in whole-cell recording are capable of passing larger amounts of currents than are sharp electrodes, especially depolarizing currents. The major problems associated with whole-cell patch recording are the series resistance and response rundown. The access resistance is in series with the membrane. Any current passing through the pipette will induce a voltage across this series resistance and thus an error in the voltage clamp. The contribution of the access resistance to total series resistance can introduce a substantial error when whole-cell recording in the slice. Therefore, a proper series resistance compensation is required to minimize this error. The rundown or gradual decrease of responses in the whole-cell recording configuration is due to dialysis of the intracellular solution and loss of energy sources, second messenger components or cofactors necessary for normal physiological functions. To minimize rundown of responses, some specific substances such as ATP and GTP are often added to the electrode internal solution.

Using these electrophysiological recording techniques described above except the whole-cell patch recording, I examined the effects of MeHg on central synaptic transmission in hippocampal and cerebellar slices.

CHAPTER THREE

METHYLMERCURY ACTS AT MULTIPLE SITES TO BLOCK HIPPOCAMPAL SYNAPTIC TRANSMISSION

ABSTRACT

To explore the mechanisms by which MeHg blocks central synaptic transmission, intracellular recordings of action potentials and resting membrane potentials were made in CA1 neurons of rat hippocampal slices. At 4 - 100 uM, MeHg blocked action potentials in a concentration- and time-MeHg also depolarized CA1 neuronal membranes. dependent manner. However, this effect occurred more slowly than did block of action potentials because the resting membrane potentials remained unchanged when threshold stimulation-evoked action potentials were blocked. Thus, MeHg may initially alter the threshold level of neuronal membrane excitability and subsequently depolarize the membrane leading to block of synaptic transmission. To identify potential sites of action of MeHg, effects of MeHg on the responses of CA1 neurons to orthodromic stimulation of Schaffer collaterals, antidromic stimulation of the alveus, direct injection of current at cell soma and iontophoretic application of glutamate were compared. At 20 and 100 µM, MeHg blocked action potentials evoked by stimulation of Schaffer collaterals and by current injection at the cell soma at similar times. In contrast, action potentials evoked by stimulation of the alveus were blocked more rapidly by 100 uM MeHg than were action potentials evoked by current injection at CA1 MeHg also blocked the responses of CA1 neurons to neuronal soma. iontophoresis of glutamate, but time to block of these responses was slower than block of the corresponding orthodromically-evoked responses by stimulation of Schaffer collaterals. Compared to EPSPs, inhibitory postsynaptic potentials (IPSPs) appeared to be more sensitive to MeHg, because block of IPSPs occurred prior to block of EPSPs. Thus MeHg apparently acts at multiple sites to block central synaptic transmission.

INTRODUCTION

The neurotoxicant MeHg disrupts sensory and motor functions following both acute and chronic exposure (Chang, 1980). Mechanisms responsible for these actions have been studied intensively at vertebrate peripheral synapses and in cells in culture using acute administration of MeHg (Juang and Yonemura, 1975; Juang, 1976; Atchison and Narahashi, 1982; Shafer and Atchison, 1991; 1992). However, considerably less is known of the mechanisms by which MeHg acutely alters central synaptic function. At the neuromuscular junction, MeHg primarily affects presynaptic mechanisms to disrupt transmission (Atchison and Narahashi, 1982; Atchison, 1986; 1987; Traxinger and Atchison, 1987a; 1987b; Shafer and Atchison, 1992). In hippocampal slices, however, results obtained from extracellular microelectrode recordings suggest that MeHg may act at multiple sites to block central synaptic transmission (Yuan and Atchison, 1993; 1994). Acute bath application of MeHg caused concentration- and time-dependent block of the population spikes, fEPSPs and antidromically-activated population spikes recorded from CA1 neurons of hippocampal slices. The characteristics of block of these field potentials by MeHg differed somewhat in terms of the time courses and degree of reversibility. It was suggested that MeHg disrupted central neuronal membrane excitability and synaptic transmission by both presynaptic and postsynaptic mechanisms. In dorsal root ganglion cells, MeHg suppressed the GABA-induced chloride current (Arakawa et al.,1991). Thus, in addition to excitatory systems, MeHg may also act on central inhibitory nerve systems to alter central synaptic transmission.

Because of the limitations of extracellular recording techniques, it is difficult to specify where and how MeHg acts to block central synaptic transmission. Thus, to explore the mechanisms underlying these effects of MeHg, intracellular microelectrode recordings and iontophoresis techniques were applied at CA1 neurons of hippocampal slices to examine directly the effects of MeHg on synaptic and action potentials, resting membrane potentials and responses of CA1 neurons to the excitatory amino acid neurotransmitterglutamate. We sought to determine: 1) whether or not MeHg affects neuronal membrane excitability or alters the threshold for neuronal excitation; 2) which is (are) the primary site(s) of actions of MeHg to block synaptic transmission; and 3) whether or not inhibitory synaptic transmission was also affected by MeHg.

MATERIALS AND METHODS

Materials. Methylmercuric chloride, purchased from ICN Biomedical, Inc. (Costa, CA), was dissolved in deionized water to a final concentration of 5 mM to serve as stock solution. The applied solutions (4 - 100 μM) were diluted with ACSF. MeHg was applied acutely to slices by bath application at a rate of 1.5 ml/min with a Gilson infusion pump. L-glutamic acid was purchased from Sigma Chemical Co. (St. Louis, MO).

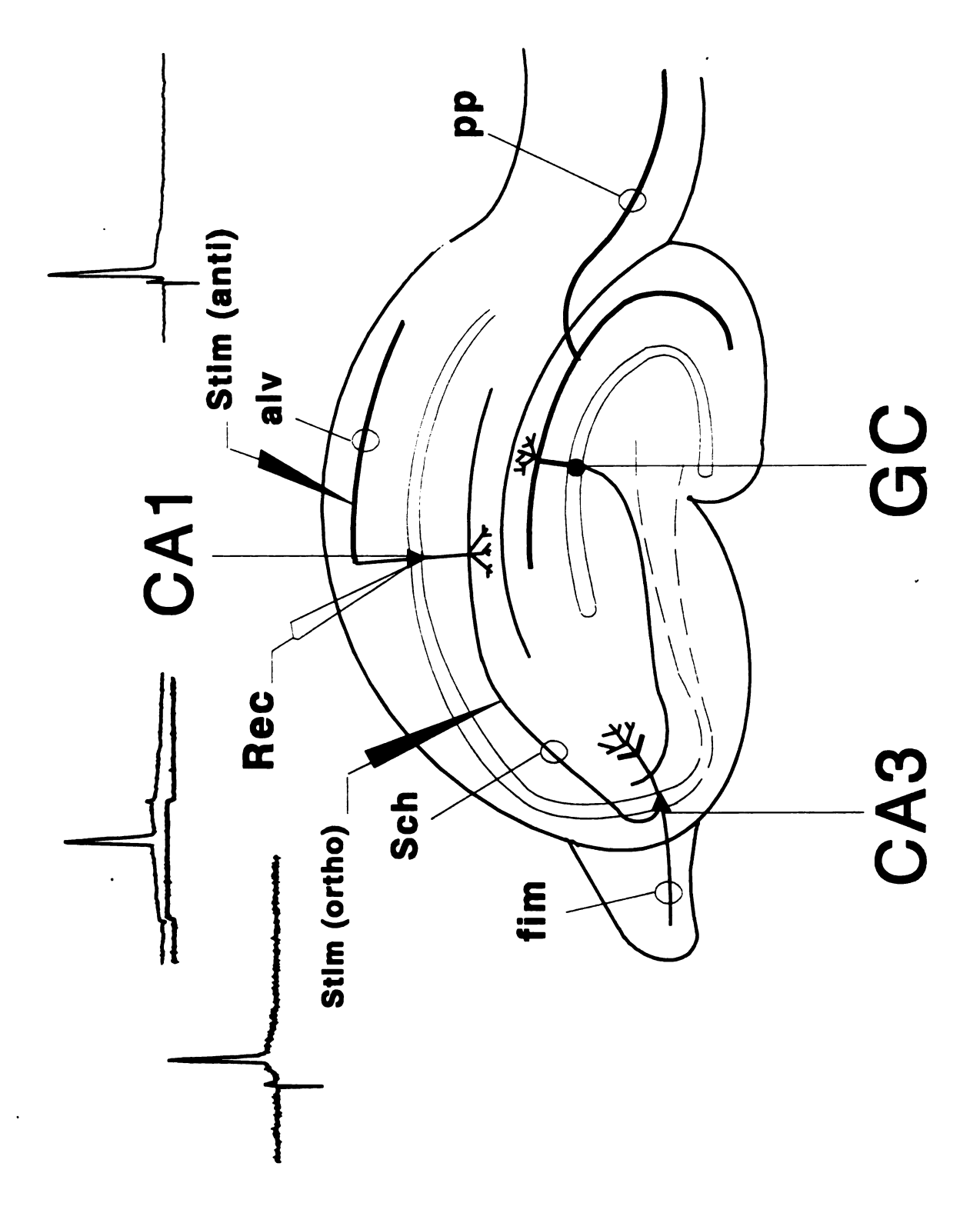
Preparation of hippocampal slices. Hippocampal slices were prepared using method described previously in Chapter Two. When recording, one or two slices were kept in the chamber at a given time. The rest were maintained in a reservoir chamber for later use. All experiments were conducted at 33 - 35 °C. One slice per rat was used.

Electrophysiological procedures. Conventional intracellular recordings were made in the CA1 neurons of hippocampal slices. 3 M Ω monopolar tungsten electrodes (FHC, Brunswick, ME) were used as stimulation electrodes. Borosilicated glass microelectrodes (o.d. 1.0 mm; i.d 0.5 mm, WPI, Inc., New Haven, CT) having impedance of 80 - 120 M Ω when filled with 3 M potassium acetate were used as recording electrodes. Action potentials were evoked orthodromically by stimulating Schaffer collaterals,

antidromically by stimulating the alveus, or directly by injection of positive current into CA1 pyramidal cell soma through the recording electrode at threshold levels (Figure 3.1). The latency to onset of action potentials evoked by threshold stimulation of Schaffer collaterals was measured as the time interval between the stimulus artifact and the peak of the action potential, because the rate of rising phase of action potentials is essentially unchanged at the earlier stage of exposure to MeHg. Intracellular EPSPs were recorded at CA1 pyramidal cell soma by stimulation of Schaffer collaterals at a level that did not evoke action potentials. Typically a 0.1 - 0.2 nA negative D.C. current was applied constantly through the recording electrode to maintain the cell membrane in a somewhat hyperpolarized state and avoid evoking action potentials. The recurrent inhibitory postsynaptic potentials (IPSPs) (Dingledine and Gjerstad, 1979; Collingridge et al., 1988) were recorded by subthreshold stimulation of the alveus. The membrane input resistance was examined by D.C. current injection through the recording electrode. The stimulus pulses were generated from a Grass S88 stimulator (Grass, Inc., Quincy, MA) at a frequency of 0.15 Hz and 0.1 msec duration and isolated with a Grass SIU5 stimulus isolation unit (Grass, Inc. Quincy, MA), which was also used to change the polarity of stimulus pulses. For iontophoretic application of Lglutamate, a third electrode (50-100 M Ω) filled with 500 mM glutamate in 100 mM NaCl (pH 8.0) was positioned at the apical dendrites of CA1 neurons. Glutamate was ejected by passing a 20 -100 nA negative current for 30 - 40 msec with a retaining current of 0 - 5 nA through the electrode. Signals from recording electrodes were amplified (Axoclamp-2, Axon Instruments, Inc., Burlingame, CA), displayed on a 2090-3 digital oscilloscope (Nicolet Instruments, Madison, WI) and stored simultaneously on floppy disks and magnetic tape by using an FM instrumentation recorder (Model B, Vetter Instruments, Rebersburg, PA) at a speed of 7-1/2 inch per second for later analysis. Only those cells in which the amplitude of action potentials was greater than 60 mV, resting membrane potentials were -55 mV or more negative, and membrane input resistances were above 20 M Ω were used for analysis.

Data analysis. Data were collected continuously before and during application of MeHg and analyzed statistically using Student's paired t-test or a one-way analysis of variance and Dunnett' procedure for post-hoc comparisons (Steel and Torrie, 1980) unless specified. Differences between values for comparisons were considered statistically significant when p < 0.05.

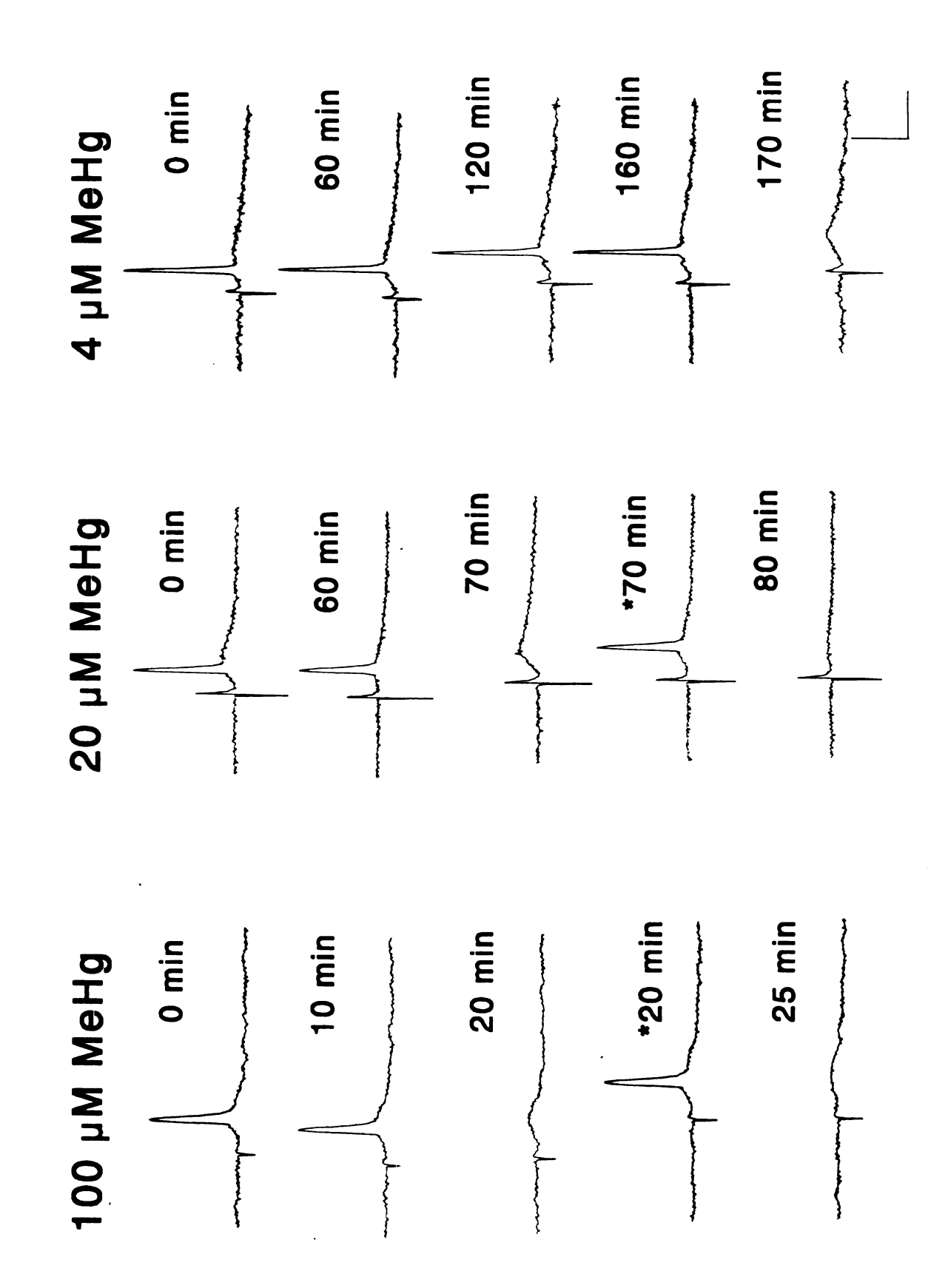
Figure 3.1 Diagrammatic depiction of the synaptic circuits of a traverse hippocampal slice and methods for recording action potentials in the CA1 pyramidal cells. Action potentials are evoked by orthodromic the recording electrode at the CA1 pyramidal cell soma. Abbreviations: pp, perforant path; GC, granule cells in the dentate region; CA3, pyramidal cell in CA3 region; fim, fimbria; Sch, Schaffer collaterals; recording electrode at the CA1 pyramidal cell soma; alv, alveus; Stim (anti), antidromic stimulation of stimulation of Schaffer collaterals, antidromic stimulation of the alveus and injection of current through Stim (ortho), orthodromic stimulation of Schaffer collaterals; CA1, pyramidal cell in CA1 region; Rec, the alveus. The upper traces depict the action potentials recorded at the CA1 pyramidal cell soma evoked by the three methods.



RESULTS

Effects of MeHg on action potentials and resting membrane Acute bath application of 4 - 100 µM MeHg caused a potentials. concentration- and time- dependent block of action potentials recorded at CA1 neurons of hippocampal slices (Figure 3.2 and Table 3.1). Time courses of effects of 4-100 µM MeHg on action potentials are illustrated in Figure 3.2. At 100 µM, MeHg suppressed generation of action potentials evoked by threshold stimulation of Schaffer collaterals within 20 min. At that time, increasing stimulation intensity slightly could again initiate action potentials, however upon returning the stimulation intensity to its original value, action potentials again disappeared. Five min later, action potentials evoked at the increased level of stimulation disappeared again. By continuously increasing stimulation intensity, action potentials could initially still be elicited in the presence of MeHg. However with continued exposure to MeHg, eventually action potentials could no longer be evoked regardless of the level of stimulation. Similar effects were observed in slices exposed to 20 and 4 µM MeHg, but time to block of action potentials was much longer. Figure 3.2 also demonstrates that at the time action potentials disappeared, EPSPs were still observable, suggesting that synaptic transmission may still be functionally intact at this moment, but the threshold for initiating action potentials was altered. The mean time to block of action potentials evoked at the threshold

Figure 3.2. Time courses of effects of 4, 20 and 100 µM MeHg on action potentials of hippocampal CA1 pyramidal cells. The asterisk (*) indicates that a slight increase in stimulation intensity caused recovery of action potentials. Each trace is a representative depiction of 6 - 9 separate experiments. Calibration bars: vertical, 40 Mv; horizontal, 10 ms.



threshold stimulation and the maximum stimulation of Schaffer collaterals. Table 3.1. Time to MeHg-induced block of action potentials evoked at the

Time to block of action potentials evoked at the threshold stimulation.

Time to block of action potentials evoked at the maximum stimulation. Mean ± SE (n). Averaged from 4 of 6 experiments that showed block

of action potentials in 180 min.

^d Not determined.

and maximum level of stimulation are summarized in Table 3.1. At 4 µM MeHg, only 4 of 6 slices exhibited complete block of action potentials within 180 min. However, if exposure of slices to 4 µM MeHg was continued for longer times, action potentials in the remaining slices would be expected to be blocked as well. At the time action potentials evoked by threshold stimulation were blocked, in most cases the amplitudes of action potentials just before block remained essentially unchanged (Table 3.2). However, with continued exposure to MeHg and gradual depolarization of membranes (Figure 3.3), the amplitudes of action potentials declined progressively until eventually they disappeared completely. For a given stimulus intensity, the latency to onset of action potentials was gradually prolonged after exposure to MeHg. At 100 µM MeHg, the latency to onset of action potential generation just before block of action potentials evoked by threshold stimulation of Schaffer collaterals was 2.0 ± 0.8 msec longer than those of the pre-treatment control (5.8 ± 0.5 msec). The shape or rates of rising phase of action potential spike were usually unchanged at the same time (Figure 3.2). However, at the late stage of exposure to MeHg, spikes usually arise directly from the base line (resting membrane potential) level, and often two or more spikes appeared simultaneously in response to a single stimulus. Spontaneous neuronal activity seemed less sensitive to the effects of MeHg, since in many slices even after evoked action potentials were blocked, the spontaneous spikes remained observable, but often occurred accompanying depolarization of the neuronal

Table 3.2. Amplitudes of the action potentials and the resting membrane potentials just before or at the time that action potentials were blocked by MeHg

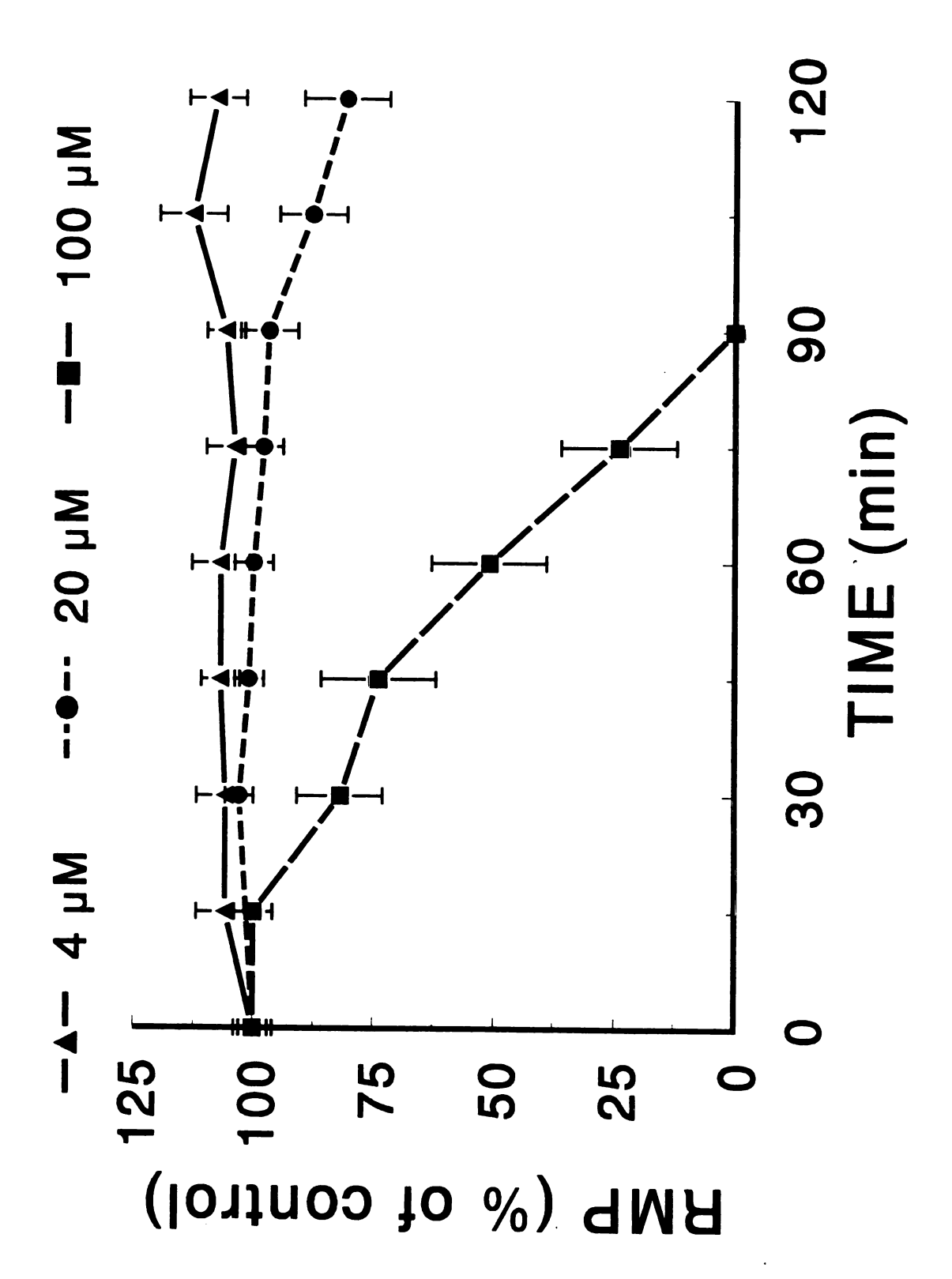
$\underset{(\%)^b}{\text{RMP}}$	$103 \pm 4 (15)$	$96 \pm 4 (22)$
AP Amplitude (%) ^a	$99 \pm 7 (15)^{\circ}$	$99 \pm 2 (22)$
MeHg (µM)	20	100

Resting membrane potentials expressed as a percent of the control. Mean \pm SE (n) Action potentials amplitude expressed as a percent of the control. . က က က

membrane. This suggests that the initial effects of MeHg on action potentials are due to reduced neuronal excitability or altered threshold for initiating action potentials and the late effects may be due to nonspecific effects of membrane depolarization. However, after action potentials were blocked completely, injection of D.C. current to return resting membrane potentials to their original values generally did not restore the action potentials. Thus, MeHg-induced block could not simply be ascribed to membrane depolarization.

MeHg also caused concentration- and time-dependent depolarization of CA1 neuronal membranes (Figure 3.3). At 100 μ M, MeHg depolarized CA1 neuronal membranes to 55 % of control at 60 min and to almost 0 % of control by 90 min. At 120 min, 20 μ M MeHg depolarized membranes to 81 % of control, whereas 4 μ M caused a slight hyperpolarization that was not statistically significant. However, if exposure of slices to 4 μ M MeHg was prolonged to 180 min, membranes also gradually depolarized to 72 % of control (results not shown in Figure 3.3). Most slices exposed to 4 - 100 μ M MeHg showed a slight hyperpolarization prior to depolarization, which is masked in Figure 3.3 by averaging due to the variation of time courses among individual experiments. Thus, the maximum hyperpolarization was averaged and compared from each individual experiment instead of the time-dependent averages shown in Figure 3.3. In all six slices exposed to 4 μ M MeHg, the average maximum hyperpolarization of membranes was 115 \pm 6 % of control

Figure 3.3. Time courses of effects of 4 - 100 µM MeHg on resting membrane potentials of hippocampal CA1 pyramidal cells. Values are expressed as percentages of pre-MeHg exposure control. All values are the mean \pm SE of recordings from slices of 6 - 22 animals.



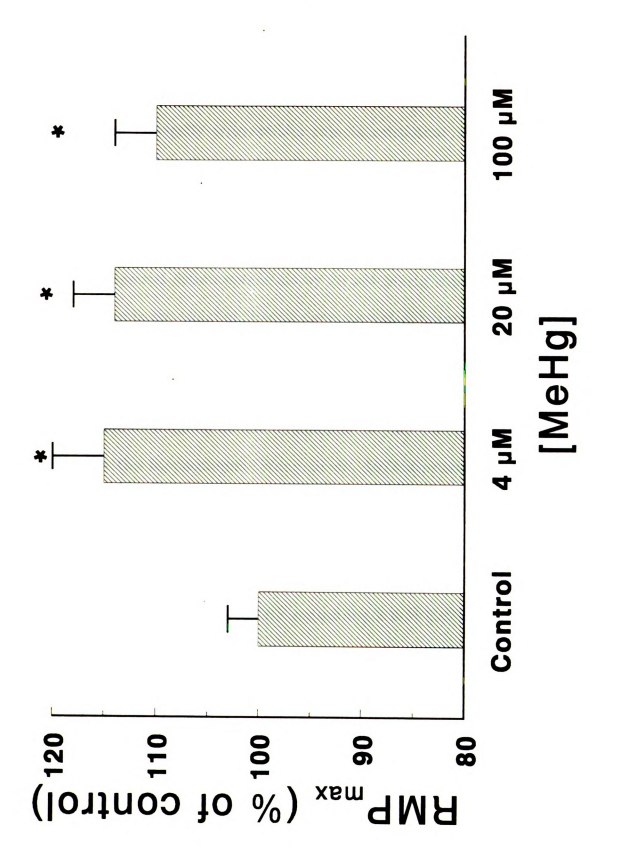
(p < 0.05). In 12 of 15 slices exposed to 20 μ M MeHg and 16 of 22 slices exposed to 100 µM MeHg, a slight hyperpolarization was also observed prior to depolarization. The averaged maximum hyperpolarizations were $114 \pm 4 \%$ and 110 ± 4 % of their control for 20 and 100 µM MeHg, respectively. These also differed significantly from their own pre-treatment control (Figure. 3.4). During hyperpolarization of the membrane, input resistance was reduced from $33 \pm 4 \text{ M}\Omega$ to $21 \pm 1 \text{ M}\Omega$ (p < 0.05). However during depolarization, changes in input resistance were inconsistent, even though many cells showed an increase in membrane input resistance at the late stage of exposure to MeHg. Thus, MeHg typically caused biphasic changes in resting membrane potentials. In contrast to the actions of MeHg on action potentials, the effects of MeHg on the resting membrane potentials occurred relatively slowly. At the time that action potentials evoked by threshold stimulation were blocked by 20 and 100 µM MeHg, the resting membrane potentials remained essentially unchanged (Table 3.2).

The effects of MeHg on population spikes were at best only partially reversible (Yuan and Atchison, 1993; 1994). To examine whether or not the effects of MeHg on action potentials and resting membrane potentials are reversible, we washed slices with 1 mM D-penicillamine, a MeHg chelator, after action potentials evoked by threshold stimulation of Schaffer collaterals were blocked by 100 µM MeHg. Only one of eight slices demonstrated recovery of the action potential and two of eight slices showed a recovery of resting

Figure 3.4. The maximum hyperpolarization of CA1 neuronal membranes caused by 4 - 100 µM MeHg.

(*) indicates a value statistically different from its own control (p < 0.05, paired *t*-test).

Values are averaged from each individual maximum hyperpolarization of 6 - 16 recordings. The asterisk



membrane potentials. In the remaining slices, washing did not restore action potentials and also did not prevent membrane depolarization to progress. Thus, it appears that the effects of MeHg on action potentials and resting potentials were generally irreversible; this is consistent with the results obtained from extracellular recordings (Yuan and Atchison, 1993; 1994).

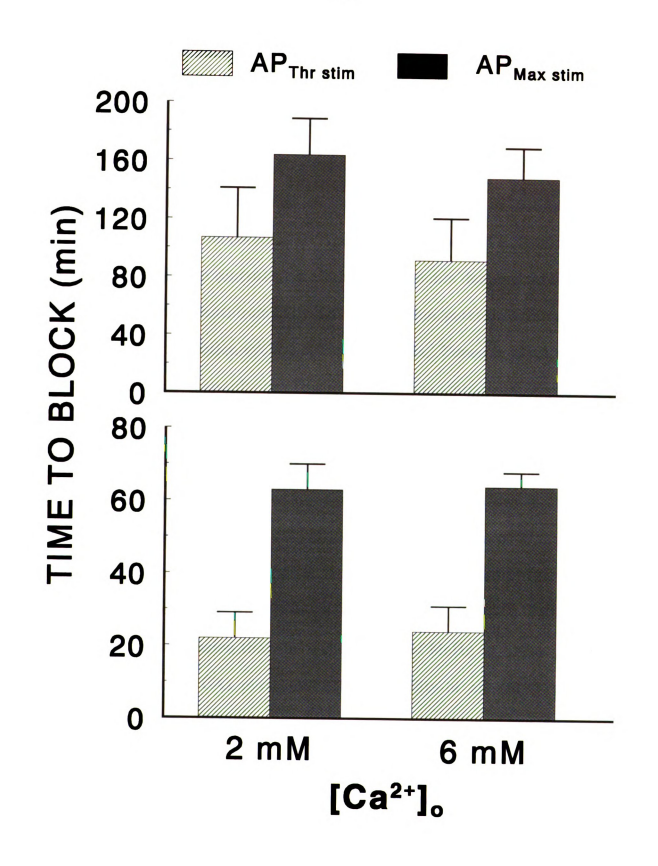
At the superior cervical ganglion of the rabbit, increasing bath Ca2+ concentration from 2.2 to 6.6 mM delayed the onset and slowed the progression of block of compound action potentials by 20 µM MeHg (Alkadhi and Taha, 1982). However, in the isolated phrenic nerve-hemidiaphragm preparations of the rat, elevating [Ca²⁺]_e did not significantly change the latency to block by MeHg of the end-plate potentials (Atchison et al., 1986; Traxinger and Atchison, 1987a). Because of the importance of Ca²⁺ currents in dendritic excitability in the hippocampus (Wong, et al., 1979; Spruston, et al., 1995; Magee and Johnson, 1995), we sought to determine if increasing [Ca²⁺]_e would alter the latency to MeHg-induced block of action potentials. To do this, we compared time to block of action potentials by 20 and 100 µM MeHg in ACSF containing 2 or 6 mM Ca2+. In ACSF containing 2 mM Ca2+, 20 and 100 µM MeHg blocked action potentials evoked by threshold stimulation at 107 ± 34 and 22 \pm 7 min and by maximum stimulation at 176 \pm 28 and 63 \pm 7 min, respectively. In ACSF containing 6 mM Ca2+, the same concentrations of MeHg blocked action potentials evoked by threshold stimulation at 92 ± 29 and 24 ± 7 min and by maximum stimulation at 149 ± 21 and 64 ± 4 min,

respectively (Figure 3.5). Thus, similar to the results obtained from phrenic nerve-hemidiaphragm preparations (Atchison *et al.*, 1986; Traxinger and Atchison, 1987a), increasing [Ca²⁺]_e from 2 to 6 mM did not significantly alter the latency to MeHg-induced block of action potentials.

Sites of actions for MeHg-induced block of synaptic transmission.

To identify the primary sites of action of MeHg in blocking hippocampal synaptic transmission, we compared the time courses of MeHg-induced block of action potentials evoked simultaneously by maximum orthodromic stimulation of Schaffer collaterals or by maximum antidromic stimulation of alveus with those by maximum current injection directly through recording electrodes at CA1 cell soma. At 20 µM MeHg, four of nine recordings demonstrated that block of action potentials evoked by stimulating Schaffer collaterals occurred earlier than block of action potentials evoked by current injection at the cell soma. At 100 µM MeHg, block of synaptically-evoked action potentials occurred slightly faster than block of current injection-induced action potentials in only four of twelve recordings. In most slices, block of action potentials evoked by the two methods occurred at the same time, usually accompanying rapid depolarization of the membrane. Overall, times to block of action potentials evoked by stimulation of Schaffer collaterals and by current-injection at the cell soma were 136 ± 19 and 142 ± 18 min, respectively for 20 μ M MeHg, and 47 \pm 6 and 49 \pm 6 min, respectively for 100

Figure 3.5. Effects of increased $[Ca^{2+}]_e$ on time to MeHg-induced block of action potentials evoked at threshold $(AP_{Thr\,Stim})$ and maximum $(AP_{Max}\,S_{tim})$ stimulation of Schaffer collaterals. Action potentials were recorded continuously in ACSF containing 2 or 6 Mm $CaCl_2$ before and during application of 20 and 100 μ M MeHg. Values are the mean \pm SE of recordings from slices of 5 - 6 rats.



uM MeHg. Thus there were no significant differences between the times to block of action potentials evoked by the two methods. Similarly, no significant difference was observed between the times to block of antidromically-generated action potentials and of current injection-evoked action potentials at 20 µM MeHg, even though three of five experiments did show that MeHg blocked antidromically-generated action potentials faster than it blocked current injection-evoked action potentials. Times to block were 164 ± 24 and 172 ± 26 min, respectively. In contrast, six of nine experiments demonstrated that 100 uM MeHg blocked antidromically-activated action potentials faster than it blocked current injection-evoked action potentials. Times to block were 42 ± 4 and 49 ± 5 min, respectively. This difference was statistically significant (p < 0.05) due to the paired nature of the study (Figure 3.6). In addition, similar to the effect of MeHg on action potentials evoked by stimulating Schaffer collaterals, initial block of action potentials evoked by threshold current injection at the CA1 pyramidal cell soma could be restored completely by increasing current injection. Later, action potentials evoked by the increased current injection were also blocked (Figure 3.7). These results further confirmed the conclusion that the initial effects of MeHg on action potentials are due to reduced CA1 pyramidal cell excitability or altered threshold for initiation of action potentials.

Next we sought to determine the contribution of presynaptic and postsynaptic mechanisms to the actions of MeHg on synaptic transmission. To

Figure 3.6. Comparison of times to MeHg-induced block of action potentials evoked by different stimulation methods. Top: times to block by MeHg of action potentials evoked by stimulating Schafer collaterals (AP_{Schaffer}) and by current injection through a recording electrode at the cell soma (AP_{soma}); Bottom: Times to block of action potentials evoked by antidromic stimulation of the alveus (AP_{anti}) and by current injection through a recording electrode at the cell soma (AP_{soma}). Values are the mean ± SE of recordings from 5 - 9 rats. The asterisk (*) indicates a significant difference between time to block of action potentials evoked by antidromic stimulation of the alveus and current injection at cell soma (p < 0.05, paired *t*-test).

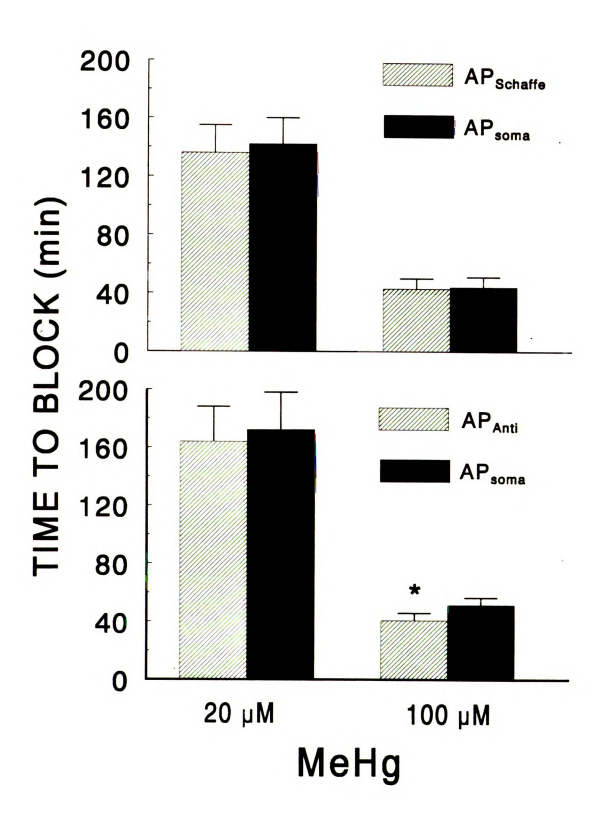
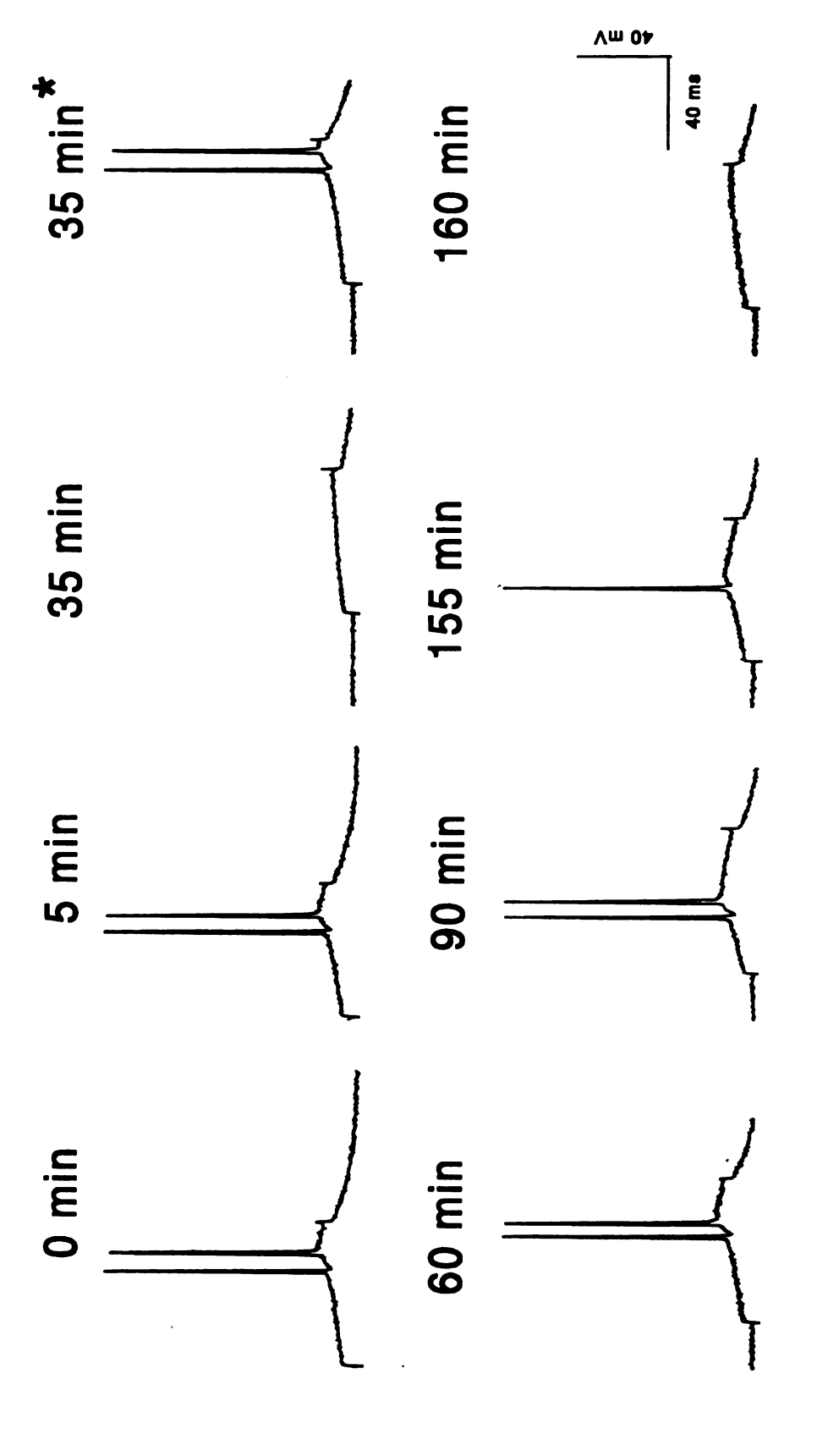


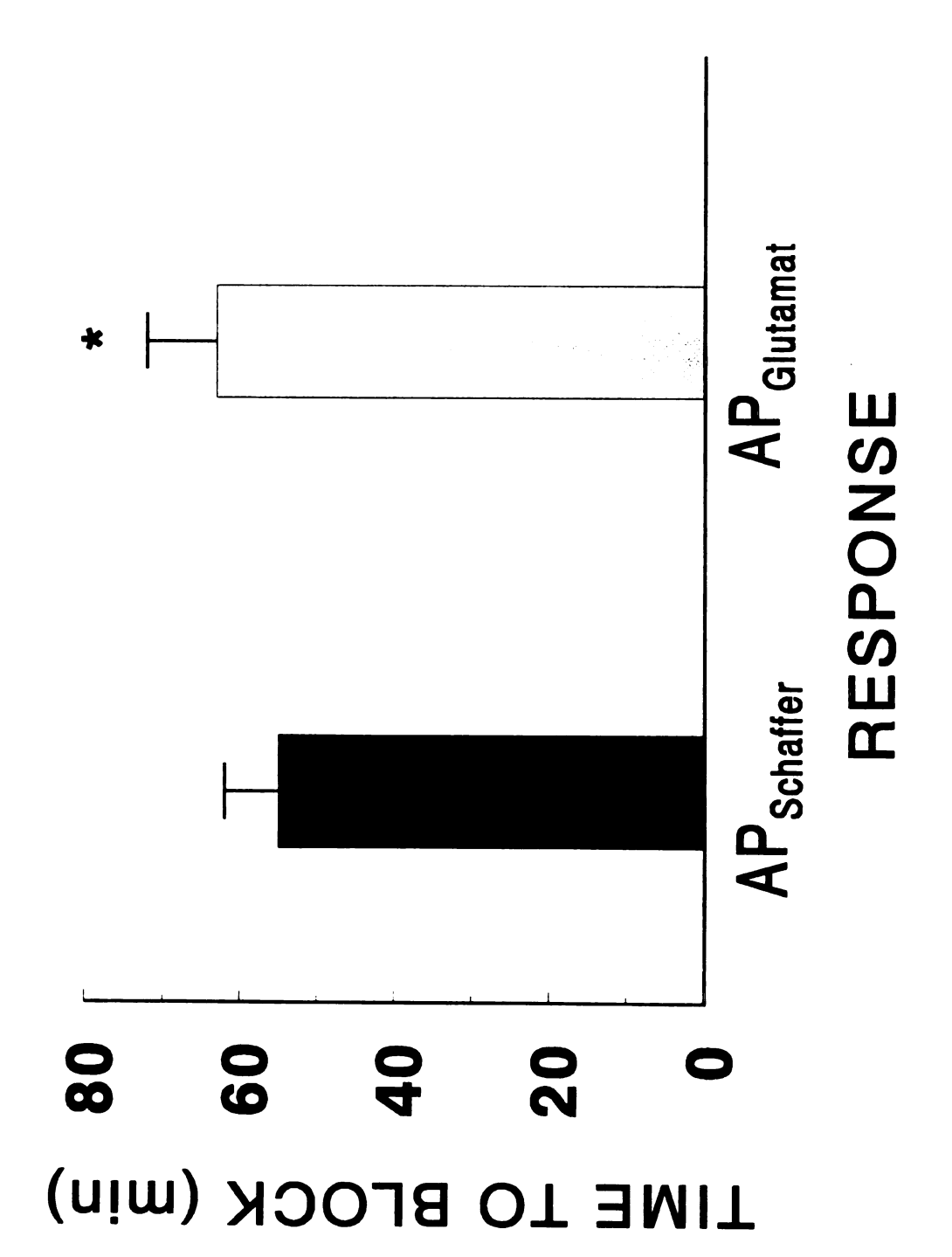
Figure 3.7 Time course of effect of 20 µM MeHg on action potentials evoked by depolarizing current evoked by threshold current injection were blocked at 35 min after application of 20 µM MeHg. At this potentials. Action potentials evoked at the increased current pulses were blocked again at 160 min after injection through a recording electrode at the CA1 pyramidal cell soma. Initially, action potentials time (indicated by the asterisk), increasing amplitude of depolarizing current pulse again initiated action exposure to MeHg. Each trace is a representative depiction of 5 experiments.



do this, we compared effects of MeHg on responses of CA1 neurons to presynaptic electrical stimulation of Schaffer collaterals and to direct iontophoretic application of glutamate onto their apical dendrites simultaneously in the same cell. At 100 μ M, MeHg blocked action potentials evoked by maximum stimulation of Schaffer collaterals at 55 \pm 7 min and blocked iontophoresis-evoked responses at 63 \pm 9 min. This difference was statistically significant (p < 0.05, Figure 3.8). Responses of CA1 neurons to iontophoresis of glutamate usually disappeared after membrane potentials were depolarized below -40 mV. At this point, however, injection of D.C. current to hold membrane potentials at -60 to -70 mV failed to reverse responses of CA1 neurons to glutamate, suggesting that block of glutamate-induced responses by MeHg could not be ascribed to membrane depolarization alone.

Effects of MeHg on EPSPs and IPSPs. In the hippocampus, inhibitory interneurons release (GABA) onto both pre- and postsynaptic sites to control or influence excitatory synaptic transmission (Dutar and Nicoll, 1988a; 1988b; Thompson and Gähwiler, 1992; Isaacson et al., 1993). Therefore, if MeHg affects these inhibitory interneurons, we may expect that it also plays a role in alteration of excitatory synaptic transmission. To test this, effects of MeHg on both EPSPs and antidromically-activated recurrent IPSPs were assessed. The time course of effects of MeHg on EPSPs

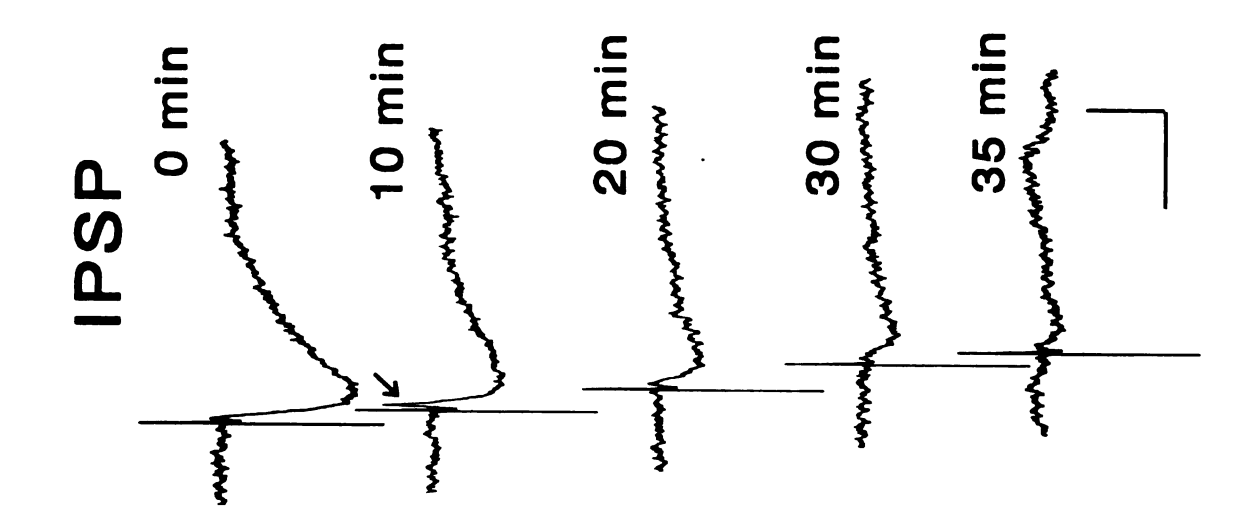
stimulation of presynaptic terminals (Schaffer collaterals, AP_{Schaffer}) and to iontophoretic application of glutamate (AP $_{\text{Glutamate}}$) on the apical dendrites of CA1 pyramidal cells. Values are the mean \pm SE of 5-9 Figure 3.8. Comparison of times to block by 100 µM MeHg of responses of CA1 neurons to electrical recordings. The asterisk (*) indicates a significant difference between time to block of responses of CA1 neurons to electrical stimulation and iontophoresis of glutamate (p < 0.05, paired *t*-test).

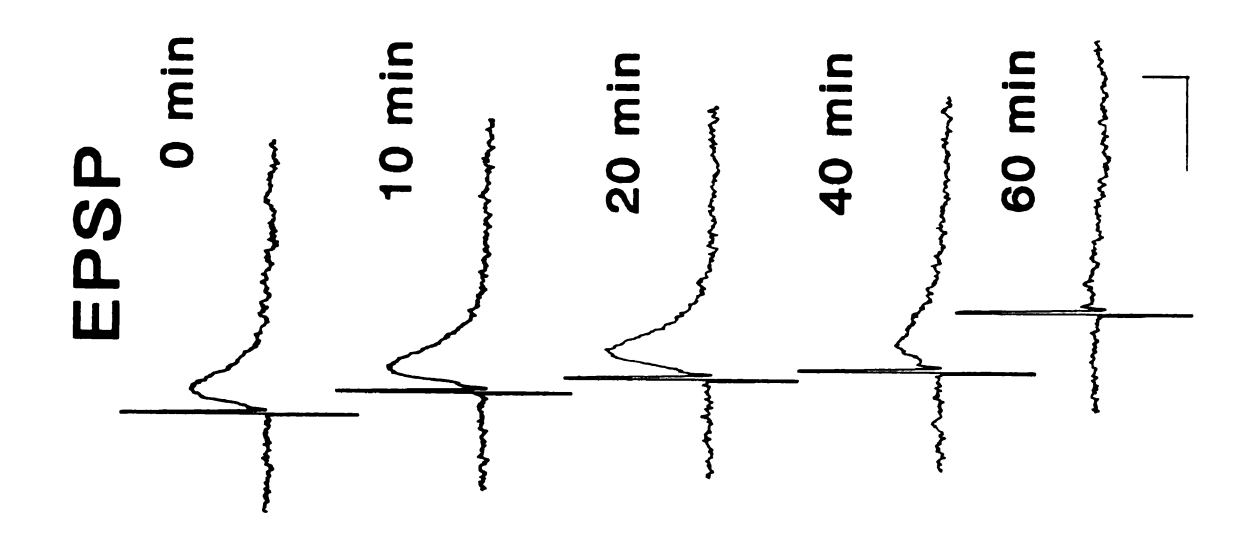


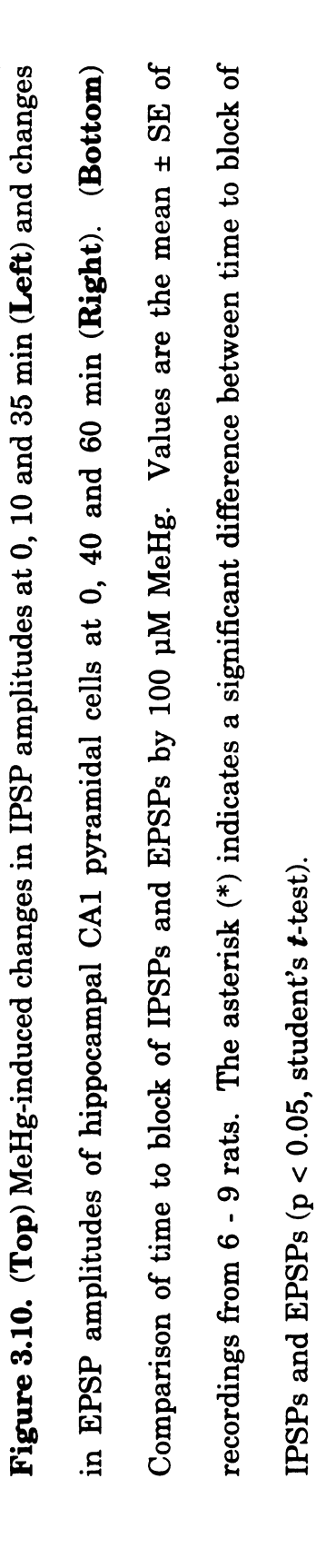
or IPSPs recorded at the CA1 neurons of hippocampal slices is shown for two separate representative cells in Figure 3.9. At 100 µM, MeHg first increased EPSP amplitudes during the first 10 to 20 min and then gradually decreased them to complete block at 60 min (Figure 3.9, Left). Often, action potentials emerged superimposed on the EPSPs during that period when EPSP amplitude was increased by MeHg (results not shown). This was not observed under normal (pre-treatment control) conditions, since the EPSPs were activated by stimulation of Schaffer collaterals at a level that does not evoke action potentials and under slightly hyperpolarizing conditions. This suggests that neuronal excitability was initially increased by MeHg. Conversely, 100 µM MeHg reduced IPSP amplitudes relatively rapidly (Figure 3.9, Right). Interestingly, at 10 min an increased EPSP phase could be observed prior to the decreased IPSP in the same recording (Fig. 3.9, Right). However in general, the time to decreased IPSP amplitudes appeared to correspond to the time to increased EPSP amplitudes, suggesting that the increased EPSPs may be due partially to reduced amplitude of IPSPs. The mean time to MeHginduced block of EPSPs and IPSPs is shown in Figure 3.10. At 100 µM, MeHg caused complete block of IPSPs at an earlier time than EPSPs. Thus, IPSPs may be more sensitive to MeHg than were EPSPs.

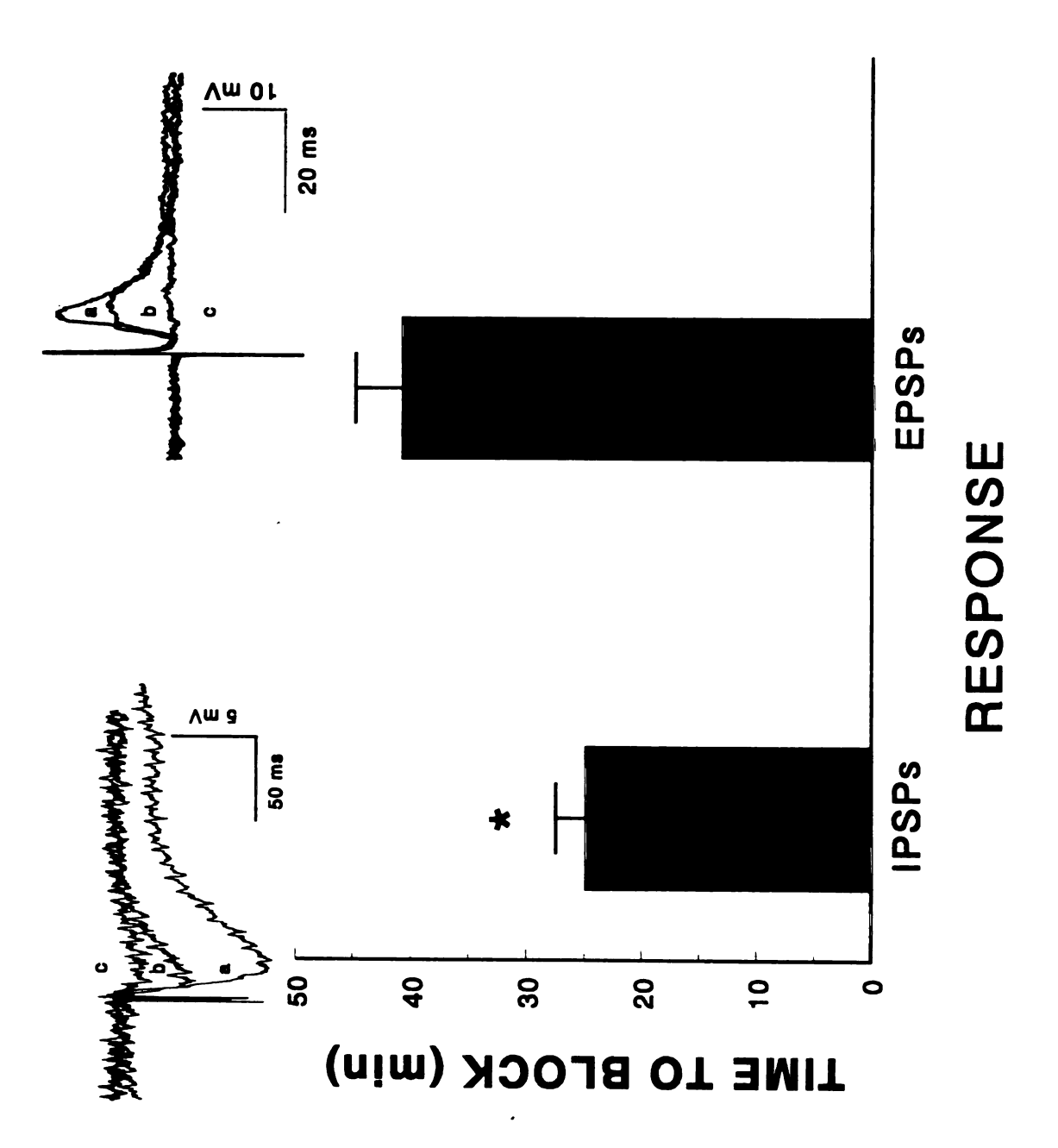
Figure 3.9. Comparison of time course of effects of 100 µM MeHg on EPSPs (Left) and IPSPs (Right).

The arrow (<) indicates the increase in EPSP phase which occurs prior to the IPSP phase. Each trace is a representative depiction of recordings from 6 - 9 animals. Calibration bars: vertical, 5 Mv for both EPSP and IPSP; horizontal, 20 ms for EPSP and 50 ms for IPSP.









DISCUSSION

The present study was undertaken with the objective of describing in more detail, the cellular actions of MeHg on central synaptic activity. Results are consistent with the following conclusions. First, at 4-100 µM, MeHg caused a concentration- and time-dependent block of action potentials and depolarization of CA1 neuronal membranes in hippocampal slices. Second, effects of MeHg on the resting membrane potentials occurred more slowly than did effects on action potentials. Third, the time to MeHg-induced block of action potentials evoked by orthodromic stimulation of Schaffer collaterals or by current injection at the cell soma was not statistically significant, but block of action potentials evoked by antidromic stimulation of the alveus occurred faster than block of action potentials generated by current injection at the cell Fourth, MeHg also suppressed the responses of CA1 neurons to soma. iontophoresis of glutamate, but effects of MeHg on these responses were relatively slow in onset, in contrast to the rapid effects of MeHg on the responses to presynaptic electrical stimulation. Finally, IPSPs seemed to be more sensitive to MeHg than were EPSPs.

Using extracellular recording, we demonstrated previously that MeHg first increased and than gradually decreased to complete block population spikes recorded from CA1 neurons of hippocampal slices. These effects were concentration- and time-dependent (Yuan and Atchison, 1993; 1994). In the

present study, the time-courses of effects of MeHg on action potentials were generally similar to those of MeHg on population spikes. However, MeHg initially blocked action potentials evoked by threshold stimulation without any significant changes in the action potential amplitudes, i.e. MeHg blocked action potentials in an all or none manner rather than gradually. In addition, the resting membrane potentials remained essentially unchanged and EPSPs were still observable after block of action potentials. Increasing stimulation intensity at the time of block completely restored the action potentials. These results suggest that at the time action potentials were blocked, synaptic transmission may remain functionally intact, but the threshold level for neuronal excitation may have been altered by MeHg. Using voltage-clamp techniques in squid axon, Shrivastav et al. (1976) demonstrated that 25 - 100 µM MeHg caused a steady increase in the threshold for action potential generation and eventual block of conduction without changing the resting membrane potentials. These effects were thought to be due to suppression of both peak Na⁺ current and steady-state K⁺ current by MeHg. Similar effects of 20 -60 µM MeHg on peak Na⁺ current and steady-state K⁺ current were observed in N1E-115 neuroblastoma cells (Quandt et al., 1982). Shafer and Atchison (1992) also demonstrated that 50 - 100 µM MeHg disrupted Na⁺ channel function in mouse triangularis sterni motor nerves. Therefore, the initial effects of MeHg on action potentials may be mediated by an action on Na⁺ channels which alters the threshold for generation of action potentials and

blocks current conduction. However, effects of MeHg on Ca2+ channels or homeostasis of Ca^{2+}_{i} may also be involved in these effects since MeHg rapidly and effectively blocks Ca2+ channels in neurons (Shafer and Atchison, 1989; Shafer et al., 1990; Shafer and Atchison, 1991; 1992; Hewett and Atchison, 1992; Sirois and Atchison, 1996, 1997) and disturbs homeostasis of Ca²⁺, (Komulainen and Bondy, 1987; Levesque and Atchison, 1991; Levesque et al., 1992; Denny et al., 1993; Hare et al., 1993; 1995; Marty and Atchison, 1997). In this regard, increasing external Ca²⁺ concentration delayed the onset of MeHg-induced block of action potentials in rabbit superior cervical ganglia (Alkadhi and Taha, 1982), supporting the suggestion that effects of MeHg on Ca²⁺ channels could be reversed by raising [Ca²⁺]_e. However, our results suggest that raising [Ca2+], alone cannot overcome effects caused by MeHg in hippocampal slices, a situation identical to that at the rat neuromuscular junction (Atchison et al., 1986; Traxinger and Atchison, 1987a) and in cortical synaptosomes (Atchison et al., 1986; Hewett and Atchison, 1992). The late effects of MeHg to decrease amplitude of action potentials to complete block may be due to the nonspecific effects of depolarization of neuronal membranes (Juang, 1976a,b; Shrivastav et al., 1976; Quandt et al., 1982; Kauppinen et al., 1989; Hare and Atchison, 1992). However, other mechanisms are probably also involved, because injection of D.C. current to hold membrane potentials around their original values did not prevent or reverse the effects of MeHg on action potentials.

At the neuromuscular junction and peripheral ganglia, 40 - 100 µM MeHg had no effects on postsynaptic resting membrane potentials (Juang and Yonemura, 1975; Juang, 1976a; Atchison and Narahashi, 1982). In the present study, 4 - 100 µM MeHg typically caused biphasic changes in the resting potentials of CA1 neurons, i.e. MeHg first hyperpolarized and then depolarized CA1 neuronal membranes. The hyperpolarizing effect was especially prominent at lower concentrations of MeHg (4 - 20 µM). phenomenon was also observed in synaptosomes exposed to 1 µM MeHg although the difference was not statistically significant (Hare and Atchison, 1992). It may be that the initial plasma membrane hyperpolarization was caused by activation of Ca2+- sensitive K+ channels as a result of MeHg-induced elevation in $[Ca^{2+}]_i$. In NG108-15 cells, the initial effect of MeHg on $[Ca^{2+}]_i$ is to increase $[Ca^{2+}]_i$ due to release of Ca^{2+} from IP_3 -sensitive pool (Hare and Atchison, 1995a). In this cell line, mobilization of this intracellular Ca²⁺ pool results in membrane hyperpolarization (Higashida and Brown, 1986). A similar phenomenon may be applicable to hippocampal slices. decreases in membrane input resistance during membrane hyperpolarization seem to support this possibility. Differences in the effects of MeHg on resting membrane potentials at neuromuscular junctions and peripheral ganglia and those reported here may be due to differences in exposure duration and concentration of MeHg. High concentrations of MeHg (400 or 500 µM) depolarize muscle fibers (Juang, 1976a,b) and squid axons (Shrivastav et al., 1976), whereas prolonged exposure of tissues to low concentration of MeHg (4 - $20~\mu\text{M}$) in this study also depolarized CA1 neuronal membranes. However, these effects of MeHg occurred more slowly than did those of MeHg on action potentials, suggesting that different mechanisms may be involved in the effects of MeHg on action potentials and resting membrane potentials.

In general, effects of MeHg on both action potentials and resting membrane potentials could not be reversed by washing slices with D-penicillamine. This is consistent to our previous results in hippocampal slices (Yuan and Atchison, 1993; 1994) and those of others in alternate systems (Juang, 1976; Shrivastav *et al.*, 1976; Alkadhi and Taha, 1982; Quandt *et al.*, 1982; Atchison and Narahashi, 1982; Traxinger and Atchison, 1987b).

The effects of MeHg on peripheral synapses have generally been ascribed to be primarily presynaptic, because at relatively high concentrations (40 or 100 µM), MeHg has no effects on either action potential amplitude or resting membrane potentials of postsynaptic muscle fibers despite blocking neuromuscular transmission (Juang, 1976a). Moreover, responses to iontophoretic application of acetylcholine to end-plates were unaffected by 100 µM MeHg at times that nerve-evoked end-plate potentials were blocked (Atchison and Narahashi, 1982). However, previous results from extracellular recordings suggest that MeHg acts at multiple sites, especially postsynaptic sites, to block hippocampal synaptic transmission, because of differential sensitivity of block of orthodromically- and antidromically-activated population

spikes compared with fEPSPs to reversal with D-penicillamine (Yuan and Atchison, 1993; 1994). The block of fEPSPs could be completely restored by Dpenicillamine, whereas population spikes were only partially restored. A goal of the present study was to identify further the primary sites at which MeHg acts to block hippocampal synaptic transmission. As such we first compared the time courses of block of action potentials evoked by orthodromic stimulation of the presynaptic nerve fibers-the Schaffer collaterals, or antidromic stimulation of the axons of CA1 neurons-the alveus, with the time course of block of action potentials evoked directly by current injection through recording electrodes at the cell soma. The rationale was that if MeHg acts primarily on presynaptic sites, then block of orthodromically-activated action potentials would be expected to occur earlier than block of action potentials evoked by current injection at the cell soma, and may also differ from the time to block of antidromically-activated action potentials. If MeHg acts primarily postsynaptically, then the time to block as assessed by the three methods might be similar or could differ depending on the sites and mechanisms of actions. MeHg blocked action potentials evoked both by orthodromic stimulation of Schaffer collaterals and by current-injection at a similar time even though some slices showed a trend that block of action potentials evoked by orthodromic stimulation was faster than by current-injection, suggesting that the primary sites of action may be at the cell soma. These results are consistent with the findings that MeHg heavily accumulated in the cell bodies of CA1 pyramidal neurons, compared with other areas in hippocampus (Møller-Madsen, 1990; 1991). However, presynaptic action or block of current conduction from apical dendrites to cell soma could not be excluded completely based on these data, because membrane depolarization caused by prolonged exposure to MeHg may mask the real procession of effects of MeHg. In contrast, 100 µM MeHg blocked antidromically-evoked action potentials significantly faster than it blocked current injection-evoked action potentials, suggesting that current conduction from axon to cell soma may be affected by higher concentrations of MeHg.

To identify whether presynaptic mechanisms were involved in the effect of MeHg on synaptic transmission, we compared the latencies to block of responses of CA1 neurons to maximum stimulation of Schaffer collaterals and the response of CA1 neurons to direct application of glutamate on their apical dendrites. The rationale for comparing these responses was that iontophoretic application of glutamate directly onto the dendrites of CA1 cells could mimic the process of synaptic activation yet bypass the presynaptic release processes. If MeHg acts primarily at presynaptic sites to influence transmitter release, then responses of CA1 cells to electrical stimulation of Schaffer collaterals would be expected to be blocked, whereas responses of CA1 cells to iontophoresis of glutamate may not be blocked or be blocked more slowly. On the other hand, if MeHg primarily acts at postsynaptic sites, no matter where they are, then time to block of responses of CA1 to either electrical stimulation

or iontophoresis of glutamate would be similar. MeHg blocked action potentials evoked by electrical stimulation of Schaffer collaterals significantly faster than it blocked responses to iontophoretic application of glutamate. This suggests that MeHg may also affect transmitter release from presynaptic terminals, albeit less prominently compared to the postsynaptic actions of MeHg. Block of responses of CA1 neurons to either electrical stimulation of presynaptic terminals or direct application of neurotransmitter to apical dendrites of neurons often coincided with progressive depolarization of membranes. Nevertheless, this effect could not be ascribed simply to membrane depolarization because injection of current to hold membrane potentials at approximately their original values did not reverse the responses to either form of stimulation. Thus, mechanisms other than membrane depolarization may be involved as well.

Block of IPSPs by MeHg preceded block of EPSPs, suggesting that inhibitory interneurons may be more sensitive to MeHg than the CA1 pyramidal neurons. MeHg appeared first to increase EPSP amplitude prior to block. Actually, during the time of increase in EPSPs, action potentials were often superimposed on the EPSPs by stimulation at what had been a subthreshold stimulus prior to MeHg exposure, suggesting that excitability was increased. The time to suppress IPSPs generally appeared to correspond to the time of increased amplitude of EPSPs and also corresponded to the time of increased amplitude of population spikes obtained from previous extracellular

recordings (Yuan and Atchison, 1993; 1994). High concentrations of MeHg may act directly on GABA, receptors, since 100 µM MeHg decreased the GABA-induced Cl current of dorsal root ganglion neurons (Arakawa et al., 1991). Thus, MeHg may suppress GABA-induced Cl current resulting in decreased IPSPs and lessened inhibitory effects of interneurons on excitatory synaptic transmission. This disinhibition, in turn, may contribute in part to the increase in EPSP amplitude, firing of action potentials in response to a preset subthreshold stimulus and occurrence of multiple spikes in response to a single stimulus. However, both amplitudes of IPSPs and EPSPs are affected by the resting membrane potentials. Simply hyperpolarizing the cell membrane could result in decreased IPSP amplitude and increased EPSP amplitude. Since recordings of EPSPs and IPSPs in the present study were made under conditions in which the cells were allowed to be hyperpolarized or depolarized by MeHg, it is possible that the decreased IPSPs and increased EPSPs caused by MeHg may be due simply to the nonspecific effects of membrane hyperpolarization. Thus, further study is required to examine the relationship between the effects of MeHg on inhibitory and excitatory synaptic transmission.

In conclusion, MeHg initially alters CA1 neuronal membrane excitability and ultimately blocks hippocampal synaptic transmission. Multiple sites of action appear to be involved. The primary sites of action of MeHg appear to be the postsynaptic CA1 neurons, however, presynaptic mechanisms,

nonspecific effects of membrane depolarization and suppression of inhibitory systems and current conduction also appear to contribute to these effects caused by MeHg.

CHAPTER FOUR

ACTION OF METHYLMERCURY ON GABA, RECEPTORMEDIATED INHIBITORY SYNAPTIC TRANSMISSION IS PRIMARILY RESPONSIBLE FOR ITS EARLY STIMULATORY EFFECTS ON HIPPOCAMPAL CA1 EXCITATORY SYNAPTIC TRANSMISSION

ABSTRACT

Acute bath application of MeHg (4-100 µM) causes an early stimulation prior to block of synaptic transmission in the CA1 region of hippocampal slices. Effects of MeHg and Hg²⁺ on IPSPs or inhibitory postsynaptic currents (IPSCs) and EPSPs or excitatory postsynaptic currents (EPSCs) were compared to examine whether or not early block by MeHg of GABA_A-mediated inhibitory synaptic transmission and MeHg-induced alterations of the resting membrane potentials of CA1 neurons contribute to this initial enhancement of excitability. MeHg affected IPSPs and IPSCs similarly, and more rapidly than EPSPs and EPSCs. In contrast, while Hg²⁺ blocked IPSPs more rapidly than EPSPs, times to block of IPSCs and EPSCs by Hg2+ were virtually identical when CA1 neurons were voltage-clamped at their resting membrane potential levels. MeHg increased EPSC amplitudes prior to their subsequent decrease even when CA1 neuronal membranes were voltage-clamped at their resting This suggests that effects of MeHg on CA1 cell membrane potentials. potentials are not a major factor for MeHg-induced early stimulation of hippocampal synaptic transmission. Effects of MeHg and Hg²⁺ on the reversal potentials for IPSCs also differed. Both metals blocked all outward and inward currents generated at different holding potentials. However, MeHg shifted the current-voltage (I/V) relationship to more positive potentials, while Hg²⁺ often caused a transient and slight increase in outward currents prior to suppression

and shifted the I/V curve to more negative potentials. Hg2+ was a less potent blocker of IPSCs and EPSPs or EPSCs than was MeHg. To determine if the early increase in amplitude of population spikes or EPSPs is due to an action of MeHg at GABA, receptors, extracellular recordings of population spikes and intracellular recordings of EPSPs were compared with or without pretreatment of hippocampal slices with bicuculline. MeHg alone (20 or 100 µM) increased and then decreased amplitudes of population spikes and EPSPs to complete block. After pre-incubation of slices with 10 µM bicuculline for 30 - 60 min, MeHg only decreased the amplitudes of population spikes and EPSPs to block; no early increase of synaptic transmission occurred. Pretreatment of slices with strychnine, did not prevent MeHg-induced early increase in population spikes. MeHg also blocked responses evoked by bath application of muscimol, a GABA agonist. Thus, block by MeHg of GABA, receptor-mediated inhibitory synaptic transmission may result in disinhibition of excitatory hippocampal synaptic transmission, and appears to be primarily responsible for the initial excitatory effect of MeHg on hippocampal synaptic transmission.

INTRODUCTION

Acute bath application to hippocampal slices of the neurotoxic metal MeHg causes a concentration- and time-dependent biphasic effect on synaptic transmission in the CA1 region. Initially MeHg increases the amplitudes of field potentials recorded extracellularly (Yuan and Atchison, 1993; 1994) and EPSPs recorded intracellularly prior to suppression of them to block (Yuan and Atchison, 1995a). MeHg also blocks the recurrent IPSPs (Andersen et al.,1964a,b) in the CA1 region. IPSPs appeared to be more sensitive to MeHg than EPSPs, because block of IPSPs occurred earlier than did block of EPSPs. The time to the early suppression of IPSP amplitudes appeared to correspond to the onset of the early increase in amplitudes of both population spikes and EPSPs. This suggests that the reduced IPSPs contribute to the early increase in amplitudes of population spikes and EPSPs. MeHg suppresses the GABAinduced chloride current in dorsal root ganglion cells (Arakawa et al., 1991) and modulates the muscimol-induced increases in the [3H]flunitrazepam binding to GABA, receptors in washed cerebellar membranes (Komulainen et al., 1995). Thus, I hypothesized that block by MeHg of GABA, receptormediated inhibitory synaptic transmission results in disinhibition of hippocampal excitatory synaptic transmission, and is at least partly responsible for the initial stimulatory effects of MeHg on CA1 hippocampal synaptic transmission. However, MeHg also caused biphasic changes in

resting membrane potentials, i.e. initial hyperpolarization and then depolarization of pyramidal CA1 neurons in hippocampal slices (Yuan and Atchison, 1995a) and rat forebrain synaptosomes (Hare and Atchison, 1992). This effect alone could influence the observed changes in IPSP and EPSP amplitudes. Thus, nonspecific effects of MeHg on resting membrane potentials may also be involved in its early effects on synaptic transmission.

To test this hypothesis, extracellular recordings of population spikes, intracellular recordings of EPSPs and IPSPs and single-microelectrode voltageclamp recordings of excitatory and inhibitory postsynaptic currents (EPSCs, IPSCs) from CA1 pyramidal neurons were compared with or without pretreatment of hippocampal slices with bicuculline, a GABA, antagonist. Effects of inorganic mercury on these responses were also examined for the purpose of comparison. I sought to determine: 1) whether or not MeHg and inorganic mercury (Hg²⁺) affect IPSPs and EPSPs in hippocampal CA1 neurons differentially, since they differentially affect GABA-mediated chloride currents in dorsal root ganglion neurons (Arakawa et al., 1991; Huang and Narahashi, 1996) and field potentials recorded in CA1 neurons of hippocampal slices (Yuan and Atchison, 1994); 2) whether or not the differential block by MeHg of IPSPs and EPSPs is due to nonspecific effects of MeHg on resting membrane potentials; and 3) whether or not block of GABA_A-mediated IPSPs is primarily responsible for the early stimulation of hippocampal synaptic transmission. Since this early stimulation is a characteristic of the effects of MeHg-induced on central synaptic transmission, I sought to understand how this effect occurs, and how it pertains to the overall process of MeHg-induced neurotoxicity.

MATERIALS AND METHODS

Materials. Methylmercuric chloride, purchased from ICN Biomedical, Inc. (Costa, CA), was dissolved in deionized water to a final concentration of 5 mM to serve as stock solution. The applied solutions (4 - 500 µM) were diluted with ACSF. MeHg and other chemicals were applied acutely to slices by bath application at a rate of 1.2 - 1.5 ml/min with a Gilson (Middleton, WI) infusion pump. Strychnine hydrochloride and muscimol were purchased from Sigma Chemical Co (St. Louis, MO). Muscimol (25 - 100 µM) was applied to slices for 15 - 30 sec at an interval of 10 min to avoid desensitization of GABA 6-Cyano-7-nitroquinoxaline-2,3-dione (CNQX), receptors. dinitroquinoxaline-2,3-dione (DNQX), D(-)-2-amino-5-phosphonopentanoic acid (AP-5) and (-)-bicuculline methbromide were obtained from Research Biochemical International (Natick, MA). CNQX or DNQX were dissolved first in dimethyl sulfoxide (DMSO) and then diluted further with ACSF. The final concentration of DMSO in the applied solution was less than 0.02% (v/v), which has no significant effects on synaptic transmission.

Preparation of hippocampal slices. Hippocampal slices were prepared using methods described previously in Chapter Two and Three.

Electrophysiological procedures. Conventional extracellular and intracellular recordings were made in the CA1 region of the hippocampal slice. Monopolar tungsten electrodes (3 M Ω , FHC, Brunswick, ME) were used as stimulation electrodes. Borosilicated glass microelectrodes (o.d. 1.0 mm; i.d 0.5 mm, WPI, Inc., New Haven, CT) filled with ACSF (5 - 15 M Ω) or 3 M potassium acetate (80 - 120 M Ω) were used for extracellular or intracellular recording respectively. Population spikes were evoked by orthodromicstimulation of Schaffer collaterals at an intensity level (usually 2 - 4 V) that gives a population spike amplitude approximately 50% of the maximum amplitude as evoked by maximum stimulation. Intracellular EPSPs were recorded at CA1 cell soma by subthreshold stimulation (0.2 Hz) of Schaffer collaterals; typically a 0.1 - 0.2 nA negative D.C. current was applied through the recording electrode to maintain the cell membrane in a somewhat hyperpolarized state to avoid evoking action potentials. The recurrent IPSPs (Andersen et al., 1964a,b) were recorded by subthreshold stimulation of the alveus. IPSCs and EPSCs were recorded using single-microelectrode voltage clamp techniques (Johnston et al., 1980; Johnston and Brown, 1981; 1984). The sample frequency was set at 8 kHz or as high as possible. When measuring the current-voltage relationship, voltage step commands were generated from an internal step command generator and manually controlled by the thumbwheel switch on the front panel of an Axoclamp-2 amplifier. For each voltage step, the cell was held at that potential for 30 - 40 sec to obtain at least 3 - 5 traces of IPSCs. The membrane input resistance was monitored by D.C. current injection through the recording electrode. All stimulus pulses were generated from a Grass S88 stimulator (Grass, Inc., Quincy, MA) at 0.2 Hz and 0.1 msec duration and isolated with a Grass SIU5 stimulus isolation unit (Grass, Inc.). Recorded signals were amplified (Axoclamp-2, Axon Instruments Inc., Burlingame, CA), displayed on a 2090-3 digital oscilloscope (Nicolet Instruments, Verona, WI) and recorded simultaneously to both floppy disks and magnetic tape by using a FM instrumentation recorder (Model B, Vetter Instruments, Rebersburg, PA) for later analysis. All measurements reported in this thesis were made based on the peak amplitude of response.

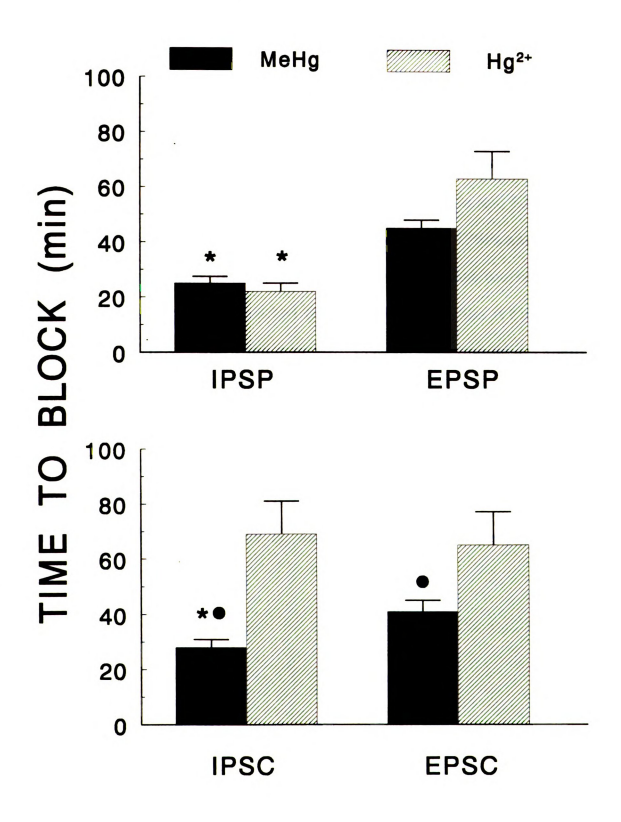
Statistical analysis. Data were collected continuously before and during application of MeHg and analyzed statistically using Student's t-test or paired t-test or a one-way analysis of variance; Dunnetts' procedure was used for *post-hoc* comparisons (Steel and Torrie, 1980). Values were considered statistically significant at p < 0.05.

RESULTS

Comparative effects of MeHg and Hg^{2+} on IPSPs and EPSPs or IPSCs and EPSCs. As shown in my previous report (Yuan and Atchison, 1995a), 100 μ M MeHg blocked IPSPs more rapidly than it did EPSPs; times to block were 25 ± 2 and 45 ± 3 min, respectively (Figure 4.1 Top). In some slices, both EPSPs and IPSPs were recorded simultaneously in the same neuron. In these recordings, an early increase in EPSP amplitude or even firing of action potentials often accompanied the decrease in IPSP amplitude at the early times of application of MeHg. At the same concentration, Hg^{2+} blocked IPSPs with a time course similar to that of MeHg. However, Hg^{2+} blocked EPSPs (63 \pm 10 min) more slowly than did MeHg.

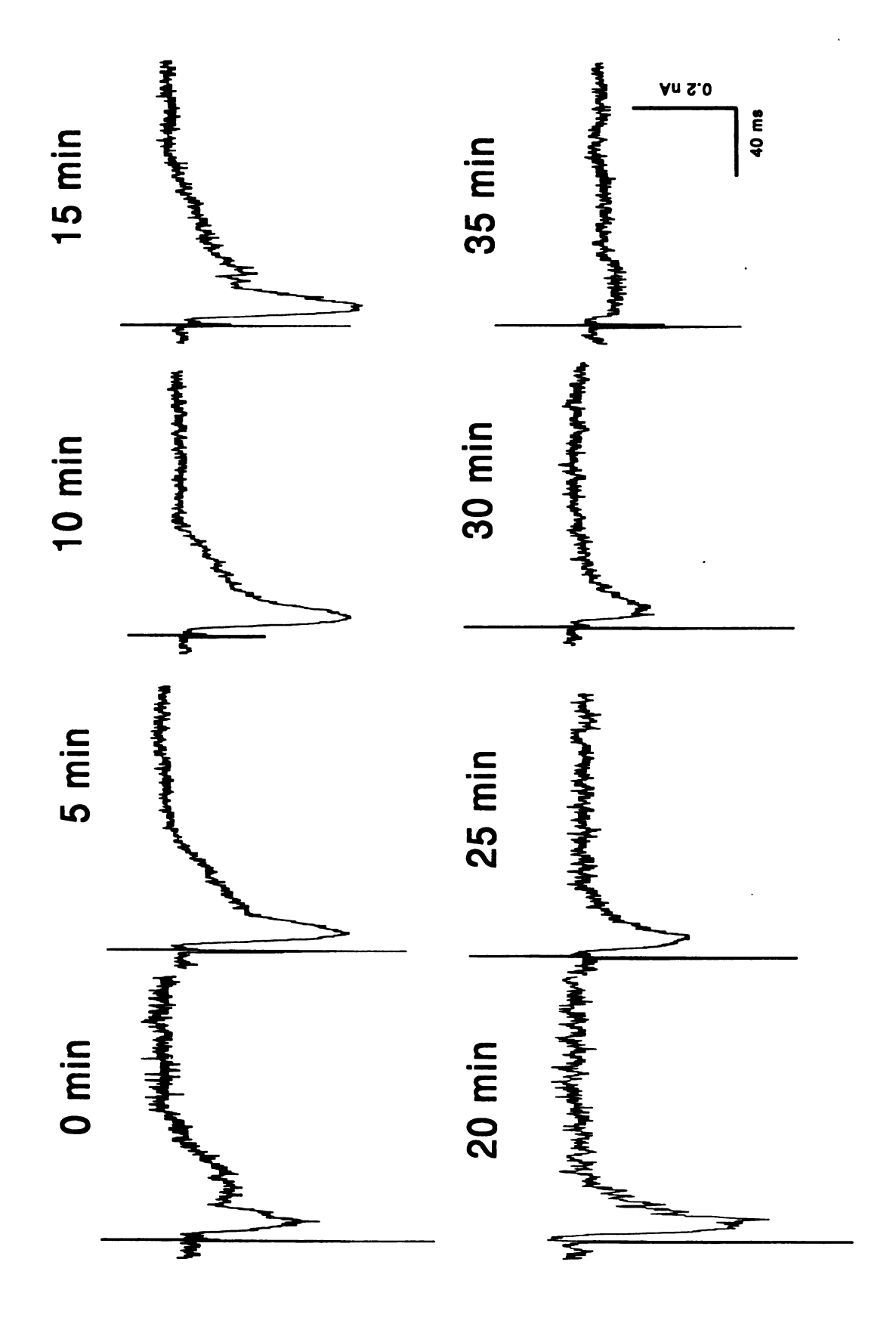
Both MeHg and Hg²⁺ alter resting membrane potentials of various excitable cells (Juang and Yonemura, 1975; Juang, 1976a,b; Shrivastav *et al.*, 1976; Miyamoto, 1983; Kauppinen *et al.*, 1989; Hare and Atchison, 1992). In hippocampal slices, acute bath application of MeHg or Hg²⁺ depolarized the CA1 neuronal membrane. However, in many slices hyperpolarization occurred prior to depolarization (Yuan and Atchison, 1995a,b). Since amplitudes of both IPSPs and EPSPs are affected by the resting membrane potentials, polarizing the cell membrane could contribute indirectly to effects of MeHg or Hg²⁺ on synaptic potential amplitude. As such, single-microelectrode voltage-clamp was used to examine the effects of mercurials on the IPSCs and EPSCs, and thus

Figure 4.1. Comparison of times to block of recurrent IPSPs and EPSPs (Top) or IPSCs and EPSCs (Bottom) by 100 μM MeHg or Hg²⁺. IPSPs and EPSPs were recorded in CA1 pyramidal cell soma by stimulating the alveus or Schaffer collaterals. IPSCs were recorded at their resting membrane potential levels in the presence of 20 μM AP-5 and 10 μM DNQX. EPSCs were evoked by presynaptic stimulation of Schaffer collaterals and recorded at CA1 pyramidal cell soma at their resting potentials levels. All values are the mean ± SE of 5 - 12 individual experiments. The asterisk (*) indicates a significant difference between times to block of IPSPs and EPSPs or IPSCs and EPSCs (p < 0.05). The black dot (●) indicates a significant difference between times to block of IPSCs or EPSCs by MeHg and Hg²⁺ (p < 0.05, student's t-test)).

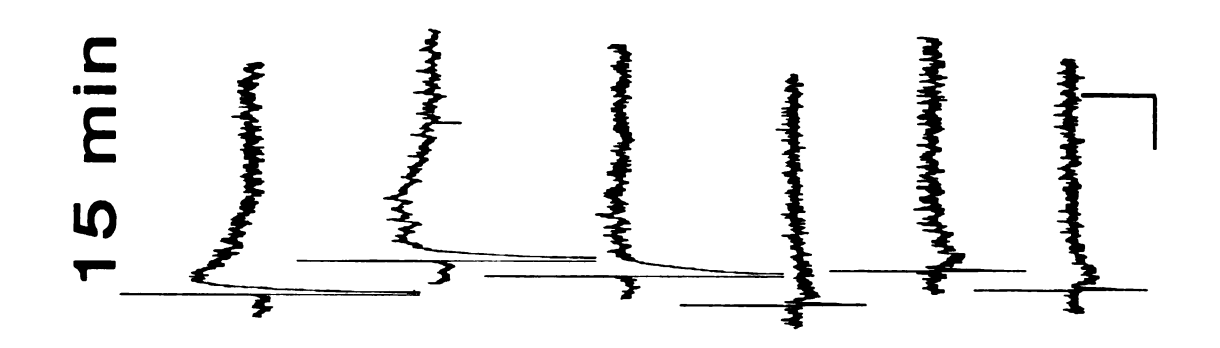


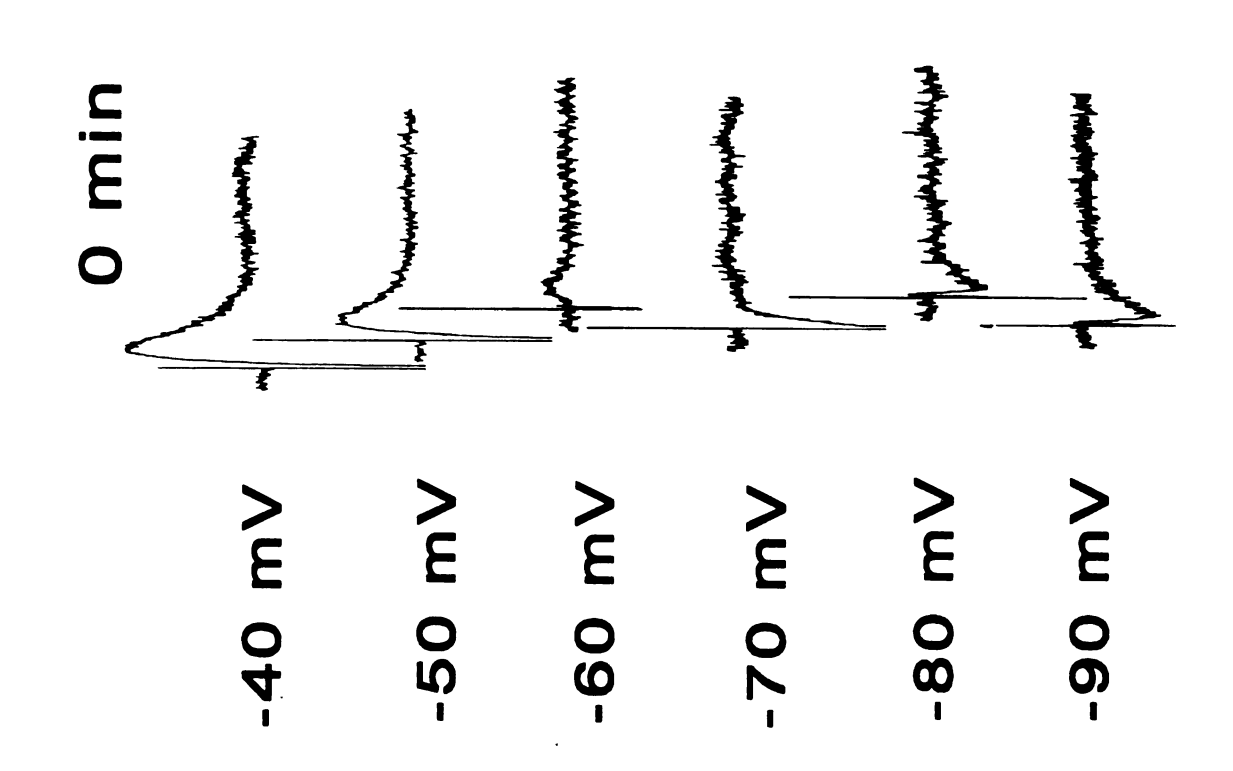
determine whether nonspecific effects of MeHg or Hg²⁺ on CA1 pyramidal cell resting potential contributed to the observed changes in EPSP and IPSP amplitude. IPSCs were recorded after pretreatment of slices for 30 min with and in the continuous presence of 20 µM AP-5 and 10 µM CNQX or DNQX in ACSF to block NMDA receptor- and non-NMDA receptor-mediated excitatory synaptic transmission. When CA1 neuronal membrane potentials were held at their resting levels (- 67 ± 2 mV), times to block of IPSCs and EPSCs for MeHg (100 µM) were virtually identical to those for block of IPSPs and EPSPs (Figure 4.1 Bottom). Hg²⁺ (100 µM) blocked EPSCs with a time course similar to that on EPSPs, however, it blocked IPSCs more slowly than it did IPSPs. Times to block of IPSCs and EPSCs by Hg^{2+} were 69 ± 12 and 65 ± 12 min, Moreover, MeHg still caused an early increase in EPSC respectively. amplitude prior to suppressing it even under voltage-clamp conditions (Figure 4.2). Thus changes in resting membrane potentials are not a primary factor for effects of MeHg on IPSPs and EPSPs or effects of Hg²⁺ on EPSPs. Effects of Hg²⁺ on IPSPs however may be due in part to alterations of resting membrane potential.

Figure 4.2. Time course of effect of 100 µM MeHg on EPSCs recorded from CA1 pyramidal cells of electrical stimulation Schaffer collaterals and recorded at the CA1 pyramidal cell soma which was voltage-clamped at its resting membrane potential (-77 mV in this case). Each trace is a representative hippocampal slices using single-microelectrode voltage-clamp techniques. EPSCs were evoked by depiction of 4 experiments which show the biphasic effects of MeHg on EPSCs.

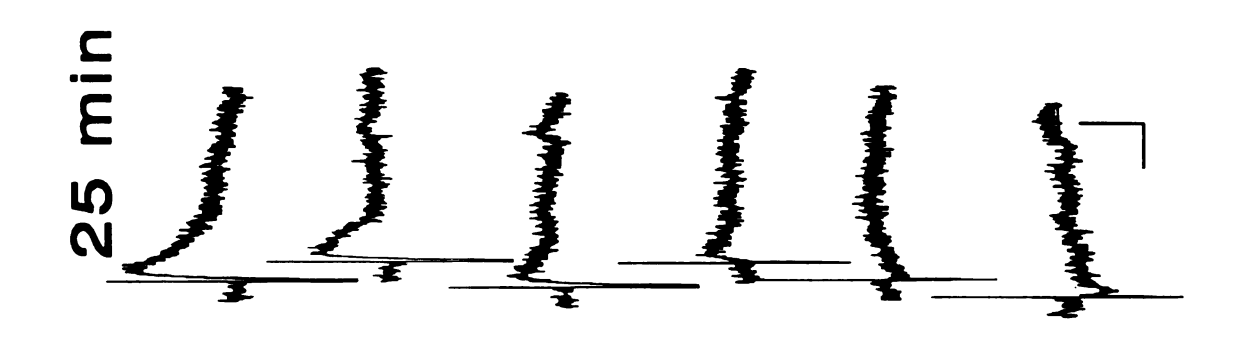


Comparative effects of MeHg and Hg2+ on current-voltage relationship of IPSCs Figures 4.3 and 4.4 compares the effects of 100 µM MeHg and Hg²⁺ on a family of IPSCs evoked at potentials of -40 to -90 mV. Figure 4.5 depicts the current-voltage relationship (I/V curve) for these IPSCs. The IPSC reversal potential is approximately -75 mV in the absence of MeHg which is close to the equilibrium potential for Cl as predicted by the Nernst equation, and similar to these values obtained by Benardo (1994) and Pitler and Alger (1994), indicating that these IPSCs are primarily GABA_A receptormediated chloride currents. MeHg suppressed both outward and inward currents; this effect usually started after 5 min of application of 100 µM MeHg. As shown in Figures 4.3 and 4.5 (left) exposure of slices to 100 µM MeHg for 15 min, resulted in depression of all IPSCs evoked at holding potentials of -40 to -90 mV. The I/V curve and the reversal potential were shifted to more positive potentials. In contrast, whereas 100 µM Hg²⁺ suppressed both outward and inward currents, Hg2+ initially caused an increase in the outward current prior to suppressing it. Moreover, Hg^{2+} shifted the I/V curve and the reversal potential to a more negative potential direction (Figure 4.4 and 4.5 right). At 20 μM the respective effects of MeHg or Hg²⁺ were similar but the latency to onset of action was much longer than at 100 µM (results not shown). Figure 4.3. Effects of 100 µM MeHg on IPSCs recorded at different holding potentials. IPSCs were evoked by presynaptic stimulation of Schaffer collaterals and recorded at CA1 pyramidal cell soma of hippocampal slices in the presence of 20 µM AP-5 and 10 µM DNQX. Time 0 min represents IPSCs recorded at different holding potentials before application of MeHg. Time 15 min indicates the time after exposure of the slice to 100 µM MeHg. Calibration bars: vertical, 300 Pa; horizontal, 50 ms.





evoked by presynaptic stimulation of Schaffer collaterals and recorded at CA1 pyramidal cell soma of Figure 4.4. Effects of 100 µM Hg²⁺ on IPSCs recorded at different holding potentials. IPSCs were hippocampal slices in the presence of 20 µM AP-5 and 10 µM DNQX. Time 0 min represents IPSCs recorded at different holding potentials before application of Hg²⁺. Time 25 min indicates the time after beginning perfusion of the slice with 100 µM Hg²⁺. Calibration bars: vertical, 300 Pa; horizontal, 50 ms.



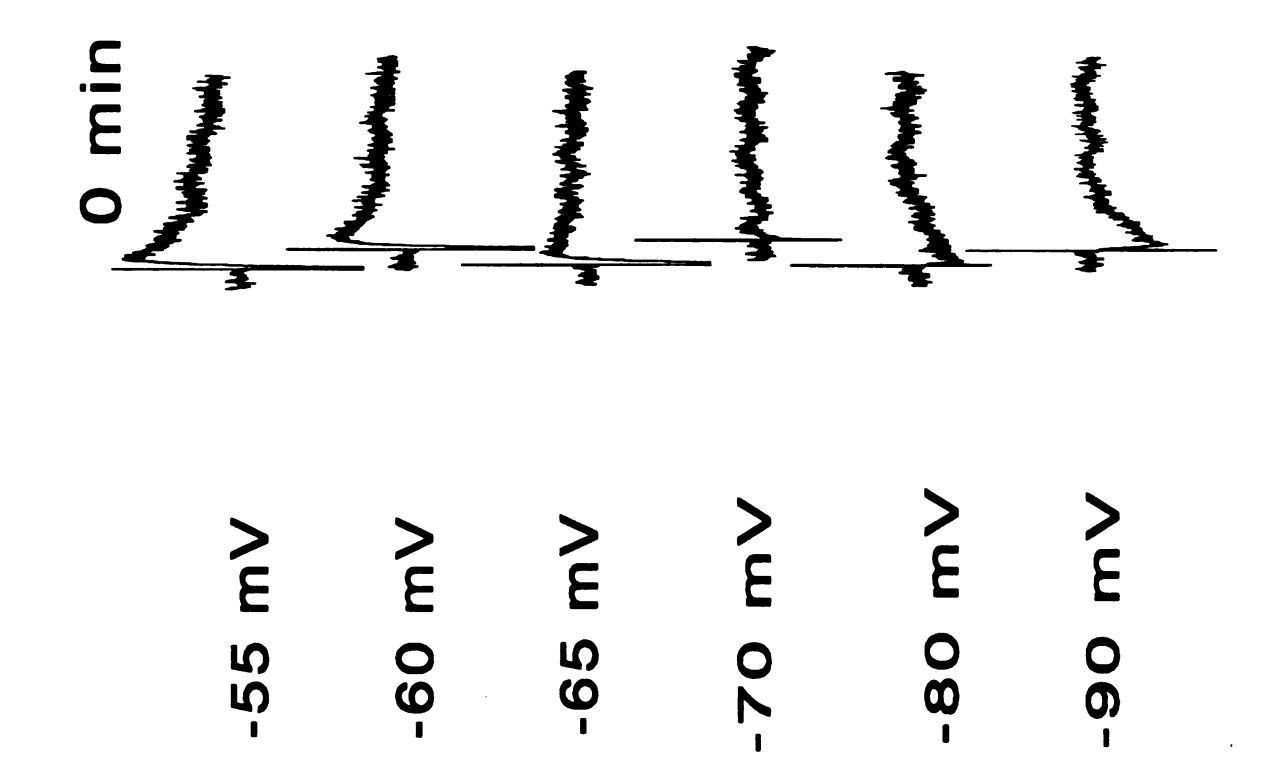
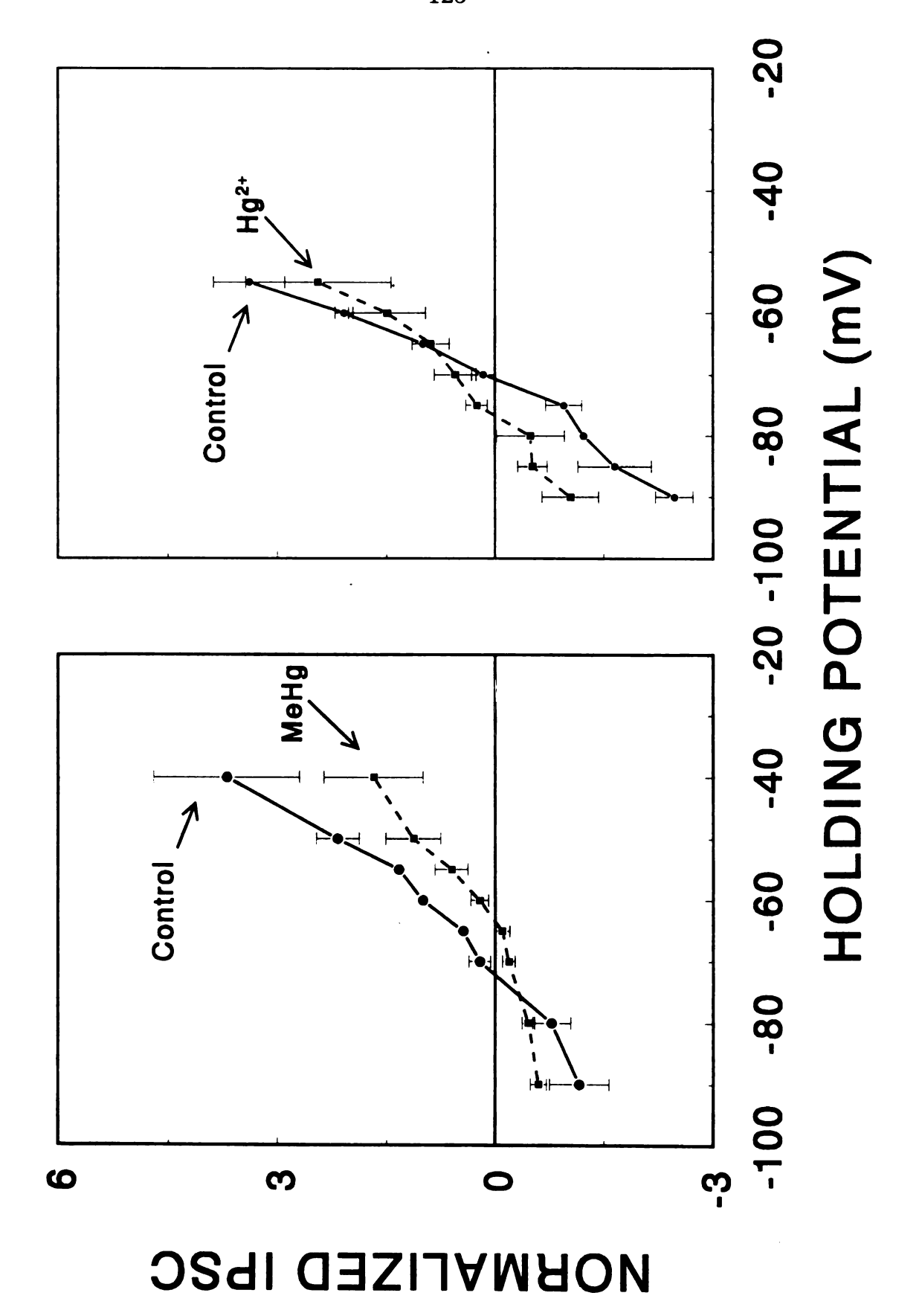


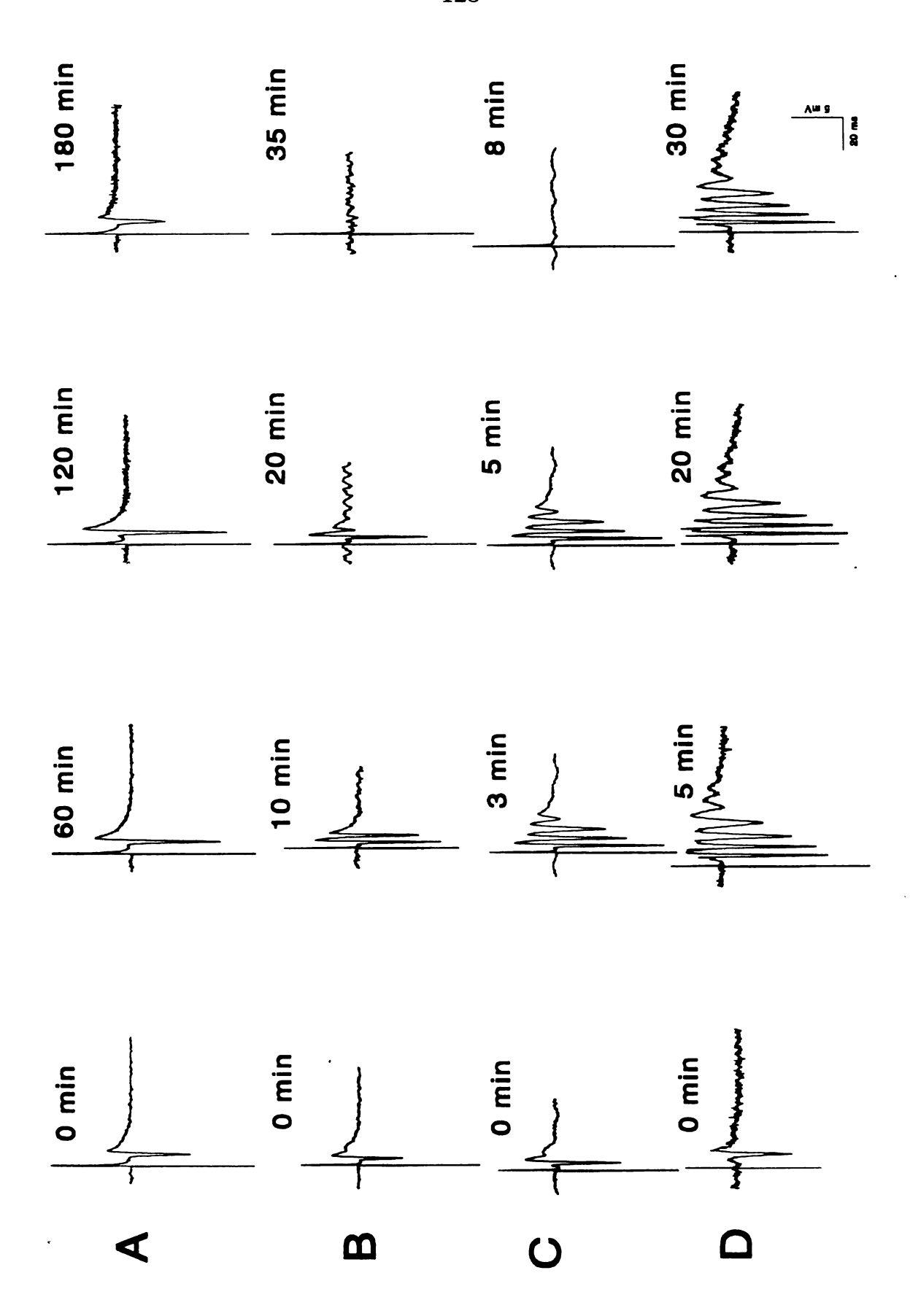
Figure 4.5. Comparison of effects of 100 µM MeHg (Left) and Hg²⁺ (Right) on the current-voltage relationship (IV curve) of IPSCs recorded in the CA1 pyramidal cells. IPSCs were normalized to their resting membrane potentials. Values are the mean ± SE of 4 - 5 individual experiments.



Comparative effects of MeHg and bicuculline on population spikes. Since MeHg suppresses the GABA_A-mediated chloride currents in hippocampal CA1 neurons, I sought to determine if its effects are similar to those of bicuculline, a selective GABA, receptor antagonist. To test this, I compared the effects of 20 - 500 µM MeHg and 10 µM bicuculline on population spikes. I used these higher concentrations of MeHg because I previously showed that the higher concentrations of MeHg induced a more rapid and noticeable increase in population spikes which was often accompanied by repetitive firing (Yuan and Atchison, 1993). At 20 - 500 µM, MeHg caused a concentration- and time-dependent early increase in amplitudes of population spikes prior to blocking them (Figure 4.6). Higher concentrations (100 and 500 µM) of MeHg induced repetitive firing in response to single shock stimuli, suggesting that membrane excitability was increased. The early stimulatory effects of MeHg on population spikes were similar to those of bicuculline on population spikes.

Effects of bicuculline pretreatment on MeHg-induced early stimulation of synaptic transmission. The early increase in excitatory synaptic transmission may be due primarily to MeHg-induced suppression of GABA_A receptor-mediated chloride currents. This in turn may lessen the inhibitory effects of interneurons on excitatory synaptic transmission. If so, then pretreatment of slices with bicuculline to block GABA_A receptor-mediated

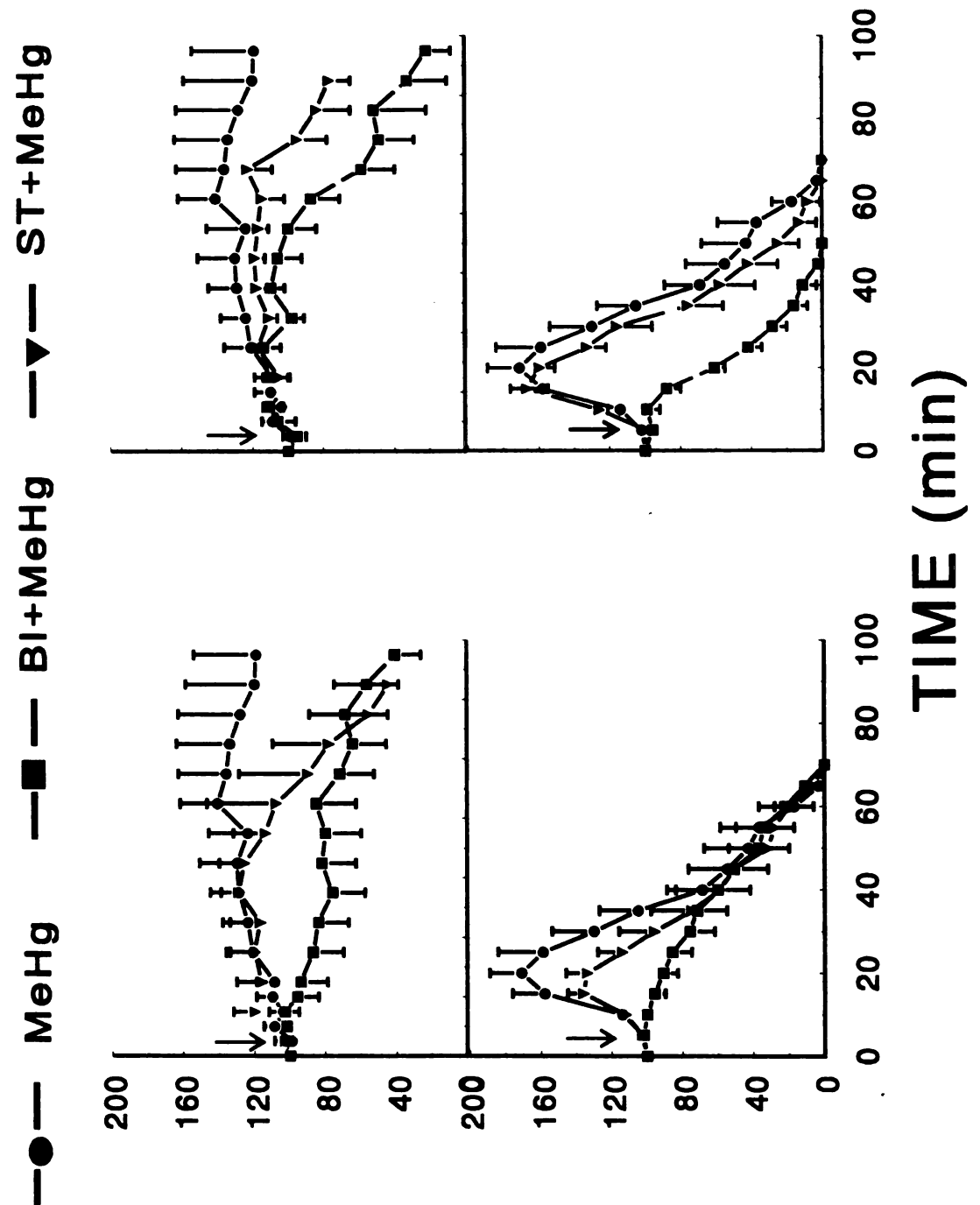
MeHg and 10 µM (D) bicuculline on population spikes. Each trace is a representative depiction of 6 to Figure 4.6. Comparison of effects of MeHg and bicuculline on population spikes of hippocampal pyramidal cells. From top to bottom are the time courses of effects of 20 (A), 100 (B) and 500 µM (C) 10 experiments. Calibration bars: vertical, 5 Mv; horizontal, 20 ms.



chloride currents should eliminate or suppress the MeHg-induced early increases in population spike amplitudes. To test this, I compared effects of 20 and 100 µM MeHg on population spike amplitudes in the presence or absence of bicuculline. Incubation of slices with 10 µM bicuculline for 5 - 10 min increased the amplitudes of population spikes significantly; moreover the single spike response gradually changed to multiple spike responses. After 30-60 min of bicuculline, population spike amplitudes typically increased to and stabilized at 150 - 200% of control (Figure 4.6D). At this point, two sets of experiments were designed to examine the effects of bicuculline on the early stimulation by MeHg of excitatory synaptic transmission. In the first set of experiments 20 or 100 µM MeHg plus 10 µM bicuculline was added to the ACSF with no change in stimulus intensity. Under these conditions, MeHg still suppressed population spike amplitude as did MeHg alone, but in 4 of 6 slices caused no further significant early increase in population spike amplitudes (Figure 4.7 Left). The second set of experiments was performed under reduced stimulus intensity. The reason for doing this was that we were concerned that pretreatment of slices with bicuculline might increase population spike amplitudes to a ceiling amplitude, above which MeHg was unable to cause further increase, thus masking the actual effect of MeHg on population spikes. Thus, the stimulus intensity was reduced to a level that gave population spike amplitudes approximately equal to the control level prior to bicuculline treatment, after the bicuculline-induced increase had stabilized.

Figure 4.7. Time courses of effects of MeHg on population spikes of hippocampal pyramidal cells with without changes in the stimulation intensity until 120 min or complete block of population spikes occurred. The starting time point for superfusion of MeHg, as indicated by the downward arrow (\downarrow) , was or without pretreatment of slices with bicuculline (BI) or strychnine (ST). Left: Slices were pretreated with ACSF containing 20 (Top) or 100 µM (Bottom) MeHg and 10 µM bicuculline or 50 µM strychnine Right: Slices were pretreated with 10 µM bicuculline or 50 µM strychnine for 30 - 60 min (Omitted in this graph), the arrow (\downarrow) , until 120 min or block of population spikes occurred. All values are the mean \pm SE of 6 - 13 with 10 µM bicuculline or 50 strychnine for 30 - 60 min (Omitted in this graph), and then superfused stimulation intensity was then reduced to a level that gave amplitudes of population spikes roughly approximate to their pretreatment values. This time point was defined as 0 min and the data collected at this point were defined as 100%. Slices were then superfused with ACSF containing 20 µM (Top) or 100 µM (Bottom) MeHg and 10 µM bicuculline or 50 µM strychnine, as indicated by the downward defined as 0 min and the data collected at this point were defined as 100%. individual experiments.

(lortnoo to %) BUUTIJ9MA



MeHg (20 or 100 µM) plus 10 µM bicuculline were then applied to the slices. As seen with the results of the first set of experiments, MeHg did not cause significant early increase in population spike amplitudes but reduced or blocked completely population spikes in 3 of 4 and 5 of 7 slices at 20 and 100 µM MeHg respectively (Figure 4.7 Right). In the remaining slices there was a 10 - 15% early increase in population spike amplitudes prior to block by MeHg. This effect was not significant, and is masked in Figure 4.7 due to averaging of the time courses from the individual experiments. Without pretreatment of slices with bicuculline, 20 and 100 µM MeHg caused the typical biphasic changes in amplitudes of population spikes, although the early increase in amplitude induced by 20 µM MeHg was not as prominent as that caused by 100 µM MeHg (Figure 4.7). Due to variations in time course of effects of MeHg among the individual experiments, Figure 4.7 does not show any decrease in population spike amplitudes after exposure to 20 µM MeHg alone for 100 min. However, prolonging exposure of slices to 20 µM MeHg to 150 - 180 min, caused suppression or block of all population spikes (Figure 1.1 and 4.6). It appears that MeHg blocked responses more rapidly in slices treated with bicuculline than in slices not pretreated with bicuculline. To test if bicuculline would prevent early increase in EPSP amplitude induced MeHg, effects of MeHg on EPSPs were examined in the presence of 10 µM bicuculline. Normally, EPSPs were evoked by subthreshold stimulation of Schaffer collaterals to avoid generation of action potentials. After application of 10 µM bicuculline for 30 - 60 min, EPSP amplitude increased dramatically and induced multiple spikes (Figure 4.8). Once the increase in EPSP amplitude reached a stable level, the stimulus intensity was then reduced to a level that gave a measurable EPSP but did not initiate action potentials. It was generally quite difficult to do this after pretreatment of slices with bicuculline, because either action potentials were generated or the EPSP at a given stimulus was not measurable. Thus I am only able to obtain a few successful recordings for this experiment. However, in those experiments MeHg failed to cause a significant early increase in EPSP amplitude in the presence of 10 µM bicuculline as was seen in Figure 4.7 for field potential recordings. Thus MeHg-induced early increases in amplitudes of population spikes and EPSPs appear to be related to its actions on GABA_A receptors.

The results of the previous experiment do not rule out the possibility that MeHg directly affects GABA release from interneurons via a presynaptic mechanism. Thus, to test if the effects of MeHg are due to a direct action on GABA_A receptors I examined the effects of MeHg on responses evoked by muscimol, a GABA_A agonist. Bath application of 25 - 100 µM muscimol to slices for 15 - 30 sec caused a concentration-dependent depolarization of CA1 pyramidal neurons. It usually took about 6 to 10 min of wash to restore the depolarized membrane back to the pre-muscimol application baseline. The muscimol-evoked responses were blocked rapidly by 20 µM bicuculline (Figure 4.9 Top), suggesting that they are GABA_A receptor-mediated responses. MeHg

Figure 4.8. Time course of effects of 100 µM MeHg on EPSPs of hippocampal CA1 pyramidal cells evoked in the presence of bicuculline. EPSPs were recorded from a CA1 neuron of a hippocampal slice min (from -30 min to 0 min), EPSPs were increased greatly in amplitude and had multiple spikes that for traces at other time points). At 0 min, the stimulation intensity was reduced to a level that S by subthreshold stimulation of the Schaffer collaterals. After perfusion with 10 µM bicuculline for 30 failed to evoke any spikes. The slice was then superfused with ACSF containing 100 µM MeHg and 10 superimposed on them (note that the vertical calibration bar for the trace at -10 min is different from µM bicuculline until complete block of EPSPs occurred. Each trace is a representative depiction of recordings

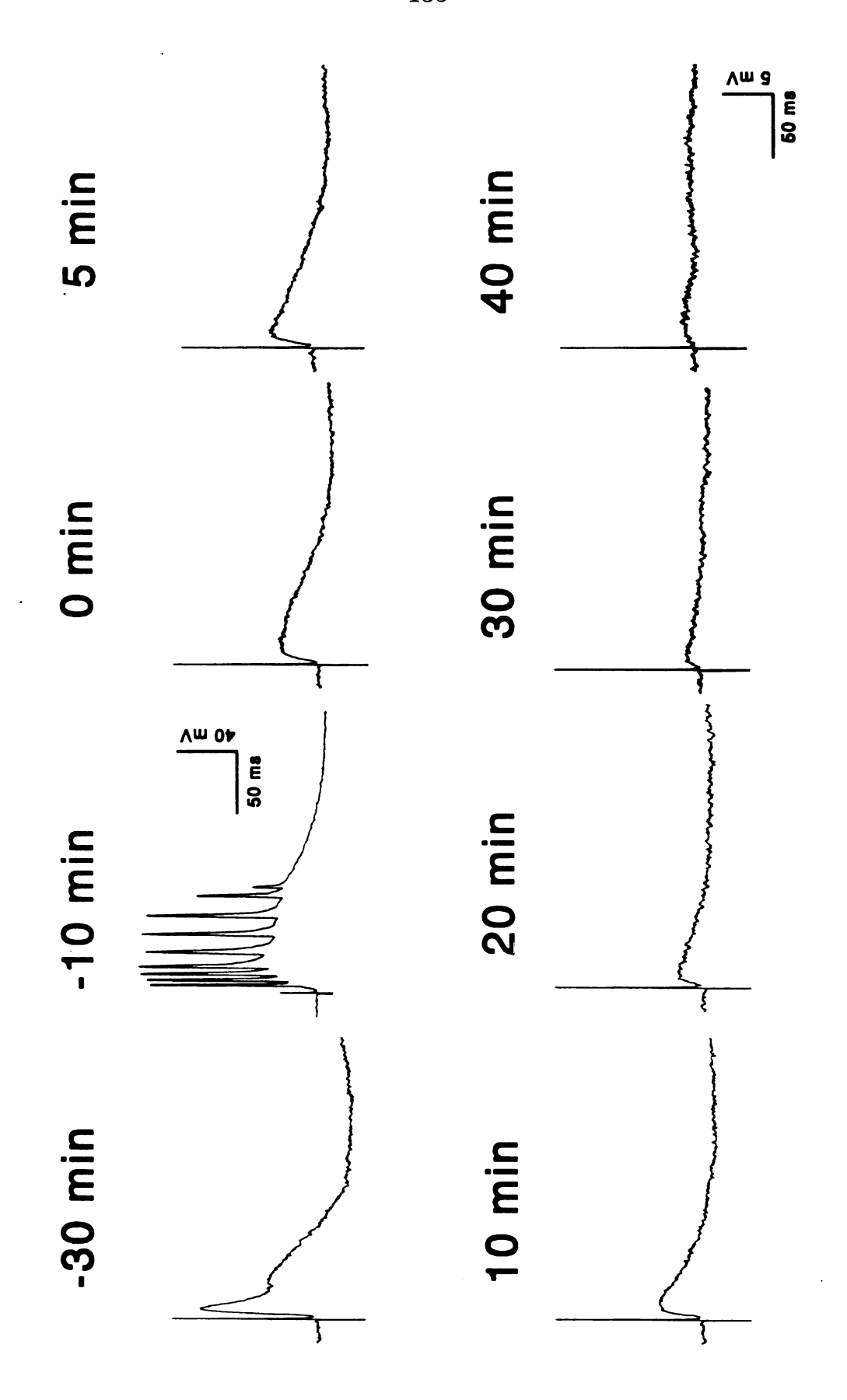
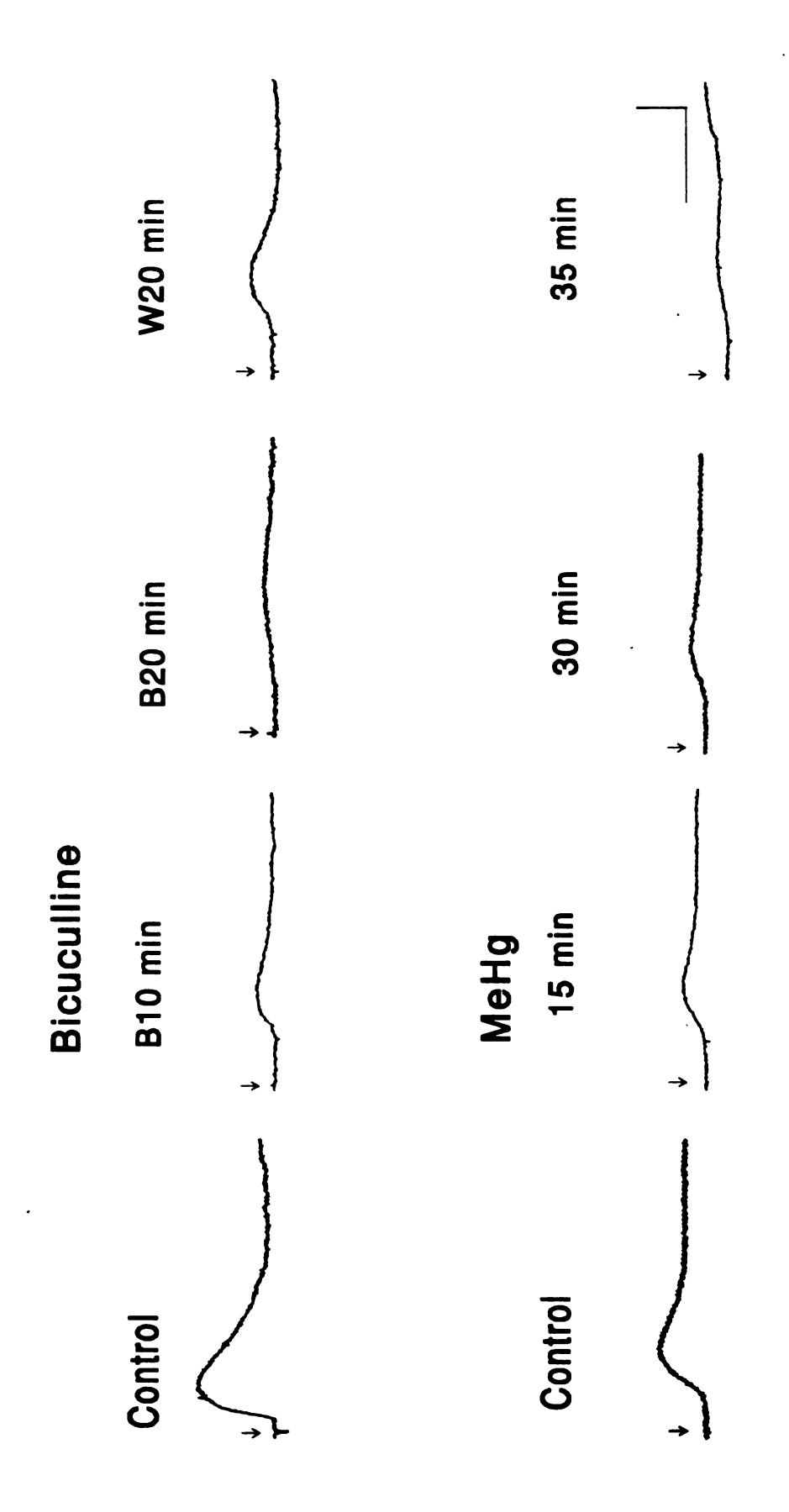


Figure 4.9. Effects of 20 µM bicuculline and 100 µM MeHg on muscimol-evoked responses in CA1 pyramidal cells in the presence of 20 µM AP-5 and 10 µM DNQX in ACSF. Bath application to muscimol-evoked responses. After the muscimol-evoked response was blocked completely, washing the hippocampal CA1 pyramidal cells. Conventional intracellular microelectrode recordings were made in effects of application of 20 µM bicuculline for 10 min (B10 min) and 20 min (B20 min) on 100 µM slices of 100 µM (Top) or 50 µM (Bottom) muscimol for 15 sec caused a depolarizing response. Top: slice with bicuculline-free ACSF for 20 min partially reversed its effect. Bottom: time course of effect of 100 µM MeHg on 50 µM muscimol-evoked response. Arrows indicate the starting point of application of muscimol. Each trace is a representative depiction of 3 - 9 experiments. Calibration bars: vertical, 20 Mv; horizontal, 100 sec.



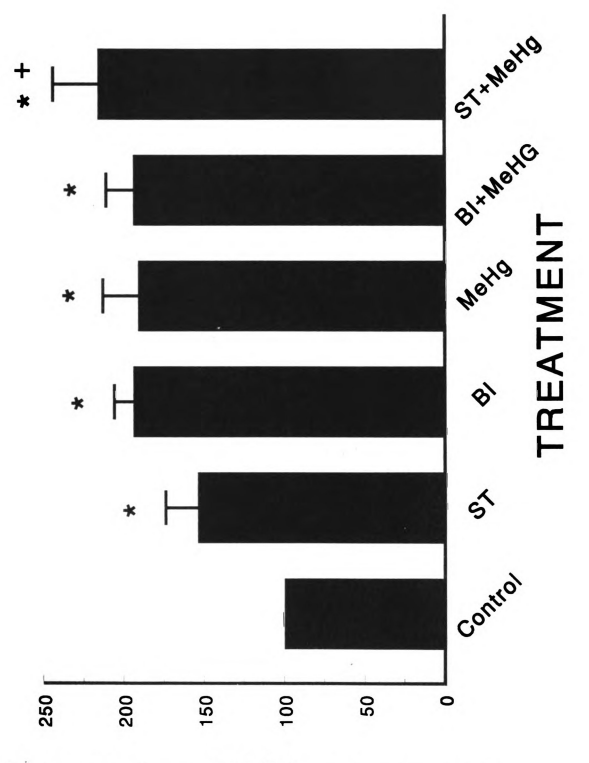
also blocked these muscimol-evoked responses (Figure 4.9 Bottom), which was consistent with the report of Komulainen et al., (1995). Times to block by 100 µM MeHg of muscimol-evoked depolarization varied from 20 to 50 min in 11 experiments, depending on the concentration and duration of muscimol application. MeHg blocked the depolarization evoked by 25 µM muscimol more rapidly than that evoked by 50 or 100 µM muscimol. In these experiments, it was difficult to determine the exact time to block by MeHg of muscimol-evoked responses due to the long time interval required for washing out muscimol from slices before the next application. However, the times to block of muscimol-evoked responses, especially those evoked by lower concentrations of muscimol, were generally similar to those to block of IPSPs or IPSCs by MeHg. This suggests a direct action of MeHg at the GABA_A receptor sites although additional presynaptic mechanisms could still occur.

Effects of strychnine on MeHg-induced early stimulation of CA1 synaptic transmission. GABA is generally believed to be the major inhibitory transmitter in the mammalian CNS. However, glycine also serves as an inhibitory transmitter in the CNS, especially in the spinal cord and brain stem (Aprison and Daly, 1978; Pycock and Kerwin; 1981; McCormick, 1990). Additionally, glycine can potentiate the action of glutamate at NMDA receptors (Johnson and Ascher, 1987), although this response is generally assumed to be strychnine-insensitive (Kishimoto et al., 1981). To test whether or not a

putative glycine receptor also plays a role in MeHg-induced early stimulatory effects on hippocampal synaptic transmission, slices were perfused with 50 µM strychnine, a glycine receptor antagonist, prior to and during exposure to 20 or 100 µM MeHg. In a similar manner to that of bicuculline, strychnine also caused a significant increase in population spike amplitudes and induced repetitive firing, although not as prominently as did bicuculline. However, unlike the effects of MeHg on population spikes in the presence of bicuculline, MeHg caused a further significant increase of population spike amplitude above that already elevated by strychnine. This effect occurred irrespective of whether or not stimulus intensity was reduced (Figure 4.7). Thus glycine receptors do not play a major role in the MeHg-induced early stimulation of hippocampal synaptic transmission. Figure 4.10 summarizes the effects of MeHg, bicuculline and strychnine alone and in combination with MeHg on population spike amplitude. Clearly, MeHg, bicuculline and strychnine all increase population spike amplitudes significantly. However, pretreatment of slices with bicuculline prevented the MeHg-induced early increase in population spike amplitudes, whereas pretreatment of slices with strychnine failed to do so.

pyramidal cell population spikes by strychnine (ST, 50 µM), bicuculline (BI, 10 µM) and MeHg alone, with the combinations of MeHg with bicuculline (BI + MeHg) or strychnine (ST + MeHg). In the BI + MeHg or ST + MeHg- groups, slices were superfused first with strychnine or bicuculline for 30 to 60 min, and then with ACSF containing both MeHg and strychnine or bicuculline. The asterisk (*) indicates a significant difference between values of control and slices treated with ST, BI, MeHg or BI + MeHg (p < 0.05, ANOVA). The dagger indicates a significant difference between values of ST and ST + MeHg Figure 4.10. Comparison of the maximum stimulation of population spikes of CA1 hippocampal (p < 0.05, paired t test)

AMPLITUDE PEAK (% of control)



DISCUSSION

Previously I showed that acute bath application of MeHg caused an initial stimulation of hippocampal synaptic transmission prior to suppression to block (Yuan and Atchison, 1993, 1995a). Under similar conditions, Hg²⁺ blocked synaptic transmission in the CA1 region of hippocampal slices but did not induce the early stimulatory effects (Yuan and Atchison, 1994). The primary objective of the present study was to identify the potential factor(s) responsible for the early stimulatory effects of MeHg on hippocampal synaptic transmission. Previous results of microelectrode current-clamp recordings suggested that effects of MeHg on inhibitory synaptic transmission and on resting membrane potentials may be involved in the MeHg-induced early stimulation of hippocampal synaptic transmission, because MeHg blocked IPSPs more rapidly than it did EPSPs, and caused biphasic changes in resting membrane potentials of CA1 pyramidal neurons (Yuan and Atchison, 1995a). In the present study, I reconfirmed that IPSPs are more sensitive to MeHg than are EPSPs, and demonstrated that this effect is not related to MeHginduced changes in resting membrane potentials of CA1 neurons, because times to block by MeHg of IPSCs and EPSCs recorded under voltage-clamp conditions were similar to those for block of IPSPs and EPSPs recorded under current-clamp conditions. Moreover, voltage-clamp of neuronal membranes at their resting potential levels failed to prevent the MeHg-induced early increase

in EPSC amplitude. In contrast, Hg^{2+} also blocked IPSPs more rapidly than it did EPSPs. However, it blocked IPSCs and EPSCs similarly when CA1 neuronal membranes were voltage-clamped at their resting potentials, suggesting that the early block by Hg^{2+} of IPSPs compared with that for EPSPs may be due simply to changes in resting membrane potential. Thus, MeHg blocked inhibitory synaptic transmission more preferentially, although it also blocked excitatory synaptic transmission, whereas Hg^{2+} blocked both inhibitory and excitatory transmission to the same extent and relatively slowly. This is consistent with our previous observations that MeHg caused early stimulatory effects on hippocampal synaptic transmission, while Hg^{2+} did not (Yuan and Atchison, 1994).

In dorsal root ganglion neurons, MeHg suppressed GABA-mediated chloride currents, while Hg²⁺ greatly enhanced these currents in a concentration-dependent manner (Arakawa et al., 1991; Huang and Narahashi, 1996). In the present study, the IPSCs recorded at CA1 neurons appear to be primarily GABA_A-mediated chloride currents, since their reversal potentials are close to the equilibrium potential of Cl⁻ and these currents can be blocked by bicuculline. At 20 and 100 µM, MeHg suppressed all inward and outward currents generated at different holding potentials and shifted the I/V curve to more positive potentials, suggesting that MeHg may block the GABA_A-mediated chloride channels. MeHg has also been shown to inhibit muscimol-stimulated agonist binding in cerebellar P₂ membrane fractions (Komulainen

et al., 1995). In contrast, whereas Hg²⁺ also suppressed to block all inward and outward Cl⁻ currents, it took longer to do so than did MeHg. Unlike the effects of MeHg on GABA_A-activated Cl⁻ currents, Hg²⁺ initially caused an increase in GABA_A-mediated outward Cl⁻ currents prior to suppressing them, indicating that Hg²⁺ may, as it did to the GABA_A-mediated chloride channels in dorsal root ganglion neurons (Arakawa et al., 1991; Huang and Narahashi, 1995), initially increase the open probability of GABA_A-activated chloride channels. Moreover, similar to its effects on the tetrodotoxin-, bicuculline- and picrotoxin-insensitive slow inward currents induced in dorsal root ganglion neurons (Arakawa et al., 1991), Hg²⁺ shifted the I/V curve and the reversal potential to more negative potentials, indicating that ions other than Cl⁻ may be also involved. These differential effects of MeHg and Hg²⁺ on GABA_A receptors may explain why MeHg causes the early stimulatory effects on hippocampal synaptic transmission, while Hg²⁺ does not.

If effects of MeHg on GABA_A receptors are indeed responsible for the MeHg-induced early increase in population spike or EPSP amplitude, then pretreatment of slices with the GABA_A antagonist bicuculline should eliminate the early increased phase in either population spikes or EPSPs. After pretreatment of slices with bicuculline, MeHg no longer caused an initial increase in population spike and EPSP amplitudes but still decreased them to block. The failure to induce the early increase in amplitude of population spikes was not due to a ceiling effect caused by bicuculline, although

bicuculline significantly increased population spike amplitude to 180 - 200% of control. At the time bicuculline-stimulated amplitudes of population spikes reached maximal levels, increasing stimulation intensity still caused a further increase in population spike amplitude. Moreover, MeHg failed to cause the early stimulatory effects even under conditions in which the stimulation intensity was reduced to pre-bicuculline control level after bicuculline had increased population spike amplitude to a stable level. The most likely explanation for these results is that MeHg may directly act at GABA_A receptors to cause disinhibition in a similar manner to the effects of bicuculline on GABA_A receptors. This explanation was further supported by the observation that MeHg blocks responses evoked by bath application of muscimol with a similar time course to that of block of IPSPs or IPSCs.

In the hippocampal CA1 region, at least two subtypes of GABA_A receptors coexist in pyramidal neurons (Pearce, 1993; Gordey *et al.*, 1995). One type is located at the soma or initial segment of the axon. When activated, it hyperpolarizes the CA1 pyramidal cell membrane. The other type is located in the dendrites. When activated, it depolarizes the CA1 pyramidal cell membrane (Gordey *et al.*, 1995). The responses evoked by bath application of muscimol in the present study are likely to represent a net response of both types of GABA_A receptor to muscimol. Thus, block of responses evoked by bath application of muscimol indicated that MeHg affects both types of GABA_A-mediated responses. We cannot exclude the possibility that presynaptic effects

of MeHg on the interneurons or some factors other than $\mbox{GABA}_{\!\mbox{\tiny A}}$ receptors contribute to the increase effect in hippocampal excitability, since in some slices pretreated with bicuculline, MeHg still caused a delayed increase of about 10 - 15 % in population spike amplitude, although this was not statistically significant. In hippocampus, in addition to GABA, receptors, GABA_B receptors are located both pre- and postsynaptically in the CA1 region and regulate synaptic transmission (Dutar and Nicoll, 1988a,b; Thompson et al., 1992; Otis et al., 1993; Isaacson et al., 1993; Pitler and Alger, 1994; Wu and Saggau, 1995). At postsynaptic CA1 neurons, GABA_B receptors are coupled to K⁺ channels via a G-protein to cause hyperpolarization of cells. This is expressed as the slow EPSP (Dutar and Nicoll, 1988b; Thompson and Gähwiler, 1992; Otis et al., 1993; Pitler and Alger, 1994). Perhaps the delayed increase in population spike amplitude by MeHg-induced in the presence of bicuculline was due to an effect on GABA_B receptors. Alternatively, effects of MeHg on intracellular Ca2+ homeostasis may also be involved in the early stimulatory effects of MeHg on hippocampal synaptic transmission, since MeHg increases intracellular Ca2+ concentrations in several types of neurons (Denny et al., 1993; Hare et al., 1993; 1995; Marty and Atchison, 1997). In fact, in hippocampal slices after block of voltage-dependent Na⁺ channels using the local anesthetic QX-314, MeHg also caused an initial increase in Ca²⁺ spike amplitudes prior to decreasing them to block (Yuan and Atchison, unpublished observation).

Earlier findings from ligand binding studies (Young and Snyder, 1973) and autoradiography (Zarbin et al., 1981; Frosholm and Rotter, 1985; Probst et al., 1986) using [3H]strychnine indicated that glycine receptors are predominately confined to the spinal cord, brain stem and other areas of the lower neuraxis. However, recent studies using immunocytochemistry with monoclonal antibodies (Van den Pol and Gorcs, 1988; Becker et al., 1988), autoradiography with [3H]glycine (Bristow et al., 1988), Northern blot hybridization (Grenningloh et al., 1990; Kuhse et al., 1990a,; Malosio et al., 1991) and polymerase chain reaction (Kuhse et al., 1990a,b; 1991) demonstrated a wide distribution of glycine receptors in the higher regions of the CNS including cerebral cortex and hippocampus. These glycine receptors, differ from those in the spinal cord and brain stem which primarily express the α1 subunit, a component of the "classical" strychnine-sensitive glycine receptor (Bristow et al., 1986; Becker et al., 1988; Belz, 1990a). Instead, these receptors express a different ligand binding subunit (α 2), which displays only low affinity for binding of strychnine (Bristow et al., 1986; Becker et al., 1988) or low sensitivity to strychnine upon heterologous expression in Xenopus oocytes (Kuhse et al., 1990a). To date, however, we are unaware of any direct report of the existence and the physiological role of functional glycine receptors in hippocampal CA1 neurons, although the above evidence suggests their presence in the hippocampus. In the present study, pretreatment of slices with strychnine caused a dramatic increase in population spike amplitude and induced multiple spike responses, although it was not as effective in this regard as was bicuculline. This suggests either that there may be a small population of strychnine-sensitive subtype of glycine receptors located in the CA1 hippocampal region, or that strychnine cross-reacts with GABA, receptors, since they both belong to a superfamily of ligand-gated ion channels and share significant sequence similarity in primary structure and transmembrane topology (Grenningloh et al., 1987; Schofield et al., 1987; Langosch et al., 1988; Schmieden et al., 1993). The latter possibility seems less likely, inasmuch as strychnine did not prevent or suppress the MeHg-induced early stimulation, as bicuculline pretreatment did. Another possible explanation for the failure of strychnine pretreatment to block MeHg-induced early stimulation of synaptic transmission is that these heterologous glycine receptors in hippocampal neurons may be not blocked completely by strychnine due to their low sensitivity to strychnine as suggested by previous studies (Young and Snyder, 1973; Frostholm and Rotter, 1985; Probst et al., 1986; Bristow et al., 1986; Kuhse et al., 1990). This may be one of the reasons why strychnine was less potent in increasing population spike amplitude than was bicuculline. This possibility also seems less likely, because pretreatment of slices with bicuculline alone completely suppressed MeHg-induced early increase in field Thus, if there are glycine receptors located on postsynaptic potentials. membranes, they do not play a primary role in MeHg-induced early stimulation of hippocampal synaptic CA1 cell transmission.

In conclusion, the preferential block by MeHg of inhibitory synaptic transmission, mediated primarily by GABA_A receptors, appears to be primarily responsible for the MeHg-induced early stimulatory effects on hippocampal synaptic transmission. The importance of this disinhibition caused by MeHg to its overall neurotoxicity also remains unknown.

CHAPTER FIVE

COMPARATIVE EFFECTS OF METHYLMERCURY ON PARALLEL-FIBER AND CLIMBING-FIBER RESPONSES IN RAT CEREBELLAR SLICES

ABSTRACT

Previous studies showed that MeHg blocked both inhibitory and excitatory synaptic transmission in the CA1 region of hippocampal slices. However, following exposure to MeHg in vivo, the primary target in the CNS for neurotoxicity is the cerebellum. Thus, in the present study, effects of MeHg on synaptic transmission between parallel fibers and Purkinje cells and between climbing fibers and Purkinje cells were compared in 300 - 350 µm cerebellar slices using extracellular and intracellular microelectrode recording techniques. Field potentials of parallel-fiber volleys (PFVs) and the associated postsynaptic responses (PSRs), presumably evoked by glutamate released from parallel-fiber terminals, were recorded in the molecular layer by stimulating parallel fibers in the same layer in transverse slices. The climbing-fiber responses (CFRs) were also recorded in the molecular layer by stimulating white matter in sagittal slices. At 20, 100 and 500 µM, MeHg blocked both PFVs and the associated PSRs, however, it blocked PSRs more rapidly than it did PFVs. Times to block of PSRs by 500, 100 and 20 μ M MeHg were 6 \pm 0.5, 32 ± 4 , and 101 ± 24 min, respectively, while times to block of PFVs by 500, 100 and 20 μ M MeHg were 10 \pm 0.5, 51 \pm 5 and 184 \pm 27 min, respectively. In addition, MeHg caused an initial slight increase in PFV and PSR amplitudes prior to suppressing them to block. Similarly, MeHg first increased and then decreased amplitudes of CFRs to complete block. Times to block of CFRs by 100 and 20 μ M MeHg were 45 \pm 3 and 115 \pm 18 min, respectively. Thus, MeHg blocks both parallel-fiber and climbing-fiber responses. However, it blocks the glutamate-evoked PSRs and CFRs more rapidly than it does PFVs. This suggests that MeHg may either affect the process of neurotransmitter release from the presynaptic fibers or act at the postsynaptic Purkinje cells. As a means of identifying the primary sites of action of MeHg in blocking these field potentials, intracellular recordings of excitatory postsynaptic potentials evoked by activation of parallel fiber (PF-EPSPs), climbing fibers (CF-EPSPs) and repetitive firing of Purkinje cells evoked by direct injection of depolarizing current at the somata were compared. At 100 and 20 µM, MeHg blocked all voltage-dependent responses with a similar time This included the Na⁺-dependent fast somatic spikes evoked by parallel fiber stimulation or by direct depolarization of Purkinje cells as well as the Ca²⁺-dependent slow dendritic spike bursts evoked by climbing fiber stimulation or by direct depolarization of Purkinje cells. MeHg appears to block voltage-dependent responses more rapidly than it does glutamatemediated responses. Thus, it may affect voltage-gated ion channels and glutamate-activated channels differently. MeHg also hyperpolarized and then depolarized Purkinje cell membranes, suppressed current conduction from parallel fiber or climbing fibers to dendrites of Purkinje cells and blocked MeHg might affect Purkinje cell synaptically-activated local responses. membrane ion conductances because it switched the patterns of repetitive firing of Purkinje cells generated spontaneously or by depolarizing current injection at Purkinje cell somata from one of predominantly Na⁺-dependent, fast somatic spikes to one of predominantly Ca²⁺-dependent, low amplitude, slow dendritic spike bursts. Thus, in the cerebellum, as in the hippocampus, acute exposure to MeHg causes a complex pattern of disruption of synaptic function. The time course of block of synaptic function in the two different regions is generally similar. Multiple sites of action appear to be involved, however, MeHg appears to act primarily at the postsynaptic Purkinje cells to block synaptic transmission between parallel fibers and Purkinje cells and between climbing fibers and Purkinje cells.

INTRODUCTION

Previously, I demonstrated that acute bath application of MeHg disrupted neuronal membrane excitability and synaptic transmission in the CA1 region of hippocampal slices in a concentration- and time-dependent manner (Yuan and Atchison, 1993, 1994, 1996 and 1997). MeHg appears to act at multiple sites to cause these effects; it blocked excitatory synaptic transmission, inhibitory synaptic transmission and antidromically-activated responses, it hyperpolarized and then depolarized the CA1 pyramidal cell membranes; and possibly also affected the process of presynaptic release of neurotransmitter. The primary sites of actions of MeHg on hippocampal synaptic transmission in the CA1 region appear to be the postsynaptic CA1 pyramidal neurons, at least at the early stage of exposure to MeHg. However, presynaptic mechanisms, nonspecific effects of membrane depolarization, and suppression of current conductance may be also involved in the actions of MeHg in blocking hippocampal synaptic transmission.

Among the specific brain regions, the cerebellum, especially the cerebellar cortex, appears to be a primary target of MeHg in the CNS. Chronically, MeHg accumulates most in the cerebellum, particularly in the Purkinje cells and the Golgi cells in the granular layer, and to a lesser extent in the granule cells, stellate cells and basket cells (Glomski, 1971; Olszewski et al., 1974; Chang, 1977, 1980; Møller-Madsen, 1990, 1991; Leyshon-Sørland,

1994). However, pathological examination of patients and experimental animals with acute and chronic MeHg poisoning indicated that the cerebellar cortex, especially the granule cells, was particularly sensitive to MeHg (Hunter and Russell, 1954; Takeuchi et al., 1962; Chang, 1977, 1980; Syversen et al., 1981). In MeHg poisoning, especially in chronic cases, there was a characteristic atrophy of the cerebellar cortex, particularly the granular layer in the lateral lobes and in the vermice, due to extensive loss of granule cells (Hunter and Russell, 1954; Takeuchi et al., 1962; Chang, 1977, 1980). In addition, the basket cells, climbing and parallel fibers were also severely involved. The Purkinje cells were more resistant, but were also typically affected in chronic cases (Hunter and Russell, 1954; Takeuchi, 1962; Chang, 1977, 1980). Possibly, the interactions of MeHg with cerebellar neurons are responsible for the motor deficits caused by acute and chronic exposure to MeHg. Thus, a specific examination of effects of MeHg on cerebellar synaptic transmission may aid our understanding of potential mechanisms of MeHginduced neurotoxicity.

To date, to my knowledge, no direct study of the effect of MeHg on cerebellar synaptic transmission has been reported, although many studies done in this and other labs have shown that *in vitro* acute exposure to MeHg affects function of cells or cell fractions derived from the cerebellum. For example, MeHg reduced influx of ⁴⁵Ca²⁺ induced by depolarization of rat cerebellar synaptosomes (Yan and Atchison, 1996), reduced currents carried

through K⁺ and Ca²⁺ channels (Sirois and Atchison, 1995, 1996, 1997) and increased [Ca²⁺], in primary cultures of rat cerebellar granule cells (Marty and Atchison, 1997). MeHg also affected protein phosphorylation and synthesis in cerebellar granule cells (Sarafian and Verity, 1986, 1990a,b, 1992; Sarafian, 1993), inhibited migration of granule cells in cerebellar organotypic cultures (Kunimoto and Suzuki, 1997), and induced rapid death of cerebellar granule cells (Sarafian et al., 1989; Nagashima et al., 1996). The unique architecture of the cerebellar cortex suggests that Purkinje cells may be a key element in the cerebellar synaptic circuitry, since they receive and integrate synaptic inputs from both parallel-fibers and climbing-fibers. Furthermore, their axons are the only output from the cerebellar cortex to the deep cerebellar nuclei to modulate activities of these nuclei. Thus, I feel it would be important to examine if Purkinje cells are functionally sensitive to MeHg, even though pathologically they are more resistant to MeHg compared to granule cells (Hunter and Russell, 1954; Takeuchi et al., 1962; Syversen et al., 1981). As such, the present study was designed to determine if MeHg affects synaptic transmission between the parallel- or climbing-fibers and Purkinje cells and whether or not MeHg affects these two synaptic pathways differently since their electrophysiological characteristics differ. Additionally, I sought to compare whether or not MeHg affects cerebellar synaptic transmission differently from its effects on hippocampal synaptic transmission.

MATERIALS AND METHODS

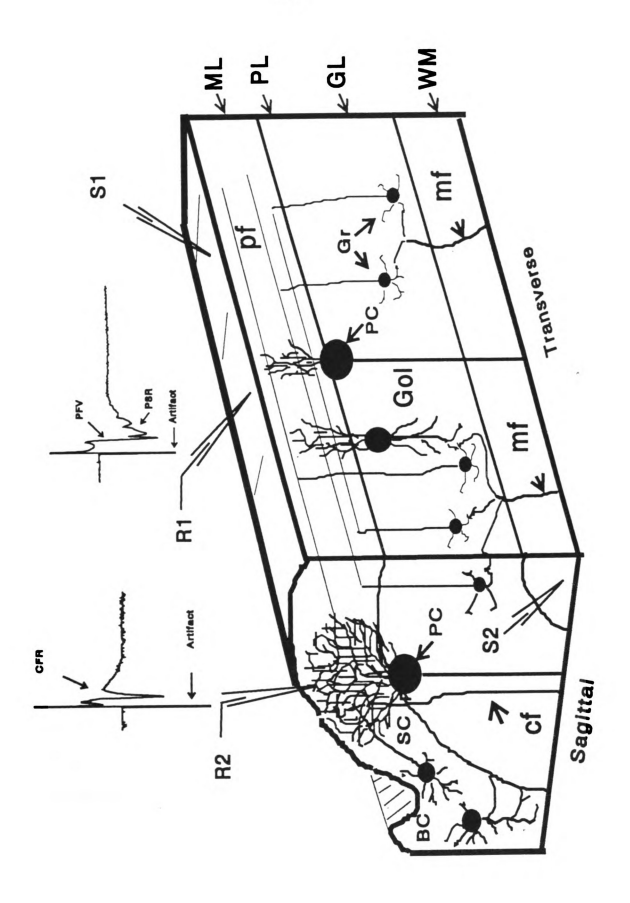
Materials. Methylmercuric chloride, purchased from ICN Biomedical, Inc. (Costa, CA), was dissolved in deionized water to a concentration of 5 mM to serve as stock solution, which was used for one week. The applied solutions (20-100 μM) were diluted with modified ACSF consisting of (in mM): 125 NaCl, 2.5 KCl, 2 CaCl₂, 1 MgCl₂, 1.25 KH₂PO₄, 26 NaHCO₃ and 20 mM d-glucose (pH 7.4) just before superfusion. MeHg and other chemicals were applied acutely to slices by bath application at a rate of 1.2 - 1.5 ml/min with a Gilson infusion pump (Middleton, WI). DNQX and AP-5 were purchased from Sigma Chemical Co. (St. Louis, MO). DNQX was dissolved first in DMSO and then diluted further with modified ACSF. The final concentration of DMSO in the applied solution was less than 0.02% (v/v), which has no significant effects on synaptic transmission.

Preparation of cerebellar slices. Cerebellar slices were prepared using the methods described previously in Chapter Two. One cerebellar slice was transferred to the recording chamber and the remaining slices were incubated in a holding chamber for later use if needed. The entire process from decapitating the rat to transferring the slices to the recording or holding chamber was finished in less than 10 min and under a temperature of 4 °C. The slice in the recording chamber was incubated and superfused (1.2 - 1.5

ml/min) continuously with the modified ACSF saturated with 95% $O_2/5\%$ CO_2 for at least 60 min before the electrophysiological recordings began. All experiments were conducted at room temperature. Only one slice per rat was used.

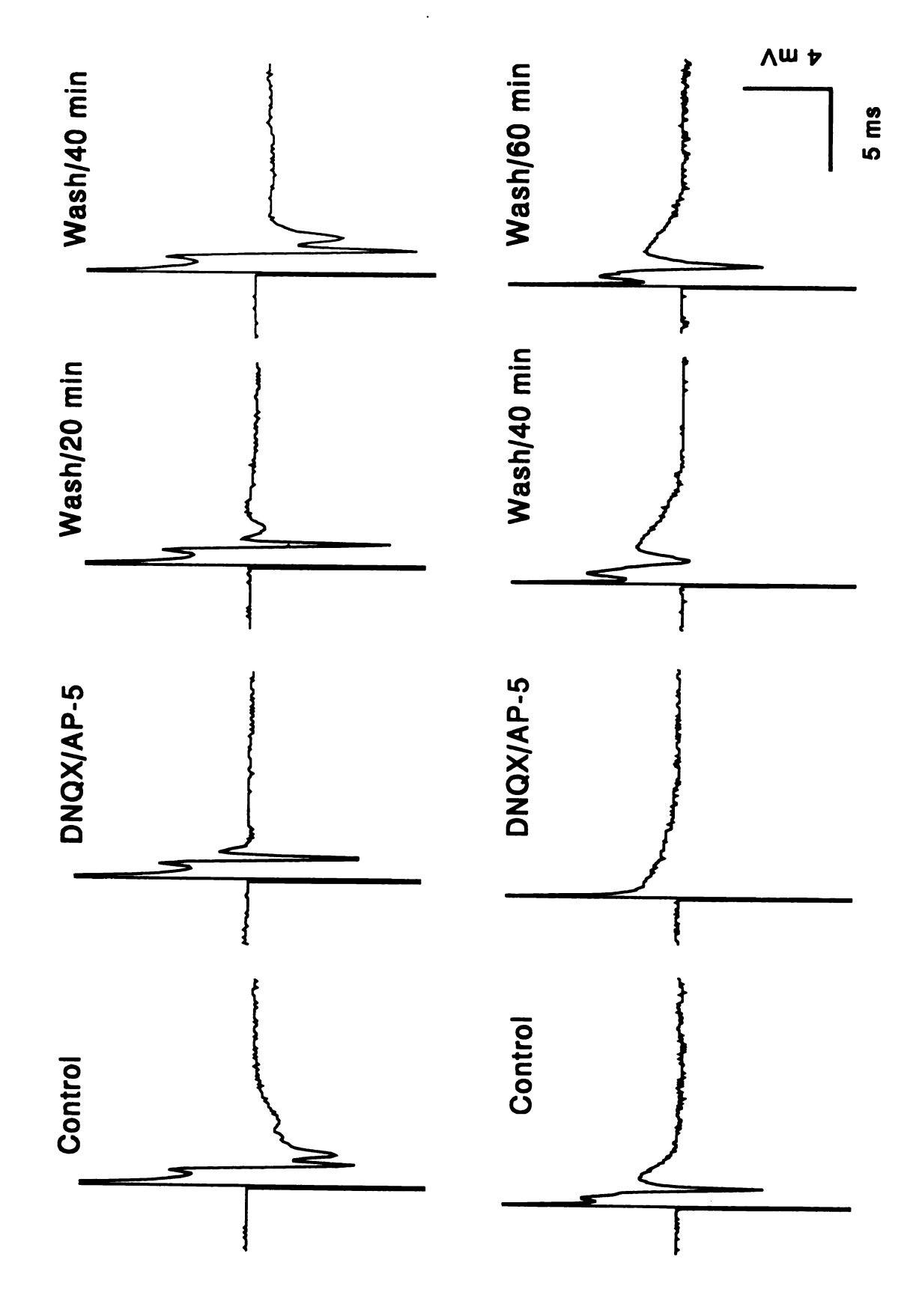
Electrophysiological procedures. A concentric bipolar metal electrode or monopolar tungsten electrode (3 M Ω , FHC, Brunswick, ME) was used as the stimulation electrode. Borosilicated glass microelectrodes (o.d. 1.0 mm, i.d. 0.5 mm, WPI, Inc., orlando, FL) filled with ACSF (5 - 15 M Ω impedance) or 3 M potassium acetate (60 - 80 M Ω impedance) were used as extracellular or intracellular recording electrodes, respectively. Conventional extracellular recordings were made in the molecular layer of the cerebellar cortex. To record extracellular responses of Purkinje cells to local extracellular activation of the parallel fibers, the stimulating electrode was positioned on the surface of the molecular layer of a transverse slice (S1 in Figure 5.1), just below the pia, and a recording electrode (R1 in Figure 5.1) was positioned on the same track which parallel fibers travel along, so-called "on beam" (Crepel and Delhaye-Bouchaud, 1978; Crepel et al., 1981), in the molecular layer (R1 in Figure 5.1). The typical extracellular response evoked by activation of parallel fibers consists of an initial triphasic potential with positive-negative-positive components and followed by another prolonged negative potential. The initial triphasic component corresponds to the current generated by action potentials

Figure 5.1. Diagrammatic depiction of the structure of the cerebellar cortex in sagittal and transverse slices and methods for recording field potentials of Purkinje cells following activation of parallel-fibers climbing fiber response; Gol, Golgi cell; GL, granule cell layer, Gr, granule cell; mf, mossy fiber; ML, PSR, postsynaptic response; R1, extracellular recording electrode in the molecular layer for "on beam" electrode on the surface of molecular layer in transverse slice for stimulation of the parallel fibers; S2, stimulating electrode; WM, white matter. Top traces represent response evoked by stimulation of or climbing-fibers. Abbreviations: Artifact, stimulating artifact; BC, basket cell; cf, climbing fiber; CFR, molecular layer; PC, Purkinje cell; pf, parallel fiber; PFV, parallel fiber volley; PL, Purkinje cell layer; recording parallel fiber response in a transverse cerebellar slice; R2, extracellular recording electrode in the molecular layer for recording climbing fiber responses in a sagittal cerebellar slice; S1, stimulating stimulating electrode in white matter for stimulation of the climbing fibers; SC, stellate cell; Stim, climbing fibers and parallel fibers, respectively.



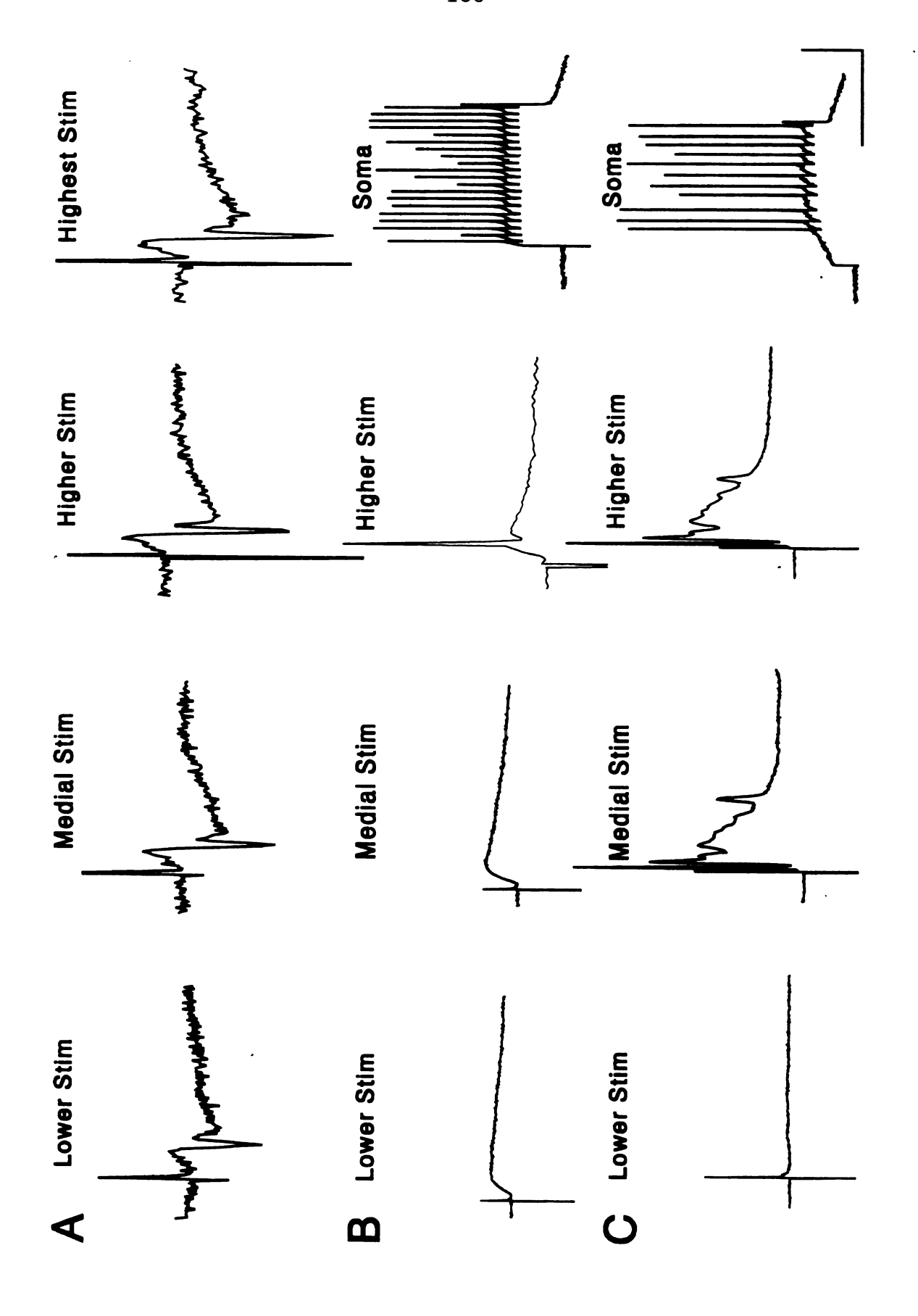
propagating along parallel fibers, defined as parallel-fiber volley (PFV in Figure 5.1). The prolonged negative potential corresponds primarily to the postsynaptic excitatory potentials evoked by glutamate released from parallel fibers onto the molecular layer dendrites of Purkinje cells, and defined as the postsynaptic response (PSR in Figure 5.1). It can be blocked reversibly by the kainate/AMPA type glutamate receptor antagonist DNQX (Figure 5.2) (Salin et al., 1996). To record field responses of Purkinje cells to activation of climbing fibers, the stimulating electrode was positioned on the white matter immediately at the base of the *folium* in a parasagittal slice (S2 in Figure 5.1); a recording electrode was positioned in the molecular layer (R2 in Figure 5.1). The field potentials evoked by stimulation of the climbing fibers are also glutamate-evoked responses because they are blocked by DNQX (Figure 5.2). Normally, amplitudes of these field potentials require stabilization for at least 20 - 30 min before beginning the experiments, because most of recordings showed increases in amplitudes of the field responses within the first 30 min after establishment of recordings in the absence of any treatment. intracellular recordings of parallel- or climbing-fiber excitatory postsynaptic potentials (PF-EPSPs or CF-EPSPs), the positions of stimulating electrodes were similar to those for extracellular recordings, however, the recording electrodes were positioned in the somata of an identified Purkinje cell with the aid of an Olympus BHWI upright microscope (Olympus Optical Co., Tokyo, Japan) equipped with Normaski optics and 10 X and 40 X water-immersion

Figure 5.2. Effects of DNQX and AP-5 on field potentials evoked by stimulating the parallel or climbing fibers in cerebellar slices. Top: effects of 10 µM DNQX and 20 µM AP-5 on responses evoked by consists of an initial triphasic wave, positive-negative-positive, followed sometimes by a prolonged negative wave (control). After application of 10 µM DNQX and 20 µM AP-5 for 5 - 20 min, the prolonged wave disappeared completely while the triphasic response remain unchanged. The prolonged response effects of DNQX and AP-5 on responses evoked by stimulating the climbing fibers in a sagittal cerebellar stimulating the parallel fibers in a transverse cerebellar slice. A typical parallel fiber response usually appeared again after washing the slice with DNQX- and AP-5-free solution for 30 - 60 min. Bottom: slice. Application of 10 µM DNQX and 20 µM AP-5 for 5 - 20 min completely blocked the climbing fiber response. Washing the slice with DNQX- and AP-5-free solution for 60 min causes completely recovery of this response.



objective lenses. The stimulus pulses were generated from and isolated using a Grass S88 stimulator and a Grass SIU5 stimulus isolation unit (Grass, Inc., Quincy, MA) at 0.15 Hz, 0.1 ms duration at an initial intensity that produced approximately 50 - 60 % of the maximum response for a given slice. Recorded signals were amplified (Axoclamp-2, Axon instruments Inc., Foster City, CA), displayed on a 2090-3 digital oscilloscope (Nicolet Instruments, Verona, WI) and recorded simultaneously to a 5X86 computer at a digital sampling interval of 0.2 or 1.0 ms. The 1 ms digital sampling interval was used to record those responses generated by injection of long duration of depolarizing current pulses at Purkinje cell soma. The responses of Purkinje cells to activation of parallelfibers and climbing-fibers were identified further based on their electrophysiological properties (Llinás and Sugimori, 1980a; Crepel et al., 1981; The responses, recorded extracellularly or Stuart and Häusser, 1994). intracellularly, generated by activation of parallel-fibers are graded events (Figure 5.3A,B), whereas responses evoked by stimulating climbing fibers are so-called all or none complex spikes regardless of the stimulus intensity (Figure 5.3C). Directly depolarizing Purkinje cells by injection of 500 - 1000 ms positive current pulses at the threshold intensity using the recording electrode in the somata generate Purkinje cell-specific repetitive spikes (Figure 5.3B,C).

At Figure 5.3. Effects of stimulus intensity on parallel fiber responses and climbing fiber responses. (A) An extracellular recording of parallel fiber responses from the molecular layer of a transverse cerebellar intracellular recording of PF-EPSPs and action potentials from a Purkinje cell by stimulating the parallel fibers in a transverse cerebellar slice. Amplitude of PF-EPSPs increased as the stimulus intensity increased. A full action potential was generated by a suprethreshold stimulus (Higher Stim). (C) Traces the subthreshold stimulation (Lower Stim), no responses occurred except the stimulus artefact. Once the or complex spikes were generated. Increasing stimulus intensity further (Higher Stim) did not cause In both B and C (Soma), direct injection of Calibration bars: 5 mV for A, 20 mV for B and C, 400 ms for Soma response in B and 200 ms for Soma stimulus intensity reached the threshold level (Medial Stim), a typical climbing fiber response (CF-EPSP) depolarizing current through the recording electrodes at Purkinje cell soma caused repetitive firing. demonstrated the **all or none** nature of responses of a Purkinje cell to activation of climbing fibers. Parallel fiber responses increased in amplitude as the stimulus intensity increased. further increase in the amplitude of the CF-EPSP. response in C, 20 ms for the rest responses.

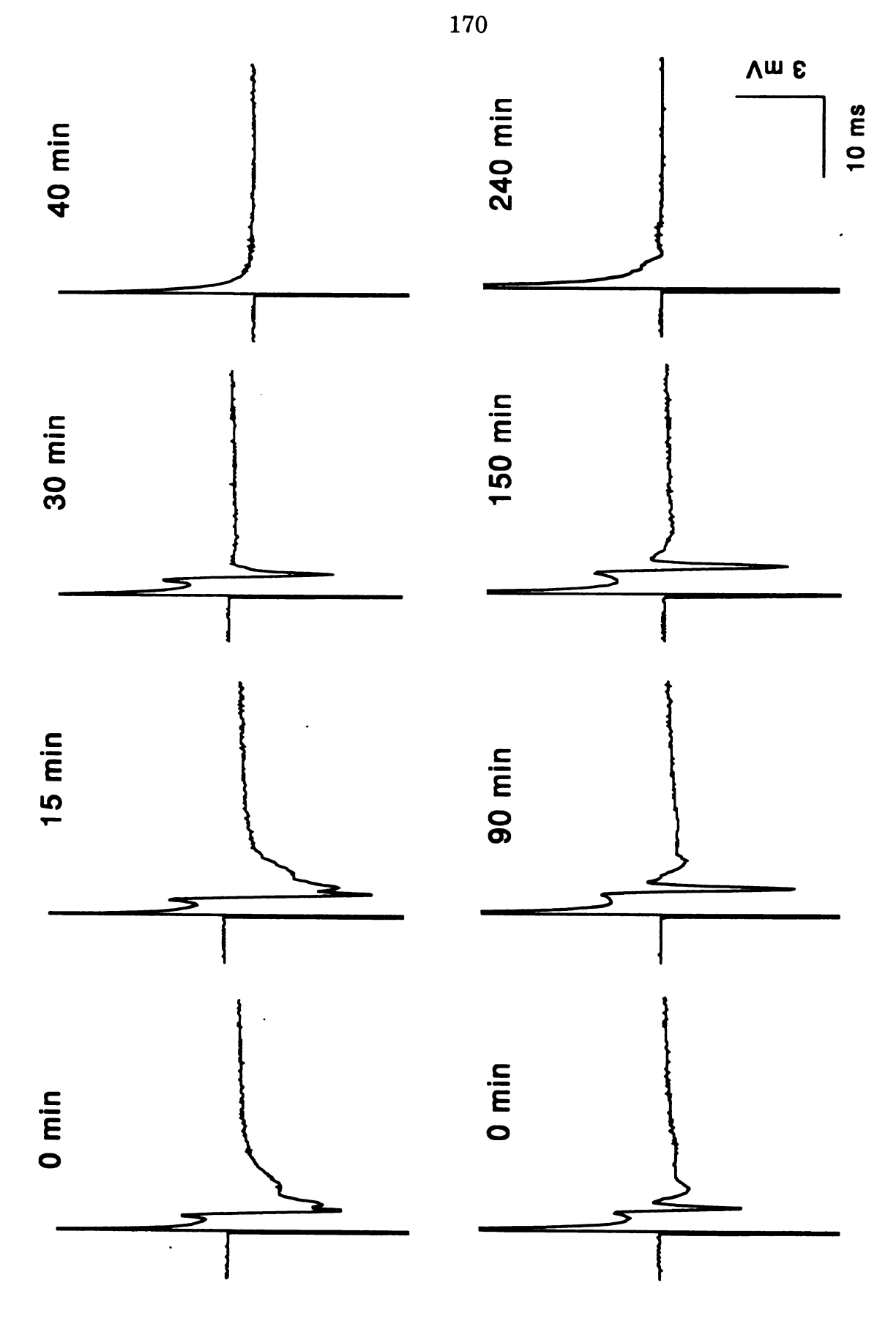


Statistical analysis. Data were collected continuously before and during application of MeHg and analyzed statistically using student's paired t test and one-way analysis of variance. Dunnetts' procedure was used for post hoc comparisons. Values were considered statistically significant at p < 0.05.

RESULTS

Comparative effects of MeHg on field potentials evoked by stimulating parallel fibers or climbing fibers. The pattern of effects of MeHg on field potentials recorded from the molecular layer of cerebellar slices was similar to that on potentials recorded from the CA1 pyramidal neurons in hippocampal slices (Yuan and Atchison, 1993, 1994). Acute bath application of 20, 100 and 500 µM MeHg caused a concentration- and time-dependent biphasic effect on the PFV and the associated postsynaptic responses-PSRs generated by stimulation of parallel fibers in transverse cerebellar slices. Initially, 20, 100 and 500 µM MeHg increased amplitudes of PFVs and PSRs (Figure 5.4 and 5.7, data for 500 µM are not shown to simplify the figures). The time-dependent averages of amplitudes of these field potentials are shown in Figure 5.7. The percentages of peak increases in amplitudes of PFVs and PSRs, averaged from each individual experiment, were 157 ± 17% and 128 ± 8% of control for 100 uM MeHg and $211 \pm 25\%$ and $178 \pm 19\%$ of control for 20 µM MeHg, respectively. The mean times to peak stimulation of PFVs and PSRs averaged from each individual experiment were 21 ± 4 and 9 ± 2 min for 100 μ M MeHg and 91 \pm 22 and 49 \pm 12 min for 20 μ M MeHg, respectively. As exposure of slices to MeHg was increased, both PFV and PSR amplitudes were reduced progressively until complete block occurred. In general, MeHg blocked PSRs more rapidly than it did PFVs. As shown in Figure 5.4, at 30 or 150 min

Figure 5.4. Time course of effects of 100 (Top) and 20 µM (Bottom) MeHg on field potentials recorded from the molecular layer of transverse cerebellar slices following stimulation of the parallel fibers. Each trace represented 8-12 individual experiments.



after exposure to 100 (Top) or 20 μ M MeHg (Bottom), the PSR components were completely blocked while the PFV components remained essentially unchanged. The mean times to block PSRs by 500, 100 and 20 μ M MeHg were 6 \pm 0.5, 32 \pm 4 and 101 \pm 24 min, respectively; the mean times to block PFVs by 500, 100 and 20 μ M MeHg were 10 \pm 0.5, 51 \pm 5 and 184 \pm 27 min, respectively (Figure 5.6). Differences between times to MeHg-induced block of PSRs and PFVs were statistically significant (p<0.05). Thus, the glutamate-mediated PSRs appear to be more sensitive to MeHg than were the presynaptic PFVs.

Similarly, 20 and 100 μ M MeHg initially stimulated the amplitude of field potentials evoked by stimulation of climbing fibers in sagittal slices prior to blocking them (Figure 5.5). The percentages of peak increases in CFR amplitudes stimulated by 100 and 20 μ M MeHg were 128 \pm 6% and 131 \pm 7% of control (p<0.05), respectively. Times to block of CFRs by 100 and 20 μ M MeHg were 45 \pm 3 and 115 \pm 18 min (Figure 5.6), respectively. These values are similar to those for MeHg-induced block of the PSRs, and appear to be more rapid than those for MeHg-induced block of the PFVs although the differences were not statistically significant. Figure 5.7 summarizes the time-courses of effects of MeHg on PFVs, PSRs and CFRs. MeHg first increased and then decreased amplitudes of all three responses to complete block. Whereas the effect of MeHg on PSRs appeared to be slightly more rapid than

Figure 5.5. Time course of effects of 100 (Top) and 20 µM (Bottom) MeHg on field potentials recorded from the molecular layer of sagittal cerebellar slices following stimulation of the climbing fibers. Each

trace is representative depiction of 5-7 individual experiments.

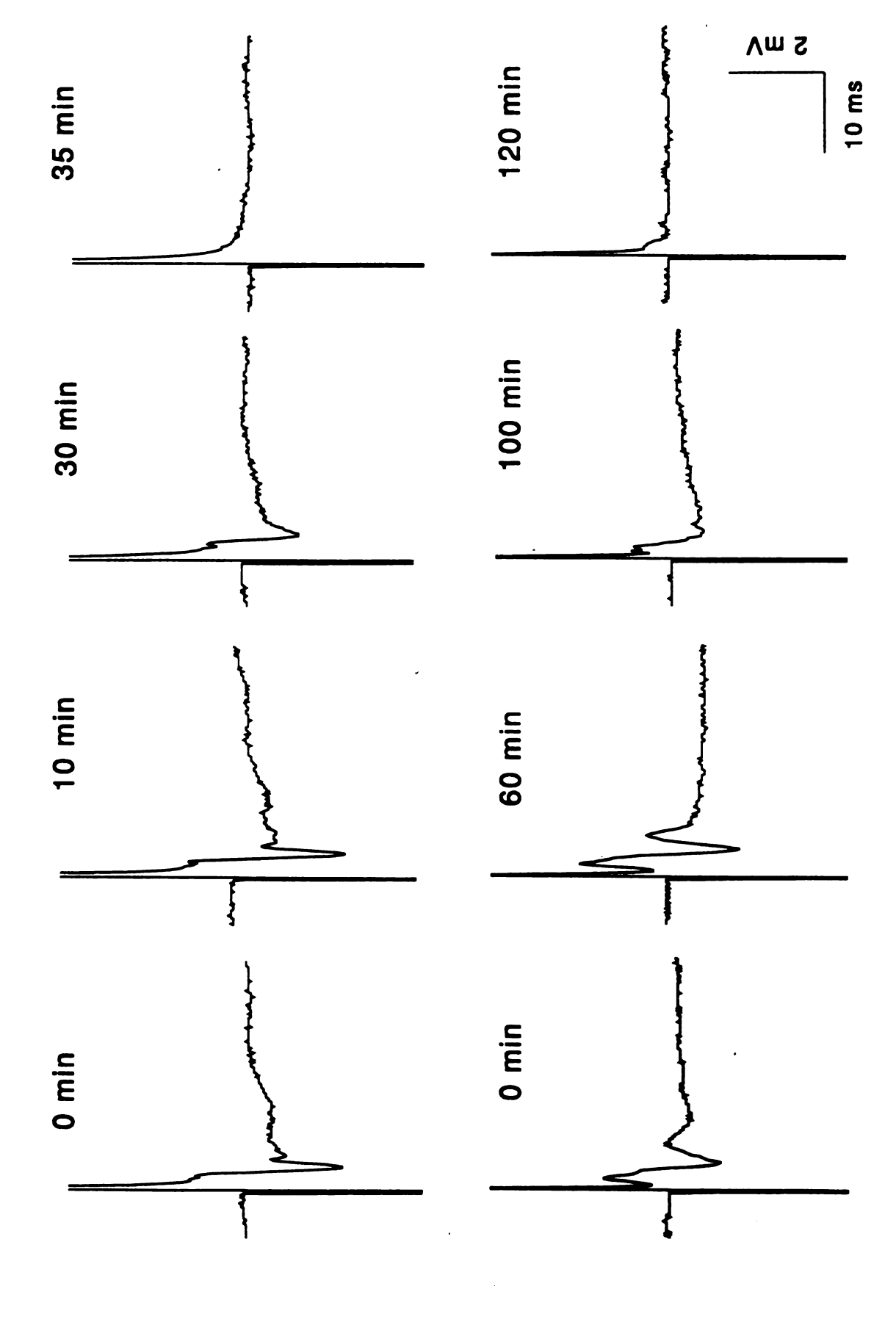


Figure 5.6. Comparison of times to block by 100 and 20 µM MeHg of field potentials representing the parallel fiber volleys (PFVs), postsynaptic responses (PSRs) and climbing fiber responses (CFRs). All values are the mean \pm S.E of 5-12 individual experiments. The asterisk indicates a significant difference between times to block of PSRs and PFVs by 100 and 20 µM MeHg (p<0.05, ANOVA).

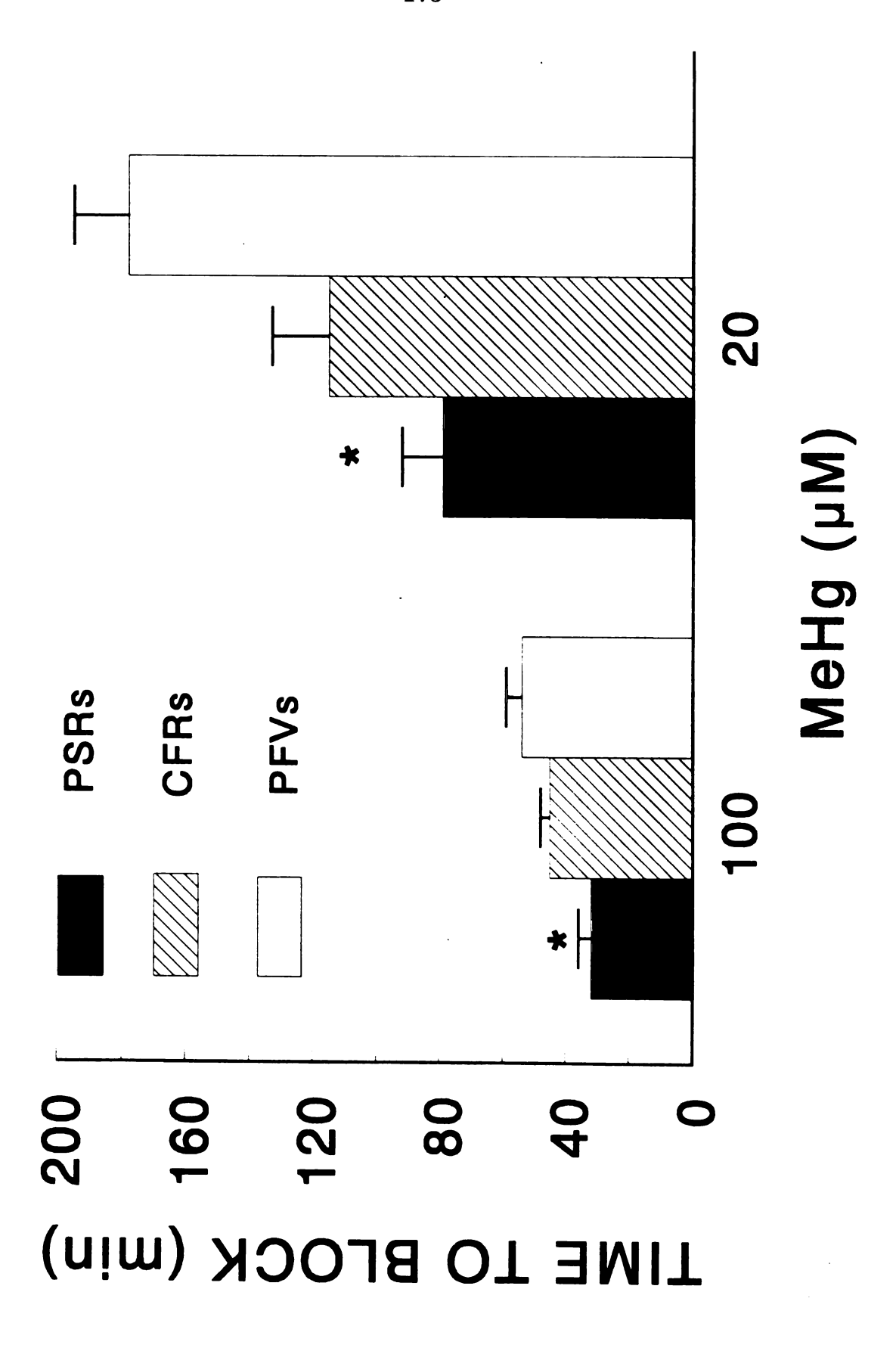
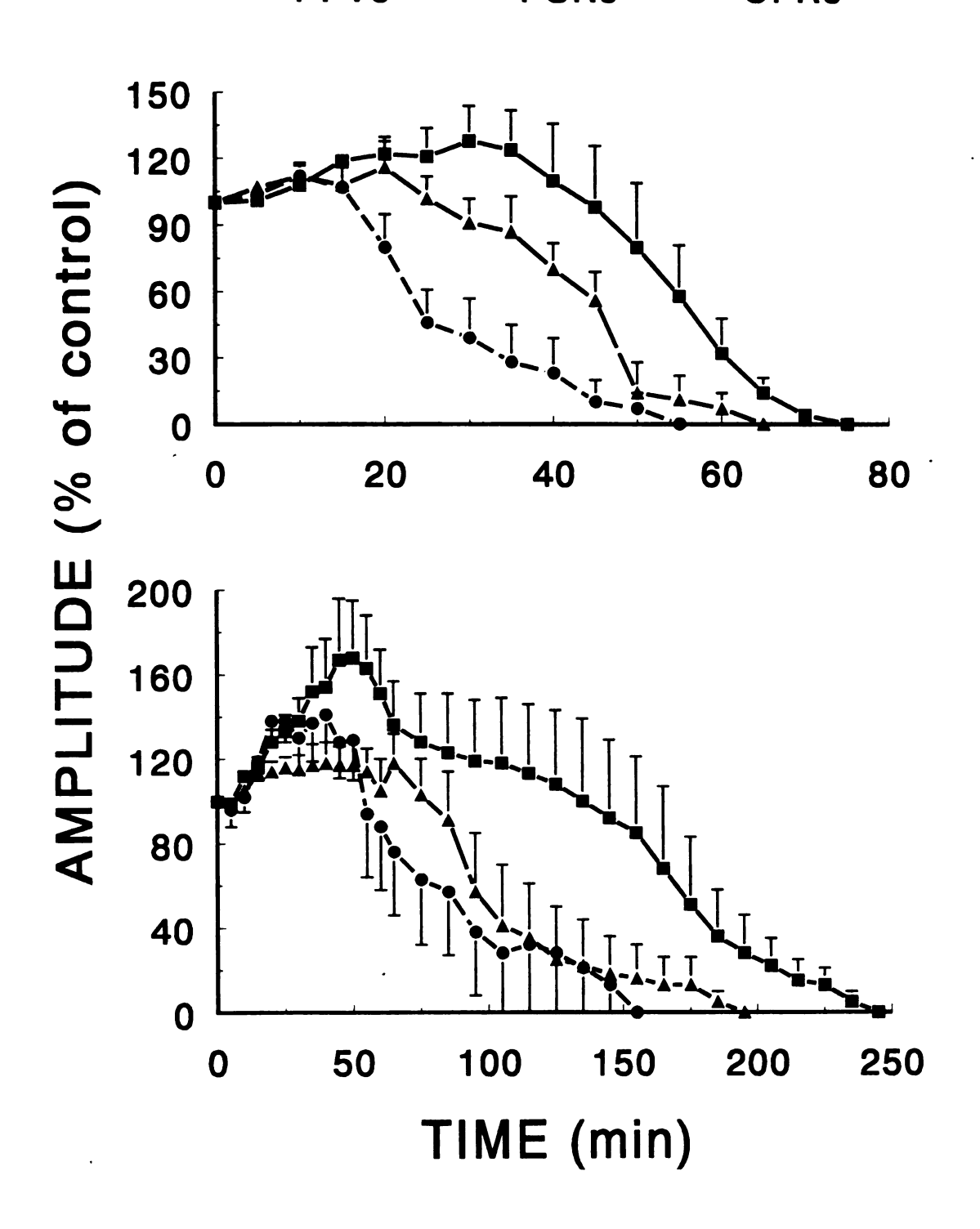


Figure 5.7. Time course of effects of 100 (Top) and 20 μ M (Bottom) MeHg on field responses representing the PFVs, PSRs and CFRs. All values are the mean \pm S.E. of 5-12 individual experiments. Values obtained prior to exposure to MeHg are considered as control.

--- PFVs --- PSRs --- CFRs



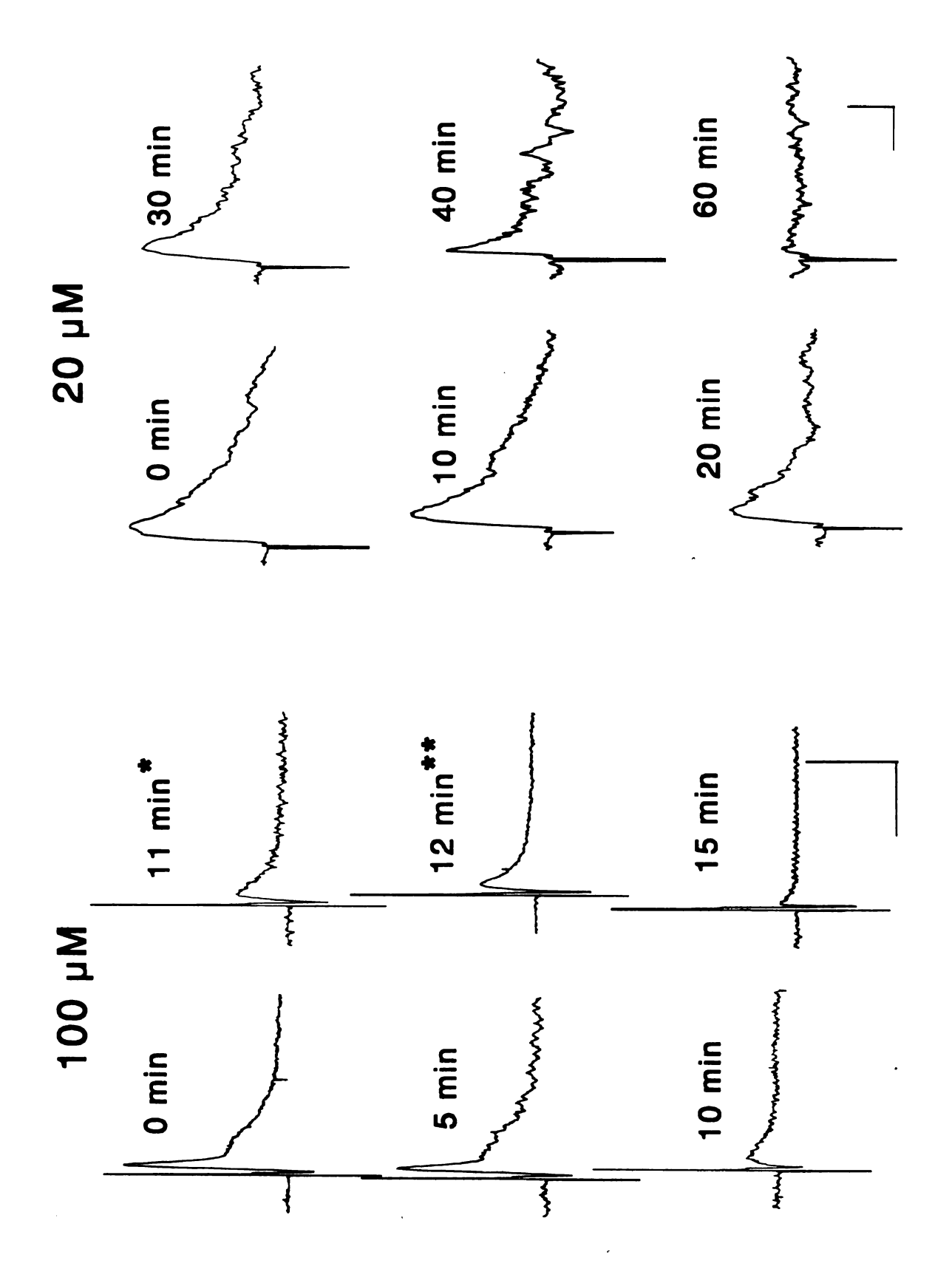
its effect on CFRs, the difference was not statistically significant. Block of both PSRs and CFRs occurred earlier than did block of PFVs. Thus, MeHg blocked glutamate-mediated postsynaptic responses activated either by stimulating parallel fibers or climbing fibers similarly, suggesting that MeHg may affect either the postsynaptic glutamate receptors or the process of transmitter release from parallel- or climbing-fiber terminals to block synaptic transmission by these two pathways.

Effects of MeHg on parallel-fiber EPSPs (PF-EPSPs) and climbing-fiber EPSPs (CF-EPSPs). To explore the mechanisms underlying the effects of MeHg on field potentials recorded in the molecular layer by activation of parallel fibers or climbing fibers, intracellular recording techniques were applied to the Purkinje cells to examine effects of MeHg on PF-EPSPs, CF-EPSPs and resting membrane potentials. Stimulation of the parallel fibers in the molecular layer of the cerebellar cortex in transverse slices initiates a negative parallel-fiber volley followed by a PF-EPSP. The PF-EPSPs were graded amplitude responses with a range of 1.5 - 2.3 ms latencies from the stimulus artefact to the onset of EPSPs, depending on the stimulus intensity and the distance between the stimulating and recording electrodes. After exposure to 100 and 20 μM MeHg, these latencies were prolonged, suggesting that current conduction from the parallel fibers to Purkinje cells was affected. Unlike the biphasic effects of MeHg on those field potentials, 100

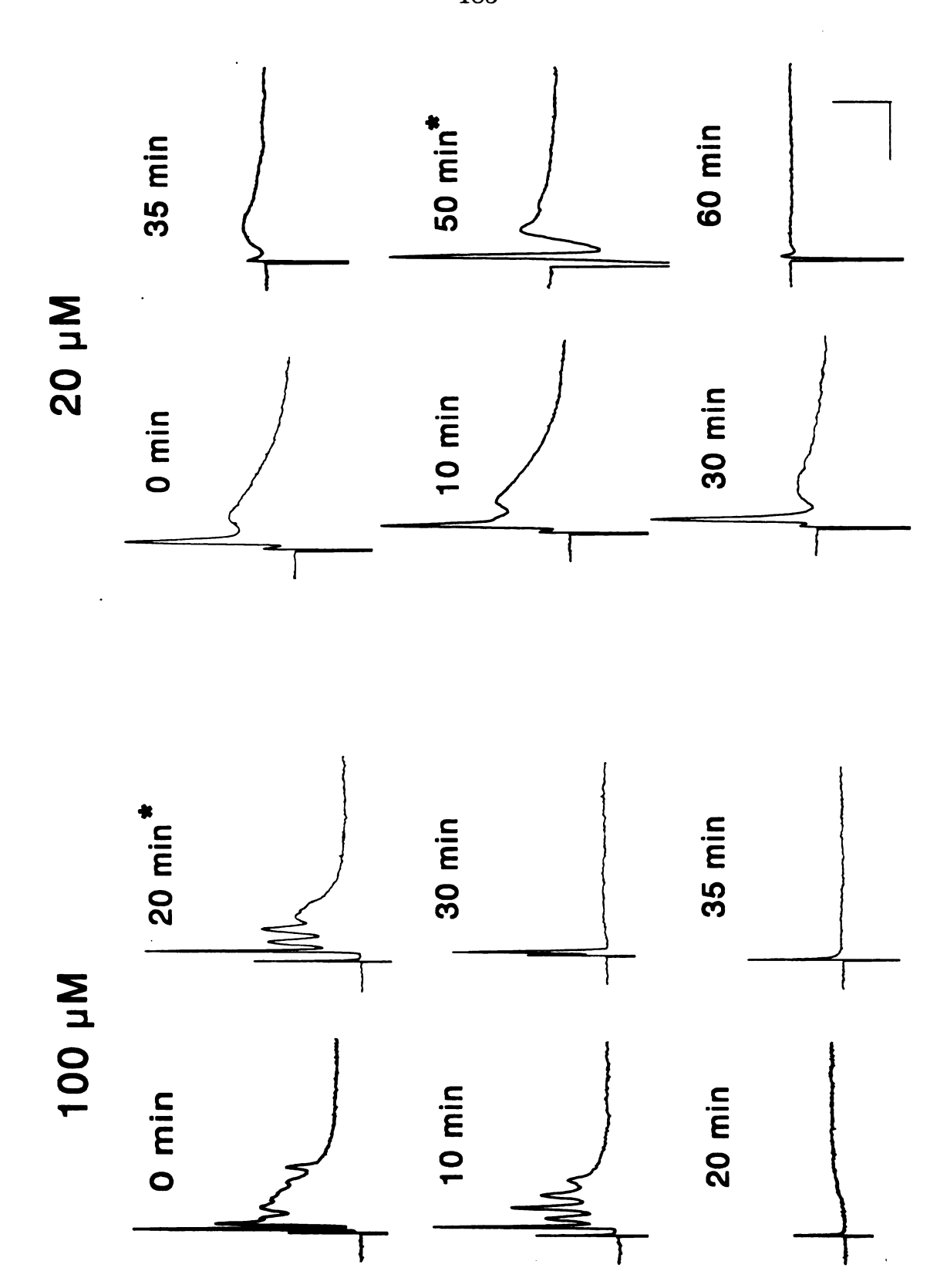
and 20 μ M MeHg blocked the PF-EPSPs without causing an early increase in EPSP amplitude, although a transient slight increase in amplitude of EPSPs occurred in some slices prior to suppression of the EPSPs. Times to block of EPSPs by 100 and 20 μ M MeHg were 33 \pm 7 and 63 \pm 3 min, respectively. However, as shown in Figure 5.8 (Left), the parallel-fiber volley responses appeared less sensitive to MeHg than did PF-EPSPs since PFV amplitudes remained essentially unchanged when EPSPs were reduced significantly (10 min) or blocked completely by MeHg (100 μ M). This was consistent with results obtained from extracellular recordings in that PFVs were less sensitive to MeHg than were the associated PSRs. In addition, the early block of EPSPs by MeHg could be partially restored by increasing the stimulus intensity (Figure 5.8 Left), suggesting that MeHg may initially suppress neuronal membrane excitability and/or transmitter release.

In contrast, stimulation of climbing fibers in sagittal cerebellar slices usually generated a full antidromically-activated action potential followed by a typical *all or none* complex spike response or CF-EPSPs (Figures 5.3, 5.9). The complex spikes consist of several small spikes superimposed on a pronounced plateau of depolarization. In some recordings, the typical complex spikes did not occur because the resting membrane potentials were more depolarized than -60 mV. The latency from the stimulus artefact to onset of CF-EPSPs was 1.9 ± 0.3 ms. After exposure of slices to $100 \mu M$ MeHg, the latency was prolonged to 2.7 ± 0.4 ms (p < 0.05), indicating that impulse

Purkinje cell soma by subthreshold stimulation of the parallel fibers using intracellular recording techniques. The single asterisk indicates that PF-EPSPs were blocked at 11 min; then increasing stimulus intensity at that time caused partial recovery of the responses. The double asterisks indicates Figure 5.8. Time courses of effects of 100 (Left) and 20 µM (Right) MeHg on PF-EPSPs recorded from that the PF-EPSPs evoked at the increased stimulus were again blocked and increasing stimulus intensity further could still cause partial recovery of these responses until they were subsequently blocked completely. Each trace is a representative depiction of 5-7 individual experiments. Calibration bars: vertical, 5 Mv; horizontal, 20 ms.



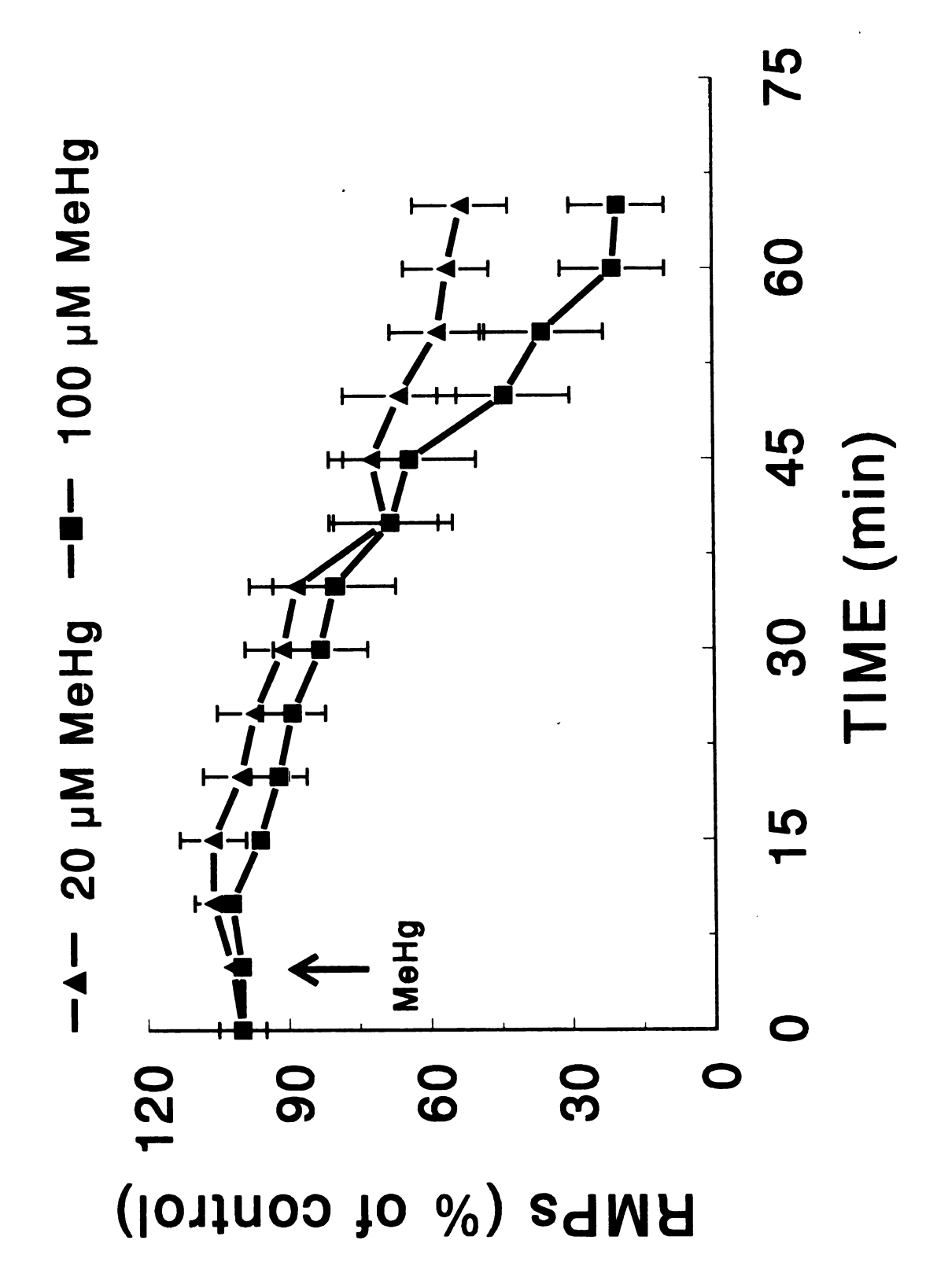
Purkinje cell soma by stimulating climbing fibers in sagittal cerebellar slices. The asterisk indicates that followed by a partial recovery of CF-EPSPs (Right). Note that in both cases suppression of the depolarizing plateau occurred before block of action potentials or complex spikes. Each trace is a Figure 5.9. Time courses of effects of 100 (Left) and 20 µM (Right) MeHg on CF-EPSPs recorded from after CF-EPSPs were blocked at 20 min by 100 µM MeHg or at 50 min by 20 µM MeHg, increasing stimulus intensity could still induce a full recovery of complex spikes (Left) or a full antidromic spike representative depiction of 8 individual experiments.



conduction from climbing fibers to Purkinje cells was affected by MeHg. Also shown in Figure 5.9, at 100 and 20 μ M MeHg, the amplitudes of the steady-state depolarization were almost always reduced prior to block of the complete climbing fiber response. Moreover, the complex spikes appeared to be more sensitive to MeHg than were the antidromically-activated action potentials because the antidromically-activated action potentials remained after complex spikes were blocked completely at 30 min and 50 min by 100 and 20 μ M MeHg, respectively. Initially, block of CF-EPSPs could be restored by increasing stimulation intensity, which was similar to effects of MeHg on PF-EPSPs. Times to complete block of CF-EPSPs by 100 and 20 μ M MeHg were 36 \pm 4 and 67 \pm 16 min, respectively, which were similar to those for block of PF-EPSPs. Thus, MeHg appears to affect the PF-EPSPs and CF-EPSPs similarly.

The resting membrane potentials of Purkinje cells recorded from 24 slices were -60 ± 4 mV under our experimental conditions. Similar to effects of MeHg on hippocampal CA1 pyramidal neuronal membrane potentials, 100 and 20 µM MeHg first hyperpolarized and then depolarized Purkinje cell membranes (Figure 5.10). At 100 and 20 µM MeHg, 11 of 15 and 8 of 9 recordings showed a hyperpolarization prior to depolarization of Purkinje cell membranes. In most cases, decreases in amplitudes of PF-EPSPs or CF-EPSPs to complete block were usually accompanied with a gradual progressive depolarization of Purkinje cell membranes. However, injection of current to restore the membrane potentials to their original levels after PF-EPSPs and

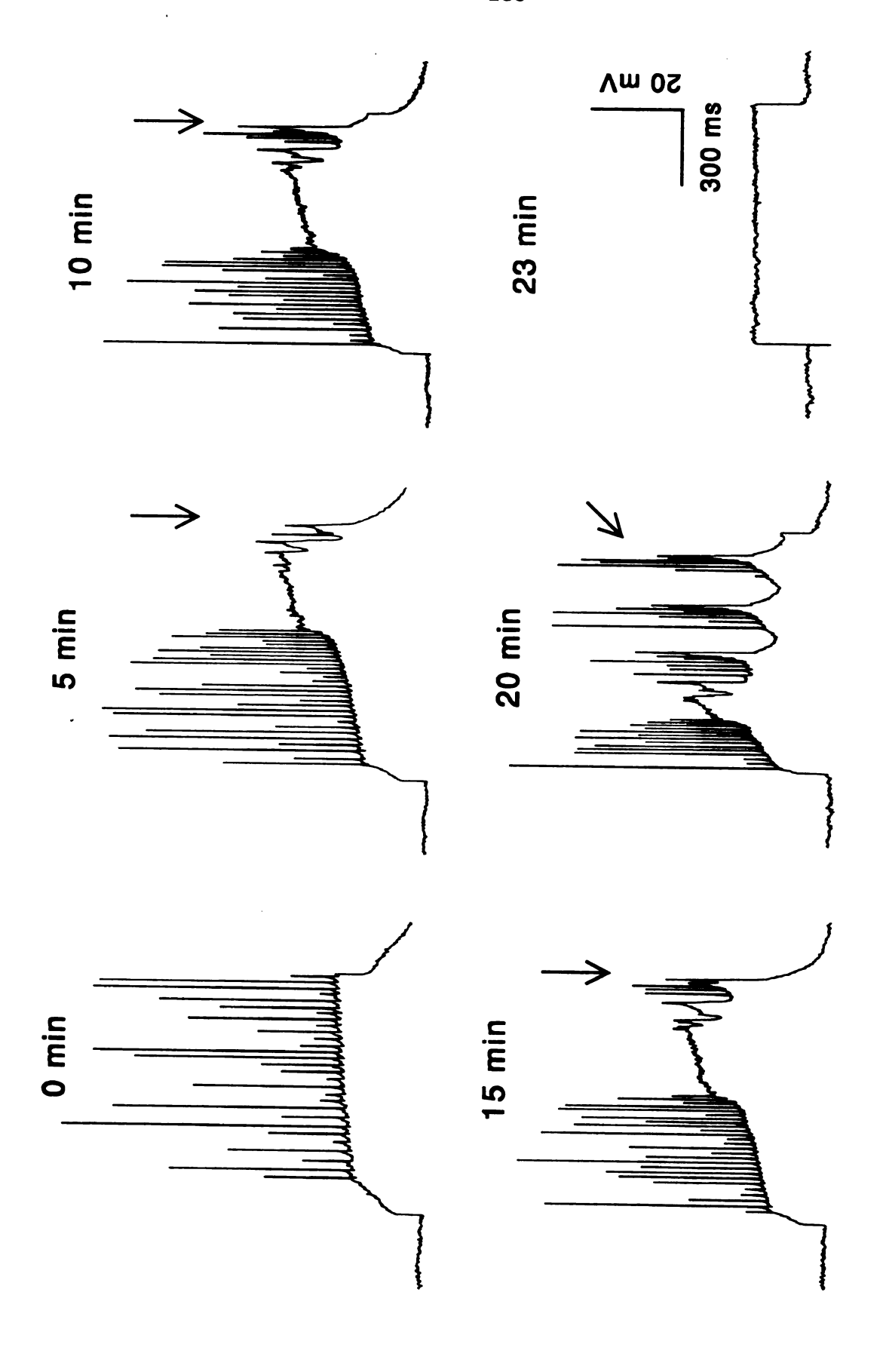
Figure 5.10. Time courses of effects of 100 and 20 µM MeHg on resting membrane potentials of Purkinje cells. The arrow indicates the starting time of application of MeHg. Values are expressed as percentages of pre-MeHg exposure control. All values are the mean ± S.E. of experiments of 7-15 individual experiments.



CF-EPSPs were blocked completely failed to cause recovery of either PF-EPSPs or CF-EPSPs, indicating that while membrane depolarization caused by MeHg may contribute to the effects of MeHg on PF-EPSPs and CF-EPSPs, it was not the primary cause of MeHg-induced block of PF-EPSPs and CF-EPSPs.

Effects of MeHg on somatic action potentials evoked by direct depolarization of Purkinje cells. A characteristic electrical property of Purkinje cells is that direct depolarization of Purkinje cell somata by current injection just above the threshold level through the recording electrode usually generates regular, repetitive firing. The patterns of repetitive firing can be changed by alterations of the amplitude and duration of the injection current pulses (Llinás and Sugimori, 1980a). To determine if MeHg acts directly on Purkinje cells to affect their electrophysiological activity, its effects on evoked repetitive firing activity of Purkinje cells were examined. Bath application of MeHg also altered the patterns of repetitive firing of Purkinje cells. Under conditions similar to those described by Llinás and Sugimori (1980), injecting 500 - 1000 ms positive current pulses at a level slightly higher than the threshold generated a form of regular repetitive firing with a frequency of 30 -40 spikes/second (Figure 5.11). After exposure to 100 µM MeHg, the firing pattern was changed in several respects as shown in Figure 5.11. First, the frequency of firing or the number of so-called fast somatic spikes, described by

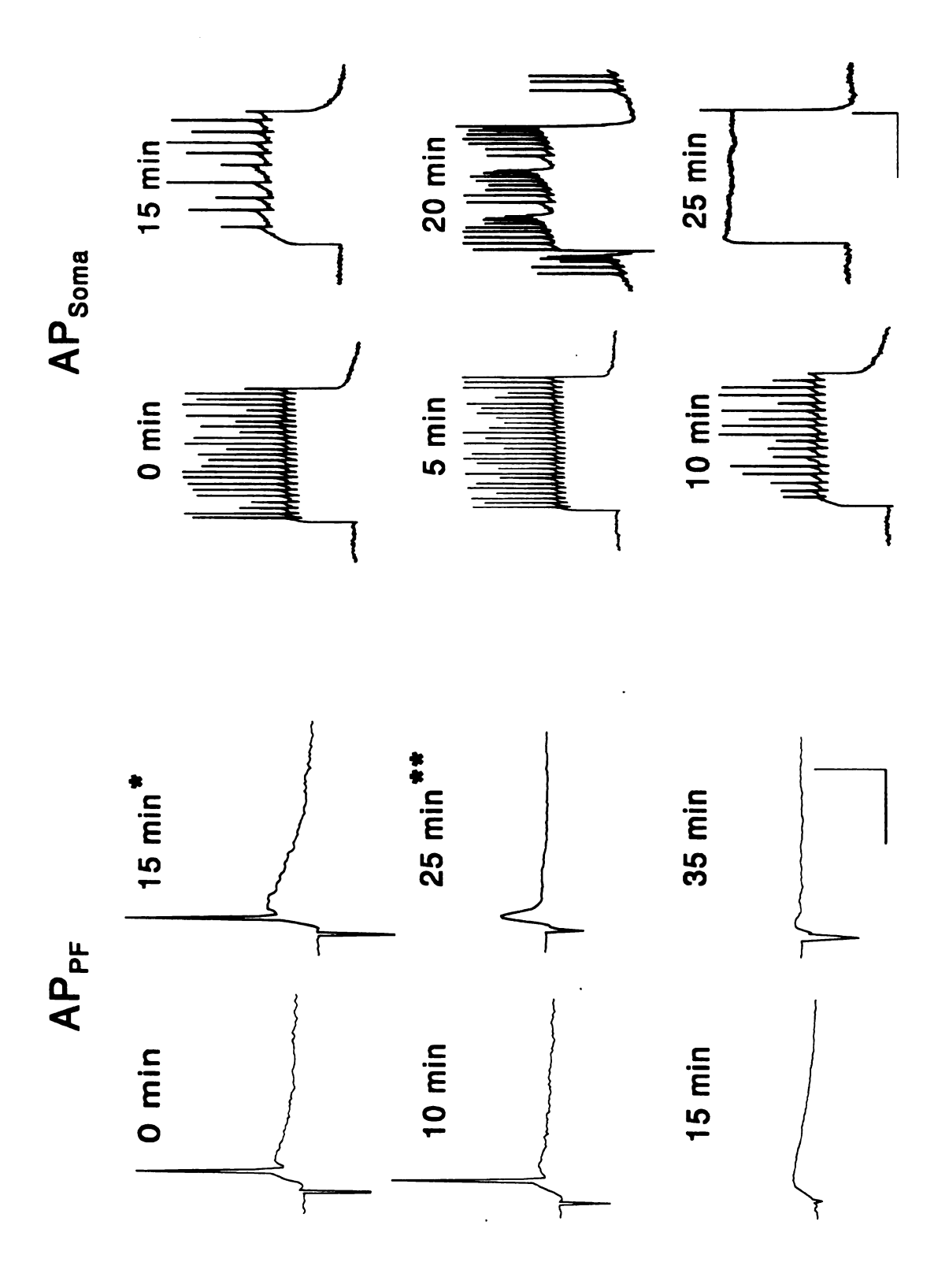
Time course of effects of 100 µM MeHg on responses evoked by direct injection of depolarizing current through the recording electrode at Purkinje cell soma. Normally, threshold current the late half of membrane depolarization plateau became more positive and the fast somatic repetitive injection caused regular repetitive firing (Na*-dependent fast somatic spikes). In the presence of MeHg, spikes disappeared and were replaced by low-amplitude Ca2+ spike burst with a slow rate of rise (as indicated by arrows). Each trace is a representative depection of 8 individual experiments. Note that due to the long digital sampling interval, the Na*-dependent fast somatic spikes varied in amplitude (same reason for those repetitivew firing in Figure 12, 13, 14 and 16). Figure 5.11.



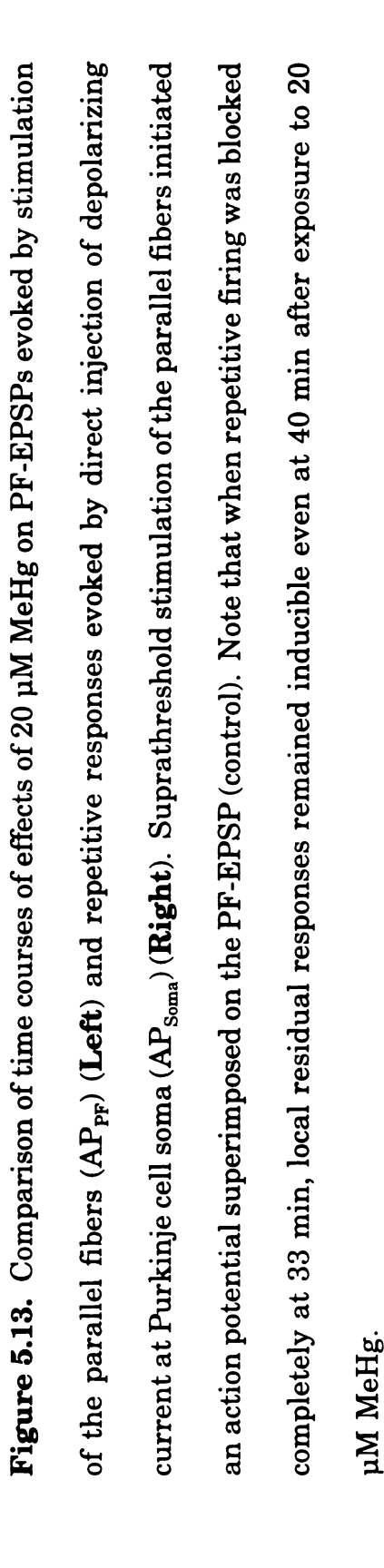
Llinás and Sugimori (1980a), was gradually reduced. Second, the late half portion of the steady-state depolarization became more pronounced and the fast somatic spikes were virtually abolished (at 5, 10 and 15 min in Figure 5.11); replacing them were small amplitude, burst-like spikes (as indicated by arrows). Third, at the late stage of exposure to MeHg, oscillatory bursting activity or so-called depolarizing spike bursts (Llinás and Sugimori, 1980a) were superimposed on the late half of the steady-state depolarization (20 min in Figure 5.11). Finally, all responses were blocked completely by MeHg. Increasing current injection did not restore these responses. Clearly, these results demonstrated that MeHg acted directly on Purkinje cells to block their electrophysiological activity.

The question is then what is(are) the primary site(s) of action of MeHg in blocking PF-EPSPs or CF-EPSPs. To test this, I compared the time-courses of MeHg-induced block of action potentials and PF-EPSPs evoked by stimulation of parallel fibers with responses evoked simultaneously by direct depolarization of Purkinje cell soma through the recording electrode. At 100 µM, MeHg blocked action potentials evoked by stimulating parallel fibers at a level slightly higher than threshold within 15 min (Figure 5.12 Left). At this time, slightly increasing the stimulus intensity could restore an action potential. Ten min later, action potentials evoked at the increased level of stimulation were blocked again; further increasing stimulus intensity only evoked a low-amplitude and narrow-duration EPSP or local responses without

Figure 5.12. Comparison of time courses of effects of 100 µM MeHg on PF-EPSPs evoked by stimulation of parallel fibers (AP PF) (Left) and repetitive responses evoked by direct injection of depolarizing current at Purkinje cell soma (AP_{Soma}) (**Right**). Suprathreshold stimulation of parallel fibers initiated an action potential superimposed on the PF-EPSP (control). The single asterisk indicates that increasing stimulus intensity could again initiate action potentials after they were blocked at 15 min after exposure of the slice to 100 µM. The double asterisks indicates that action potentials evoked at the increased stimulus residual responses remain inducible. Calibration bars: vertical, 20 Mv; horizontal, 20 ms for AP_{PF}, 400 were blocked again at 25 min; further increases of stimulus intensity at this time only produced a local responses or residual PF-EPSP. Note that when repetitive firing was blocked completely at 25 min, local ms for AP_{Soma} .



an action potential superimposed on them. The residual synaptic responses were blocked eventually at 35 min. At the same time, repetitive firing of Purkinje cells evoked by depolarizing current pulses were first reduced significantly in number, then changed to burst-like firing and finally blocked completely at 25 min (Figure 5.12 Right). In almost all recordings, block of action potentials evoked by stimulating parallel fibers and of repetitive firing evoked by current injection occurred at the same time, suggesting that they resulted from the same effect. However, complete block of the residual PF-EPSPs or local responses required a slightly longer time. The same was true for effects of 20 µM MeHg on these responses. As shown in Figure 5.13, at 35 min the repetitive firings evoked by depolarizing current pulses were blocked completely by 20 µM MeHg (Figure 5.13 Right), whereas the residual PF-EPSPs could still be initiated at 40 min and were blocked completely only after 60 min exposure to MeHg (Figure 13 Left). We also compared time-courses of block of CF-EPSPs evoked by stimulating climbing fibers with responses evoked simultaneously by direct depolarization of Purkinje cell soma through the recording electrode. In Figure 5.14, the somatic repetitive firings were evoked by a short current pulse (50 ms). At 100 µM, MeHg blocked action potentials or complex spikes evoked by stimulating climbing fibers and the somatic repetitive firings evoked by direct depolarization of Purkinje cells



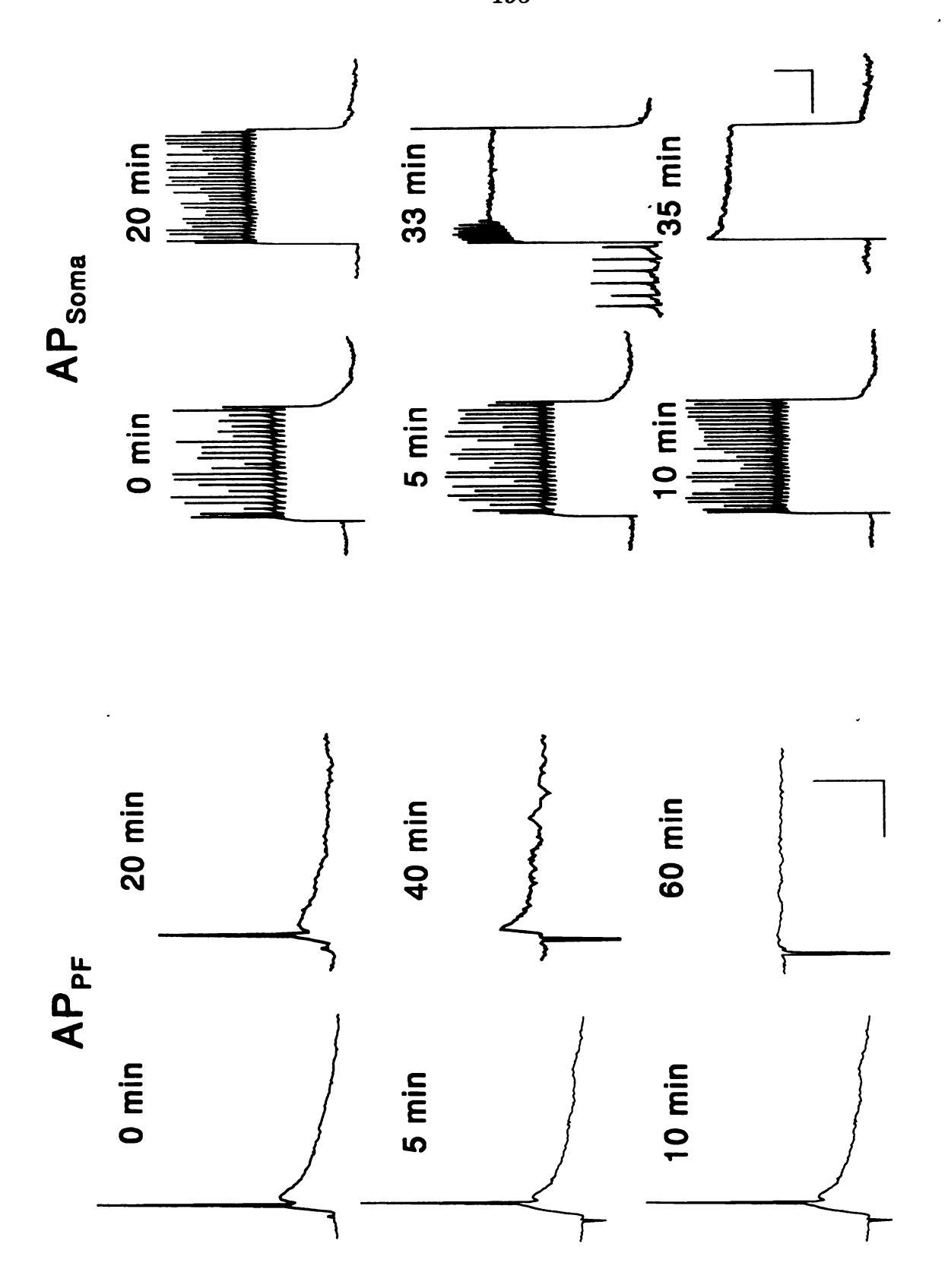
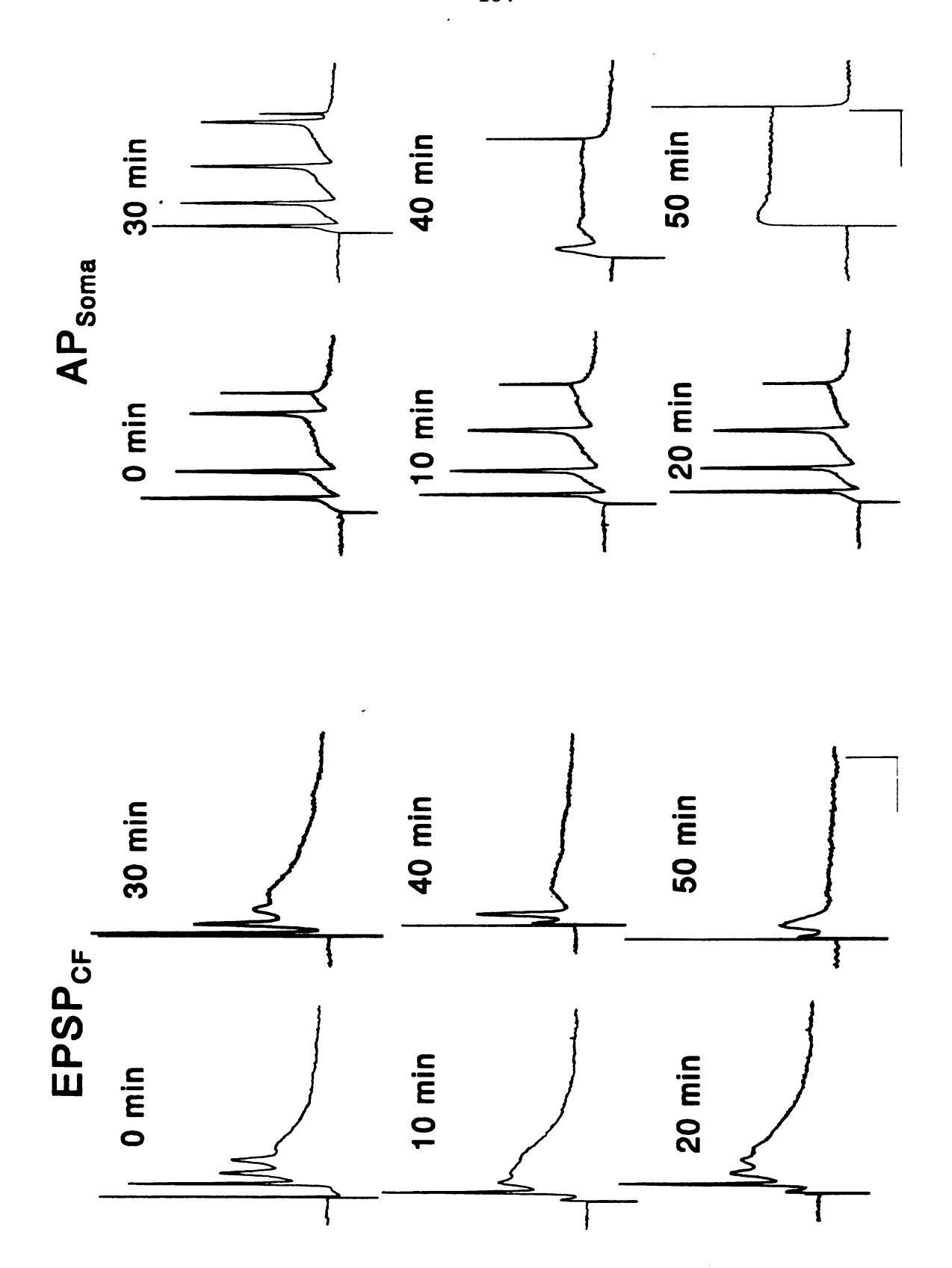


Figure 5.14. Comparison of time courses of effects of 100 µM MeHg on CF-EPSPs evoked by stimulation was blocked completely at 50 min, local residual EPSP responses remained inducible. Each trace is a of the climbing fibers (EPSP_{pr}) (Left) and repetitive responses evoked by injection of short duration depolarizing currents at Purkinje cell soma (AP_{Soma}) (**Right**). Suprathreshold stimulation of parallel fibers initiated an action potential superimposed on PF-EPSP (control). Note that when repetitive firing representative depiction of 8 individual experiments.

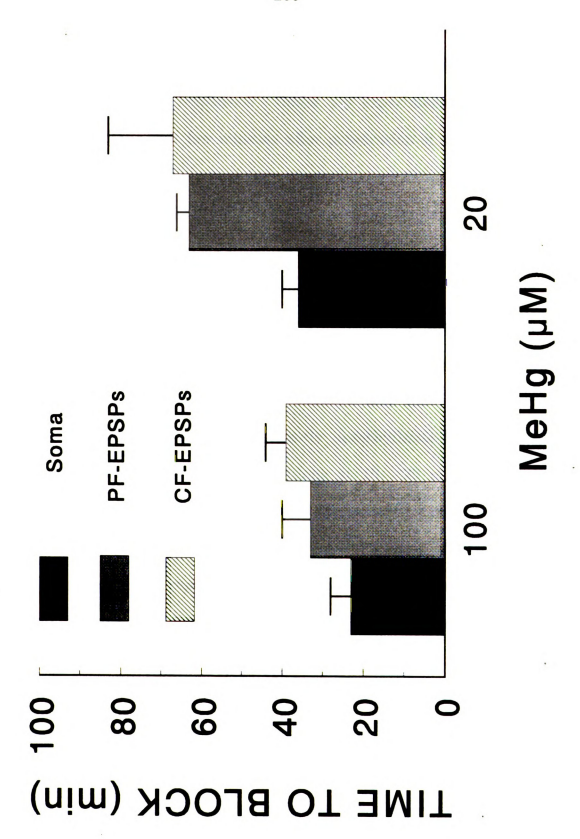


through current injection similarly. However, block of the residual synaptic responses evoked by stimulating climbing fibers took slightly longer (Figure 5.14). In this case, complete block of the residual synaptic responses occurred at 55 min. Thus, these results suggest that the voltage-dependent responses or action potentials evoked by stimulating parallel fibers, climbing fibers or by direct depolarization of Purkinje cells were equally sensitive to MeHg. However, the residual synaptic responses or local responses evoked by stimulating parallel or climbing fibers were slightly less sensitive to MeHg than were those voltage-dependent responses. Thus, the primary sites of action of MeHg in blocking PF-EPSPs and CF-EPSPs appear to be the postsynaptic Purkinje cells. Figure 5.15 summarizes the times to block of PF-EPSPs, CF-EPSPs and responses evoked by current injection. MeHg blocked PF-EPSPs and CF-EPSPs similarly but slightly more slowly than it blocked somatic responses if the residual synaptic responses are taken into account.

Effects of MeHg on spontaneous activity of Purkinje cells. In addition to those unique evoked responses, Purkinje cells also displayed another well-described electrical property-spontaneous firing or autorhythmic oscillatory activity, which was observed in both extracellular and intracellular recordings (Llinás and Sugimori, 1980a,b; Aubry et al., 1991; Chang et al., 1993). In hippocampal slices, spontaneous activity appeared to be less sensitive to MeHg than were evoked responses in CA1 pyramidal neurons

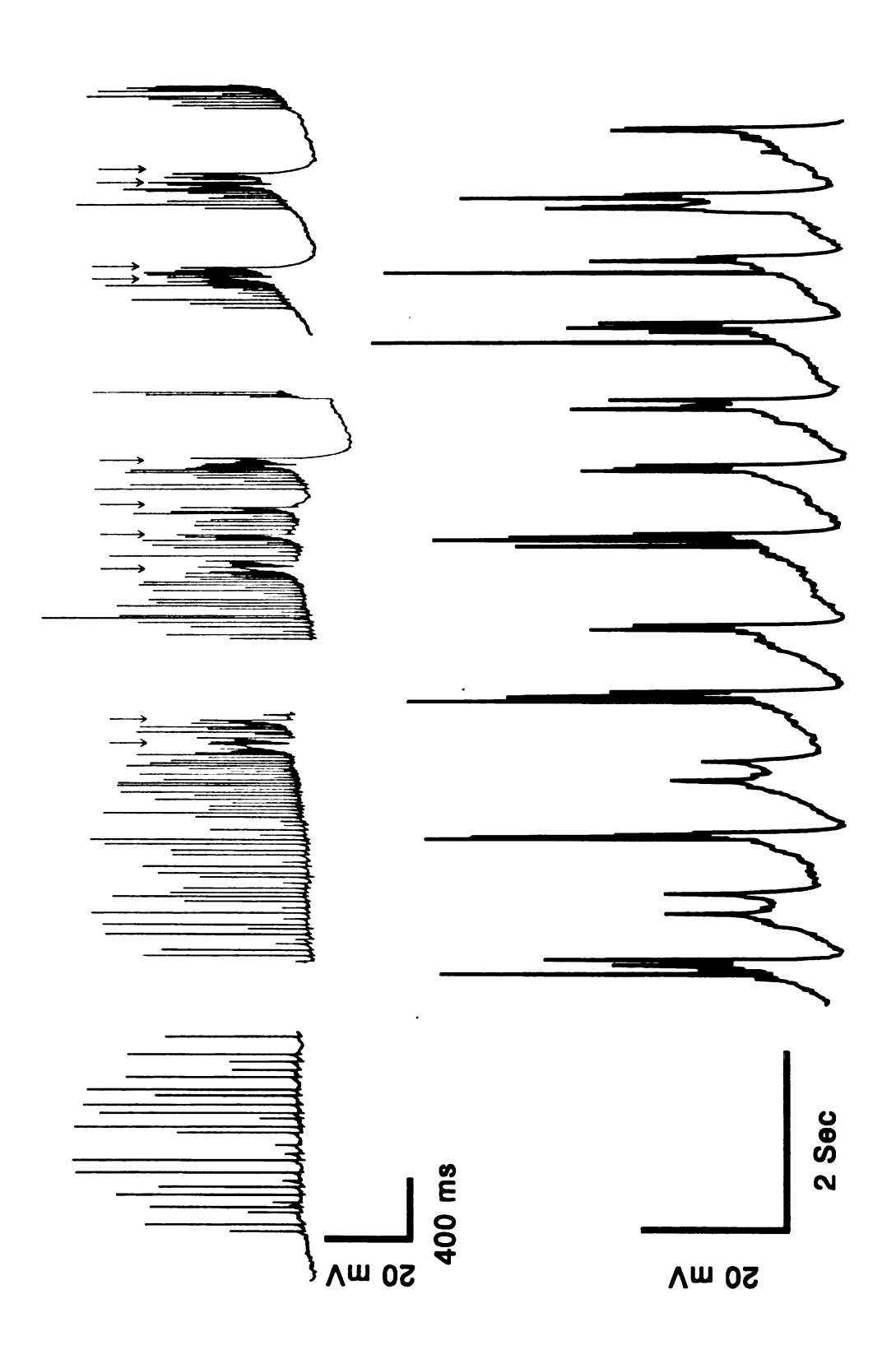
Figure 5.15. Comparison of times to block of PF-EPSPs, CF-EPSPs and repetitive firing responses

(Soma) of Purkinje cell by 100 and 20 μM MeHg. All values are the mean ± S.E. of 3-12 experiments.



(Yuan and Atchison, 1993). To test if this was also the case for Purkinje cells, effects of MeHg on spontaneous firing activity were examined simultaneously with those on evoked responses. Under my experimental conditions, in general, within the first few minutes after penetration of their membranes, Purkinje cells displayed a mixed form of spontaneous firing including the socalled Na⁺-dependent, fast somatic repetitive action potentials, Ca²⁺-dependent slow dendritic spikes or bursting, as described by Llinás and Sugimori (1980a,b) (Figure 5.16). After recordings were stable for 5 - 10 min, the pattern of spontaneous firing became predominantly the repetitive, fast somatic spike form. However, after exposure to 100 µM MeHg, initially, the number of fast somatic spikes was reduced and then the patterns of spontaneous firing became predominantly autorhythmic bursting activity separated by interburst hyperpolarizations at 15 - 20 min (Figure 5.17). Subsequently, all spikes were blocked and the remaining responses were the slow rate of rise, low-amplitude oscillatory local responses. At the same time, all action potentials or repetitive spikes evoked by stimulating parallel fibers or climbing fibers or by direct depolarization of Purkinje cell soma and even by antidromic stimulation of Purkinje cell axons were blocked as well, except for residual PF-EPSPs and CF-EPSPs. Later, the remaining responses including the low-amplitude oscillatory local responses, the residual PF-EPSPs and CF-EPSPs were also blocked (Figure 5.17). These results suggest that all these somatic action potentials or repetitive spikes either occurring spontaneously

Figure 5.16 Spontaneous repetitive firing of a Purkinje cell just after penetration with a glass recording microelectrode. Top: spontaneous repetitive firing recorded on a rapid time scale. Bottom: spontaneous repetitive firing recorded on a slow time scale. Arrows indicate the low-amplitude Ca²⁺-dependent, dendritic spike bursts.



responses were also blocked with the exception of the residual local responses evoked by stimulation of Figure 5.17. Effects of 100 µM MeHg on spontaneous repetitive firing of Purkinje cells. Traces are from 3 individual experiments. The asterisks indicate that at the same time, all evoked voltage-dependent parallel fibers or climbing fibers.

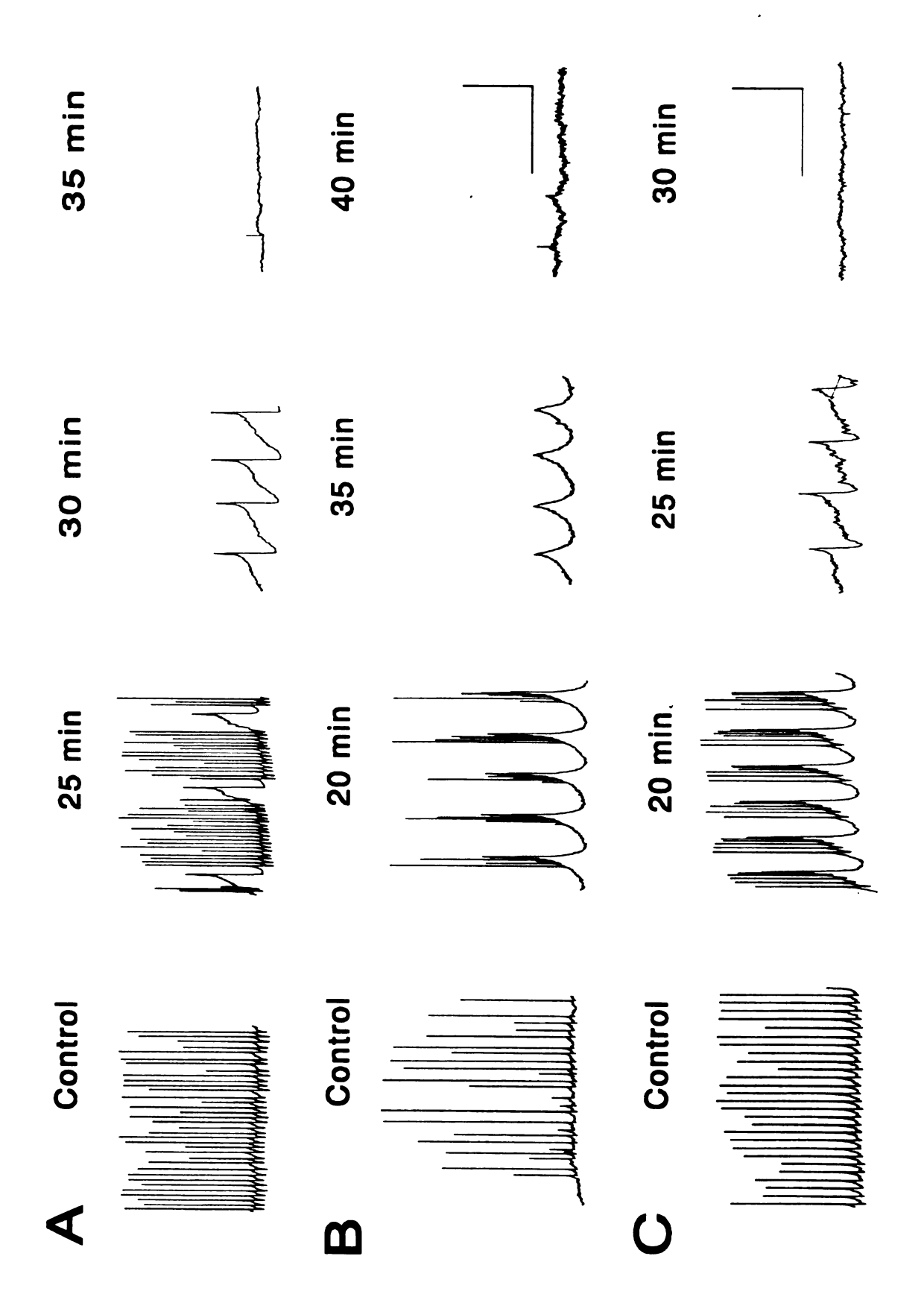
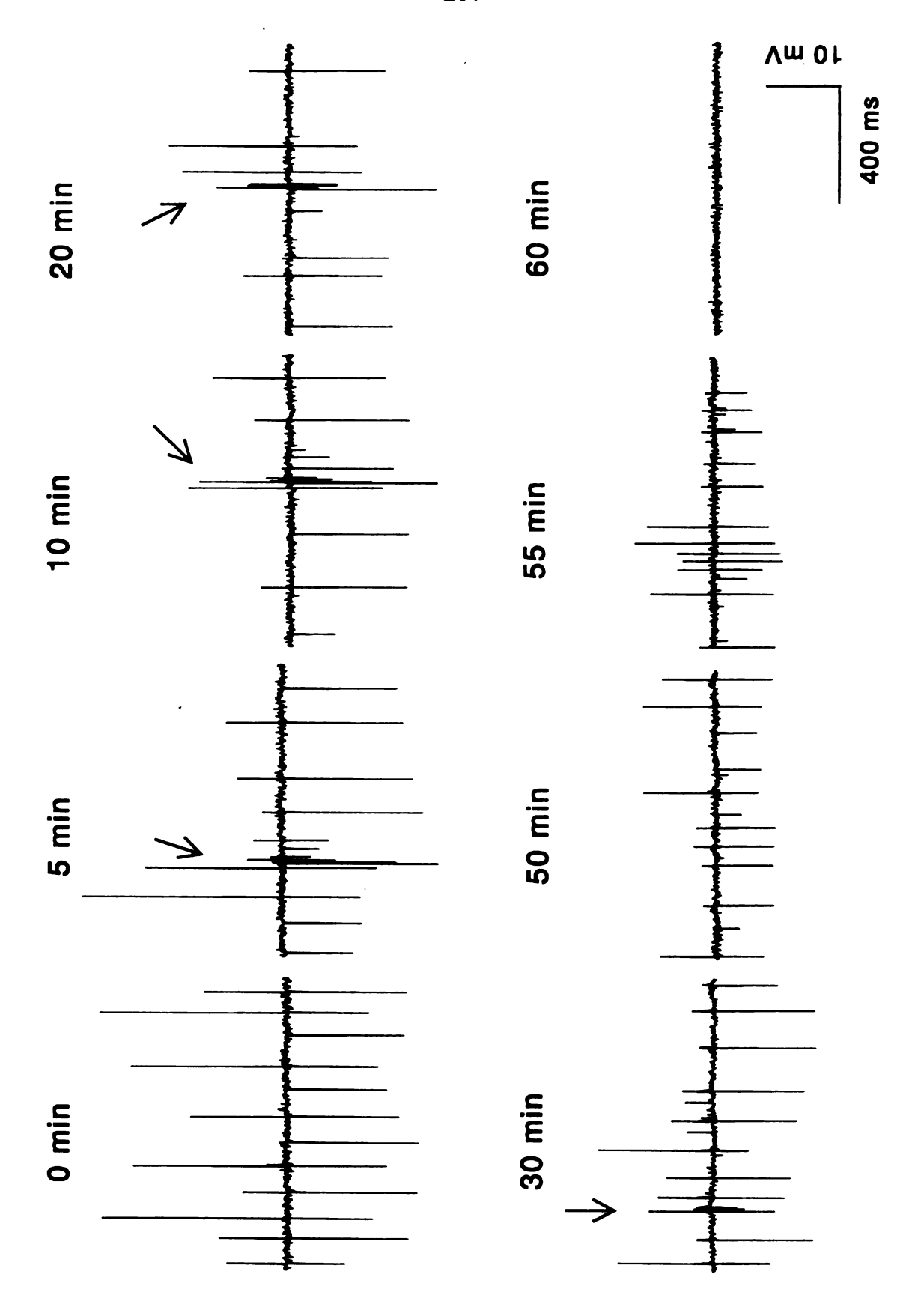
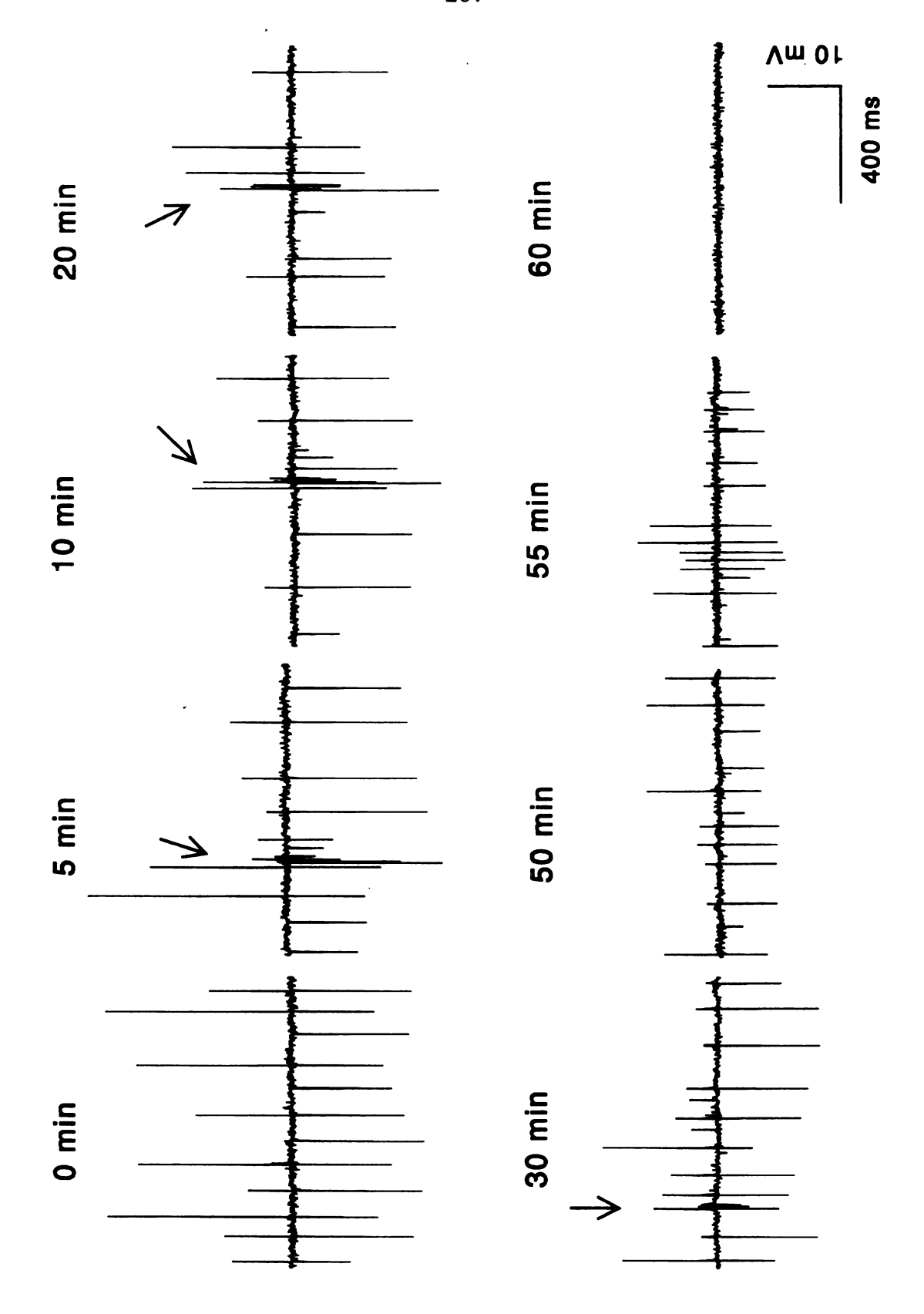


Figure 5.18. Effects of 100 µM MeHg on spontaneous firing of Purkinje cells recorded from the Purkinje cell layer of a transverse cerebellar slice using extracellular recording techniques. Arrows indicate responses evoked by stimulating the parallel fibers on the surface of the molecular layer. Each trace is a representative depiction of 5 individual experiments.



cell layer of a transverse cerebellar slice using extracellular recording techniques. Arrows indicate Figure 5.18. Effects of 100 µM MeHg on spontaneous firing of Purkinje cells recorded from the Purkinje responses evoked by stimulating the parallel fibers on the surface of the molecular layer. Each trace is a representative depiction of 5 individual experiments.



or evoked were equally sensitive to MeHg. Interestingly, in many cases after responses recorded from intracellular recordings were blocked completely, withdrawing recording electrodes out of cells could still pick up some extracellular spontaneous firing activity. Thus, I examined effects of MeHg on the spontaneous activity obtained from extracellular recordings. Figure 5.18 shows representative extracellular spontaneous firing activity. After exposure of a transverse slice to 100 µM MeHg for 5 to 30 min, stimulating parallel fibers could initiate population spikes, as indicated by the arrows. After 40 min, no further evoked responses could be observed, however, spontaneous firing remained until complete block occurred at 60 min. Thus, spontaneous activity appears to be less sensitive to MeHg than are evoked responses.

DISCUSSION

Previously, we demonstrated that MeHg affects both excitatory and inhibitory synaptic transmission in hippocampal slices. However, a more sensitive and primary target of MeHg in the CNS is the cerebellum, especially Thus, a direct examination of effects of MeHg on the cerebellar cortex. cerebellar synaptic transmission should be especially relevant to its in vivo neurotoxicity. As a first step, the objective of the present study was to determine if MeHg differentially affects synaptic transmission between parallel-fibers or climbing-fibers and Purkinje cells. Acute bath application of 20 and 100 µM MeHg caused a biphasic effect-namely an initial increase of amplitude followed by a decrease to block of the field potentials recorded from the molecular layer of cerebellar slices. This pattern was observed for PFVs, PSRs and CFRs evoked by stimulation of parallel fibers and climbing fibers. Moreover, this pattern is a characteristic effect of MeHg also seen in MeHg appears to block the glutamate-mediated hippocampal slices. postsynaptic responses PSRs and CFRs with a similar time course and more rapidly than it did PFVs. Intracellular recordings supported this conclusion as MeHg blocked both PF-EPSPs and CF-EPSPs with similar time courses. The primary site of action of MeHg in blocking these responses appears to be the postsynaptic Purkinje cells because MeHg blocked responses evoked by direct depolarization of Purkinje cell soma with a similar time course to its

effects on PF-EPSPs and CF-EPSPs. Moreover, MeHg also hyperpolarized and then depolarized Purkinje cell membranes and suppressed spontaneous activity.

Purkinje cells differ from most neurons in the CNS in that a single Purkinje cell receives two major excitatory synaptic inputs: the parallel fibers and climbing fibers. One Purkinje cell may make synaptic contacts with as many as 200,000 parallel fibers. On the other hand, a given Purkinje cell only makes synaptic contact with one climbing fiber, however, as many as 200 contacts may be formed between each Purkinje cell and each climbing fiber (Llinás and Walton, 1990). When activated, both synaptic responses can be recorded easily in the molecular layer of the cerebellar cortex using extracellular recording techniques. In addition, when parallel fibers are activated, action potential propagation along the parallel fibers can be picked up and recorded as the PFV by an extracellular recording electrode in the molecular layer. As expected, exposure of cerebellar slices to MeHg caused stimulation and then suppression to complete block of these field potentials. In hippocampal slices, MeHg caused similar effects on population spikes recorded from CA1 pyramidal neurons. The early stimulatory effects of MeHg on hippocampal CA1 excitatory synaptic transmission are apparently due primarily to a preferential action of MeHg on GABA, receptor-mediated inhibitory synaptic transmission leading to disinhibition of excitatory synaptic function (Yuan and Atchison, 1997). The same mechanism may apply to the

stimulatory effects of MeHg on the glutamate-mediated postsynaptic responses in Purkinje cells such as PSRs evoked by stimulating parallel fibers and CFRs evoked by stimulating climbing fibers. Purkinje cells also receive inhibitory inputs directly from two types of GABAergic interneurons- the stellate and basket cells and indirectly from Golgi cells (Llinás and Walton, 1990). Golgi cells, which are excited by mossy, climbing and parallel fibers, exert an inhibitory action on granule cells and indirectly modulate activity of Purkinje It is possible that this disinhibition in response to MeHg is also responsible for the early increase in PFV amplitude. It may be also related to changes in the long-term depression induced by interaction among the parallelfiber, climbing-fiber excitatory pathways and Purkinje cells (Sakurai, 1990; Crepel and Jaillard, 1990; Konnerth et al., 1992; Kano et al., 1992; Linden et al., 1993; Aiba et al., 1994; Schotter, 1995). The unexpected result is that MeHg blocked the presynaptic PFVs apparently more slowly than it blocked the glutamate-mediated PSRs and CFRs. Pathologically, the granule cells are well-known to be highly sensitive to MeHg (Hunter and Russell, 1954; Takeuchi et al., 1962; Chang, 1977, 1980; Syversen et al., 1981) and their axons, which form the parallel fibers, are unmyelinated and injured by MeHg during chronic exposure. Thus, theoretically, initiation and propagation of action potentials along parallel fibers should be affected by MeHg at least as readily as were the postsynaptic responses. It is unclear why PFVs are relatively less sensitive to MeHg than are PSRs and CFRs. Perhaps, it is in part due to the relatively high Na⁺ channel density in the presynaptic parallel fibers making them more resistant to MeHg, or perhaps it simply reflects a preferential effect of MeHg on either the glutamate release processes from parallel fibers and climbing fibers or postsynaptic glutamate receptor functions.

To determine further how MeHg caused the effects on the field potentials, PF-EPSPs and CF-EPSPs were examined using intracellular recording techniques. Consistent with the results obtained from extracellular recordings, MeHg blocked both PF-EPSPs and CF-EPSPs with similar time courses, although the two responses were generated from two different synaptic pathways with distinct electrophysiological characteristics. The PF-EPSPs generated by stimulation of parallel fibers are single-peaked and graded amplitude responses, the simple spike. Each parallel fiber, when activated, produces a small synaptic current that must sum at the initial segment of Purkinje cells to produce an action potential. Thus, activation of parallel fibers leads to generation of voltage- and Na⁺-dependent simple spikes graded as a function of the summation of synaptic currents from many parallel fiber synapses. Conversely, the CF-EPSPs generated by stimulation of climbing fibers are all or none Ca2+-dependent responses (Crepel and Delhaye-Bouchaud, 1978; Llinás and Sugimori, 1980a,b; Crepel et al., 1981, 1982; Humura et al., 1985; Anderson, 1989; Llinás and Walton, 1990; Llano et al., 1991; Stuart and Häusser, 1994). Stimulation of climbing fibers produces a large synchronized depolarization of Purkinje cell dendrites, which then activates the dendritic Ca²⁺ channels to initiate the slow dendritic Ca²⁺ spikes. It is not surprising that MeHg blocked both responses since it reduces currents carried through voltage-dependent Na⁺ channels (Shrivastav et al., 1976; Quandt et al., 1982; Shafer and Atchison, 1992; Leonhardt et al., 1996) and Ca2+ channels (Shafer and Atchison, 1989; Shafer et al., 1990; Shafer and Atchison, 1991, 1992; Hewett and Atchison, 1992; sirois and Atchison, 1996; Leonhardt et al., 1996). The similarity in blocking both responses suggests that MeHg acts via a similar mechanism to block both PF-EPSPs and CF-EPSPs. In CF-EPSPs recordings, on the other hand, the early suppression of the depolarization plateau and block of complex spikes almost always occurred before block of the antidromically-activated spikes, suggesting that the orthodromically-activated synaptic responses may be more sensitive to MeHg than were antidromically-activated responses and implying that effects of MeHg on the process of synaptic transmission were involved. Unlike the effects of MeHg on EPSPs recorded from the CA1 region of hippocampal slices, overall, MeHg did not cause a significant early stimulatory effect on PF-EPSPs and CF-EPSPs although it caused a slight and transient early increase in some slices. These results were also inconsistent with those obtained from extracellular recordings, in which MeHg caused a significant early increase prior to suppression of the field potentials. The difference between results obtained from extracellular and intracellular recordings may indicate that MeHg does not affect the response of an individual Purkinje cell to a given stimulus, but rather affects the recruitment of additional Purkinje cells which fire synchronously at the early stage of exposure to MeHg.

To determine if MeHg preferentially acts on Purkinje cells to block PF-EPSPs or CF-EPSPs, effects of MeHg on responses evoked by direct depolarization of Purkinje cells with current injection at the somata were examined and compared with those of MeHg on PF-EPSPs and CF-EPSPs. Normally, injection of a short (50 - 100 ms) or long current pulse (500 - 1300 ms) at the threshold levels in Purkinje cell somata generates regular, repetitive firing, fast somatic spikes. As the intensity of current injection pulse is increased, particularly for long current pulses, the regular repetitive firing form was replaced, near the end of the pulse, by the complex, low-amplitude spike burst-depolarizing spike burst (Llinás and Sugimori, 1980a). The fast somatic spike is a low-threshold, voltage- and Na⁺-dependent response, which is blocked by removal of extracellular Na⁺ or by application of TTX. The depolarizing spike burst, on the other hand, is a slow rate of rise, highthreshold, voltage- and Ca2+-dependent response, which is TTX-insensitive and blocked by removal of extracellular Ca²⁺ or by application of Ca²⁺ channel blockers such as Co²⁺, Cd²⁺ or Mn²⁺ (Llinás and Sugimori, 1980a,b; Aubry et al., 1991; Chang et al., 1993). However, in the presence of MeHg and without changing the amplitude of threshold current injection, the patterns of the repetitive firing induced were altered such that they resembled responses caused by increasing current pulses under normal conditions. Thus, MeHg appears to alter Purkinje cell membrane ion conductances in the same way that they are altered by increasing stimulus intensity. Normally, generation of this Ca²⁺-dependent depolarizing spike burst requires higher stimulus intensity because of its high-threshold nature. However, exposure of slices to MeHg induced an identical response even at normal threshold stimulus level. That suggests that MeHg may initially change the threshold level for activation of Ca2+ channels. Again, as it did with CA1 pyramidal cells in hippocampal slices, MeHg blocked all voltage-dependent responses including both Na⁺- and Ca²⁺-dependent spikes evoked by stimulation of parallel or climbing fibers or by direct current injection at Purkinje cell somata with a similar time course. This suggests that MeHg primarily acts at the Purkinje cells via a similar mechanism to block these voltage-dependent responses. However, a slightly longer time was required for complete block by MeHg of the synaptically-activated local responses or the residual PF-EPSPs or CF-EPSPs compared with those required for blocking voltage-dependent responses. This implies that glutamate receptor functions may be also affected by MeHg, although they appear to be relatively less sensitive to MeHg than are those voltage-dependent channels. This is consistent with the results that MeHg blocked orthodromically-activated synaptic responses more rapidly than it did antidromically-activated responses. In addition, the prolonged latencies from stimulus artefact to onset of PF-EPSPs and CF-EPSPs suggest that the current conduction from parallel fibers or climbing fibers to the dendrites of Purkinje cells were affected by MeHg. Thus, once again MeHg apparently acts at multiple sites to block synaptic transmission between parallel fibers or climbing fibers and Purkinje cells. The primary sites appear to be the postsynaptic Purkinje cells, although the presynaptic actions may be also involved.

In addition to effects of MeHg on the evoked repetitive firing of Purkinje cells, MeHg also changed the patterns of spontaneous repetitive firing of Purkinje cells. Normally, the spontaneous repetitive firing consists of predominantly the Na⁺-dependent fast somatic spikes and some low-amplitude Ca²⁺-dependent slow dendritic spike bursts (Llinás and Sogimori, 1980a). After exposure to MeHg, the patterns of spontaneous firing changed to predominantly Ca²⁺-dependent autorhythmic burst. This effect of MeHg is very similar to effects of TTX on Purkinje cell spontaneous firing (Aubry et al., 1991; Chang et al., 1993). Application of TTX, a specific Na⁺-channel blocker, to cerebellar slices suppressed Na⁺ spikes of Purkinje cells and induced Ca²⁺dependent oscillatory firing activity. This oscillatory firing activity was thought to be maintained by an intrinsic property of Purkinje cells inasmuch as it remained after block of both excitatory and inhibitory synaptic inputs to Purkinje cells (Chang et al., 1993). The mechanism proposed to be responsible for TTX-induced oscillatory activity of Purkinje cells was block of Na⁺ channels leading to activation of the Na⁺/Ca²⁺ exchanger with a net gain of intracellular Ca2+ (Aubry et al., 1991; Chang et al., 1993). Compared with TTX, MeHg blocks both Na⁺ and Ca²⁺ channels, and increases [Ca²⁺]_i in a variety of cells (Komulainen and Bondy, 1987; Kauppinen et al., 1989; Hare and Atchison, 1992b; Denny et al., 1993; Hare et al., 1993, 1995) including primary cultures of cerebellar granule cells (Marty and Atchison, 1997). Thus, the MeHginduced oscillatory burst activity may be related to an effect on regulation of [Ca²⁺], of Purkinje cells. Perhaps, initially, MeHg blocks Na⁺ channels in the same way as TTX does to activate the Na⁺/Ca²⁺ exchanger (Aubry et al., 1991; Chang et al., 1993), which unmasks intrinsic oscillatory activity of Purkinje cells by an unknown mechanism, increases [Ca2+], and depolarize Purkinje cell membranes to generate the slow Ca2+ spikes. Subsequently, the increase in [Ca²⁺], activates Ca²⁺-dependent K⁺ channels leading to hyperpolarization of Purkinje cells to return their membrane potentials toward the resting level. As the K⁺ channels close, another cycle begins. However, at the late stage of exposure of slices to MeHg, all action potentials or voltage-dependent responses were blocked and what was left were only those low-amplitude oscillatory local responses. These local oscillatory responses were later blocked completely along with the synaptically-activated local responses (residual PF-EPSPs and CF-EPSPs) at the same time, suggesting that the Ca2+-dependent oscillatory burst activity of Purkinje cells is of dendritic origin. This is consistent with the conclusion of Llinás and Sugimori (1980a,b). Spontaneous firing activity is also observed in extracellular recordings. Interestingly, MeHg blocked the spontaneous responses more slowly than it did the evoked responses.

addition, in many cases, after evoked responses recorded by intracellular recording were blocked, the extracellular spontaneous responses often remained, suggesting that the spontaneous responses were less sensitive to MeHg than were evoked responses. This is consistent with the effects of MeHg on neuromuscular transmission (Atchison and Narahashi, 1982), in which spontaneous release of ACh remained observable at the time of evoked release of ACh were blocked completely by MeHg. Thus, mechanisms responsible for block by MeHg of spontaneous and evoked responses were differently. Moreover, it appears that MeHg takes longer time to block extracellular responses than it does intracellular responses. This may be due simply to (1) in intracellular recording, penetration of cell with recording electrode causes injury of membrane, which accelerates the action of MeHg on cell; (2) accessibility of MeHg to cells located on the surface and in the deep tissue of slices differs; extracellular recording electrode picks up firing from a population of cells which may include those located in both surface and deep tissues. For those cells in the deep tissue, it will take a longer time for MeHg to access them, and hence a longer time to block their responses.

In conclusion, MeHg caused biphasic effects on synaptic transmission between parallel-fibers or climbing-fibers and Purkinje cells in cerebellar slices. MeHg appears to act primarily at the postsynaptic Purkinje cells to cause these effects because it blocked responses evoked by directly depolarizing Purkinje cells. However, multiple actions including hyperpolarizing and

depolarizing the Purkinje cell membranes, blocking current conduction and affecting glutamate receptor functions may be also involved in these effects. MeHg blocked spontaneous firing of Purkinje cells and acted in a manner similar to TTX to induce a Ca²⁺-dependent, spontaneous oscillatory burst activity in Purkinje cells. This is superficially consistent with the findings that MeHg increases [Ca²⁺]_i in a variety of cell types. In general, the effects of MeHg on electroresponsesiveness of Purkinje cells in cerebellar slices are similar to those on CA1 pyramidal cells in hippocampal slices.

CHAPTER SIX

SUMMARY AND CONCLUSION

A. SUMMARY

Previous studies have extensively examined effects of MeHg on peripheral synaptic transmission at the neuromuscular junction and autonomic ganglia. However, little is known of the effects and underlying mechanisms of MeHg on central synaptic transmission. Using extracellular recording techniques I previously demonstrated that acute bath application of MeHg to hippocampal slice preparations disrupted CA1 neuronal membrane excitability and synaptic transmission (Yuan and Atchison, 1993, 1994). However, due to the limitations of extracellular recording techniques, it is difficult to identify where and how MeHg caused these effects. In addition, to date, there are no reports of effects of MeHg on cerebellar synaptic transmission even though it is well-known that the cerebellum, and especially the cerebellar cortex, is one of the major neurotoxic targets of MeHg in the CNS. Also, it is unclear whether or not the data obtained following acute exposure of the hippocampus to MeHg can be used to predict effects of MeHg on other CNS targets. Thus, the present study was designed primarily to compare and characterize the in vitro effects of acute exposure to MeHg on synaptic transmission in both hippocampal slices and cerebellar slices and to explore the potential mechanisms underlying these effects. To do this, conventional electrophysiological recording methods including extracellular and intracellular microelectrode recording, SEVC recording and iontophoresis techniques were used.

Concentrations of MeHg used in this dissertation varied from 4 to 500 µM, which are similar to those used in other studies in isolated cells, tissues, etc. The concentrations of 4 and 20 µM MeHg was used because they are within the range of those reported to be found in blood of patients poisoned with MeHg during acute exposure episode in Iraq. My previous results have demonstrated that the effects of MeHg on those field potentials recorded from CA1 region of hippocampal slices were concentration- and time-dependent. Moreover, the characteristics of effects of MeHg at lower (4 and 20 µM) or higher concentrations (100 and 500 µM) on hippocampal synaptic transmission are generally similar (Yuan and Atchison, 1993, 1994), except that latencies to onset of effects of MeHg occurred at lower concentrations of MeHg were much longer than those that occurred at higher concentrations of MeHg. Thus, relatively higher concentrations of MeHg (100 and 500 µM) were also used in the present study to shorten the latency to onset of effects of MeHg on electrophysiological responses and to examine the concentration-dependence of any responses observed. This is especially helpful when intracellular recordings were made in relatively small neurones, because it is usually difficult to maintain a stable, long duration of intracellular recording in small neurons.

Several new findings presented in this dissertation are consistent with the following conclusions: (1) acute bath application of MeHg blocked central synaptic transmission in brain slice in a concentration- and time-dependent manner; (2) MeHg initially stimulates and then suppresses excitatory synaptic transmission in both hippocampal and cerebellar slices; (3) MeHg hyperpolarizes and then depolarizes both hippocampal CA1 pyramidal and cerebellar Purkinje cell membranes; (4) it appears that inhibitory synaptic transmission is more sensitive to MeHg than is excitatory synaptic transmission in hippocampal slices, which may be primarily responsible for the early apparent stimulatory effects of MeHg on hippocampal synaptic transmission. (5) MeHg appears to act at multiple sites to block central synaptic transmission, however, the primary sites of action of MeHg on synaptic transmission in the tested synaptic pathways (Schaffer collateral-CA1 pyramidal pathway in hippocampal slice, parallel fiber- and climbing fiber-Purkinje cell pathways in cerebellar slices) appear to be the postsynaptic neurons (CA1 pyramidal and Purkinje cells); (6) MeHg appears to affect voltage-dependent responses more rapidly than does synaptically-activated responses; (7) MeHg appears to block evoked responses more rapidly than does the spontaneous responses.

One of the characteristic effects of MeHg on central synaptic transmission is that MeHg caused a concentration- and time-dependent biphasic effect on synaptic transmission in both hippocampal and cerebellar slices. In hippocampal slices, 4 - 500 µM MeHg initially increased and then suppressed amplitudes of population spikes and EPSPs to complete block. Similarly, MeHg caused a transient stimulation prior to suppression of field

potentials recorded from the molecular layer of cerebellar slices by activation of either the parallel or climbing fibers. Thus, the biphasic effects of MeHg on synaptic transmission in both hippocampal and cerebellar slices appear to be a general feature of effects of MeHg in the CNS. However, such biphasic effects of MeHg on synaptic transmission were not limited in the CNS; they were also observed at peripheral synapses. At neuromuscular junctions, MeHg first stimulated and then suppressed to block of spontaneous release of ACh from the presynaptic nerve terminals (Juang and Yonemura, 1975; Juang, 1976b; Atchison and Narahashi, 1982; Atchison, 1986, 1987; Traxinger and Atchison, 1987a, b; Levesque and Atchison, 1987, 1988). In addition, in some cases, MeHg also transiently increased EPP amplitude prior to block (Manalis and Cooper, 1975; Juang, 1976b; Traxinger and Atchison, 1987b). Thus, the biphasic changes caused by MeHg in synaptic transmission may be a general characteristic of its effects in both central and peripheral nervous systems. The question is what factor(s) is(are) responsible for these early stimulatory effects of MeHg on central synaptic transmission. Data obtained from intracellular microelectrode and sSEVC recordings in CA1 pyramidal neurons of hippocampal slices indicated that an effect of MeHg on the resting membrane potential was not a major factor in causing the early stimulatory effects on hippocampal synaptic transmission, because MeHg affected synaptic responses evoked under both current clamp (EPSPs) and voltage clamp (EPSCs) similarly, and still caused a biphasic effect on EPSCs even though the CA1 pyramidal cell membrane was voltage-clamped at its resting membrane potential. However, by comparison of effects of MeHg on IPSP or IPSCs and EPSPs or EPSCs, I found that a preferential block by MeHg of inhibitory synaptic transmission was primarily responsible for the early apparent stimulatory effect of MeHg on hippocampal synaptic transmission. Pretreatment of hippocampal slices with bicuculline, the GABA_A receptor antagonist, completely eliminated the initial increase in amplitudes of population spikes and EPSPs induced by MeHg. Normally, neuronal membrane excitability of central neurons is regulated by the integrated activity from both excitatory and inhibitory inputs. If inhibition on a given cell is lost or reduced for any reason, this cell will become overexcited. Perhaps, MeHg preferentially suppresses GABA_A (maybe also GABA_B) receptor-mediated inhibitory synaptic transmission, which results in disinhibition of excitatory synaptic transmission via both pre- and postsynaptic mechanisms and leads to an initial hyperexcitation of CA1 pyramidal cells. Three possible events might occur following the disinhibition: (1) increased release of transmitter from presynaptic terminals due to loss of presynaptic inhibition; (2) individual neurons become more excited; and (3) more neurons are recruited to fire synchronously in response to a given stimulus. One or all of the these events may be involved in the early stimulatory effect of MeHg on hippocampal CA1 synaptic transmission. To date, no such experiments have been done in the cerebellar slices. It is reasonable to predict that effects of MeHg on inhibitory synaptic transmission in cerebellar slices will be also primarily responsible for the early stimulation of cerebellar synaptic transmission, because similar inhibitory synaptic circuits exist in the cerebellum. However, the lack of an early increase in amplitude of both PF-EPSPs and CF-EPSPs recorded from individual Purkinje cells suggests that the early stimulatory effects on field potentials recorded from the molecular layer of cerebellar slices may be due primarily to increased recruitment of more Purkinje cells to fire synchronously. In neuromuscular junction and autonomic ganglion preparations, the early increase in spontaneous release of ACh or frequency of MEPPs was postulated to be the result of depolarization of the presynaptic nerve terminal membranes, which caused the opening of Na⁺ and Ca²⁺ channels leading to increasing Ca²⁺ influx, and subsequent increases in spontaneous release of ACh (Atchison and Narahashi, 1982).

The second feature of effects of MeHg on central synaptic transmission presented in this dissertation is that MeHg initially reduced neuronal membrane excitability or altered the threshold level for initiation of action potentials and subsequently depolarized neuronal membranes leading to complete block of synaptic transmission. In hippocampal slices, at the time action potentials evoked by threshold stimulation of Schaffer collaterals or by directly depolarizing CA1 pyramidal cells were initially blocked, simply increasing the stimulus intensity slightly could temporarily again initiate action potentials. In addition, the amplitude of action potentials recorded just

prior to conduction block remained essentially unchanged (all or none manner). The same was true for effects of MeHg on action potentials evoked by stimulating the parallel fibers or CF-EPSPs evoked by stimulating the climbing fibers in cerebellar slices. Normally, an action potential is generated at the initial segment of the axon when the neuronal membrane is depolarized to reach a threshold level that leads to an explosive opening of Na⁺ channels. Theoretically, the threshold for a given cell can be changed by a variety of factors. MeHg may alter the distance between resting membrane potentials and the threshold by hyperpolarizing the cell membrane such that the resting membrane potential is farther from its threshold level or by moving the threshold level farther from a given resting membrane potential level. In either situation, a higher stimulus intensity will be required to initiate action potentials. MeHg did cause an initial hyperpolarization prior to depolarization of hippocampal CA1 pyramidal and cerebellar Purkinje cell membranes, however, the fact is that the resting membrane potentials were very close to the pre-MeHg treatment control level at the time action potentials evoked by threshold stimulation were blocked. Therefore, hyperpolarization alone cannot explain how MeHg changes the threshold level. Another possibility is that MeHg moves the threshold level farther from the resting membrane potentials. Using voltage-clamp techniques in squid axons, Shrivastav et al., (1976) demonstrated that 25 - 200 µM MeHg caused a steady increase in the threshold for initiation of action potentials and eventual block of conduction without significant changes in the resting membrane potentials. The authors proposed that the increased threshold levels were due to MeHg-induced suppression of both peak Na⁺ currents and steady-state K⁺ currents. If this is also true in hippocampal and cerebellar slice preparations, the amplitude of action potentials would be expected to decline progressively. This is true for the effects of MeHg on action potentials at the late stage of exposure to MeHg. However, at the early stage of exposure to MeHg in my experiments, amplitudes of action potentials just before block remained essentially unchanged and moreover, amplitudes of action potentials regenerated by increased stimulus were the same as those before block. One possible explanation is that MeHg may initially change the open probability of Na⁺ channels or increase the threshold for opening Na⁺ channel via certain mechanisms to result in the increased threshold for initiation of action potentials. Another possible explanation is that MeHg may suppress neurotransmitter release from the presynaptic terminals so that a higher stimulus intensity is required to release enough transmitter to act at the postsynaptic receptors and cause membrane depolarization toward the threshold level. Additionally, effects of MeHg on Ca2+ channels or Ca2+ homeostasis may be also involved, since Ca2+ plays a crucial role in both neurotransmitter release and maintenance of neuronal membrane excitability.

Much is known of effects of MeHg on resting membrane potentials in a variety of types of cells. Exposure to MeHg caused depolarization of muscle

fibers (Juang, 1976), squid axon membranes (Shrivastav et al. 1976), neuroblastoma cell membranes (Quandt et al., 1982) and synaptosomes (Kauppinen et al. 1989; Hare and Atchison, 1992). Results presented in this dissertation consistently demonstrated that MeHg initially hyperpolarizes and then depolarizes both hippocampal CA1 pyramidal cell and cerebellar Purkinje cell membranes in a concentration- and time-dependent manner. Actually, a similar effect also occurred in synaptosomes exposed to 1 µM MeHg (Hare and Atchison, 1992). Leonhardt et al. (1996) also demonstrated that MeHg caused a biphasic change, a transient inward current followed by a larger, sustained outward current, in the holding membrane current or the "resting membrane current" at the potential of -80 mV in 25 % of the experiments in rat dorsal root ganglion neurons. The ionic conductances responsible for the inward and outward currents are unknown. However, the authors hypothesized that these effects may be related to functional changes in some ion channels such as K⁺ and Cl channels that are regulated directly by increased [Ca2+];. The same may be true for effects of MeHg on hippocampal CA1 pyramidal cells. The initial membrane hyperpolarization induced by MeHg may be due to activation of Ca2+-sensitive K+ channels as result of MeHg-induced elevation in [Ca2+]; In rat synaptosomes, NG108-15 cells and primary culture of cerebellar granule cells, MeHg caused two phases of elevation in [Ca²⁺]; (Denny et al. 1993; Hare and Atchison, 1995; Marty and Atchison, 1997). The first phase of increase in [Ca²⁺], was believed to be due to release of Ca²⁺ from intracellular Ca²⁺ pools (eg. IP₃-sensitive pool) (Hare and Atchison, 1995; Marty and Atchison, 1997). It was believed that in NG108-15 cells, mobilization of an intracellular Ca²⁺ pool activates K+ channels and subsequently results in membrane hyperpolarization (Higashida and Brown, 1986). In addition, there is a difference in the effects of MeHg on resting membrane potentials at somatic motor end-plates or autonomic ganglia and those presented in this dissertation in that lower concentrations of MeHg (40 - 100 uM) had no effects on postsynaptic resting membrane potentials (Juang and Yonemura, 1975; Juang, 1976; Atchison and Narahashi, 1982). Depolarization of cell membranes only occurred at very high concentrations (500 µM) of MeHg (Shrivastav et al., 1976). However, in both hippocampal and cerebellar slices, lower concentrations of MeHg (4 - 20 µM) caused typical hyperpolarization and subsequent depolarization of CA1 pyramidal and Purkinje cell membranes. Differences between the effects of MeHg on resting membrane potentials in peripheral and central postsynaptic membranes may be due to differences in site of cells, underlying conductances (for example skeletal muscle cells have a very large endogeous Cl conductance) or duration and manner of exposure to MeHg. Alternatively, it may be that excitable cells in the CNS are more sensitive to MeHg than those at peripheral synapses, or at least with regards to the resting membrane potentials of postsynaptic muscle fibers.

MeHg appears to block voltage-dependent responses more rapidly than synaptically-activated local responses in both hippocampal and cerebellar slices. At the time that action potentials evoked by threshold stimulation of Schaffer collaterals in hippocampal slices were blocked by MeHg, EPSPs remained observable. Similarly, when action potentials (both Na⁺-dependent, fast somatic spikes and Ca²⁺-dependent, slow dendritic spike bursts) evoked by stimulating parallel or climbing fibers were blocked completely, synaptically-activated local responses or EPSPs remained observable. These results suggest that the voltage-dependent responses may be more sensitive to MeHg than are the synaptically-activated or glutamate-mediated responses. Thus, MeHg may affect both voltage-gated ion channels and glutamate receptors to block synaptic transmission. Further experiments to compare effects of MeHg on responses evoked by iontophoretic application of glutamate and by injection of depolarizing current at Purkinje cell soma should be designed to test this conclusion.

MeHg blocks both evoked and spontaneous responses in hippocampal and cerebellar slices. However, MeHg appears to block the evoked responses more rapidly than it does the spontaneous responses. In many cases, after evoked responses were blocked by MeHg, spontaneous responses remained observable in both intracellular and extracellular recordings. Similar phenomena were also observed in the neuromuscular preparations (Atchison and Narahashi, 1982). At neuromuscular junction, normal amplitude and duration of MEPPs remained to occur at the time EPPs were blocked. These results suggest that the mechanisms by which MeHg blocks the evoked and

spontaneous responses may differ. Perhaps, the differential effects of MeHg on evoked and spontaneous responses are resulted from different requirements and process for spontaneous and evoked release of neurotransmitters.

Apparently, multiple sites and effects were involved in MeHg-induced disruption of central synaptic transmission in both hippocampal and cerebellar slices, however, the mechanisms responsible for these effects appear to be predominantly postsynaptic. Thus, the mechanisms by which MeHg blocks neurotransmission in brain slices and at neuromuscular junction appear to differ; the effects of MeHg on transmission at the neuromuscular junction are generally considered to be primarily presynaptic. The difference between effects of MeHg on neurotransmission in brain slices and neuromuscular junction may be due to their different synaptic components. In central synapses, both pre- and postsynaptic parts consist of the neuronal components, while at neuromuscular junction, the postsynaptic components are muscle fibers, which may be more resistant to MeHg than are neurons.

In CF-EPSP recordings, MeHg almost always blocked the steady-state depolarization evoked by stimulating the climbing fibers first prior to suppression to block of Na⁺-dependent action potentials evoked by antidromic stimulation of Purkinje cell axons, *i.e.* the orthodromically-activated synaptic or climbing fiber responses are more sensitive to MeHg than are the antidromically-activated responses. These results further support the conclusion that effects of MeHg on synaptic process are involved. These results

may also indirectly imply that the Ca²⁺-dependent responses (climbing fiber responses) are more sensitive to MeHg than are Na⁺-dependent responses (antidromically-evoked action potentials), because voltage-activated Ca²⁺ and K⁺ channel currents were five times more sensitive to MeHg than were voltage-activated Na⁺ channel currents in dorsal root ganglion neurons (Leonhardt *et al.*, 1996).

Thus, the in vitro effects of MeHg on synaptic transmission in the tested pathways in hippocampal and cerebellar slices are generally similar. However, differences between effects of MeHg on hippocampal synaptic transmission and cerebellar synaptic transmission also existed at least in the following aspects: (1) MeHg appears to block evoked responses in Purkinje cells more rapidly than it does those evoked in hippocampal CA1 pyramidal cells, especially at lower concentrations of MeHg (Table 6.1, 6.2). However, the results obtained from hippocampal slices and cerebellar slices in this dissertation were conducted in separated experiments. Thus, direct comparison under similar conditions may be required before making a final conclusion about their sensitivity to MeHg; (2) due to Purkinje cells receiving inputs from both parallel and climbing fibers, characteristic effects of MeHg on repetitive firing of Purkinje cells which occurred spontaneously or was evoked by injection of depolarizing current were not observed in the CA1 pyramidal cells; and (3) in most hippocampal slices, MeHg caused an initial increase in amplitudes of EPSPs evoked by activation of Schaffer collaterals, whereas in most cerebellar

slices, MeHg did not induce early increase in amplitudes of PF-EPSPs or CF-EPSPs.

Effects of MeHg on the central synaptic transmission in brain slices also share many similarities with those of MeHg on peripheral neuromuscular transmission such as similar time courses, concentration-dependence and reversibility.

Table 6.1. Comparison of times to MeHg-induced block of population spikes (PSs) and field excitatory postsynaptic potentials (fEPSPs) in the CA1 region of hippocampal slices.

MeHg (µM)	20	100	500
PSs	$139 \pm 16(5/8)^{a}$	$41 \pm 4(8)$	$9 \pm 0.8 (11)$
fEPSPs	$177 \pm 3(3/8)$	$42 \pm 4(7)$	$9 \pm 0.5 (8)$

^a Mean \pm SE(n), fraction (5/8 or 3/8) means that in 5 or 3 of 8 slices, PSs or fEPSPs were blocked completely during 180 min application of 20 μM MeHg. The mean values are averaged based on the 5 or 3 experimental results. Actual times to block of PSs or fEPSPs by 20 μM should be longer than these means.

Table 6.2. Comparison of times to MeHg-induced block of parallel-fiber responses (PFRs), parallel-fiber post-synaptic responses (PSRs) and climbing-fiber responses (CFRs) in cerebellar slices.

MeHg (µM)	20	100	500
PSRs	$110 \pm 27(7)^{a}$	$40 \pm 4(8)$	$6 \pm 0.5(3)$
PFRs	$200 \pm 26(7)$	$61 \pm 3(9)$	$10 \pm 0.5(5)$
CFRs	$113 \pm 15(6)$	47 ± 3(8)	ND^{b}

^a Mean \pm SE(n) min.

^b Not determined.

Table 6.3. Comparison of times to MeHg-induced block of action potentials evoked by stimulating Schaffer collaterals (AP_{Sch}) and by current-injection (AP_{Soma}) in CA1 pyramidal cells of hippocampal slices.

MeHg (µM)	20	100
$\mathrm{AP}_{\mathrm{Sch}}$	$136 \pm 19(9)^a$	$47 \pm 6(12)$
$\mathrm{AP}_{\mathrm{Soma}}$	$142 \pm 18(9)$	49 ± 6(12)

^a Mean \pm SE(n).

Table 6.4. Comparison of times to MeHg-induced block of parallel fiber excitatory postsynaptic potentials (EPSP_{PF}), climbing fiber excitatory postsynaptic potentials (EPSP_{CF}) and repetitive firing of Purkinjec ells evoked by current injection (AP_{Some}) in cerebellar slices.

MeHg (µM)	20	100
$\mathrm{EPSP}_{\mathrm{PF}}$	$57 \pm 6(3)^{a}$	$33 \pm 7(7)$
$\mathrm{EPSP}_{\mathrm{CF}}$	$60 \pm 8(7)$	$36 \pm 4(8)$
AP _{Soma}	$36 \pm 4(3)$	$23 \pm 5(5)$

^a Mean \pm SE(n) min.

B. Conclusion.

Acute bath application of MeHg caused a concentration- and timedependent biphasic effect on central synaptic transmission in both hippocampal and cerebellar slices. Multiple effects or sites of action of MeHg, including presynaptic mechanisms, nonspecific membrane depolarization, suppression of current conductances and inhibitory synaptic transmission, are apparently involved, however, the primary sites of action of MeHg on central synaptic transmission appear to be the postsynaptic, which is different from those of effects of MeHg on peripheral neurotransmission at neuromuscular junction and autonomatic ganglia. The effects of MeHg on synaptic transmission in both hippocampal and cerebellar slices are similar in terms of the time course and concentration-dependence. This result suggests that under in vitro conditions and acute exposure, hippocampal pyramidal and cerebellar Purkinje cells, and perhaps other central neurons, may have similar sensitivity to MeHg. Also, these effects are also generally similar to those of acute exposure to MeHg of neuromuscular junctions in terms of the time course, concentrationdependence and reversibility. Thus, a similar and nonspecific mechanism may be responsible for acute effects of MeHg on neurotransmission in both central and peripheral nervous systems.

C. Future direction.

In short term, the following questions should be asked. (1) are the inhibitory synaptic circuits also more sensitive to MeHg than are the excitatory synaptic circuits in cerebellar slices? If so, do effects of MeHg on the inhibitory synaptic transmission contribute to the early stimulatory effects of MeHg on cerebellar excitatory synaptic transmission? (2) Are Ca²+-dependent responses more sensitive to MeHg than are Na+-dependent responses? Earlier block of depolarization plateau evoked by stimulation of the climbing fibers than action potentials evoked antidromically indirectly implied that Ca²+-dependent responses may be more sensitive to MeHg than Na+-dependent responses; (3) Are cerebellar granule cells functionally more sensitive to MeHg than are Purkinje cells? and (4) are there any relationships between effects of MeHg on Ca²+ homeostasis and synaptic transmission?

In long term, since previous studies of effects of MeHg on Ca²⁺ homeostasis, synaptic transmission and ion channels (Ca²⁺ channels) were performed in different experimental systems, a combination of Ca²⁺ imaging techniques, electrophysiological techniques and molecular biological techniques should be used to study effects of MeHg on central synaptic transmission in brain slices. In addition, previous and present studies primarily focus on the *in vitro* acute effects of MeHg on synaptic transmission, future research should be designed to examine the chronic effects of low concentrations of MeHg on

central synaptic transmission using brain slice cultures and eventually in vivo systems.

REFERENCES

- ALGER, B. E., DHANJAI, S. S., DINGLEDINE, R., GARTHWAITE, J., HENDERSON, G., KING, G. L., LIPTON, A. N., SCHWARTZKROIN, P. A., SEARS, T. A., SEGAL, M. WHITTINGHAM, T. S. AND WILLIAMS, J.: Brain Slice Methods. In: Brain Slices, ed. by R. Dingledine, pp. 381-437, Plenum Press, New York and London, 1984.
- ALKADHI, K. AND TAHA, M.N.: Antagonism by calcium of the inhibitory effect of methylmercury on sympathetic ganglia. Arch. Toxicol. **51**: 175-181, 1982.
- ANDERSEN, P., ECCLES, J.C. AND LØYNING, Y: Location of postsynaptic inhibitory synapses on hippocampal pyramids. J. Neurophysiol. 27: 592-607, 1964a.
- ANDERSEN, P., ECCLES, J.C. AND LØYNING, Y: Pathway of post-synaptic inhibition in the hippocampus. J. Neurophysiol. 27: 608-619, 1964b.
- ANDERSON, M. E.: The cerebellum. *In*: Textbook of Physiology: Excitable Cells and Neurophysiology, eds. by H. D. Patton, A. F. Fuchs, B. Hille, A, M. Scher and R. Steiner, pp 632-648, W. B. Saunders Company, Philadelphia, 1989.
- APRISON, M.H. AND DALY, E.C.: Biochemical aspects of transmission at inhibitory synapses. *In:* Advances in Neurochemistry, Vol. 3, eds. by B.W. Agranoff and M.H. Aprison, pp 203-294, Plenum Press, New York, 1978.

- ARAKAWA, O., NAKAHIRO, M., AND NARAHASHI, T.: Mercury modulation of GABA-activated chloride channels and non-specific cation channels in rat dorsal ganglion neurons. Brain Res. **551**: 58-63, 1991.
- ATCHISON, W.D., AND NARAHASHI, T.: Methylmercury-induced depression of neuromuscular transmission in the rat. NeuroToxicology 3: 37-50, 1982.
- ATCHISON, W.D.: Extracellular calcium-dependent and -independent effects of methylmercury on spontaneous and potassium-evoked release of acetylcholine at the neuromuscular junction. J. Pharmacol. Exp. Ther. 237: 672-680, 1986.
- ATCHISON, W.D., JOSHI, U. AND THORNBURG, J.E.: Irreversible suppression of calcium entry into nerve terminals by methylmercury. J. Pharmacol. Exp. Ther. 238: 618-624, 1986.
- ATCHISON, W.D.: Effects of activation of sodium and calcium entry on spontaneous release of acetylcholine induced by methylmercury. J. Pharmacol. Exp. Ther. 241: 131-139, 1987.
- ATCHISON, W.D.: Neurophysiological effects of mercurials. *In*: The Toxicity of Methyl Mercury, ed. by C.U. Eccles and Z. Annau, pp 189-219, The John Hopkins University Press, Baltimore, 1988.
- AUBRY, A., BATINI, C., BILLARD, J.M., KADO, R.T. AND MORAIN, P.: Tetrodotoxin induced calcium spikes: in vitro and in vivo studies of normal and differentiate Purkinje cells. Exp. Brian Res. 84: 297-302, 1991.

- BAKIR, F., DAMLUJI, S. F., AMIN-ZAKI, L., MURTADHA, M., KHALIDI, A., ALRAWI, N. Y., TIKRITI, S., DHAHIR, H. I., CLARKSON, T.W., SMITH, J.C. AND DOHERTY, R. A.: Methylmercury poisoning in Iraq. Science 181: 230-241, 1973.
- BASKYS, A.: Metabotropic receptors and "slow" excitatory actions of glutamate agonists in the hippocampus. TINS 15: 92-96, 1992.
- BECKER, C.M., HOCH, W. AND BETZ, H.: Glycine receptor heterogeneity in rat spinal cord during postnatal development. EMBO J. 7: 3717-3726, 1988.
- BELZ, H: Ligand-gated ion channels in the brain: The amino acid receptor superfamily. Neuron 5: 383-392, 1990.
- BENARDO, L.S.: GABA_A receptor-mediated mechanisms contribute to frequency-dependent depression of IPSPs in the hippocampus. Brain Res. **601**: 81-88, 1993.
- BIRKE, G., JONELS, A.G., PLANTIN, L-O., SJÖSTRAND, B. SKERFVING, S., WESTERMARK, T. AND STOCKHOLM, S.D.: Studies on humans exposed to methylmercury through fish consumption. Arch Environ Health 25: 77-91, 1972.
- BLANTON, M.G., LO TURCO, J.J. AND KRIEGSTEIN, A.R.: Whole cell recording from neurons in slices of reptilian and mammalian cerebral cortex. J. Neurosci. Meth. **30**: 203-210.
- BLITZER, R.D. AND LANDAU, E.M.: Whole-cell patch recording in brain slices. Meth. Enzymol. 238: 375-384, 1994.

- BOXALL, A.R., LANCASTER, B. AND GARTHWAITE, J.: Tyrosine kinase is required for long-term depression in the cerebellum. Neuron 16: 805-813, 1996.
- BONDY, S.C., ANDERSON, C.L., HARRINGTON, M.E. AND PRASAD, K.N.:

 The effects of organic and inorganic lead and mercury on
 neurotransmitter high-affinity transport and release mechanisms.

 Environ. Res. 19: 102-111, 1979.
- BRISTOW, D.R., BOWERY, N.G. AND WOODRUFF, G.N.: Light microscopic autoradiographic location of [³H]strychnine binding sites in rat brain. Eur. J. Pharmacol. **126**: 303-307, 1986.
- BRAOWN, T.H. AND ZADOR, A.M.: Hippocampus. *In*: The synaptic Organization of The Brain, 3rd edition, ed by G. M. Shepherd, pp 346-388, Oxford University Press, New York, 1990.
- CARPENTER, M. B.: The cerebellum. In: Core Text of Neuroanatomy, ed. by M. B. Carpenter, pp 224-249, Williams & Wilkins, Baltimore, 1991.
- CHANG, L.W. AND HAUTMANN, H.A.: Ultrastructural studies of the nervous system after mercury intoxication. I. Pathological changes in the nervous cell bodies. Acta Neuropath 20: 122-138, 1972.
- CHANG, L.W.: Neurotoxic effects of mercury. A review. Environ. Res. 14: 329-373, 1977.

- CHANG, L.W.: Mercury. *In* Experimental and Clinical Neurotoxicology, ed. by P.S. Spencer and H.H. Schaumburg, pp. 508-526, Williams and Wilkins, Baltimore, 1980.
- CHANG, W., STRAHLENDORF, J.C. AND STRAHLENDORF, H.K.: Ionic concentrations to the oscillatory firing activity of rat Purkinje cells in vitro. Brain Res. **614**: 335-341, 1993.
- COLLINGRIDGE, G.L., HERRON, C.E. AND LESTER, R.A.J.: Synaptic activation of N-methyl-D-aspartate receptors in the Schaffer Collateral-commissural pathway of rat hippocampus. J. Physiol. (Lond.) **399**: 283-300, 1988.
- COLLINGRIDGE, G.L. AND SINGER, W: Excitatory amino acid receptors and synaptic plasticity. Trends Pharmacol. Sci. 11: 290-296, 1990.
- CONNORS, B. W. AND PRINCE, D. A.: Effects of local anesthetic QX-314 on the membrane properties of hippocampal pyramidal neurons. J. Pharmacol. Exp. Ther. 220: 476-481, 1982.
- CREPEL, F. AND DELHAYE-BOUCHAUD, N.: Intracellular analysis of synaptic potentials in cerebellar Purkinje cells of the rat. Brain Res. 155: 176-181, 1978.
- CREPEL, F., DHANJAL, S. S. AND GARTHWAITE, J.: Morphological and electrophysiological characteristics of rat cerebellar slices maintained *in vitro*. J. Physiol. (Lond.) **316**: 127-138, 1981.

- CREPEL, F., DHANJAL, S. S. AND SEARS, T. A. Effect of glutamate, aspartate and related derivatives on cerebellar Purkinje cell dendrites in the rat: an *in vitro* study. J. Physiol. (Lond.) **329**: 297-317, 1982.
- CREPEL, F. AND JAILLARD, D.: Protein kinases, nitric oxide and long-term depression of synapses in the cerebellum. NeuroReport 1: 133-136, 1990.
- D'ANGELO, E., ROSSI, P. AND GARTHWAITE, J.: Dual-component NMDA receptor currents at a single central synapse. Nature (Lond.) **346**: 467-470, 1990.
- D'ANGELO, E., FILIPPI, G. D., ROSSI, P. AND TAGLIETTI, V.: Synaptic excitation of individual rat cerebellar granule cells *in situ*: evidence for the role of NMDA receptors. J. Physiol.(Lond.) **484**: 397-413, 1995.
- DENNY, M.F., HARE, M.F. AND ATCHISON, W.D.: Methylmercury alters intrasynaptosomal concentrations of endogenous polyvalent cations. Toxicol. Appl. Pharmacol. 122: 222-232, 1993.
- DINGLEDINE, R.B. AND GJERSTAD, L.: Penicillin blocks hippocampal IPSPs, unmasking prolonged EPSPs. Brain Res. 168: 205-209, 1979.
- DINGLEDINE, R.: Hippocampus: Synaptic pharmacology. *In*: Brain Slices, ed. by R. Dingledine, pp 87-112, Plenum, New York, 1984.
- DUTAR, P. AND NICOLL, R.A.: A physiological role for GABA_B receptors in the central nervous system. Nature (Lond.) **332**: 156-158, 1988a.

- DUTAR, P. AND NICOLL, R.A.: Pre- and postsynaptic GABA_B receptors in the hippocampus have different pharmacological properties. Neuron 1: 585-591, 1988b.
- DYCK, R.H. AND O'KUSKY, J.R.: Increased cytochrome oxidase activity of mesencephalic neurons in developing rats displaying methylmercury-induced movement and postural disorders. Neurosci. lett. 89: 271-276, 1988.
- EDWARD, F.A., KONNERTH, A., SAKMANN, B. AND TAKAHASHI, T.: A thin slice preparation for patch recordings from neurons of the mammalian central nervous system. Pflügers Archiv 414: 600-612, 1989
- EILLERS, J.: Calcium signaling in a narrow somatic submembrane shell during synaptic activity in cerebellar Purkinje neurons. Proc. Natl. Acad. Sci. USA 92: 10272-10276, 1995.
- EVANS, R.D.: Source of mercury contamination in the sediments of small headwater lakes in south-central Ontario, Canada. Arch. Envirn. Toxicol. 15: 505-512, 1986.
- FEJTL, M., GYÖRL, J. AND CARPENTER, D.O.: Hg²⁺ increases the open probability of carbachol-activated Cl⁻ channels in *Aplysia* neurons. NeuroReport **5**: 2317-2320, 1994.
- FRANCK, J.A., SCHWARTTZKRION, P.A., PHILLIPS, J.O. AND FUCHS, A.: The Limbic System. In: Textbook of Physiology: Excitable Cells and Neurophysiology, ed. by H. D. Patton, A. F. Fuchs, B. Hille, A, M. Scher and R. Steiner, pp 693-717, W. B. Saunders Company, Philadelphia, 1989.

- FROSTHOLM, A. AND ROTTER, A.: Glycine receptor distribution in mouse CNS: autoradiographic localization of [3H] strychnine binding sites. Brain Res. Bull. 15: 473-486, 1985.
- GARTHWAITE, J. AND BRODBELT, A.R.: Synaptic activation of N-methyl-D-aspartate and non-N-methyl-D-aspartate receptors in the mossy fiber pathway in adult and immature rat cerebellar slices. Neuroscience 29: 401-412, 1989.
- GLOMSKI, A. AND BRODY, H.: Distribution and concentration of mercury in autopsy specimens of human brain. Nature 232: 200-201, 1971.
- GORDEY, M., KANG, M., OLSEN, R.W. AND SPIGELMAN, I: Zinc modulation of GABA_A receptor-mediated chloride flux in rat hippocampal slices. Brain Res. **691**:125-132, 1995.
- GRENNINGLOH, G., GUNDELFINGER, E.D., SCHMITT, B., BETZ, H., DARLISON, M.G., BARNARD, E.A., SCHOFIELD, P.R. AND SEEBURG, P.H.: Glycine vs GABA receptors. Nature (Lond.) 330: 25-26, 1987.
- GRENNINGLOH, G., SCHMIEDEN, V., SCHOFIELD, P.R., SEEBURG, P.H. AND SIDDIQUE, T.: Alpha subunit variants of the human glycine receptor: primary structures, functional expression and chromosomal localization of the corresponding genes. EMBO J. 9: 771-776, 1990.
- HACKETT, J. T., HOU, S.-M. AND COCHRAN, S. L.: Glutamate and synaptic depolarization of Purkinje cells evoked by parallel fibers and by climbing fibers. Brain Res. 170: 377-380, 1979.

- HARE, M.F. AND ATCHISON, W.D.: Comparative actions of methylmercury and divalent inorganic mercury on nerve terminal and intraterminal mitochondrial membrane potentials. J. Pharmacol. Exp. Ther. **261**: 166-172, 1992.
- HARE, M.F., McGINNIS, K.M. AND ATCHISON, W.D.: Methylmercury increases intracellular concentration of Ca⁺⁺ and heavy metals in NG108-15 cells. J. Pharmacol Exp. Ther. **266**: 1626-1635, 1993.
- HARE, M.F. AND ATCHISON, W.D.: Methylmercury mobilizes Ca⁺⁺ from intracellular stores sensitive to inositol 1,4,5-trisphosphate in NG108-15 cells. J. Pharmacol. Exp. Ther. **272**: 1016-1023, 1995a.
- HARE, H.F. AND ATCHISON, W.D.: Nifedipine and tetrodotoxin delay the onset of methylmercury-induced increase in [Ca²⁺]_i in NG108-15 cells. Toxicol. Appl. Pharmacol. **135**: 299-307, 1995b.
- HENDERSEN, G.: Pharmacological analysis of synaptic transmission in brain slices. *In*: Electrophysiology, ed. by D. I. Walls, pp 89-107, 1993.
- HEWETT, S.J. AND ATCHISON, W.D.: Effects of charge and lipophilicity on mercurial-induced reduction of ⁴⁵Ca²⁺ uptake in isolated nerve terminals of the rat. Toxicol. Appl. Pharmacol. **113**: 267-273, 1992.
- HIGASHIDA, H. AND BROWN, D.A.: Two polyphosphatidylinositide metabolites control two K⁺ currents in a neuronal cell. Nature (Lond.) **323**:333-335, 1986.

- HIMURI, H., OKAMOTO, K AND SAKAI, Y.: Climbing and parallel fiber responses recorded intracellularly from Purkinje cell dendrites in guinea pig cerebellar slices. Brain Res. **348**: 213-219, 1985.
- HUANG, C-S. AND NARAHASHI, T.: Mercury chloride modulation of the GABA_A receptor-channel complex in rat root ganglion neurons. Toxicol. Appl. Pharmacol. **140**: 508-520, 1996.
- HUNTER, D. AND RUSSELL, D.S.: Focal cerebellar atrophy in human subject due to organic mercury compounds. J. Neurol. Neurosyrg. Psych. 17: 235-241, 1954.
- ISAACSON, J.S., SOLIS, J.M. AND NICOLL, R.A.: Local and diffuse synaptic actions of GABA in the hippocampus. Neuron 10: 165-175, 1993.
- JOHNSTON, D., HABLITZ, J.J. AND WILSON, W.A.: Voltage clamp discloses slow inward current in hippocampal burst-firing neurones. Nature (Lond.) **286**: 391-393, 1980.
- JOHNSTON, D AND BROWN, T.H.: Giant synaptic potential hypothesis for epileptiform activity. Science 211: 294-297, 1981.
- JOHNSTON, D. AND BROWN, T.H.: Biophysics and Microphysiology of Synaptic Transmission in Hippocampus. *In:* Brain Slice, ed. by R. Dingledine, pp 51-86, Plenum Press, New York, 1984.
- JOHNSON, J.W. AND ASCHER, P.: Glycine potentiates the NMDA response in cultured mouse brain neurons. Nature (Lond.) **325**: 529-531, 1987.

- JOHNSTON, D., MAGEE, J.C., COLBERT, C.M. AND CHRISTIE, B.R.: Active properties of neuronal dendrites. Annu, rev. Neurosci. 19: 165-186, 1996.
- JUANG, M.S. AND YONEMURA, K.: Increased spontaneous transmitter release from presynaptic nerve terminal by methylmercuric chloride.

 Nature (Lond.) **256**: 211-213, 1975.
- JUANG, M.S.: An electrophysiological study of action of methylmercuric chloride and mercuric chloride on the sciatic nerve-sartorius muscle preparation of the frog. Toxicol. Appl. Pharmacol. 88: 77-86, 1976a.
- JUANG, M.S.: Depression of frog muscle contraction by methylmercuric chloride and mercury chloride. Toxicol. Appl. Pharmacol. **35**: 183-185, 1976b.
- KANO, M., SCHNEGGENBURGER, R., VERKHRATSKY, A. AND KONNERTH, A.: Depolarization-induced calcium signals in the somata of cerebellar Purkinje neurons. Neurosci. Res. 24: 87-95, 1995.
- KAUPPINEN, R.A., KOMULAINEN, H. AND TAIPALE, H.: Cellular mechanisms underlying the increase in cytosolic free calcium concentration induced by methylmercury in cerebrocortical synaptosomes from guinea pig. J. Pharmacol. Exp. Ther. 248: 1248-1254, 1989.
- KENNEDY, M.B. AND MARDER, E.: Cellular and molecular mechanisms of neuronal plasticity, In: An Introduction to Molecular Neurobiology. ed by Z.W. Hall, pp463-495, Sinaure Associates, Inc, Sunderland, 1992.

- KIMURA, H., OKAMOTO, K. AND SAKAI, Y.: Climbing and parallel fibre responses recorded intracellularly from Purkinje cell dendrites in guinea pig cerebellar slices. Brain Res. 348: 213-219, 1985.
- KISHIMOTO, H., SIMON, J.R. AND APRISON, M.H.: Determination of the equilibrium dissociation constants and number of glycine binding sites in several areas of the rat central nervous system, using a sodium-independent system. J. Neurochem. 37: 1015-1024, 1981.
- KISHIMOTO, T., OGURI, T. AND TADA, M.: Effect of methylmercury (CH₃HgCl) injury on nitric oxide synthase (NOS) activity in cultured human umbilical vascular endothelial cells. Toxicology **103**: 1-7, 1995.
- KOMULAINEN, H. AND BONDY, S.: Increased free intrasynaptosomal Ca²⁺ by neurotoxic organometals: Distinctive mechanisms. Toxicol. Appl. Pharmacol. **88**:76-86, 1987.
- KOMULAINEN, H.: Neurotoxicity of methylmercury: cellular and subcellular aspects. *In*: Metal Neurotoxicity, ed. by S.C Bondy and K.N. Prasad, pp 167-182, CRC, Inc. Boca Raton, Florida, 1988.
- KOMULAINEN, H., KERÄNEN, A. AND SAANO, V.: Methylmercury modulates GABA_A receptor complex differentially in rat cortical and cerebellar membranes *in vitro*. Neurochem. Res. **20**; 659-662, 1995.
- KONNERTH, A., LLANO, I. AND ARMSTRONG, C. M.: Synaptic currents in cerebellar Purkinje cells. Proc. Natl. Acad. Sci. USA 87: 2662-2665, 1990.

- KONNERTH, A., DREESSEN, J. AND AUGUSTINE, G.J.: Brief dendritic calcium signals initiate long-lasting synaptic depression in cerebellar Purkinje cells. Pro. Natl. Acad. USA 89: 7051-7055, 1992.
- KUHSE, J., SCHMIEDEN, V. AND BETZ, H.: A single amino acid exchange alters the pharmacology of neonatal rat glycine receptor subunit. Neuron 5: 867-873, 1990a.
- KUHSE, J., SCHMIEDEN, V. AND BETZ, H.: Identification and functional exchange of a novel ligand binding subunit of the inhibitory glycine receptor. J. Biol. Chem. **265**: 22317-22320, 1990b.
- KUHSE, J., KURYATOV, A., MAULET, Y., MALOSIO, M.L., SCHMIEDEN,
 V. AND BETZ, H.: Alternative splicing generates two isoforms of the α2 subunit of the inhibitory glycine receptor. FEBS Lett. 283: 73-77, 1991.
- KUNIMOTO, M. AND SUZUKI, T.: Migration of granule neurons in cerebellar organotypic cultures is impaired by methylmercury. Neurosci. Lett. **226**: 183-186, 1997.
- KURLAND, T. L., FARO, S. N., AND SIEDLER, H.: Minamata disease. World Neurol. 1:370-395, 1960.
- LANGMOEN, I. A. AND ANDERSON, P.: The hippocampal slice in vitro. A description of the technique and some examples of the opportunities it offers. In: Electrophysiology of isolated Mammalian CNS Preparations, ed. by G. A. Kerkut and H. V. Wheal, pp 51-105, Academic Press, London, 1981.

- LANGOSCH, D., THOMAS, L. AND BETZ, H.: Conserved quaternary structure of ligand-gated ion channels: the postsynaptic glycine receptor is a pentamer. Proc. Natl. Acad. Sci. USA 85: 7394-7398, 1988.
- LEONHARDT, R., HAAS, H. AND BÜSSELBERG, D.: Methyl mercury reduces voltage-activated currents of rat dorsal root ganglion neurons.

 Naunyn-Schmiedeberg's Arch. Pharmacol. **354**: 532-538, 1996.
- LEVESQUE, P.C. AND ATCHISON, W.D.: Interaction of mitochondrial inhibitors with methylmercury on spontaneous quantal release of acetylcholine. Toxicol. Appl. Pharmacol. 87: 315-324, 1987.
- LEVESQUE, P.C. AND ATCHISON, W.D.: Effect of alteration of nerve terminal Ca²⁺ regulation on increased spontaneous quantal release of acetylcholine by methylmercury. Toxicol. Appl. Pharmacol. **94**: 55-65, 1988.
- LEVESQUE, P.C. AND ATCHISON, W.D.: Disruption of brain mitochondrial calcium sequestration by methylmercury. J. Pharmacol. Exp. Ther. **256**: 236-256, 1991.
- LEVESQUE, P.C., HARE, M.F. AND ATCHISON, W.D.: Inhibition of mitochondrial Ca²⁺ release diminishes the effectiveness of methyl mercury to release acetylcholine from synaptosomes. Toxicol. Appl. Pharmacol. 115: 11-20, 1992.
- LEYSHON-SØRLAND, K., JASANI, B. AND MORGAN, A.J.: The localization of mercury and metallothionein in the cerebellum of rats experimentally exposed to methylmercury. **26**: 161-169, 1994.

- LINDEN, D.J., SMEYNE, M. AND CONNOR, J.A.: Induction of cerebellar long-term depression in culture requires postsynaptic action of sodium ions. Neuron 11: 1093-1100, 1993.
- LLANO, I., MARTY, A., ARMSTRONG, C. M. AND KONNERTH, A.: Synapticand agonist-induced excitatory currents of Purkinje cells in rat cerebellar slices. J. Physiol. (Lond.) 434: 183-213, 1991.
- LLINÁS, R. AND HESS, R.: Tetrodotoxin-resistant dendritic spikes in avian Purkinje cells. Proc. Natl. Acad. Sci. USA 73: 2520-2523, 1976.
- LLINÁS, R. AND SUGIMORI, M.: Electrophysiological properties of *in vitro* purkinje cell somata in mammalian cerebellar slices. J. Physiol. (Lond.) **305**: 171-195, 1980a.
- LLINÁS, R. AND SUGIMORI, M.: Electrophysiological properties of *in vitro*Purkinje cell dendrites in mammalian cerebellar slices. J. Physiol.

 (Lond.) **305**: 197-213, 1980b.
- LLINÁS, R. AND WALTON, K.D.: Cerebellum. In The synaptic organization of the brain. 3rd edition, ed by Gordon M. Shepherd. pp215-245, Oxford University Press, New York, 1990.
- LYNCH, G.: The use of *in vitro* brain slices for multidisciplinary studies of synaptic function. Ann. Rev. Neurosci. 3: 1-22, 1980.
- MAGEE, J. C. AND JOHNSTON. D.: Synaptic activation of voltage-gated channels in the dendrites of hippocampal pyramidal neurons. Science **268**: 301-304, 1995.

- MALOSIO, M-L.V., MARQUÈZE-POUEY, B., KUHSE, J.A. AND BETZ, H.: Widespread expression of glycine receptor subunit mRNAs in the adult and developing rat brain. EMBO J. 10: 2401-2409, 1991.
- MANALIS, R.S. AND COOPER, G.P.: Evoked transmitter release increased by inorganic mercury at frog neuromuscular junction. Nature **257**: 690-691, 1975.
- MARTY, M. S. AND ATCHISON, W. D.: Methylmercury may utilize voltage-operated channels for Ca²⁺ influx and/or MeHg entry into cerebellar granule cells. Fundam. Appl. Toxicol. (Suppl.) **30** (1): 174, 1996.
- MARTY, M.S. AND ATCHISON, W.D.: Pathways mediating Ca²⁺ entry in rat cerebellar granule cells following *in vitro* exposure to methylmercury. Toxicol. Appl. Pharmacal. 1997 (in press).
- MINNEMA, D.J., COOPER, G.P. AND GREENLAND, R.D.: Effects of methylmercury on neurotransmitter release from rat brain synaptosomes. Toxicol. Appl. Pharmacol. 99: 510-521, 1989.
- MINTZ, I.M., SABATINI, B. L., and REGEHR, W. G.: Calcium control of transmitter release at a cerebellar synapse. Neuron 15: 675-688, 1995.
- McCORMICK, D.A.: Membrane properties and neurotransmitter actions. *In:*The Synaptic Organization of the Brain, ed. by Gordon M. Shepherd, pp
 32-66, Oxford University Press, New York, 1990.
- MIYAKAWA, T., DESHIMARU, M., SUMIYOSHI, S., TERAOKA, A., UDO, N., HATTORI, E. AND TATETSU S.: Experimental organic mercury poisoning-pathological changes in peripheral nerves. Acta Neuropath. (Berl.) 15: 45-55, 1970.

- MIYAMOTO, M.D.: Hg^{2+} causes neurotoxicity at an intracellular site following entry through Na⁺ and Ca²⁺ channels. Brain Res. **267**: 375-379, 1983.
- MÔLLER-MADSEN, B.: Localization of mercury in CNS of the rat. II: Intraperitoneal injection of methylmercury chloride (CH₃HgCl) and mercuric chloride (HgCl₂). Toxicol. Appl. Pharmacol. **103**: 303-323, 1990.
- MÖLLER-MADSEN, B.: Localization of mercury in CNS of the rat. III: Oral administration methylmercury chloride (CH₃HgCl). Fund. Appl. Toxicol. **16**: 172-187, 1991.
- MOMIYAMA, A. AND TAKAHASHI, T.: Calcium channels responsible for potassium-induced transmitter release at rat cerebellar synapses. J. Physiol. (Lond.) 476: 197-202, 1994.
- MÜLLER, W. AND CONNOR, J. A.: Dendritic spines as individual neuronal compartments for synaptic Ca²⁺ responses. Nature (*Lond.*) **354**: 73-79, 1991.
- NADLER, J.V., THOMPSON, M.A. AND McNAMARA, J.O.: Kindling reduces sensitivity of CA3 hippocampal pyramidal cells to competitive NMDA receptor antagonists. Neuropharmacol. 33: 147-153, 1994.
- NAGASHIMA, K., FUJII, Y., TSUKAMOTO, T., NUKUZUMN, S., SATOH, M. FUJITA, M. FUJIOKA, Y. AND AKAGI, H.: Apoptotic process of cerebellar degeneration in experimental methylmercury intoxication of rats. Acta Neuropathol. **91**: 72-77, 1996.

- NATER, E.A. AND GRIGAL, D.F.: Regional trends in mercury distribution across the great lakes states, north central USA. Nature (Lond.) **358**: 139-141, 1992.
- NELSON, N., KOLBYE, Jr., A.C., KULAND, L,T., SHAPIRD, R.E., SHIBKO, S.I, STICKEL, W.H., THOMPSON, J.E., VAN DEN BERG, L.A AND WEISSLER, A.: Hazards of mercury. Environ. Res. 4 (1) 1-69, 1971.
- NICOLLS, J., MARTIN, A. R. AND WALLACE, B. G.: From Neuron to Brain, pp 538-543, Sinauer Associates, Inc., Sunderland, Massachusetts, 1992.
- NRIAGU, J.O., PFEIFFER, W.C., MALM, O., SOUZA, C.M.M. AND MIERLE, G.: Mercury pollution in Brazil. Nature (Lond.) **356**: 389, 1992.
- NRIAGU, J.O.: Legacy of mercury pollution. Nature (Lond.) 365: 589, 1993.
- OLSZERWSKI, W.A., PILLAY, K.K.S., GLOMSKI, C.A. AND BRODY, H.:

 Mercury in the human brain. Acta Neurol. Scandinav. 50: 581-588,
 1974.
- OMATA, S., HIRAKAWA, E., DAIMON, Y. UCHIYAMA, M., NAKASHITA, H., HORIGOME, T., SUGANO, I. AND SUGANO, H.: Methylmercury-induced changes in the activities of neurotransmitter enzymes in nervous tissues of the rat. Arch. Toxicol. 51: 285-294, 1982.
- OMATA, S., KASAMA, H., HASWGAWA, H., HASEGAWA, K., OZAKI, K. AND SUGANO, H.: Species difference between rat and hamster in tissue accumulation of mercury after administration of methylmercury. Arch. Toxicol. **59**: 249-254, 1986.

- OTIS, T.S., KONINCK, Y.V. AND MODY, I.: Characterization of synaptically elicited GABA_B responses using patch-clamp recordings in rat hippocampal slices. J. Physiol. (Lond.) **463**: 391-407, 1993.
- PEARCE, R.A.: Physiological evidence for two distinct GABA_A responses in rat hippocampus. Neuron 10: 189-200, 1993.
- PETROZZINO, J. J. AND CONNOR, J. A.: Dendritic Ca²⁺ accumulations and metabotropic glutamate receptor activation associated with an N-Methyl-D-Aspartate receptor-independent long-term potentiation in hippocampal CA1 neurons. Hippocampus, **5**: 546-558, 1994.
- PETROZZINO, J. J., POZZO MILLER, L. D. AND CONNOR, J. A.: Micromolar Ca²⁺ transients in dendritic spines of hippocampal pyramidal neurons in brain slices. Neuron 14: 1223-1231, 1995.
- PITLER, T.A AND ALGER, B.E.: Differences between presynaptic and postsynaptic GABA_B mechanisms in rat hippocampal pyramidal cells. J. Neurophysiol. **72**: 2317-2327, 1994.
- PLANT, T.D., EILERS, J. AND KONNERTH, A.: Patch-clamp technique in brain slices. *In*: Neuromethods, Vol. 26: Patch-Clamp Application and Protocols, eds. by A. A. Boulton, G. B. Baker and W. Walz, pp 233-257, Humana Press Inc., Totowa, 1995.
- PROBST, A., CORTES, R. AND PALACIOS, J.M.: The distribution of glycine receptors in the human brain. A light microscopic autoradiographic study using [3H]strychnine. Neuroscience 17: 11-35, 1986.

- PYCOCK, C.J. AND KERWIN, R.W.: The status of glycine as a supraspinal neurotransmitter. Life Sci. 28: 2679-2686, 1981.
- QUANDT, F.N., KATO, E. AND NARAHASHI, T.: Effects of methylmercury on electrical responses of neuroblastoma cells. NeuroToxicology 3: 205-220, 1982.
- REDMAN, S. J.: Single-electrode voltage clamp. *In*: Practical Electrophysiological Methods, eds. by H. Kettenmann and R. Grantyn, pp 263-270, Willey-Liss Inc., New York, 1992
- REGEHR, W. G. AND TANK, D. W.: Selective fura-2 loading of presynaptic terminals and nerve cell processes by perfusion in mammalian brain slices. J. Neurosci. Meth. 37: 111-119, 1991.
- REGEHR, W. G., KONNERTH, A. AND ARMSTRONG, C. M.: Sodium action potentials in the dendrites of cerebellar Purkinje cells. Proc. Natl. Acad. Sci. USA 89: 5492-5946, 1992
- REGEHR, W. G. AND MINTZ, I. M.: Participation of multiple calcium channel types in transmission at single climbing fiber to Purkinje cell synapses.

 Neuron 12: 605-613, 1994.
- REGEHR, W. G. AND ATLURI, P.: Calcium transients in cerebellar granule cell presynaptic terminals. Biophys. J. **68**: 2156-2179, 1995.
- ROSS, W.N. AND WERMAN, R.: Mapping calcium transients in the dendrites of Purkinje cells from the guinea-pig cerebellum *in vitro*. J. Physiol. (Lond.) **389**: 319-336, 1987.

- RUSTAM, H. AND HAMDI, T.: Methyl mercury poisoning in Irag. A neurological study. Brain 97: 499-510, 1974.
- RUSTAM, H., VON BURG, R., AMIN-ZAKI, L. AND HASSANI, S.E.: Evidence for a neuromuscular disorder in methylmercury poisoning. Clinical and electrophysiological findings in moderate to severe cases. Arch. Envir. health 30: 190-195. 1975.
- SAKMANN, B. AND STUART, G.: Patch-pipette recordings from the soma, dendrites, and axon of neurons in brain slices. *In*: Single-Channel Recording, Second edition, eds. by B. Sakmann and E. Neher, pp 199-211, Plenum Press, New York, 1995.
- SAKURI, M.: Calcium is an intracellular mediator of the climbing fiber in induction of cerebellar long-term depression. Proc. Natl. Acad. Sci. USA 87: 3383-3385, 1990.
- SALIN, P.A., MALENKA, R.C. AND NICOLL, R.A.: Cyclic AMP mediates a presynaptic form of LTP at cerebellar parallel fiber synapses. Neuron 16: 797-803, 1996.
- SARAFIAN, T.A.; HAGLER, J., VARTAVARIAN, L. AND VERITY, M.A.:
 Rapid cell death induced by methyl mercury in suspension of cerebellar
 granule neurons. J. Neuropathol. Exp. Neurol. 48: 1-10, 1989.
- SARAFIAN, T.A. AND VERITY, M.A.: Methyl mercury stimulates protein ³²P phospholabelling in cerebellar cell culture. J. Neurochem. **55**: 913-921, 1990a.

- SARAFIAN, T.A. AND VERITY, M.A.: Altered patterns of protein phosphorylation and synthesis caused by methyl mercury in cerebellar granule cell culture. J. Neurochem. **55**: 922-929, 1990b.
- SARAFIAN, T.A. AND VERITY, M.A.: Changes in protein phosphorylation in cultured neurons after exposure to methyl mercury. Ann. N.Y. Acad. Sci. **679**: 65-77, 1992
- SARAFIAN, T.A.: Methyl mercury increases intracellular Ca²⁺ and inositol phosphate levels in cultured cerebellar granule neurons. J. Neurochem. **61**: 648-657, 1993.
- SARAFIAN, T.A., VARTAVARIAN, L. KANE, D.J. BREDESEN, D.E. AND VERITY, M.A.: bcl-2 expression decreases methyl mercury-induced free-radical generation and cell killing in a neural cell line. Toxicol. lett. 74: 149-155, 1994.
- SCHMIEDEN, V., HUHSE, J. AND BETZ, H.: Mutation of glycine receptor subunit creates β-alanine receptor responsive to GABA. Science 262: 256-258, 1993.
- SCHOFIELD, P.R., DARLISON, M.G., FUJITA, N., RODRIGUEZ, H., BURT, D.R., STEPHENSON, F.A. RHEE, L.M., RAMACHANDRAN, J., GLENCORSE, T.A., REALE, V., SEEBURG, P.H. AND BARNARD, E.A.: Sequence and functional expression of the GABA_A receptor shows a ligand-gated receptor superfamily. Nature (Lond.) 328: 221-227, 1987.
- SCHUTTER, E.: Cerebellar long-term depression might normalize excitation of Purkinje cells: a hypothesis. Trends Neurosci. 18: 291-295, 1995.

- SCHWARTZKROIN, P. A. AND SLAWSKY, M: Probable calcium spikes in hippocampal neurons. Brain Res. 135: 157-161, 1977.
- SCHWARTZKROIN, P. A.: To slice or not to slice. In: Electrophysiology of Isolated Mammalian CNS Preparations, ed. by J.A.Kerkut and H.V Wheal, pp15-50, Academic Press, London, 1981.
- SEGAL, M.: Imaging of calcium variations in living dendritic spines of cultured rat hippocampal neurons. J. Physiol. (*Lond.*) **486**: 283-295, 1995.
- SHAFER, T.J. AND ATCHISON, W.D.: Block of ⁴⁵Ca²⁺ uptake into synaptosomes by methylmercury: reversibility, state, and Na⁺-dependency. J. Pharmacol. Exp. Ther. **248**: 696-702, 1989.
- SHAFER, T.J., CONTRERAS, M.L. AND ATCHISON, W.D.: Characterization of interactions of methylmercury with Ca²⁺ channels in synaptosomes and pheochromocytoma cells: radiotracer flux and binding studies. Mol. Pharmacol. **38**: 102-113, 1990.
- SHAFFER, T.J. AND ATCHISON, W.D.: Methylmercury blocks N- and L-type Ca²⁺ channels in nerve growth factor-differentiated pheochromocytoma (PC12) cells. J. Pharmacol. Exp. Ther. 258: 149-157, 1991.
- SHAFER, T.J. AND ATCHISON, W.D.: Effects of methylmercury on perineurial Na⁺ and Ca²⁺-dependent potentials at neuromuscular junctions of the mouse. Brain Res. **595**: 215-219, 1992.
- SHEPHERD, G.M.: Cerebellum. *In*: The Synaptic Organization of The Brain, Third edition, ed. by G. M. Shepherd, pp 215-245, Oxford University Press, New York, 1990.

- SHIRASAKI, T., HARATA, N. AND AKAIKE, N.: Metabotropic glutamate response in acutely dissociated hippocampal CA1 pyramidal neurones of the rat. J. Physiol. (Lond.) 475: 439-453, 1994.
- SHRIVASTAV, B.B., BRODWICK, M.S. AND NARAHASHI, T.: Methylmercury: Effects on electrical properties of squid axon membranes. Life Sci. 18: 1077-1082, 1976.
- SILVER, R.A., TRAYNELIS, S. F. AND CULL-CANDY, S. G.: Rapid-time-course miniature and evoked excitatory currents at cerebellar synapses in situ. Nature (Lond.) **355**: 163-166, 1992.
- SILVER, R.A., CULL-CANDY, S.G. AND TAKAHASHI, T.: Non-NMDA glutamate receptor occupancy and open probability at a rat cerebellar synapse with single and multiple release sites. J. Physiol. (Lond.) **494**: 231-250, 1996.
- SIROIS, J. E., BICKMEYER, U. and ATCHISON, W. D.: Methylmercury modulation of whole cell outward current in cerebellar granule cells. The Toxicologist 15: 14, 1995.
- SIROIS, J. E. and ATCHISON, W. D.: Methylmercury (MeHg) decreases whole cell barium current (I_{Ba2+}) in cerebellar granule neurons. Fundam. Appl. Toxicol. (Suppl.) **30** (1): 26, 1996.
- SOMER, B. AND SEEBURG, P.H.: Glutamate receptor channels: novel properties and new clones. Trends Pharmacol. Sci. 13: 291-296, 1992.

- SPRUSTON, N., SCHILLER, Y., STUART, G. AND SAKMANN. B.: Activity-dependent action potential invasion and calcium influx into hippocampal CA1 dendrites. Science **268**: 297-300, 1995a.
- SPRUSTON, N. JONAS, P. AND SAKMANN, B.: Dendritic glutamate receptor channels in rat hippocampal CA3 and CA1 pyramidal neurones. J. Physiol. **482**: 325-352, 1995b.
- STEEL, R.G.D. AND TORRIE, J.H.: *In* Principles and Procedures of Statistics, pp. 137-194. McGraw-Hill, New York, 1980.
- STUART, G.J., DOLT, H.-U. AND SAKMANN, B.: patch-clamp recordings from the soma and dendrites of neurons in brain slices using infrared video microscopy. Pflügers Arch. 423: 511-518, 1993.
- STUART, G. AND HÄUSSER, M.: Initiation and spread of sodium action potentials in cerebellar Purkinje cells. Neuron 13: 703-712, 1994.
- SYVERSEN, T.L.M.: Effects of methyl mercury on protein synthesis in vitro.

 Acta Pharmacol. Toxicol. 49: 422-426, 1981.
- TAKEUCHI, T., KAMBARA, T., MORIKAWA, N., MATSUMOTO, H., DHIRAISHI, Y. AND ITO, H.: Pathologic observations of the Minamata disease. Acta path. Jap. 9 (Suppl.): 769-783, 1959.
- TAKEUCHI, T., MORIKAWA, N. MATSUMOTO, H. AND SHIRAISHI, Y.: a pathological study of Minamata disease in Japan. Acta Neuropath. 2: 40-57, 1962.

- TAYLOR, C.B.: The effect of mercurial diuretics on adenosinetriphosphatase of rabbit kidney in vitro. Biochem. Pharmacol. 12: 539-550, 1963.
- TEYLER, T. J.: Brain slice preparation: hippocampus. Brain Res. Bull. 5: 391-403, 1980.
- TEYLER, T. L: The Introduction of Brain Slices to Neurophysiology, In: Brain Slices: Fundamentals, Applications and Implications, ed. by A. Schurr, T. J. Teyler and M. T. Tseng, pp 1-9, Academic Press, London, 1986.
- TOKUOMI, H., OKAJIMA, T., KANAI, J., TSUNODA, M., ISHIYASU, Y., MISUMI., H., SHIMOMURA, K. and TAKABA, M.: Minamata disease. World Neurol. 2: 536-545, 1961.
- THOMAS, D., FISHER, H.L., SMULER, M.R., MARCUS, A.H. MUSHAK. P. AND HALL, L.L.: Sexual differences in the distribution and retention of organic and inorganic mercury in methyl mercury-treated rats. Environ. Res. 41: 219-234, 1986.
- THOMPSON, S. AND GÄHWILER, B.H.: Comparison of the actions of baclofen at pre- and postsynaptic receptors in the rat hippocampus in vitro. J. Physiol. (Lond.) 451: 329-345, 1992.
- TRAXINGER, D.L. AND ATCHISON, W.D.: Comparative effects of divalent cations on the methylmercury-induced alterations of acetylcholine release. J. Pharmacol. Exp. Ther. 240: 451-459, 1987a.
- TRAXINGER, D.L. AND ATCHISON, W.D.: Reversal of methylmercury-induced block of nerve-evoked release of acetylcholine at the neuromuscular junction. Toxicol. Appl. Pharmacol. **90**: 23-33, 1987b.

- TRAYNELIS, S. F., SILVER, R. A. AND CULL-CANDY, S. G.: Estimated conductance of glutamate receptor channels activated during EPSCs at the cerebellar mossy fiber-granule cell synapse. Neuron 11: 279-289, 1993.
- TUNNICLIFF, G. AND WOOD, J.D.: The inhibition of mouse brain neurotransmitter enzymes by mercury compounds and a comparison with the effects of hyperbaric oxygen. Comp. Gen, Pharmacol. 4: 101-105, 1973.
- VAN DEN POL, A. AND GORCS, T.: Glycine and glycine receptor immunoreactivity in brain and spinal cord. J. Neurosci. 8: 472-492, 1988.
- VERITY, M.A., BROWN, W.J. AND CHEUNG, M.: Organic mercury encephalopathy: in vivo and in vitro effects of methylmercury on synaptosomal respiration. J. Neurochem. 25: 759-766, 1975.
- VON BURG, R. AND LANDRY, T.: Methylmercury induced neuromuscular dysfunction in the rat. Neurosci. lett. 1: 169-172, 1975.
- VON BURG, R. AND LANDRY, T.: Methylmercury and the skeletal muscle receptor. J. Pharm. Pharmacol. 28: 548-551, 1976.
- WALSH, T. J. AND EMERCH, D. F.: The hippocampus as a common target of neurotoxic agents. Toxicology 49: 137-140, 1988.
- WENDRO, A.P.: Domestic mercury pollution. Nature (Lond.) 347: 623, 1990.

- WONG, R. K. S. and PRINCE, D. A.: Participation of calcium spikes during intrinsic burst firing in hippocampal neurons. Brain Res. **159**: 385-390, 1978.
- WONG, R.K.S., PRINCE, D.A. AND BASBAUM, A.I.: Intradendritic recordings from hippocampal neurons. Proc. Natl. Acad. Sci. USA **76**: 986 990, 1979.
- WU, L. G. and SAGGAU, P.: Presynaptic calcium is increased during normal synaptic transmission and paired-pulse facilitation, but not in long-term potentiation in area CA1 of hippocampus. J. Neurosci. 14: 645-654, 1994.
- WU, L.G. AND SAGGAU, P.: GABA_B receptor-mediated presynaptic inhibition in guinea-pig hippocampus is caused by reduction of presynaptic Ca²⁺ influx. J. Physiol. (Lond.) **485**: 649-657, 1995.
- YAN, C. and ATCHISON, W. D.: Characterization of interaction of methylmercury with Ca²⁺ channels of rat cerebellar synaptosomes. Fundam. Appl. Toxicol. (Suppl.) **30** (1): 187, 1996.
- YASUTAKE, A. AND HIRAYAMA, K.: Strain difference in mercury excretion in methylmercury-treated mice. Arch. Toxicol. **59**: 99-102, 1986.
- YOSHINO, Y., MOZAI, T. AND NAKAO, K.: Distribution of mercury in the brain and its subcellular units in experimental organic mercury poisonings. J. Neurochem. 13: 397-406, 1966a.
- YOSHINO, Y., MOZAI, T. AND NAKAO, K.: Biochemical changes in the brain in rats poisoned with an alkylmercuric compound, with special reference

- to the inhibition of protein synthesis in brain cortex slice. **13**: 1223-1230, 1996b.
- YOUNG, A.B. AND SNYDER, S.H.: Strychnine binding associated with glycine receptors of the central nervous system. Proc. Natl. Acad. Sci. USA 70: 2832-2836, 1973.
- YUAN, Y. AND ATCHISON, W.D.: Disruption by methylmercury of membrane excitability and synaptic transmission of CA1 neurons in hippocampal slices of the rat. Toxicol. Appl. Pharmacol. 120: 203-215, 1993.
- YUAN, Y. AND ATCHISON, W.D.: Comparative effects of inorganic divalent mercury, methylmercury and phenylmercury on membrane excitability and synaptic transmission of CA1 neurons in hippocampal slices of the rat. NeuroToxicology 15: 403-412, 1994.
- YUAN, Y. AND ATCHISON, W.D.: Methylmercury acts at multiple sites to block hippocampal synaptic transmission. J. Pharmacol. Exp. Ther. **275**: 1308-1316, 1995a.
- YUAN, Y. AND ATCHISON, W.D.: Differential effects of Hg²⁺ and methylmercury on excitatory and inhibitory transmission in hippocampal slices. Soc. Neurosci. abstr. 21: 1985, 1995b.
- YUAN, Y AND ATCHISON, W.D.: Action of MeHg on GABA_A receptor-mediated inhibitory synaptic transmission is primarily responsible for its early apparent stimulatory effects on hippocampal CA1 excitatory transmission in hippocampal slices. J. Pharmacol. Exp. Ther. 282: 64-73, 1997.

ZARBIN, M.A., WAMSLEM, J.K. AND HUHSE, M.J.: Glycine receptor: light microscopic autoradiographic localization with [3H]strychnine. J. Neurosci. 1: 532-547, 1981.

